Mechanisms of S-nitrosothiols intestinal permeability and NO store formation within vascular wall to improve NO oral delivery systems

Yi Zhou

Ecole Doctorale BioSE (Biologie-Santé-Environnement)

Thèse

Présentée et soutenue publiquement pour l'obtention du titre de

DOCTEUR DE l'UNIVERSITE DE LORRAINE

Mention : « Sciences de la Vie et de la Santé » par

Yi ZHOU

Mechanisms of *S*-nitrosothiols intestinal permeability and NO store formation within vascular wall to improve NO oral delivery systems

Le 17 octobre 2019

Membres du jury:

Rapporteurs:	**Gilles PONCHEL**	**Pr, UMR CNRS 8612 Université Paris-Sud**
	Céline DEMOUGEOT	**Pr, PEPITE EA 4267, Université de Franche-Comté**
Examinateurs:	**Mourad ELHABIRI**	**DR-CNRS, UMR CNRS 7042-LIMA, ECPM, Université de Strasbourg**
	Cédric BOURA	**MCU, HDR, UMR CNRS 7039-CRAN, Université de Lorraine**
	Caroline GAUCHER	**MCU, HDR, CITHEFOR EA 3452, Université de Lorraine, directeur de thèse**
	Marianne PARENT	**MCU, CITHEFOR EA 3452, Université de Lorraine, co-directeur de thèse**

EA 3452 CITHEFOR "Cibles thérapeutiques, formulation et expertise préclinique du médicament", Campus Brabois Santé 9, avenue de la Forêt de Haye - BP 20199
54505 Vandoeuvre Les Nancy Cedex

Acknowledgements

The completion of my PhD thesis would not have been possible without the support of many people whom I wish to thank for their contributions and diligent efforts.

I would like to express my sincerely thanks to Pr. Ponchel (Université Paris-Sud), Pr. Demougeot (Université de Franche-Comté), Dr. Elhabiri (DR-CNRS, Université de Strasbourg) and Dr. Boura (MCU, Université de Lorraine) for accepting to be my reviewers of this work. To Pr. Ponchel and Dr. Boura, thank you for their participation in this thesis committee and valuable comments which have enriched this work.

I would like to express my deepest and sincere gratitude to my supervisors: Caroline Gaucher and Marianne Parent, who supported me during the all the research and writing of this thesis. Caroline had a large impact on my work by sharing her insight and experience. I deeply appreciate her smart mind and efficient work capacity. Her bright ideas and optimism on work always inspired me. I learned a lot from Marianne about Pharmaceutics. She let me know the importance of standardization and details in experiments. She always spends her time listening to all the developments in my work and providing help and support every step of the way. I am lucky to have these two supervisors and friends: not only guided me in the thesis, but also helped me make my casual life easier in France.

I gratefully acknowledge Pr. Hu (my supervisor during master study in Wuhan University), Pr. Maincent (Université de lorraine) and Pr. Leroy (Université de lorraine). They provided me this precious opportunity to start my PhD here. Pr. Hu taught me a lot about basic experiment knowledge during the three years of master study in Wuhan. Pr. Maincent gave me a lot of useful suggestions of the formulation part and Pr. Leroy let me know the importance of serous and detailed attitude in the experiments.

I would like to express my thanks to Ariane Boudier (leader of EA3452), Anne Sapin-Minet and Igor Clarot for their supporting and advices during the experiments and life. Their smile and words always comfort and inspire me especially during the discussion.

I would like to express my gratitude to Isabelle Lartaud, Isabelle Fries and Caroline Perrin-Sarrado for their help and contributions about the work during pharmacological evaluations.

My grateful words should go to Philippe Giummelly. for his help on GSNO preparation, apparatus validation as well as the operation teaching on different apparatus.

I also need to express truthful gratitude to Arnaud, Romain, Justine, Jordan and Margaux… for their help and suggestions during the cooperation and daily experiments. Special gratitude is sent to Hui and Haiyan, who accompanied and help me from my master study to PhD work.

I also own my sincere gratitude to Pascale, Nathalie and all my colleges for their help at any time for any cases.

At last, the deepest thanks and heartfelt goes to my parents in China, who have always supported me about every decision, that motivated me to keep going.

Table of contents

Scientific works

Publications

(1) *Bonetti, J. & *****Zhou, Y., Parent, M., Clarot, I., Yu, H., Fries-Raeth, I., Leroy, P., Lartaud, I. & Gaucher, C. (2018). Intestinal absorption of S-nitrosothiols: Permeability and transport mechanisms. Biochemical pharmacology (IF = 4.8), 155, 21-31. *** equal contribution**

(2) Sahyoun, T., Gaucher, C., Zhou, Y., Ouaini, N., Schneider, R., & Arrault, A. (2018). Synthesis of novel mono and bis nitric oxide donors with high cytocompatibility and release activity. Bioorganic & medicinal chemistry letters (IF = 2.53), 28(20), 3329-3332

(3) *Perrin-Sarrado. C. & *****Zhou, Y., Salgues. V., Parent, M., Giummelly.P., Lartaud.I. & Gaucher, C. *S*-nitrosothiols as potential therapeutics to induce a mobilizable vascularstore of nitric oxide to counteract endothelial dysfunction (under review). Biochemical pharmacology (IF = 4.8), *** equal contribution**

(4) Zhou, Y., Gaucher, C., Fries-Raeth, I. Hobbekaya, M., Martin, C., Sapin-Minet, A… & Parent, M. Enhancing intestinal permeability of nitric oxide with storable microparticles for *S-nitro*soglutathione oral delivery (submitted) Journal: *International Journal of Pharmaceutics* (IF = 4.2).

Oral presentations (international congress)

(1) Zhou, Y., Gaucher, C., Fries-Raeth, I. & Parent, M. Nano or micro: 3 different particles to deliver and protect *S*-nitrosoglutathione for oral route administration: COST meeting, 25th to 27th March 2019 in Luxemburg. (published in Proceedings)

(2) Parent, M., Zhou, Y., Bonetti, J., Perrin-Sarrado, C., Lartaud, I., Sapin-Minet, A. & Gaucher, C. Antioxidant properties of *S*-nitrosoglutathione and

nanotechnologies: COST meeting, 25th to 27th March 2019 in Luxemburg. (published in Proceedings)

(3) Zhou, Y., Gaucher, C., Fries-Raeth, I., Hobbekaya, M-A., Martin, C. & Parent, M. Nano- versus micro-particles for *S*-nitrosoglutathione formulation: PDDS meeting, 24th to 26th June 2019 in Marne-La-Vallée, France.

Poster communications

(1) Zhou, Y., Gaucher, C., Parent, M. :Système d'administration orale de *S*-nitrosoglutathion pour les maladies cardiovasculaires. DocLor – Doctorial de Lorraine 2018, April 16th to 20th, 2018 in La Bolle Saint-Dié (France)

(2) Zhou, Y., Gaucher, C., Fries-Raeth, I., Hobbekaya, M-A., Martin, C. & Parent, M: Nano- versus Micro-particles for *S*-nitrosoglutathione formulation. Formulation Days 2019, January 10th to 11th, 2019 in Lyon (France).

List of tables, figures and abbreviations

Tables

Introduction

Article 2

Figures

Introduction

Article 1:

Article 2:

Article 3:

Abbreviations

Abbreviations	Full names
BCS	Biopharmaceutical Classification System
BSA	Bovine serum albumin
cGMP	Cyclic guanosine monophosphate
CYP450	Cytochrome P-450 system
CVD	Cardiovascular diseases
CBR1 or CR1	Carbonyl reductase
CysNO	*S*-nitrosocysteine
DAN	2,3-Diaminonaphthalene
DNIC	Dinitrosyl iron complexes
EDRF	Endothelium-derived relaxing factor
EDTA	Ethylene diaminotetraacetic acid
eNOS	Endothelial nitric oxide synthase
GGT	*γ*-glutamyltransferase
GSH	Reduced glutathione
GSNO	*S*-nitrosoglutathione
GSNO-NP	GSNO-loaded nanoparticles
GSNO-aNCP	GSNO-loaded alginate nanocompsite particles
GSNO-cNCP	GSNO-loaded chitosan nanocompsite particles
GSNO-acNCP	GSNO-loaded chitosan nanocompsite particles
GSNOR	GSNO reductase
GSSG	Glutathione disulphide
GTP	Guanosine-5’-triphosphate
Hb	Hemoglobin

Hb-α	Hemoglobin-α
HBSS	Hank's Balanced Salt Solution
HPMC	Hydroxypropyl methylcellulose
IBD	Inflammatory bowel diseases
iNOS	Inducible NO synthase
IV	Intravenous
L-Arg	L-arginine
log P	Logarithmic value of partition coefficient
MTT	3(4,5-Dimethylthiazol-2-yl)-2,5-diphenyltetrazolium bromide
NAC	*N*-acetyl-*L*-cysteine
NACNO	*S*-nitroso-*N*-acetyl-*L*-cysteine
NADPH	Dihydronicotinamide-adenine dinucleotide phosphate
NHA	*N*-hydroxy-L-arginine
nNOS	Neuronal NO synthase
NOS	Nitric oxide synthase
NOx species	Nitrogen oxide related species
P_{app}	Apparent permeability coefficient
PCL	Poly(ε-caprolactone)
PDI	Protein disulfide isomerase
PEG	Poly(ethylene glycol)
PKG	Protein kinase G
pKa	Negative logarithmic value of acid ionisation constant
PLGA	Poly(lactide-co-glycolide)
PVAT	Perivascular adipose tissue
PVA	Poly(vinyl alcohol)

PVP	Poly(vinyl pyrrolidone)
RSNOs	*S*-nitrosothiols
SDS	Sodium dodecyl sulfate
sGC	Soluble guanylate cyclase
SMCs	Smooth muscle cells
SNAP	*S*-nitroso-*N*-acetyl-*D*-penicillamine
SNP	Sodium nitroprusside
S/O/W	Solid-in-oil-in-water
Trx	Thioredoxin
TrxR	Thioredoxin reductase
VSMCs	Vascular smooth muscle cells
TEER	Transepithelial electrical resistance
W/O/W	Water-in-oil-in-water

Aperçu de la thèse

Le monoxyde d'azote (NO) est un gaz radicalaire impliqué dans la signalisation des systèmes cardiovasculaires, immunitaires et nerveux. Au sein du système cardiovasculaire, la première cible de NO est la guanylate cyclase soluble (GCs) dont l'activation permet la synthèse de GMPc, un second messager médiant la relaxation vasculaire. Ceci constitue la voie de signalisation NO/GCs/GMPc. Cependant, le mécanisme d'action de NO emprunte également des voies de signalisation indépendantes de la voie NO/GCs/GMPc, comme la *S*-nitrosation. La *S*-nitrosation correspond à la formation d'un lien covalent entre la fonction thiol d'un résidu cystéine et NO. Elle est considérée comme une modification post-traductionnelle des protéines, aussi importante que la phosphorylation pour la modulation des activité/expression protéiques. La *S*-nitrosation forme des *S*-nitrosothiols comme les *S*-nitrosoprotéines, *S*-nitrosopeptides ou *S*-nitrosoacides aminés. En plus de moduler les voies de signalisation, ces *S*-nitrosothiols représentent également une forme de stockage et de transport de NO dont la demi-vie à l'état radicalaire n'est que de quelques secondes. Ainsi, à l'état radicalaire, le rayon d'action de NO ne peut dépasser quelques micromètres. Ces *S*-nitrosothiols sont depuis quelques années considérés comme des candidats médicaments. IIs constituent en effet des prodrogues de NO, dont la biodisponibilité est considérablement diminuée au cours des pathologies cardiovasculaires. Les donneurs de NO comme les dérivés nitrés sont utilisés depuis de nombreuses années dans le traitement de l'angor dans le cadre de sa prévention et en cas de crise. Cependant, les dérivés nitrés sont sujets au phénomène de tolérance (perte d'effet thérapeutique lors d'administration chronique), présentent une faible biodisponibilité et une faible sélectivité. Ils sont également responsables de l'amplification du stress oxydant déjà installé au cours des pathologies cardiovasculaires.

Ainsi, d'autres molécules donneuses de NO sont actuellement à l'étude. Parmi celles-ci nous nous sommes d'abord intéressés aux amidoximes. La fonction amidoxime est physiologiquement produite lors de la synthèse de NO catalysée par les NO synthases. En effet, au cours de cette catalyse en deux étapes, l'arginine est d'abord *N*-hydroxylée en *N*-hydroxyarginine présentant une fonction amidoxime. Cette fonction amidoxime est capable de libérer NO sous l'action oxydative des cytochromes

P450. Les résultats de l'étude de nouvelles molécules synthétiques, mono ou bis-amidoxime, sont présentés dans l'article 1.

Article 1: Synthesis of Novel Mono and Bis Nitric Oxide Donors with High Cytocompatibility and Release Activity

Tanya Sahyoun, Caroline Gaucher, Yi Zhou, Naïm Ouaini, Raphaël Schneider, Axelle Arrault.

Quatre composés comportant une ou deux fonctions amidoximes ont été synthétisés : (1) Le composé **2a-b** contenant une fonction amidoxime aromatique, (2) le composé **2c** présentant une fonction amidoxime aliphatique, et (3) le composé **2d** présentant deux fonctions amidoxime, une aromatique et une autre aliphatique. La capacité de ces composés à libérer du monoxyde d'azote (NO) a été évaluée *in vitro* en tirant partie du métabolisme oxydant de cytochromes P450 de microsomes de foie de rats. Les résultats obtenus démontrent que toutes les fonctions amidoxime des composés synthétisés sont capables de libérer NO, avec une plus grande capacité pour le composé **2a** qui possède une fonction amidoxime aromatique. De plus, toutes les amidoximes testées sont cytocompatibles vis-à-vis de cellules musculaires lisses humaines. En utilisant la formation de *S*-nitrosothiols intracellulaires comme marqueur de la biodisponibilité de NO, les composés **2a et 2c** ont montré leur capacité à délivrer une plus grande quantité de NO que la molécule de référence (4-chlorobenzamidoxime). Ainsi, les amidoximes sont capables de traverser la membrane cellulaire pour être ensuite oxydées par les CYP450 des cellules musculaires lisses. En revanche, la bis-amidoxime aromatique/aliphatique **2d** est de grand intérêt car sa capacité à délivrer NO et par la suite à augmenter le stockage de NO dans les cellules *via* la formation de *S*-nitrosothiols intracellulaires est similaire aux amidoximes **2a** et **2b**. En effet, en considérant que la bis-amidoxime **2d** a été étudiée à une concentration deux fois plus faible que celle des composés **2a** et **2b**, nous pouvons conclure que le composé **2d** est la molécule la plus performante de tous les composés donneurs de NO testés ici.

D’autres donneurs de NO dérivant des *S*-nitrosothiols, formes physiologiques de transport et de stockage de NO, sont également à l’étude. Parmi ces *S*-nitrosothiols, nous pouvons citer le *S*-nitrosoglutathion (GSNO), la *S*-nitroso-*N*-acétyl-*L*-cystéine (NACNO) et le *S*-nitroso-*N*-acétyl-pénicillamine (SNAP). Les *S*-nitrosothiols sont considérés comme des candidats médicaments d’avenir, puisqu’ils ne présentent pas les effets indésirables de dérivés nitrés précédemment énumérés. Les RSNO sont dénués de toxicité aigüe, et de par l’existence physiologique de certains d’entre eux, ils ne présentent probablement aucun risque dans le cadre d’application répétée. Ceci est d’autant plus important que les pathologies cardiovasculaires sont, pour la plupart, des affections chroniques nécessitant un traitement sur le long terme. Dans ce contexte, la voie d’administration orale de ces molécules est la plus indiquée du point de vue des patients (facilité, faible contrainte conduisant à une meilleure observance). De plus, la voie orale présente des avantages physiologiques comme une grande surface d’absorption (300 à 400 m^2). Néanmoins, la barrière intestinale constitue un obstacle important à franchir pour ces molécules de nature peptidique ou protéique, avec une liaison nitrosothiol fragile. Ainsi, une deuxième étude a été menée sur les mécanismes d’absorption intestinale des *S*-nitrosothiols (Article 2).

Article 2: Intestinal absorption of *S*-nitrosothiols: permeability and transport mechanisms

Absorption intestinale des *S*-nitrosothiols : Mécanismes de transport et de perméabilité

Justine Bonetti[#], Yi Zhou[#], Marianne Parent, Igor Clarot, Haiyan Yu, Isabelle Fries-Raeth, Pierre Leroy, Isabelle Lartaud, Caroline Gaucher*

[#] **Les deux auteurs ont contribué à parts égales à ce travail.**

Au cours du vieillissement ou du développement des pathologies cardiovasculaires, une diminution de la biodisponibilité du monoxyde d'azote (NO) est observée. Afin de restaurer une concentration physiologique de NO, les *S*-nitrosothiols (RSNO) font partie des donneurs de NO envisagés comme principes actifs potentiels. Les RSNO sont la forme physiologique de stockage et de transport de NO dans l'organisme, lui assurant ainsi une demi-vie supérieure à sa forme libre radicalaire (< 0,5 s). La plupart des pathologies cardiovasculaires nécessitent un traitement chronique pour lequel la voie orale est plébiscitée. Cependant, l'absorption intestinale des RSNO, première limite à leur biodisponibilité vasculaire, n'a jamais été étudiée. Ainsi, à l'aide d'un modèle *in vitro* de barrière intestinale (Caco-2), cette étude vise à élucider les mécanismes de perméabilité intestinale (passifs ou actifs, voie paracellulaire ou transcellulaire) et à prédire le site d'absorption intestinale préférentiel des RSNO. Dans notre étude, trois RSNO, le *S*-nitrosoglutathion (GSNO), la *S*-nitroso-*N*-acétylcystéine (NACNO), la *S*-nitroso-*N*-acétyl-*D*-pénicillamine (SNAP), qui diffèrent de par le squelette transportant NO, ont été évalués. Ces squelettes transporteurs de NO confèrent des propriétés physico-chimiques (lipophilie) et des activités biologiques (antioxydantes et/ou anti-inflammatoires) différentes aux RSNO. Ainsi, en montrant à l'aide de ce modèle la perméabilité apparente moyenne des RSNO, associée à leur forte solubilité, cette étude a permis de placer ces molécules entre la classe I et la classe III du Système de Classification Biopharmaceutique. L'évaluation bidirectionnelle de la perméabilité a également solutionné le mécanisme de perméabilité de RSNO selon un phénomène passif. De plus, GSNO et NACNO suivent préférentiellement la voie transcellulaire alors que SNAP préfère la voie paracellulaire. Finalement, le squelette transportant NO a une influence sur le site d'absorption des RSNO, puisque la perméabilité de NACNO est favorisée à pH 6,4, pH proche de la partie proximale du jéjunum, alors que celles de GSNO et SNAP sont meilleures à pH

7,4, pH proche de sa partie distale. Au travers de cet article, nous avons déterminé les mécanismes de perméabilité intestinale des RSNO et prouvé que leur administration par voie orale était possible. Après avoir franchi la barrière intestinale, les *S*-nitrosothiols rejoignent le compartiment vasculaire où ils joueront leurs rôles de transporteurs puis de donneurs de NO pour restaurer le pool vasculaire de NO. Ce pool se retrouve ainsi sous deux formes, une forme circulante dans le flux sanguin et une forme tissulaire stockée dans la paroi vasculaire. Ainsi, la prochaine étape de cette étude a consisté à comparer la capacité des différents *S*-nitrosothiols à promouvoir la formation d'un stock au sein de la paroi aortique et de vérifier si ce stock est mobilisable pour la vasodilation, faisant preuve de sa biodisponibilité. Enfin, les propriétés protectrices des fonctions endothéliales des *S*-nitrosothiols ont été évaluées sur des aortes dénuées d'endothélium (Article 3).

Article 3: *S*-nitrosothiols as potential therapeutics to induce a mobilizable vascular store of nitric oxide to counteract endothelial dysfunction.
Les S-nitrosothiols : de potentiels médicaments induisant la formation d'un stock mobilisable de monoxyde d'azote au sein des vaisseaux afin de contrer la dysfonction endothéliale.

Caroline Perrin-Sarrado[#], Yi Zhou[#], Valérie Salgues, Marianne Parent, Philippe Giummelly, Isabelle Lartaud, Caroline Gaucher*

[#] **Les deux auteurs ont contribué à parts égales à ce travail.**

Article soumis au journal *Biochemical Pharmacology* le 28 juin 2019, en révision

La dysfonction endothéliale prédispose au développement de certaines pathologies cardiovasculaires. Elle est définie comme un déséquilibre entre la production de substances vasodilatatrices comme le monoxyde d'azote (NO) et de substances vasoconstrictrices. Afin d'assurer ses fonctions physiologiques, NO, un radical gazeux à demi-vie très courte, a besoin d'être stocké et transporté jusqu'à son site d'action. Les *S*-nitrosothiols (RSNO) comme le *S*-nitrosoglutathion (GSNO) représentent la principale forme physiologique de stockage de NO au sein du système vasculaire. Le stock de NO formé par les RSNO reste alors biodisponible pour déclencher la vasorelaxation. Ainsi, les RSNO représentent une classe émergente de donneurs de NO pour restaurer la biodisponibilité de NO au cours des troubles cardiovasculaires.
Le but de cette étude est de comparer la capacité des *S*-nitrosothiols à produire un stock vasculaire de NO au sein d'artères dont l'endothélium est intact ou d'artères dont l'endothélium a été retiré. Un RSNO physiologique, le GSNO, ainsi que deux RSNO synthétiques, la *S*-nitroso-*N*-acétylcystéine (NACNO) et la *S*-nitroso-*N*-acétylpénicillamine (SNAP) ont été testés, permettant ainsi d'évaluer le potentiel thérapeutique des RSNO pour compenser la dysfonction endothéliale. Le nitroprussiate de sodium (SNP), un médicament bénéficiant déjà d'une autorisation de mise sur le marché, a été utilisé comme donneur de NO contrôle non RSNO. Les deux types d'artères (avec ou sans endothélium) utilisées dans cette étude ont été isolées de rats Wistar mâles normotendus et exposées aux donneurs de NO. Ensuite, les espèces dérivées de NO (NOx) représentant le stock intravasculaire de NO, ont été quantifiées en utilisant la sonde diaminonaphthalène couplée aux ions mercuriques. La biodisponibilité du stock de NO et sa capacité à produire la vasorelaxation ont été

testés à l'aide de la *N*-acétylcystéine. Ensuite la capacité de ce stock à s'opposer à la vasoconstriction produite par la phényléphrine (PHE) a été appréciée.

Tous les RSNO étudiés ont été capables de générer un stock de NO trois à cinq fois supérieur à la quantité basale de NOx au sein des artères contrôle. NACNO était le plus performant de tous les RSNO pour produire un stock vasculaire biodisponible pour la vasorelaxation et pour induire une hyporéactivité à la PHE des artères sans endothélium. L'efficacité de GSNO et SNAP était équivalente, et supérieure à celle de SNP. Au sein des artères avec endothélium, le stock de NO s'est également formé, cependant il s'est avéré moins disponible pour la vasorelaxation et n'a pas influencé la vasoconstriction induite par la PHE.

En conclusion, les RSNO, et NACNO plus particulièrement, sont capable de restaurer la biodisponibilité de NO en créant un stock fonctionnel de NO au sein de la paroi des vaisseaux sanguins et de façon plus marquée quand l'endothélium est absent. Ce phénomène a été associé à une hyporéactivité de l'artère à un agent vasoconstricteur comme la PHE. Des traitements à base de RSNO pourraient donc présenter un bénéfice pour restaurer les fonctions NO-dépendantes dans des états pathologiques associés à un endothélium lésé.

Ainsi, toutes ces études mettent en évidence que NACNO est le S-nitrosothiol qui franchit le mieux la barrière intestinale et qui produit le stock de NO vasculaire le plus grand et le plus biodisponible.

Dans la dernière partie de ce travail, nous nous sommes intéressés au développement de formulations particulaires adaptées à la voie orale et permettant d'augmenter la biodisponibilité des S-nitrosothiols. Malgré la supériorité de NACNO dans les études précédentes, c'est le GSNO qui a été utilisé pour cette étude. En effet, il présente certains avantages. D'une part, il est physiologique (contrairement à NACNO) et a été utilisé dans la majorité des essais cliniques. D'autre part, seul GSNO peut être obtenu sous la forme d'un produit à la fois pur et solide (ce qui permet plus de libertés dans la formulation).

En ce qui concerne le procédé de formulation galénique, il doit être adapté à ces molécules particulièrement fragiles et hydrophiles, tout en respectant le cahier des charges pour la voie orale : polymère adapté, charge en principe actif suffisante, libération appropriée, stabilité des caractéristiques des particules obtenues pour faciliter leur utilisation, amélioration de la perméabilité intestinale sans cytotoxicité…

Dans ce contexte, trois stratégies de formulation de GSNO basées sur des procédés de double émulsion/évaporation de solvant ont été comparées (Article 4).

Article 4: Enhancing intestinal permeability of nitric oxide with storable microparticles for *S*-nitrosoglutathione oral delivery.

Des microparticules préparables à l'avance pour la délivrance de *S*-nitroglutathion par voie orale et capables d'augmenter la perméabilité intestinale du monoxyde d'azote

Yi Zhou, Caroline Gaucher, Isabelle Fries, Mehmet Hobekkaya, Charlène Martin, Clément Leonard, Frantz Deschamps, Anne Sapin-Minet, Marianne Parent*

Article soumis au journal *International Journal of Pharmaceutics* le 21 août 2019

Trois sortes de particules encapsulant du *S*-nitrosoglutathion (GSNO), un donneur physiologique de monoxyde d'azote, ont été préparées à partir des mêmes matériaux mais avec des procédés modifiés de double émulsion/évaporation de solvant : eau dans huile dans eau (E/H/E) ou solide dans huile dans eau (S/H/E). Les nano- et micro-particules obtenues par la méthode E/H/E ont été comparées aux microparticules obtenues par la méthode S/H/E en ce qui concerne leur taille, leur capacité à encapsuler le GSNO et à le libérer *in vitro*. La cytocompatibilité des particules vis-à-vis des cellules intestinales ainsi que leur capacité à améliorer la perméabilité intestinale du GSNO *in vitro* (modèle de barrière intestinale constituée par les cellules Caco-2 différenciées) ont été évaluées.

L'efficacité d'encapsulation du GSNO est la même (environ 30 %) pour les trois sortes de particules mais les microparticules (S/H/E > E/H/E) présentent un profil de libération plus lent du GSNO *in vitro* et améliorent significativement la perméabilité intestinale de GSNO. Cette perméabilité apparente élevée lorsqu'il est encapsulé dans les microparticules, associée à une solubilité élevée, fait passer GSNO en classe III de la classification biopharmaceutique.

La réduction de la taille des grains de GSNO (de 40 µm à moins de 10 µm) initiée en collaboration avec la société StaniPharm devrait, d'après la littérature, conduire à une meilleure encapsulation et à une libération prolongée de GSNO avec les microparticules S/H/E. Cependant, les premiers essais en fluide supercritique présentés dans cet article n'ont pas été concluants, à cause de la grande fragilité et de l'hydrophilie du GSNO.

Par ailleurs, les paramètres critiques des particules (taille et contenu en GSNO) sont maintenus jusqu'à 1 mois après lyophilisation et stockage à 4°C pour les microparticules et jusqu'à 3 mois pour les nanoparticules. Les suspensions fraîches

de particules n’étant stables qu’une journée, cette stabilisation représente une avancée majeure, car elle permettra d’optimiser les campagnes de préparation des particules et de les envoyer éventuellement vers d’autres laboratoires pour la réalisation de tests précliniques. Les particules chargées en GSNO développées pourraient ainsi représenter une nouvelle opportunité thérapeutique pour un traitement chronique, par voie orale, des pathologies associées avec un déficit en monoxyde d’azote

Pour conclure, les objectifs de ce travail étaient de mettre en évidence les mécanismes de la perméabilité intestinale de différents *S*-nitrosothiols et leur capacité à former un stock de NO mobilisable dans la paroi vasculaire, ainsi que de développer des formulations adaptées pour le traitement oral des maladies cardiovasculaires. Nous avons démontré : 1) que les trois RSNO étudiés peuvent être administrés par voie orale (avec une perméabilité intestinale moyenne) ; 2) qu'ils peuvent tous trois former un stock vasculaire de NO mobilisable pour une vasorelaxation ou pour induire une hyporéactivité à un agent vasoconstricteur. Tout ceci dans le cadre d'un endothélium lésé, ce qui est prometteur dans le contexte des maladies cardiovasculaires, souvent liées à une dysfonction endothéliale ; et 3) qu'il est possible d'augmenter significativement la perméabilité intestinale du GSNO grâce à des formulations, en particulier les microparticules obtenues par la méthode d'émulsion solide-huile-eau.

Ce travail ouvre de nombreuses perspectives à la fois pharmacologiques et galéniques. Par exemple, une localisation plus fine du stock vasculaire de NO ainsi qu'une identification des protéines nitrosées (par une technique de biotin-switch associée à la spectrométrie de masse, déjà développée dans l'équipe) pourrait être entreprise afin de mettre au jour de nouvelles cibles de NO. Idéalement, les méthodes analytiques devraient également permettre de réaliser une pharmacocinétique complète des RSNO administrés (libres ou formulés). En ce qui concerne la formulation, de nombreuses optimisations pourraient être recherchées (meilleure encapsulation, libération plus longue, encapsulation d'autres donneurs de NO – RSNO, amidoximes, ou autres-, co-encapsulation de différents principes actifs, modification des polymères par exemple avec des groupements donneurs de NO, …). Cependant, les formulations développées dans ce travail pourraient d'ores et déjà être administrées chez l'animal sain, pour vérifier la formation du stock vasculaire de NO, ou dans des modèles pathologiques (athérosclérose ou accident vasculaire cérébral, par exemple).

Chapter 1. Introduction

1.1 Nitric oxide

Nitric oxide (NO) is a gaseous radical, whose biosynthesis and cellular signaling mechanisms were discovered in the 1980's[1–4]. As one of the most important signaling molecule, NO is involved in different organs and systems (such as cardiovascular system[5,6], immune system[2,3] and nervous system[7]) where it is responsible for modulating various effects[8,9] (Figure 1). Among others, NO can be regarded as a potent vasodilator, a regulator of platelet adhesion, a neurotransmitter, an antimicrobial agent, a tumor mediator and an angiogenesis promoter[10,11]. Thus, researchers from different disciplines have proposed NO as a potential therapeutic.

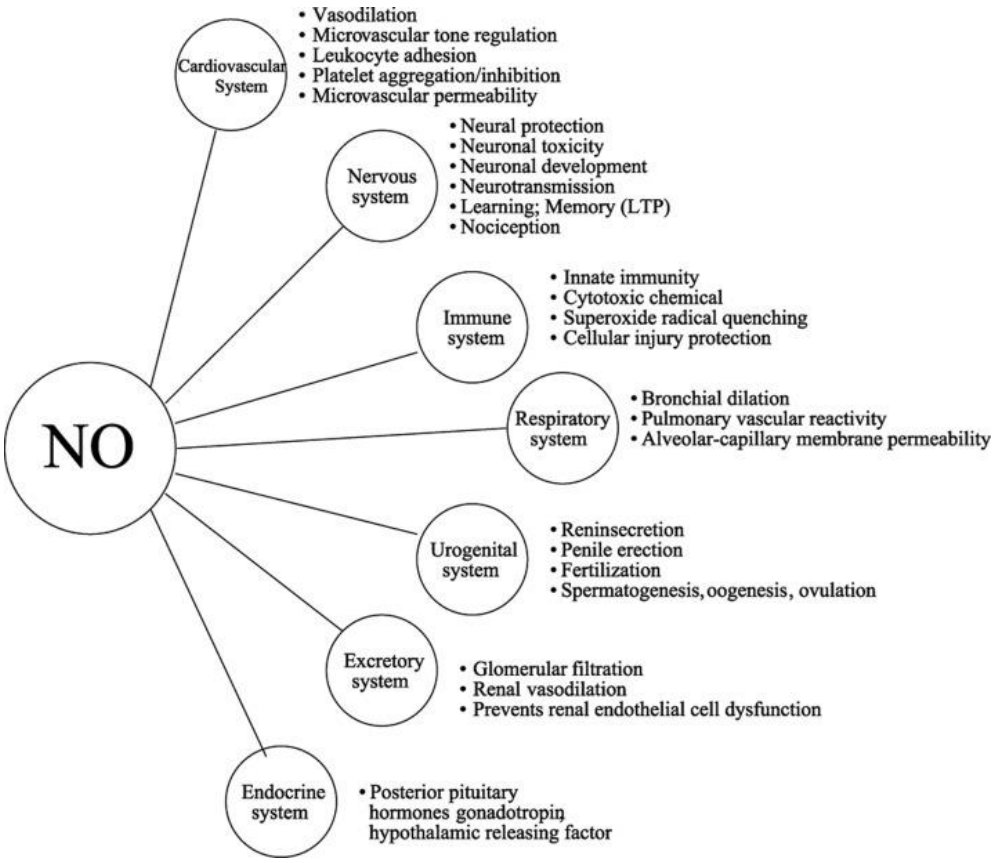

Figure 1. An overview of nitric oxide (NO) physiological activities in various systems[10].

As an important second messenger, NO is synthesized by three different isoforms of nitric oxide synthases (NOS): neuronal NOS (nNOS), inducible NOS (iNOS), and endothelial NOS (eNOS)[12]. nNOS was first discovered in neuronal tissue and eNOS in vascular endothelial cells. iNOS is the inducible isoform found in a wide range of tissues and cells. NO is constitutively generated by nNOS or eNOS at relatively small

concentration (10 nM) for signaling. However, NO synthesized by the inducible isoform (iNOS), works as a response to inflammation, leading to high (more than 1 µM) and cytotoxic local concentrations of NO[12,13]. These three NOSs isoforms catalyze the synthesis of NO through a two-step reaction starting from L-arginine (L-Arg) transformed in an amidoxime intermediate, the *N*-hydroxy-L-arginine (NHA) to finally form L-citrulline and NO[14] (Figure 2).

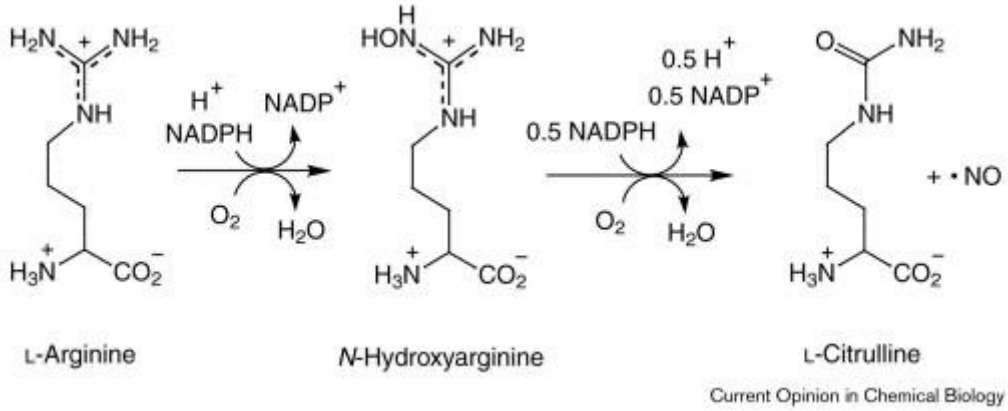

Figure 2. The synthesis of nitric oxide by nitric oxide synthases[12].

1.2 Nitric oxide and cardiovascular diseases (CVD)

1.2.1 Nitric oxide in the cardiovascular system

In cardiovascular system[15–17], eNOS is mainly expressed in endothelial cells but also in platelets, cardiac myocytes and smooth muscle cells (SMCs); nNOS is basically expressed in the sarcoplasmic reticulum from cardiac myocytes, in autonomic cardiac neurons as well as ganglia or within vascular smooth muscle cells (VSMCs) (Figure 3). However, only under oxidative or pro-inflammatory conditions, iNOS will be expressed in a large range of cells such as endothelial cells, cardiac myocytes, nerve cells, VSMCs, leukocytes and fibroblasts. NO regulates cardiovascular system *via* two distinct pathways: one is the activation of the soluble guanylate cyclase (sGC) followed with the downstream stimulation of Protein Kinase G (PKG), and one direct pathway through proteins *S*-nitrosation (the binding of a NO moiety on a thiol group from a cysteine residue to form an RSNO).

In vessels, NO synthesized by eNOS triggers the relaxation of VSMCs as well as inhibits their proliferation[17,18]. After its diffusion to the vessel lumen, it also mediates

angiogenesis and inhibits platelet aggregation and thrombosis.

In erythrocytes, NO reacts with the Fe^{2+} heme of oxyhemoglobin and produce nitrate ions. Then, the nitrate reductase existing in mammalian tissues reduces nitrate ions (NO_3^-) to nitrite ions (NO_2^-). In fact, deoxygenated hemoglobin has a nitrite reductase activity, which reduces NO_2^- to NO in hypoxic and acidic environments. In addition, reversible *S*-nitrosation of the Cys 93 of hemoglobin might transport NO for its subsequent release in hypoxic tissues. The reduction of NO_2^- and/or *S*-nitrosation of hemoglobin promotes NO release followed by-immediate relaxation of hypoxic tissues[19]. The diffusion and bioavailability of NO in VSMCs are regulated by hemoglobin-α (Hb-α) at the myoendothelial junction and by cytoglobin in muscle cells. In addition, NO synthesized through nNOS in the VSMCs also help to regulate the vascular tone[20–22].

In cardiac myocytes, the main roles of NO are the regulation of cardiac contractility through the modulation of the excitation–contraction coupling, relaxation, and mitochondrial respiration. In addition, the action of nNOS expressed in cardiac nerves and postsynaptic eNOS can reinforce the parasympathetic (vagal) transmission through modulating the sympathetic–parasympathetic balance, which finally reduces the heart rate[18].

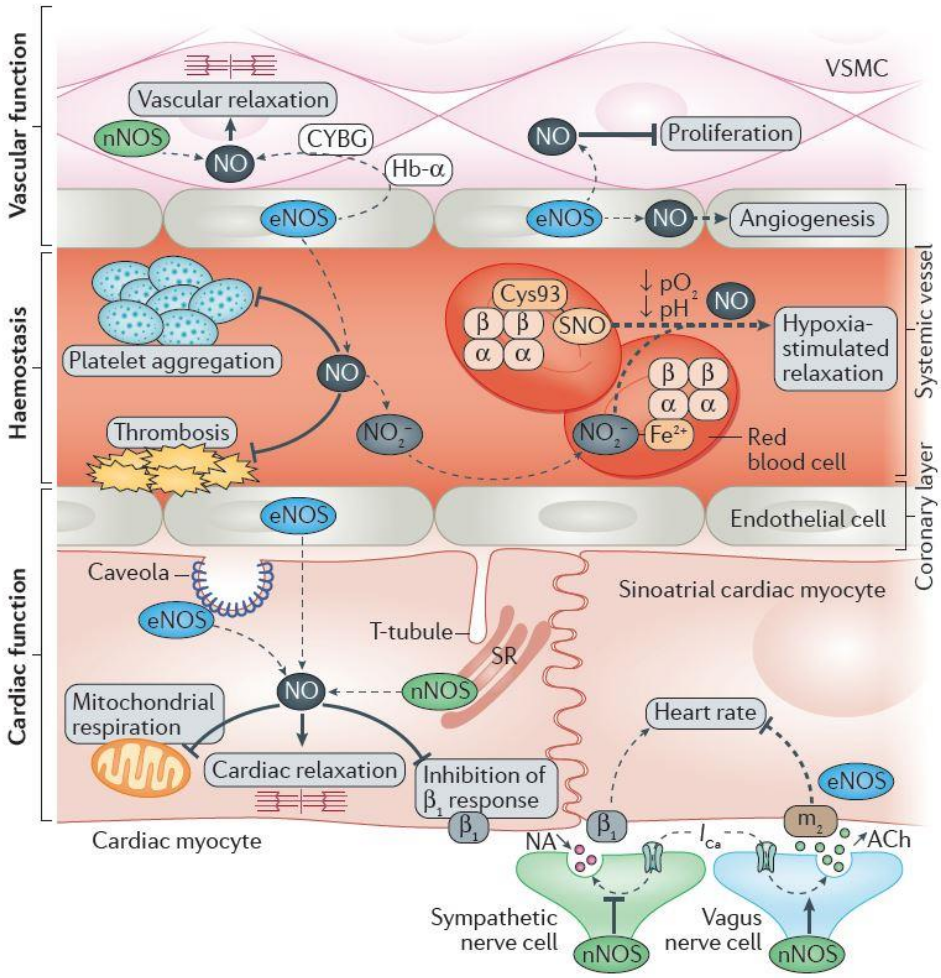

Figure 3. NO in the cardiovascular system[15]. NO, nitric oxide; eNOS, endothelial nitric oxide synthase; VSMC, vascular smooth muscle cell; NO_2^-, nitrite ions; Hb-α, haemoglobin-α; CYGB, cytoglobin; nNOS, neuronal nitric oxide synthase; β1, adrenergic receptor β1; ACh, acetylcholine; m2, muscarinic acetylcholine receptor m2; NA, noradrenaline; SNO, *S*-nitrosothiol; SR, sarcoplasmic reticulum; T-tubule, transverse-tubule.

1.2.2 NO signaling in vascular beds in health and disease.

Under physiological conditions (Figure 4a), NO synthesized by eNOS inhibits platelet aggregation and thrombosis. Basically, NO activates soluble guanylate cyclase in VSMCs by coordination to the ferrous prosthetic of the heme moiety (which is nitrosylation) which converts the guanosine-5'-triphosphate (GTP) to cyclic guanosine monophosphate (cGMP). Then, the PKG will be activated in the SMCs. Both cGMP and PKG lowered the intracellular Ca^{2+} levels through stimulating its reuptake by sarcoplasmic/ endoplasmic reticulum calcium-ATPase and its extrusion through the

plasma membrane calcium-transporting ATPase[15]. In addition, the efflux of K^+ will also be triggered by PKG through the large-conductance Ca^{2+}-sensitive potassium channel, which will hyperpolarize the cell and reduce Ca^{2+} entry through the L-type calcium channel. At last, PKG promotes the dephosphorylation of the myosin light chain through the associated phosphatase. Together these modifications mediate vasorelaxation. Perivascular adipose tissue (PVAT) contributes to this effect under healthy conditions by releasing NO and adiponectin, which activates NO production in SMCs[15,18,21].

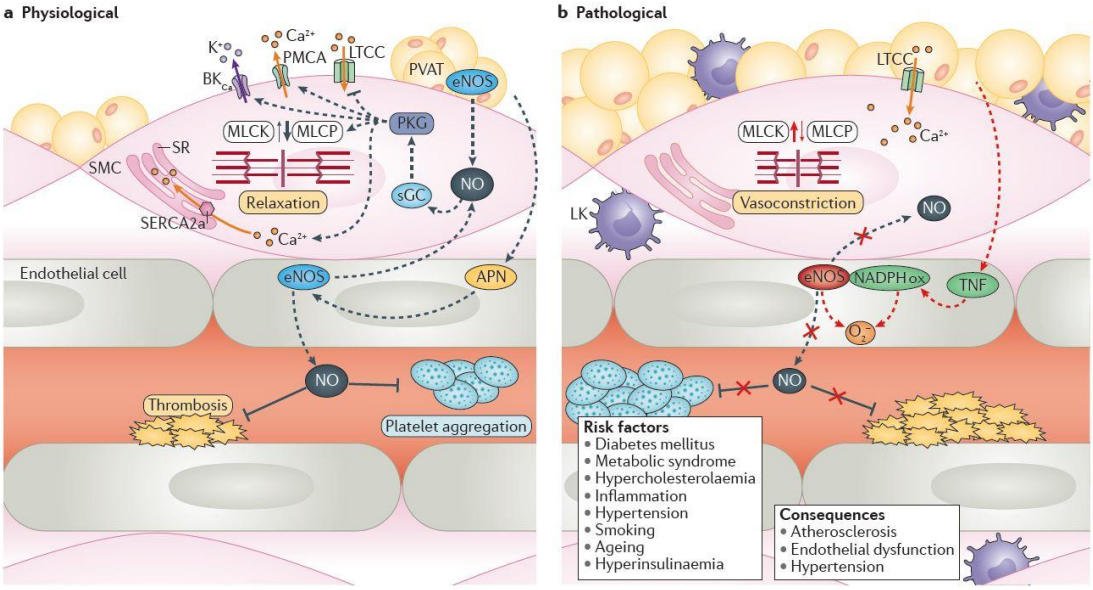

Figure 4. NO signaling in cardiovascular system under physiological (left) and pathological (right) conditions[15]. NO, nitric oxide; eNOS, endothelial nitric oxide synthase; sGC, soluble guanylate cyclase; PKG, protein kinase G; SMCs, smooth muscle cells; SERCA, sarcoplasmic/ endoplasmic reticulum calcium-ATPase; PMCA, plasma membrane calcium-transporting ATPase; BK_{Ca}, Ca^{2+}-sensitive potassium channel; LTCC, L-type calcium channel; MLCP, myosin light chain through the associated phosphatase; PVAT, Perivascular adipose tissue; APN, adiponectin; NADPH ox, NADPH oxidase; O_2^-, superoxide anion; TNF, Tumour necrosis factor; LK, leukocyte; MLCK, myosin light chain kinase; SR, sarcoplasmic reticulum.

Under pathological condition (Figure 4b)**,** NO bioavailability will be reduced by different cardiovascular risk factors through the uncoupling of eNOS and the activation of Reduced nicotinamide adenine dinucleotide phosphate (NADPH) oxidase, resulting in superoxide anion production. Reduced NO bioavailability promotes platelet aggregation, thrombosis, and vasoconstriction. Tumor necrosis factor produced from PVAT further activates NADPH oxidase. Subsequent endothelial dysfunction,

increased permeability, and leukocyte diapedesis contribute to the initiation of atherosclerosis[19]. As one of the key factors for the initiation and progress of cardiovascular diseases including atherosclerosis, heart failure, hypertension, arterial thrombotic disorders and stroke[27,28], NO deficiency may result from both endothelium dysfunction (decreased production) or NO oxidative consumption (increased metabolism)[15].

1.3 NO storage

The first target of NO is sGC, the soluble isoform of the guanylate cyclase[5]. However, it is now known that many actions of NO are in fact independent of cGMP. It has been reported that the cGMP-independent NO signaling pathways are attributed to *S*-nitrosation of structurally and functionally important cysteine residues[9]. In fact, the *S*-nitrosation process will produce different *S*-nitrosothiols (RSNOs), which are the main components of 'NO storage pool' in the body. NO synthesized from NOSs or coming from exogenous sources will be transferred into different NO storage forms like nitrite ions, RSNOs, N-nitroso proteins and other compounds like iron-nitrosyl-complexes (Figure 5). These compounds can act as NO donors or may even possess intrinsic NO-like activity[16,25].

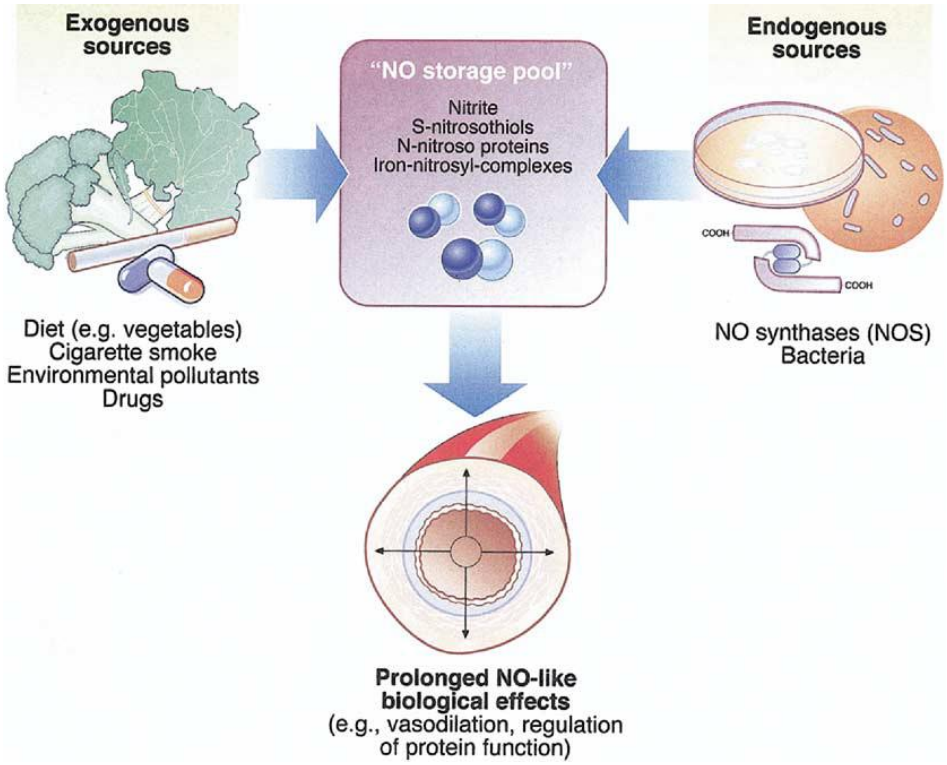

Figure 5. *S*-nitrosothiols (RSNOs) formation and degradation in the body[25].

As physiological compounds, RSNOs are generated through the *S*-nitrosation of thiols of low molecular weight (*e.g.* glutathione, cysteine) or of high molecular weight (cysteine residues of proteins like albumin, hemoglobin, …) in the body. The *S*-nitrosation reaction between NO and a thiol function is a one-electron oxidation reaction. As shown in Figure 4, the NOS activation results not only in NO production but also in NOS auto-*S*-nitrosation, followed with the transnitrosation of NO. RSNOs such as *S*-nitrosoglutathione (GSNO) or *S*-nitrosoproteins can be generated from NO through different ways: transition metal catalyzed pathway[26], thiyl radical recombination, NO oxidation or transnitrosation from other RSNOs[27,28]. Indeed, once formed, GSNO or *S*-nitrosated proteins can transfer NO to other proteins through transnitrosation reactions. RSNOs can degrade through different ways (Figure 6): for example, GSNO degrades through direct denitrosation by enzymes like GSNO reductase (GSNOR) or Carbonyl reductase (CBR1 or CR1)[27], which lead to the formation of non-bioavailable NO. Other enzymes like γ-glutamyltranspeptidase (GGT) also help the degradation of GSNO (will be discussed in the chapter about GSNO) In addition, the Thioredoxin (Trx) can denitrosate the RSNOs and regenerate through the activity of thioredoxin reductase (TrxR)[26]. The protein disulfide isomerase (PDI) also catalyzes transnitrosation and denitrosation processes through thio-disulfide exchange reactions.

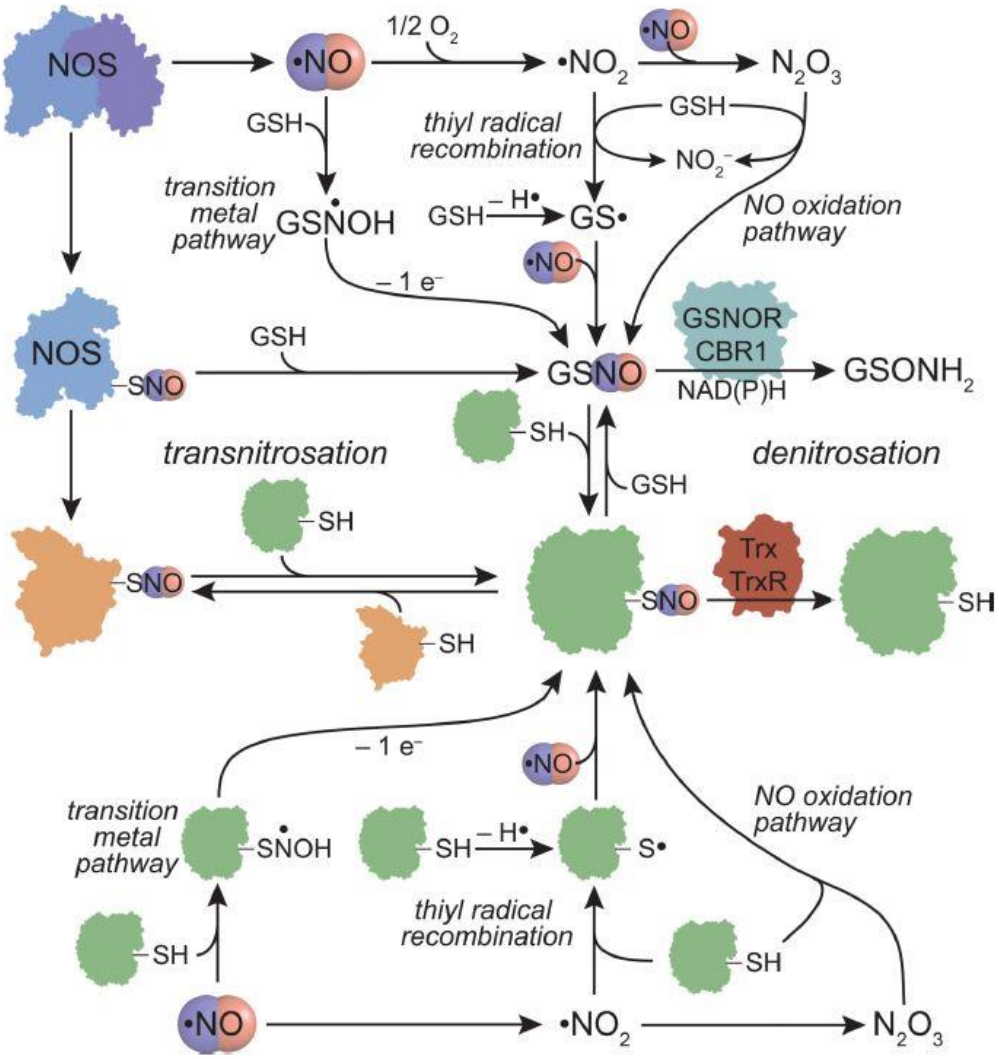

Figure 6. Potential mechanisms of *S*-nitrosothiols and *S*-nitrosoproteins formation and degradation[26]. NOS, nitric oxide synthases; GSNO, *S*-nitrosoglutathione; GSNOR, GSNO reductase; CBR1, carbonyl reductase 1; Trx, thioredoxin; TrxR, thioredoxin reductase.

1.4 Nitric oxide donors

An exogenous supply of NO is needed to restore deficient NO levels. Indeed, by applying gaseous NO directly *via* inhalation, the pulmonary hypertension was relieved without systemic vasodilation and hypotension[29]. However, this application is still limited by several shortcomings: such as, its rapid inactivation when stopping NO administration due to the short half-time of NO; complex operation conditions with high cost (specific tanks); lack of possibility to treat pathologies at distant sites (NO cannot reach more than lungs when applied through inhalation). Therefore, a lot of compounds showing the ability to release NO have been investigated for cardiovascular diseases treatment and some of them (*eg*, nitroprusside and nitroglycerin) are or even have

been used in clinic for decades[30–32]. According to different mechanism of NO formation, some of them are direct NO donors (including NO gas) whereas others require metabolism[33]. This will be discussed in the following sections. In addition, two families (related to our work) among the several new NO donors will be presented: amidoximes and RSNOs.

1.4.1 Direct Donors

Compounds, which release NO directly are pharmacological agents with either a nitroso (S-N=O) or nitrosyl (metal·NO) functional group. These direct donors can spontaneously release NOx species (nitric oxide related species: different redox forms of nitrogen monoxides produced by the donor molecule). The most common members of direct donors are NO gas, sodium nitroprusside, and sodium trioxodinitrate (Angeli's salt). NO gas is the most direct form but the complex conditions for inhalation and the short half time of NO (within second) limits its application[34]. In sodium nitroprusside (SNP), NO is coordinated to iron as a nitrosyl group (also connected to 5 nitrile ions) in a square bipyramidal complex[35]. Under physiological conditions, NO can be released spontaneously from the parent chemical structure. For decades, SNP was widely used for the acute treatment of heart failure and hypertension. However, the application of SNP was limited due to parenteral administration, tolerance and side effects (potential thiocyanate toxicity for long-time administration)[36]. Thus, SNP has been withdrawn from European market in 2017. In Angeli's salt, NO^-, a reduced form of NO, is released spontaneously under physiological conditions. Distinct from other redox forms of NO, NO^- has an unique effect on vascular smooth muscle: the relaxation mediated by NO^- from Angeli's salt were more prolonged than those induced by NO[37,38]. Besides, compounds like Diethylamine/NO and diethylenetriamine/NO (which belong to diazeniumdiolate or NONOate [N(O)NO] class) can also release NO spontaneously[39]. In these two compounds, NO is covalently linked to diethylamine and diethylenetriamine. It has been proved that diazeniumdiolates can protect the neuro system from the neurotoxicity induced by hydrogen peroxide through a rat model[40]. Other heterocyclic compounds include the oxatriazolium class (sydnonimines) and the furoxan class[41]. These two kinds of NO donors can release NO directly using some cofactors (oxidants for sydnonimines and thiols for furoxans) [42].

1.4.2 Donors Requiring Metabolism

NO donors requiring metabolism to release NO are also widely used. For example, the two classic nitrovasodilator families, nitrite esters and organic nitrates (like amyl nitrite, isosorbide dinitrate and isosorbide 5-mononitrate nitroglycerin, shown in Figure 7), have been used in cardiovascular diseases for a long time. However, there are several limitations for these NO donors, including tolerance (*i.e.* the loss of therapeutic effect under chronic administration), limited bioavailability, low selectivity as well as potentially adverse hemodynamic effects[43,44]. Though these limitations, these drugs are still one the main therapeutics for cardiovascular diseases treatment. As these organic nitrate esters are prodrugs, they require enzymes to generate NO in the body. The main enzyme systems involved in the metabolism of organic nitrate/ nitrite esters is located within microsomal membranes. A lot of evidences suggest that the cytochrome P-450 (CYP450), the presence of NADPH oxidase as well as the activity of glutathione-*S*-transferase, are necessary in the metabolic processes of both de-nitration and reduction of organic nitrate esters to authentic NO[45,46]. It has also been proved that the tolerance of these NO donors is related to the increasing angiotensin II-dependent vascular superoxide anion production from NAD(P)H oxidase and eNOS[47,48]. Superoxide anion then reacts with NO generated from the NO donors, producing peroxynitrite ions ($OONO^-$)[49]. In addition, the tolerance to organic nitrates is also associated with the cross-tolerance to endothelium-derived NO, both by the oxidative inactivation of this endogenous NO to peroxynitrite ions and by the "uncoupling" of eNOS activity[50,51].

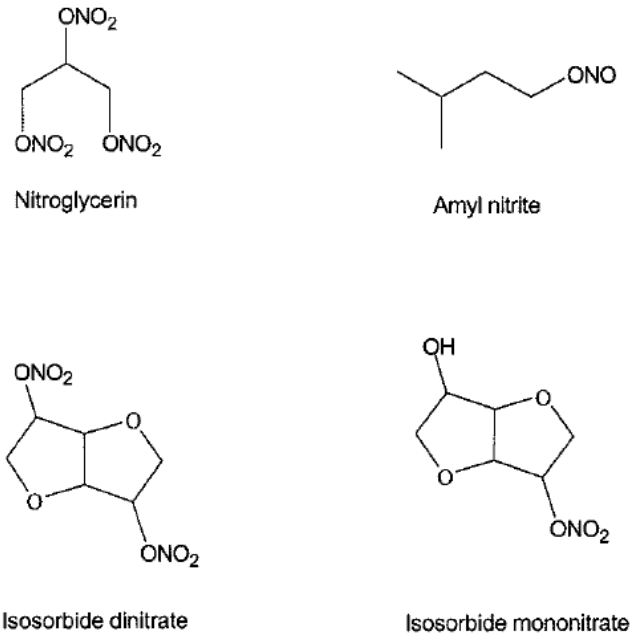

Figure 7. Structures of conventional organic nitrates and nitrite esters[42].

1.4.3 New NO donors

Amidoximes

Amidoximes are oximes of amides with general structure as in Figure 8. These molecules present many important biological effects and have the capacity of releasing NO when oxidized by enzymes such as CYP450[52].

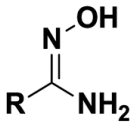

Figure 8. Structure of amidoxime function.

The oxidation of amidoxime compounds has two pathways[53]:

Nitric oxide Synthase pathway

As described in the Figure 2, nitric oxide is produced by a single pathway during the oxidation of guanidine function of the L-arginine. The oxidation is catalyzed by eNOS, in two steps. The first step is the *N*-hydroxylation of one of the two guanidino nitrogens of the L-arginine. This step consumes one mol of NADPH and of O_2. The second step is the oxidation of the intermediate product, NHA, which bears an

amidoxime function. This step consumes 0.5 mol of NADPH and 1 mol of O_2 for the oxidative cleavage of theC=N-OH bond to produce NO and citrulline. However, it seems the eNOS can only oxidize NHA, no other amidoximes.

Cytochromes P450 pathway

The first step of the oxidation by NOS resembles a classical P-450 dependent monooxygenation, which is not the case of the second step since it consumes only 0.5 mol of NADPH. This reaction has been the subject of study of many researchers, which have proven that the oxidation of not only the NHA, but also other arginine-mimetics like amidoximes, can be done by the CYP450.

It has been proven by previous work, that many molecules presenting the C=N-OH function like benzamidoximes, ketoximes, guanidoximes, and arylamidoximes are capable of releasing NO in the presence of CYP450, NADPH and dioxygen.

One of the studied molecules that released important quantities of NO is 4-chlorobenzamidoxime[54] (Figure 9).

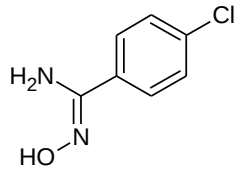

Figure 9. Structure of 4-chlorobenzamidoxime.

In this thesis, some new amidoximes molecules have been evaluated in the article 1, as follows:

Article 1: Synthesis of Novel Mono and Bis Nitric Oxide Donors with High Cytocompatibility and Release Activity

Tanya Sahyoun[a,c], Caroline Gaucher[b], Yi Zhou[b], Naïm Ouaini[c], Raphaël Schneider[d*], Axelle Arrault[a*]

[a] *Laboratoire de Chimie Physique Macromoléculaire, Université de Lorraine, CNRS, LCPM, F-54000 Nancy, France*

[b] *Université de Lorraine, CITHEFOR, F-54000 Nancy, France*

[c] *Faculty of Sciences, Holy Spirit University of Kaslik, BP446, Jounieh, Mount Lebanon, Lebanon*

[d] *Laboratoire Réactions et Génie des Procédés, Université de Lorraine, CNRS, LRGP, F-54000 Nancy, France*

Bioorganic & Medicinal Chemistry Letters 28 (2018) 3329–3332

Contents lists available at ScienceDirect

Bioorganic & Medicinal Chemistry Letters

journal homepage: www.elsevier.com/locate/bmcl

Synthesis of novel mono and bis nitric oxide donors with high cytocompatibility and release activity

Tanya Sahyoun[a,c], Caroline Gaucher[b], Yi Zhou[b], Naïm Ouaini[c], Raphaël Schneider[d,*], Axelle Arrault[a,*]

[a] Laboratoire de Chimie Physique Macromoléculaire, Université de Lorraine, CNRS, LCPM, F-54000 Nancy, France
[b] Université de Lorraine, CITHEFOR, F-54000 Nancy, France
[c] Faculty of Sciences, Holy Spirit University of Kaslik, BP446, Jounieh, Mount Lebanon, Lebanon
[d] Laboratoire Réactions et Génie des Procédés, Université de Lorraine, CNRS, LRGP, F-54000 Nancy, France

ARTICLE INFO

Keywords:
Amidoximes
Nitric oxide
Cardiovascular disease
Double donor
Oxidation

ABSTRACT

Four compounds bearing amidoxime functions were synthetized: (1) **2a,b** bearing an aromatic amidoxime function, (2) **2c** bearing an aliphatic amidoxime function, and (3) **2d** bearing aromatic and aliphatic amidoximes functions. The ability of these compounds to release NO was evaluated *in vitro* using the oxidative metabolism of cytochrome P450 from rat liver microsomes. Results obtained demonstrate that all amidoximes were able to release NO with a highest amount of NO produced by the **2a** aromatic amidoxime. Moreover, all amidoximes exhibit cytocompatibility with human aorta smooth muscle cells. Using intracellular *S*-nitrosothiol formation as a marker of NO bioavailability, compounds **2a–c** were demonstrated to deliver a higher amount of NO in the intracellular environment than the reference. Considering that the concentration of the bis-amidoxime **2d** was two times lower that than of **2a** and **2b**, we can assume that **2d** is the most potent molecule among the tested compounds for NO release.

Gasotransmitters are endogenously synthesized molecules presenting biological properties. Until today, three gasotransmitters have been identified.[1] The first described and studied gasotransmitter is nitric oxide (NO)[2] NO plays a key role in various physiological processes. In the nervous system, NO controls the neurotransmission, in the immune system, it also acts as a defense against bacteria, parasites, and tumor cells, and in the cardiovascular system, it controls vascular homeostasis including blood pressure[3,4] The second gasotransmitter is carbon monoxide (CO) which plays a role in the cardiovascular system since it relaxes the vascular vessels and therefor lowers the blood pressure. CO was also identified as a neurotransmitter. The third and recently studied gasotransmitter is hydrogen sulfide (H_2S) which was discovered to play an important role in neuromodulation and neurotransmission.[2,5]

In this study, we focus on the firstly discovered gasotransmitter, NO. *In vivo*, NO is produced by oxidation of the guanidine function of L-arginine. In the cardiovascular system, this oxidation is catalyzed by the endothelial nitric oxide enzyme (eNOS) and occurs in two steps.[6] The first one is the *N*-hydroxylation of one of guanidino nitrogen atoms of arginine consuming one mole of NADPH and one mole of dioxygen. The second step is the oxidation of the intermediate *N*-hydroxy-L-arginine (NOHA) allowing the breaking of the C=N−OH bond and producing NO and citrulline (Fig. 1).[7] This step consumes 0.5 mol of NADPH and 1 mol of dioxygen. The L-arginine oxidation resembles a classical P450 dependent monooxygenation.[8] This reaction has been the subject of extensive studies and it has been demonstrated that the oxidation of NOHA, but also of other arginine-mimetics like amidoximes, can be performed by cytochromes P450.[9]

Jousserandot et al. were the first to describe the oxidation of some amidoximes by cytochromes P450, using rat liver microsomes in the presence of NADPH and dioxygen.[10,11] Their work focused on the quantification of nitrite ions released by aromatic amidoximes substituted by para electron-donating substituents, such as Cl, that were demonstrated to exhibit the highest NO release rates.[11] Other studies were devoted to the synthesis of prodrugs bearing an amidoxime function and on their effects on many diseases like cardiovascular disease. These reports showed the capacity of seventeen different amidoxime prodrugs to inhibit platelet aggregation, thrombus formation and to decrease blood pressure in spontaneously hypertensive rats.[12,13] Some aliphatic bis-amidoximes showed the highest inhibition of thrombus formation while the aromatic mono-amidoxime bearing a p-CF_3 group was demonstrated to be of high efficiency for the decrease of

* Corresponding authors.
E-mail address: axelle.arrault@univ-lorraine.fr (A. Arrault).

https://doi.org/10.1016/j.bmcl.2018.09.009
Received 9 July 2018; Received in revised form 4 September 2018; Accepted 7 September 2018
Available online 08 September 2018
0960-894X/

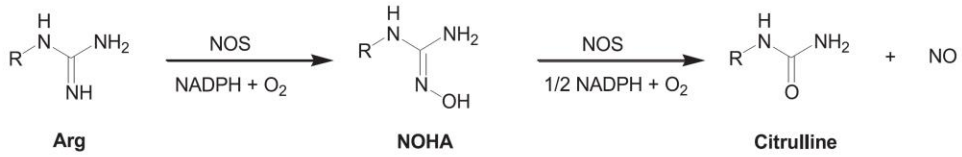

Fig. 1. *In vivo* oxidation of L-Arginine by NO Synthases.

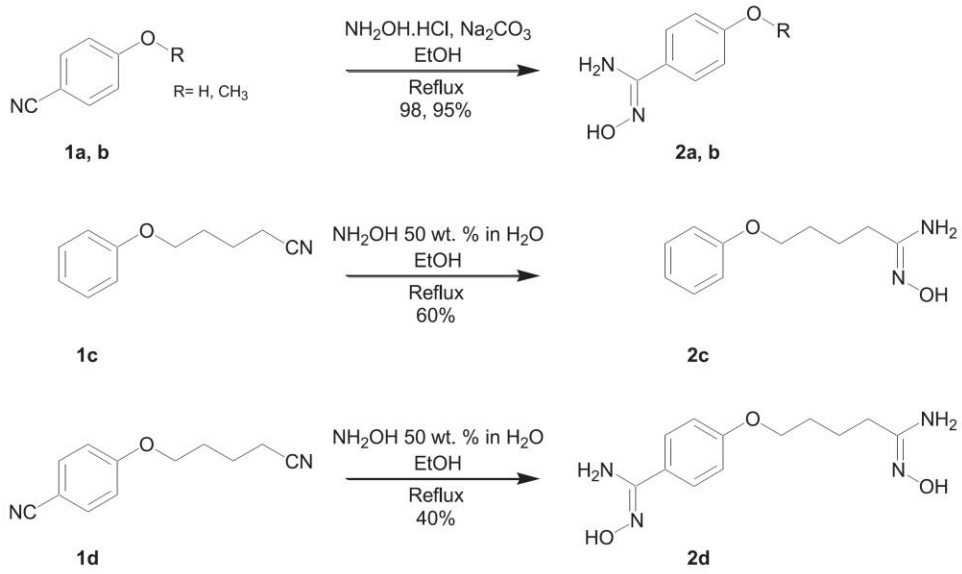

Fig. 2. Synthesis of amidoximes.

the blood pressure.[13] Furthermore, the capacity of some amidoxime functions to induce vasorelaxation of rat aortic rings after the NO release was also highlighted.[14,15]

In this work, the synthesis of mono-amidoximes **2a–c** substituted by various electron-donating groups in the para position and of a bis-amidoxime **2d**, bearing one aromatic and one aliphatic amidoxime function, is described from the corresponding nitriles (Fig. 2).

Nitriles **1a** and **1b** are commercially available, while **1c** and **1d** were prepared from the corresponding bromides by nucleophilic substitution using KCN in DMF. The synthesis of amidoximes **2** from nitriles **1** was performed either in ethanol using hydroxylamine hydrochloride associated to Na_2CO_3 or using an aqueous solution of hydroxylamine and a protocol adapted from Ovdiichuk et al.[16–18] The synthetic conditions are listed in Table 1 in the Supporting Information. Aromatic nitriles **1a and 1b** could easily be converted into amidoximes **2a**[19,20] and **2b**[19,21] using hydroxylamine hydrochloride and Na_2CO_3. Due to the lower reactivity of aliphatic nitriles compared to aromatic ones, compound **2c**[19] could only be prepared from **1c** with a modest yield of 37% under these synthetic conditions. With aliphatic nitriles, better conversions were obtained using a solution of hydroxylamine in water and **2c**[22,23] was isolated with 60% yield after column chromatography. Under these reaction conditions, bis-amidoxime **2d**[22,24] was obtained in 40% yield.

The ability of compounds **2** to release NO by oxidation was first evaluated using rat liver microsomes containing cytochromes P450 in the presence of NADPH and dioxygen (see Supporting Information). 4-Chlorobenzamidoxime (Fig. 3), which is known to release high amounts of NO in the presence of cytochrome P450,[11] was used as a reference.

After 10 min of incubation with rat liver microsomes and NADPH, supernatants were collected for nitrite ions quantification using the Griess assay (see Supporting Information). Four control samples were prepared for each molecule, namely without microsomes, without amidoximes, without NADPH and finally using nitriles **1** instead of amidoximes **2**. The amount of nitrite ions measured in these controls was subtracted from the values measured with amidoximes **2**. As can be seen from Fig. 4, all compounds **2** generate nitrite ions, indicating their ability to be oxidized by rat liver microsomes and NADPH. The nitrite ions release was the highest for compounds **2a** and **2b** (2.4 and 1.5 nmol NO_2^-/mg P450 for 10 min, respectively). Noteworthy is that these values are higher than that obtained for the reference (1.3 nmol NO_2^-/mg P450 for 10 min). The modest capacity of compounds **2c** and **2d** to produce nitrite ions may originate from their inadequate size/shape that does not allow their fast oxidation by the enzyme and/or to the lower reactivity of aliphatic amidoximes in the oxidation reaction. Compound **2a** is of high interest due to its high capacity of release NO compared to the reference.

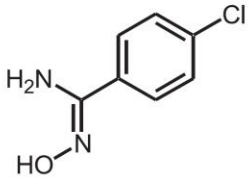

Fig. 3. Structure of 4-chlorobenzamidoxime.

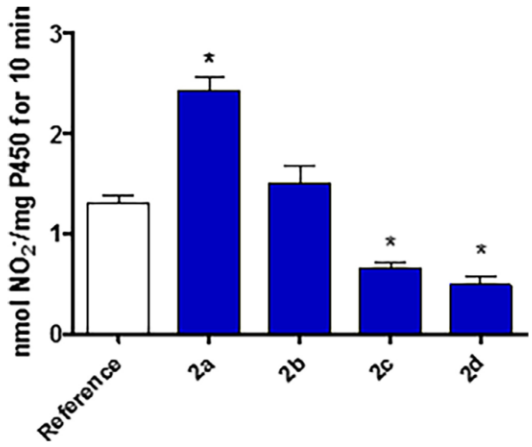

Fig. 4. Concentration of released nitrite ions from compounds **2** and the reference after a 10 min incubation with microsomes. Results are presented as mean ± SEM of three to five independent experiments and compared with a One-way ANOVA; * $p < 0.05$ *versus* reference.

We further evaluated the capacity of compounds **2** to release NO in the presence of human vascular smooth muscle cells (HVSMC). In preliminary experiments, the cytocompatibility of amidoximes **2** toward the HVSMC was evaluated (see Supporting Information). As shown in Fig. 5, except **2a** which induced the lowest cell viability at 100 μM (74.67% ± 2.03), HVSMC cells remained alive and active in the presence of amidoximes even used at high concentration. Further experiments were conducted at the 100 μM concentration to reach NO releases higher than the limit of detection of the fluorometric method used (*vide infra*). Noteworthy is also that the cytotoxicity observed at 100 μM was detected after 24 h-incubation while the release test requires only a 1 h-incubation.

For NO release experiments using amidoximes **2**, *S*-nitrosoglutathione (GSNO),[25] a well-known NO donor, able to deliver bioavailable NO for smooth muscle cells and blood vessels,[26–28] was prepared and used as a reference. HVSMC cells were seeded in 6-wells plates 48 h before incubation with compounds **2** for 1 h at 37 °C. Amidoximes **2a–c** and GSNO were used at 100 μM while compound **2d** bearing two amidoxime functions was used at 50 μM. After washing and lysis of the cells, *S*-nitrosothiols (RSNO) and nitrite ions were immediately quantified using a fluorometric method based on the reaction of N_2O_3 with 2,3-diaminonaphthlene producing naphthotriazole that

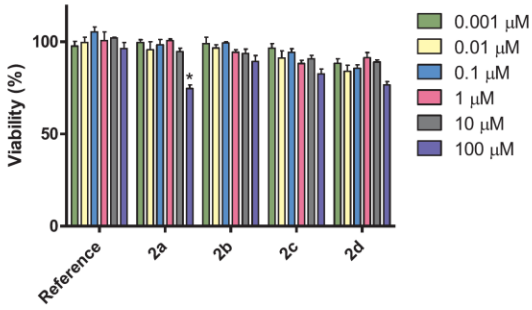

Fig. 5. Viability of the smooth muscle cells after 24 h incubation at concentrations ranging from 0.001 to 100 μM. Results are presented as mean ± SEM of three to four tests and compared with a two-way ANOVA for compound 2a; * $p < 0.001$ 100 μM *versus* all the concentrations.

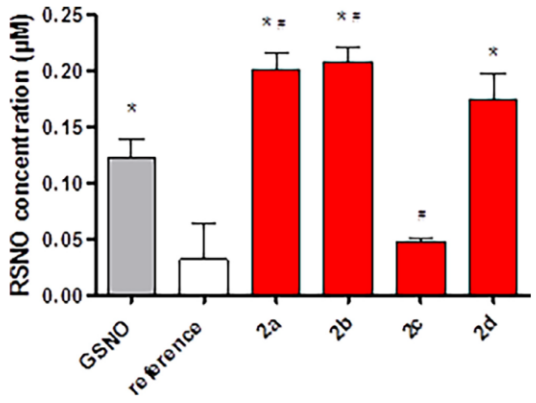

Fig. 6. RSNO intracellular concentration after a 1 h incubation of smooth muscle cells with 100 μM of each compound except **2d** that was used at 50 μM. Results are presented as mean ± SEM of three independent experiments and compared with a One-way ANOVA; * $p < 0.05$ *versus* reference; # $p < 0.05$ *versus* GSNO (Dunnett's multiple comparisons post-test).

emits at 415 nm after excitation at 375 nm (see Supporting Information).[29] The RSNO quantification corresponds to the released NO able to react with cell proteins thiol groups (intracellular *S*-nitrosation).[30] Control cells incubated with PBS containing 0.1% DMSO were under the limit of detection for both RSNO and nitrite ions. Fig. 6 shows that all compounds induced the formation of RSNO inside the cells. In all cases, the concentration of nitrite ions was under the limit of quantification of the method. GSNO, **2a**, **2b** and **2d** produced a significantly higher RSNO intracellular concentration (0.20 ± 0.01 μM, 0.21 ± 0.01 μM and 0.17 ± 0.02 μM, respectively) compared to the 4-chlorobenzamidoxime reference (0.03 ± 0.03 μM). The intracellular *S*-nitrosation process is less pronounced for **2c**, which contains a similar aliphatic amidoxime function than **2d**. Noteworthy is that compounds **2a**, **2b** and **2d** exhibit a higher potential than GSNO to generate intracellular RSNO.

Among all new synthesized amidoximes, **2a** and **2b** seem the most potent since they showed very high NO release compared to other mono-donors like the reference and GSNO. On the other hand, **2d** is also of high interest since its ability to release NO and thus to increase NO storage through RSNO formation inside the cells is similar to compounds **2a** and **2b** but at a twice lower concentration.

In summary, a series of mono- and bis-amidoximes were synthesized and tested for their capacity to release NO. Using rat liver microsomes, only the aromatic mono-amidoximes **2a-b** showed high ability to release NO in the presence of cytochromes P450, while the aliphatic mono-amidoxime **2c** and the bis-amidoxime **2d** exhibit weaker NO liberation capacity. All of the studied amidoximes were demonstrated to be cytocompatible with human vascular smooth muscle cells and were further tested for their ability to deliver NO inside the cells. Amidoximes **2a**, **2b** and **2d** showed a high capacity to form intracellular RSNO indicating that these compounds were able to enter the cells and to be oxidized by the P450 of smooth muscle cells. The lowest delivery of NO inside the cells was observed with aliphatic amidoxime **2c**. Among the amidoximes able to form a high amount of intracellular RSNO, bis-amidoxime **2d** is of high potential since its concentration was two times lower than that of other amidoximes. This makes new bis-amidoxime **2d** of interest since it should allow to halve the drug dosage and thus to reduce the potential secondary effects. Results obtained with mono-amidoximes **2a-b** show their high capability of being used as NO donors and these compounds are among the best existing mono-NO-donors reported to date.

Acknowledgments

The authors thank the Agence Universitaire de la Francophonie (AUF) middle east for financial support of this work. The authors also thank Olivier Fabre for NMR analysis and Isabelle Fries for the cyto-compatibility tests.

Appendix A. Supplementary data

Supplementary data associated with this article can be found, in the online version, at https://doi.org/10.1016/j.bmcl.2018.09.009.

References

1. Steiger AK, Zhao Y, Pluth MD. *Antioxid Redox Signal.* 2018;28:1516.
2. Fagone P, Mazzon E, Bramanti P, Bendtzen K, Nicoletti F. *Eur J Pharmacol.* 2018;834:92.
3. Schröder A, Kotthaus J, Schade D, Clement B, Rehse K. *Arch Pharm.* 2010;343:9.
4. Snyder SH, Bredt DS. *Sci Am.* 1992;266:68.
5. Shefa U, Yeo SG, Kim MS, et al. *BioMed Res Int.* 2017;2017.
6. Sennequier N, Boucher J-L, Battioni P, Mansuy D. *Tetrahedron Lett.* 1995;36:6059.
7. Mansuy D, Boucher J-L. *Free Radical Biol Med.* 2004;37:1105.
8. Mansuy D, Boucher J-L, Clement B. *Biochimie.* 1995;77:661.
9. Fylaktakidou K, Hadjipavlou-Litina D, Litinas K, Varella E, Nicolaides D. *Curr Pharm Design.* 2008;14:1001.
10. Jousserandot A, Boucher J-L, Desseaux C, Delaforge M, Mansuy D. *Bioorg Med Chem Lett.* 1995;5:423.
11. Jousserandot A, Boucher J-L, Henry Y, Niklaus B, Clement B, Mansuy D. *Biochemistry.* 1998;37:17179.
12. Rehse K, Bade S, Harsdorf A, Clement B. *Arch Pharm.* 1997;330:392.
13. Rehse K, Brehme F. *Arch Pharm.* 1998;331:375.
14. Vetrovsky P. *J Pharmacol Exp Ther.* 2002;303:823.
15. Chalupsky K, Lobysheva I, Nepveu F, et al. *Biochem Pharmacol.* 2004;67:1203.
16. Ovdiichuk O, Hordiyenko O, Medviediev V, Shishkin O, Arrault A. *Synthesis.* 2015;47:2285.
17. Ovdiichuk O, Hordiyenko O, Arrault A. *Tetrahedron.* 2016;72:3427.
18. Ovdiichuk O, Hordiyenko O, Fotou E, Gaucher C, Arrault A, Averlant-Petit M-C. *Struct Chem.* 2017;28:813.
19. General protocol for the synthesis of mono amidoximes. To a stirred solution of nitrile **1** (4 mmol) in ethanol (40 mL), were added hydroxylamine hydrochloride and sodium carbonate (see Table 1 for details). The mixture was heated to reflux for 48 h. After cooling to room temperature, the solvent was evaporated and the residue was extracted with ethyl acetate (2 x 30 mL). The organic phase was washed with water (30 mL), dried over $MgSO_4$ and finally concentrated under vacuum. Amidoximes **2** were purified by flash chromatography using methanol/dichloromethane (10/90) as eluent.
20. -Hydroxybenzamidoxime: Yellow-brown powder. $C_7H_8N_2O_2$. Yield: 596 mg (98%); mp 150.1°C; TLC: R_f = 0.15 (CH_2Cl_2/MeOH, 90:10) [silica gel]. ^{1}H NMR (300 MHz, DMSO-d_6, 25°C): δ = 9.57 (s, 1H, =N-OH), 9.33 (s, 1H, OH), 7.9-7.6 (m, 2H, H_{ar}), 6.7-6.72 (m, 2H, H_{ar}), 5.61 (s, 2H, NH_2). ^{13}C NMR (75 MHz, DMSO-d_6, 25°C): δ = 158.1, 150.8, 126.7, 12.1, 11.7. IR (neat): 33 (br), 3319 (br), 3211 (br), 165 (m), 1609 (m), 1509 (m), 1277 (m), 127 (m). 113 (m). HRMS (ESI, *m/z*): MH^+, found 153.0688. $C_7H_8N_2O_2$ requires 153.0659.
21. -Methoxybenzamidoxime: White powder. $C_8H_{10}N_2O_2$. Yield: 631 mg (95%); mp 120.2°C; TLC: R_f = 0.15 (CH_2Cl_2/MeOH, 90:10) [silica gel]. ^{1}H NMR (300 MHz, DMSO-d_6, 25°C): δ = 9.2 (s, 1H, OH), 7.62-7.59 (m, 2H, H_{ar}), 6.93-6.90 (m, 2H, H_{ar}), 5.70 (s, 2H, NH_2), 3.77 (s, 3H, CH_3). ^{13}C NMR (75 MHz, DMSO-d_6, 25°C): δ = 159.8, 150.5, 126.7, 125.7, 113., 55.1. IR (neat): 33 (s), 3353 (s), 2968 (w), 281 (w), 166 (s), 1608 (m), 1518 (s), 113 (m), 1386 (m), 1303 (m), 123 (s), 1175 (m), 1033 (m), 925 (m), 835 (s). (ESI, *m/z*): MH^+, found 167.0836. $C_8H_{11}N_2O_2$ requires 167.0815.
22. General protocol of the bis-amidoximes and aliphatic amidoxime synthesis: To a stirred solution of nitrile **1** in ethanol (40 mL), was added an aqueous hydroxylamine solution (50 wt. % in H_2O). The reaction was heated to reflux for 24 h. After cooling to room temperature, the solvent was evaporated and the residue was extracted with ethyl acetate (2 x 30 mL). The organic phase was washed with water, dried over $MgSO_4$ and finally concentrated under vacuum. The product was purified by flash chromatography using methanol/dichloromethane (10/90) as eluent.
23. N-hydroxy-5-phenoxy-pentanamidine: Black purple powder. $C_{11}H_{16}N_2O_2$. Yield: 583 mg (70%); mp 96.5°C; TLC: R_f = 0.15 (CH_2Cl_2/MeOH, 90:10) [silica gel]. ^{1}H NMR (300 MHz, DMSO-d_6, 25°C): δ = 8.70 (s, 1H, OH), 7.30-7.24 (m, 2H, H_{ar}), 6.93-6.88 (m, 3H, H_{ar}), 5.32 (s, 2H, NH_2), 3.95 (t, *J* = 6.2 Hz, 2H, O-CH_2), 2.02 (t, *J* = 7.2 Hz, 2H, CH_2), 1.73-1.61 (m, 4H, $(CH_2)_2$). ^{13}C NMR (75 MHz, DMSO-d_6, 25°C): δ = 158.6, 152.6, 129.4, 120.3, 114.4, 67.0, 30.4, 28.2, 22.9. IR (neat): 3475 (br), 3361 (br), 3229 (br), 2926 (w), 2871 (w), 1681 (w), 1589 (w), 1498 (w), 1475 (w), 1296 (w), 1255 (m), 751 (w), 660 (m). (ESI, *m/z*): MH^+, found 209.1323. $C_{11}H_{17}N_2O_2$ requires 209.1285.
24. N-Hydroxy-4-[4-(N-hydroxycarbamimidoyl)-butoxy]-benzamidine: Green powder. $C_{12}H_{18}N_4O_3$. Yield: 330 mg (40%); mp 166.6°C; TLC: R_f = 0.15 (CH_2Cl_2/MeOH, 90:10) [silica gel]. ^{1}H NMR (300 MHz, DMSO-d_6, 25°C): δ = 9.42 (s, 1H, OH), 8.72 (s, 1H, OH), 7.60-7.57 (m, 2H, H_{ar}), 6.94-6.89 (m, 2H, H_{ar}), 5.69 (s, 2H, NH_2), 5.38 (s, 2H, NH_2), 3.98 (t, *J* = 6.0 Hz, 2H, O-CH_2), 2.02 (t, *J* = 7.1 Hz, 2H, CH_2), 1.73-1.61 (m, 4H, $(CH_2)_2$). ^{13}C NMR (75 MHz, DMSO-d_6, 25°C): δ = 159.2, 152.8, 150.6, 126.7, 125.6, 113.9, 67.2, 30.3, 28.1, 22.9. IR (neat): 3452 (br), 3303 (br), 2941 (w), 2869 (w), 1679 (s), 1627 (s), 1522 (m), 1393 (m), 1306 (w), 1260 (m), 1180 (m), 920 (w), 843 (w). (ESI, *m/z*): MNa^+, found 289.1291. $C_{12}H_{18}N_4NaO_3$ requires 289.1271.
25. Parent M, Dahboul F, Schneider R, Clarot I, Maincent P. *Curr Pharm Anal.* 2013;9:31.
26. Belcastro E, Wu W, Fries-Raeth I, et al. *Nitric Oxide.* 2017;69:10.
27. Wu W, Perrin-Sarrado C, Ming H, et al. Nanomedicine: Nanotechnology. *Biol Med.* 2016;12:1795.
28. Dahboul F, Leroy P, Maguin Gate K, et al. *PLoS ONE.* 2012;7:e43190.
29. Wu W, Gaucher C, Diab R, et al. *Eur J Pharm Biopharm.* 2015;89:1.
30. Nagababu E, Rifkind JM. *Cell Biochem. Biophys.* 2013;67:385.

Please find the Appendix A from page 206 to 222.

S-nitrosothiols

As described in the Figure 5 and 6, RSNOs (such as GSNO and *S*-nitrosoproteins) can be synthesized through different ways in the body. RSNOs are regarded as promising candidates for the treatment of cardiovascular diseases because of their advantages over the existing drugs: they do not share the shortcomings of organic nitrates and nitroprusside, including oxidative stress or tolerance induction. Several initial clinical studies showed that RSNOs may be of benefit in different cardiovascular diseases[55]. As shown in Figure 10, members of this class include GSNO, *S*-nitroso-*N*-acetyl-penicillamine (SNAP), *S*-nitroso-*N*-acetyl-*L*-cysteine (NACNO)…

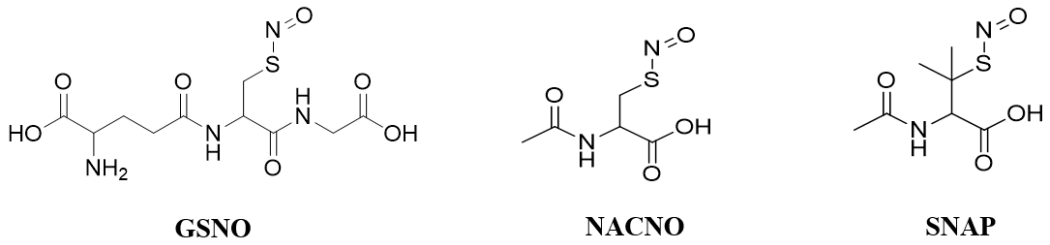

Figure 10. Structure of GSNO, NACNO and SNAP[56,57].

The stability and biological chemistry of RSNOs

One of the most important parameters for the degradation of *S*-nitrosothiols are metal ions (specifically copper and iron). Even traces of contaminating metal ions can degrade RSNOs, that is why published half-lives for *S*-nitrosothiols are more a measure of water purity than of compound stability[56] if no metal ion chelator is used. The common biological *S*-nitrosothiols are stable for several hours in the presence of the metal ion chelator diethylenetriaminepentaacetic acid. Their stabilities decrease in the order GSNO>SNAP>*S*-nitrosohomocysteine>*S*-nitrosocysteine in the absence of the

metal ion chelator in pH 7.4 phosphate buffer[57]. The decomposition caused by copper (II) leads to the formation of nitric oxide without any thiyl radicals formation, which indicates that the breakdown mechanism of S-NO bond is not homolysis [57]. Another parameter accelerating RSNOs degradation is the light. Unlike copper (II), photolysis promote the hemolytic cleavage of the S-NO bond[58]. A strong direct light can significantly reduce RSNOs concentration. The room light is sufficient to produce a small quantity of nitric oxide in a solution of RSNOs. So, RSNOs (powders or solutions) should be stored in the dark. In addition, thermal decomposition is also regarded as a key factor for the decomposition of RSNOs[57]. The mechanism of this appears to be similar to photolysis, with homolytic cleavage producing NO and an alkyl thiyl radicals. There are still other parameters, which will decrease the stability of RSNOs like enzymatic decomposition: for example, GGT can cause the decomposition of GSNO[59]. Several enzymes are involved in the degradation of RSNOs and they will be discussed later in the manuscript (*in vivo* metabolism of GSNO).

RSNOs are biologically involved in 3 main reactions (Figure 11): nitric oxide release, transnitrosation and *S*-thiolation[60].

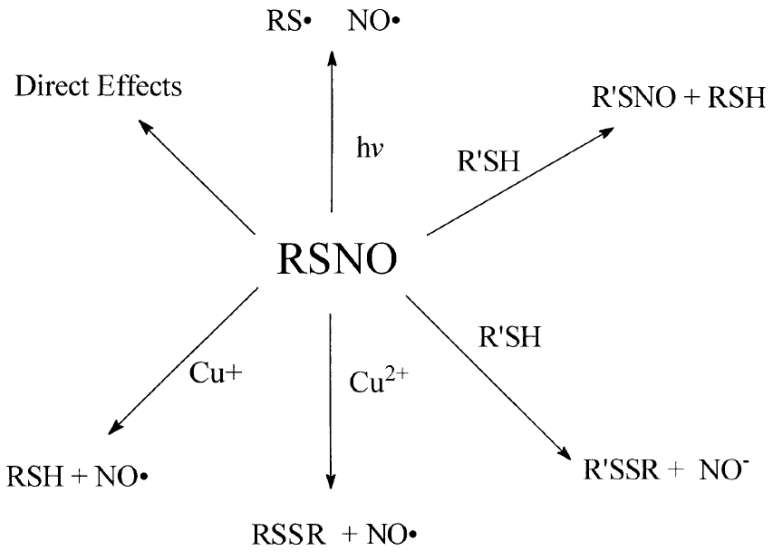

Figure 11. Biological activity of RSNOs[60].

Nitric oxide release

As mentioned above, nitric oxide is easily generated from RSNOs in the presence of metal ions such as copper ions, iron ions and reducing agents. Copper (II) can directly and catalytically decompose RSNOs. This reaction generates nitric oxide and thiol disulfide but does not appear to proceed through a thiyl radical intermediate. The mechanism is fairly well established:

$$2GSNO + Cu^{2+} \rightarrow GSSG + Cu^{2+} + 2 \cdot NO$$

$$GSNO + Cu^{+} \rightarrow GS^{-} + NO + Cu^{2+}$$

Transnitrosation

In transnitrosation process, the nitroso functional group is transferred from one *S*-nitrosothiol to another thiol function. Transnitrosation occurs by nucleophilic attack of the thiolate anion on the nitrogen of the *S*-nitrosothiol.

$$RSNO + R'SH \rightleftharpoons RSH + R'SNO$$

This reaction is reversible because its products are still a thiol and a *S*-nitrosothiol[61]. When the transition occurs from a relatively stable *S*-nitrosothiols (*e.g.* GSNO or SNAP) to the thiol function of cysteine amino acid, a relatively unstable *S*-nitrosocysteine will be formed. *S*-nitrosocysteine can decompose and release NO in the presence of Cu^{+} or spontaneously[62,63]. Transnitrosation represents an important way to transfer 'NO' from species to species inside cells, which is regarded as a potential mechanism for the modification of protein activity[64].

***S*-Thiolation**

S-thiolation reaction occurs through the nucleophilic attack of the sulfur of RSNOs by a thiolate anion, producing a disulfide and nitroxyl anion[65,66]. The *S*-thiolation of proteins has been regarded for a long time as an intracellular response to oxidative stress. When enzymes were incubated with RSNOs, both

S-nitrosation and *S*-thiolation occured[67,68]. However, exposure of cells to nitrogen oxides led to extensive intracellular *S*-thiolation[69]. Thus, *S*-thiolation is a more stable modification than *S*-nitrosation.

$$RSNO + R'S^- \rightarrow RSSR + NO^-$$

In addition to these three biological reactions, some RSNOs can have direct effects. On the one hand, it has been suggested that GSNO acts as a substrate for several enzymes utilizing glutathione (GSH), such as the GGT and the glutathione peroxides[59]. On the other hand, several RSNOs like GSNO, SNAP can *S*-nitrosate sGC, which will inactivate the enzyme[70].

1.5 GSNO

GSNO, as one of the main intracellular RSNOs, seems to be a good choice as drug candidate with several advantages over others RSNOs: i) GSNO is a physiologic RSNOs with no side effects. ii) it is relatively stable compared to other endogenous RSNOs; iii) dedicated enzymes like the GGT are able to catalyze the release of NO only from GSNO and not from other natural (*e.g*. *S*-nitrosoalbumin) nor synthetic RSNOs (*e.g.* NACNO and SNAP).

1.5.1 Chemical Synthesis of GSNO

GSNO is easy to synthesize through the reaction between GSH and nitrous acid. This reaction is efficient and fast with high yield. Unlike most low-molecular weight RSNOs, GSNO can be precipitated with acetone, which results in a pink solid powder. Other nitrosating agents could be used for GSNO synthesis, such as nitrosonium, nitrosonium chloride, tetrafluoroborate, dinitrogen tetraoxide and dinitrogen trioxide[59,71]. However, reaction between GSH and nitrous acid is the most frequently used with both a simple procedure and a high yield. The original study by Hart[72] showed an extinction coefficient for GSNO of 922 M^{-1}

cm^{-1} at λ_{max} = 335 nm, which is in agreement with the result measured in our lab with the value as 922 M^{-1} cm^{-1} at λ_{max} = 334 nm[73].

1.5.2 *In vitro* stability

Similar with other RSNOs introduced above, GSNO shows a low stability in aqueous solutions. A possible explanation is the mesomerization of the S-NO bond. The distribution of those mesomers depends on the electrophile and nucleophile groups in the S-NO bond environment.

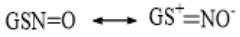

Published half-lives of GSNO are not unified and are clearly condition-dependent. Basically, several mechanisms are involved in the decomposition of GSNO, including S-NO bond homolysis in the thermal/photolysis decomposition, metal ion-catalyzed (mainly Cu^{2+}) decomposition, heterolysis, and hydrolysis.

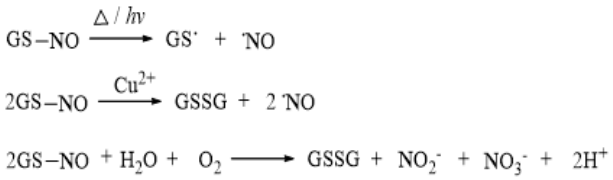

As GSNO is easy to degrade under all these conditions, it is important to develop dosage forms to protect GSNO from degradation for the different therapeutic applications.

1.5.3 *In vivo* metabolism

A summary of the four main enzymatic metabolisms of GSNO is presented in Figure 12. They will be subsequently discussed in the text.

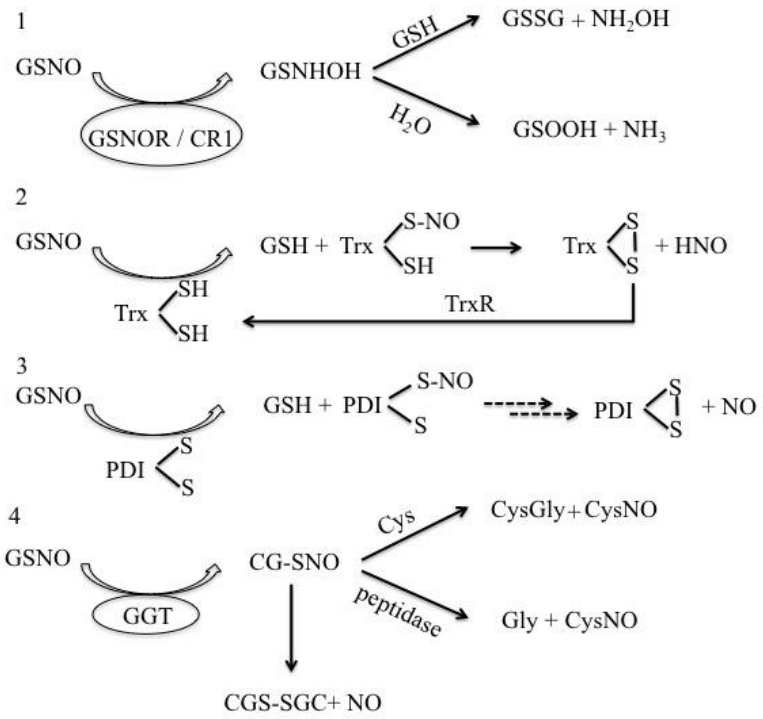

Figure 12. *In vivo* metabolism of GSNO through different enzymes: 1. GSNO reductase (GSNOR)/carbonyl reductase 1 (CR1); 2. thioredoxin system (Trx); 3. protein disulfide isomerase (PDI); 4, γ-glutamyltranspeptidase (GGT).

GSNO reductase (GSNOR) and carbonyl reductase 1 (CR1):

These two enzymes are able to catabolize GSNO without any release of NO. GSNO reductase reduces GSNO using NADH as a cofactor. The product GSNHOH is an intermediate, which can either rearrange and being hydrolyzed to produce GSO_2H and ammonia or react with GSH and produce GSSG and NH_2OH[74]. Through catalyzing the breakdown of GSNO, GSNOR can modulate intracellular reactive nitric oxide availability. In addition, it can also indirectly regulate RSNOs through GSNO-mediated protein *S*-nitrosation[75].

Compared with GSNOR, CR1 is one of the most recent addition to the list of GSNO reducing enzymes[76]. Similar to GSNOR, the catalytic reaction of GSNO by Carbonyl reductase 1 produces the same intermediate product.

Thioredoxin system (Trx) and Protein disulfide isomerase (PDI):

The thioredoxin superfamily is a large multigene family that contains five main protein groups: Trx, PDI, glutaredoxins, glutathione peroxidases, and glutathione-*S*-transferases. All the members share a common structural arrangement and are major players in oxidative protein folding. Among them, Trx and PDI play important roles in the metabolism of GSNO.

The thioredoxin system plays a critical role in both control and maintenance of redox homeostasis, and this system comprises three main members: Trx, TrxR, and NADPH[77]. Trx has two isoforms: Trx1 mainly localizes in the cytosol and the nucleus; Trx2 localizes in the mitochondria. Through their vicinal dithiols at the active site, they are able to reduce protein disulfides. Reduced Trx (Trx-$(SH)_2$) reacts directly with a protein disulfide and produces a reduced protein dithiol and oxidized Trx (Trx-S_2). Although Trx has been regarded as a target of *S*-nitrosation for a long time, it has also been identified as a main player in the reduction of low-molecular weight and protein *S*-nitrosothiols. Trx plays a critical role in both denitrosation and transnitrosation reactions[78–80].In denitrosation, reduced Trx reacts directly with the low-molecular weight RSNOs (like GSNO) and protein RSNOs. In transnitrosation, Trx is *S*-nitrosated, leaving behind a thiol. Then, the *S*-nitrosated Trx will be turned over and nitroxyl will be released to form oxidized Trx. The oxidized Trx can be reduced by the TrxR and NADPH. The Trx system has been hypothesized as the primary regulator of the *S*-nitroso proteome in most tissues because of its more ubiquitous expression than GSNO reductase and carbonyl reductase[59].

PDI is an enzyme has two catalytic sites composed of two cysteine residues, which catalyzes the breakage and formation of disulfide bonds between cysteine residues in proteins to fold proteins. The catalyzing mechanism of PDI is similar to RSH-RSNOs exchange reaction[81]. The protein

disulfide isomerase regulates intracellular transfer of nitric oxide through catalyzing transnitrosation and denitrosation. It has been reported that PDI can denitrosate GSNO and it is suggested that NO released through this reaction combines with dioxygen in the hydrophobic environment and generates N_2O_3[82]. This "NO-charged PDI" can perform both intramolecular and intermolecular *S*-nitrosation reactions. Reduced PDI can denitrosate *S*-nitrosated PDI to release NO.

γ-glutamyltranspeptidase (GGT):

As an enzyme on the extracellular cell surface, the γ-glutamyltranspeptidase is involved in the catabolism of GSH and GSH adducts and the processing of thiol-based leukotrienes [83]. The enzyme transfers the γ-glutamate group from glutathione and leaves cysteinyl-glycine through either hydrolysis or in the presence of a co-substrate like glycyl-glycine[84]. It has been reported that GGT can use GSNO as a substrate, producing *S*-nitrosocysteinylglycine to accelerate the degradation of GSNO. GGT appears to work when GSH crosses cell membranes to deliver extracellular cysteine[83]. In addition, the substrates for GGT include many substituted derivatives of GSH, and GSSG, and GGT acts to degrade and recycle both GSSG and the products of glutathione *S*-transferase activity[85].

Other enzymes-dependent mechanisms

In has been suggested that other enzymes also play a role in the metabolism/degradation of GSNO. These enzymes include glutathione peroxidase[86], xanthine oxidase[87] and CuZn superoxide dismutase[88]. In the work of Hou et al[86], glutathione peroxidase alone catalyzed the GSNO, without the presence of any thiol or H_2O_2. Under aerobic conditions, xanthine oxidase showed its ability to induce the decomposition of GSNO in the presence of purine or pteridine substrates[87]. CuZn superoxide dismutase[88] was able to

catalyze the GSNO decomposition in the presence of GSH and result in the production of NO. Through these enzymes, the reaction products are nitric oxide, GSH or glutathione disulfide. However, it has been shown by kinetic measurements that their reactions are much less efficient than the other enzymes (GSNOR, Trx system or GGT)[89].

1.6 GSNO related delivery systems and therapeutic potentials

Due to the low stability of GSNO *in vitro* and *in vivo*, an ideal formulation should protect it from decomposition while ensuring suitable localization and kinetics of drug delivery. GSNO, as a small hydrophilic drug, could diffuse very easily, which may cause two issues: low encapsulation efficiency (during formulation process) and initial burst (*i.e.* massive drug release over a short time period after administration). The main delivery systems previously reported for GSNO will be discussed in detail in the following sections. They were categorized according to the administration route: (i) intravenous, (ii) topical, (iii)parenteral other than intravenous (implants) and (iv) oral.

1.6.1 Intravenous administration

Intravenous (IV) therapy delivers liquids directly into a vein. The therapeutic potential of GSNO was evaluated in humans through IV administration, focusing on its ability to effectively decrease platelet aggregation and blood pressure (as shown in Table 1). GSNO showed its antiplatelet effect at low dosage (2.5 mg IV for healthy women) without hemodynamic changes[90]. Similarly, Moncada et al.[91] have reported that when applied to patients undergoing percutaneous transluminal coronary angioplasty, small IV doses (4.4. nmol/kg/min) of GSNO inhibited platelet aggregation without decreasing blood pressure. These results have been supported by several similarly designed experiments, which applied low dosage GSNO to reduce platelet

aggregation[28,92–94] as well as embolization[95–97]. It has been suggested that the antiplatelet effect of GSNO is driven by the high expression of cell surface protein disulfide isomerase on platelets surface, catalyzing the release of NO[98]. However, at higher dosage GSNO caused hypotension to healthy adults[98], which come from the vasodilation effect of NO. Indeed Rassaf[100] described that infusion of GSNO at 30 μmol over 1 minute induces vasodilation and causes hypotension to healthy adult humans. All these studies reported pharmacological effects (anti-platelet aggregation, embolization and hypotension) of GSNO with minimal or no side effects.

Through IV, GSNO was not only administrated as a solution, but also as a suspension of nanoparticles in some preclinical studies. For example, Duong[101] and his group obtained self-assembled nanoparticles through GSNO-conjugated diblock copolymers (2-vinyl-4,4-dimethyl-5-oxazolone and oligoethylene glycolmethacrylate), which showed a high stability with sustained release (over 80% of NO released from the nanoparticles after 24 h in the presence of ascorbic acid). After decoration with vitamin A for liver targeting (the therapeutic aim was reducing portal hypertension), these nanoparticles were intravenously administrated to rats (with GSNO concentration equivalent to 500 μM in rat blood). They preferentially accumulated in the liver as expected, so they could be applied to alleviate liver fibrosis and portal hypertension. Delivery of GSNO through IV route has several merits, such as rapid onset drug effect, direct delivery to the blood and precise control of drug quantities. However, low patient compliance and short drug duration time are the main drawbacks of intravenous delivery. Thus, other delivery systems of GSNO have been developed.

Table 1. GSNO related intravenous delivery systems

Formulation type	Effects	Application	Note	Dosage (eq infusion rate)	Ref
Free GSNO	Inhibition of platelet activation	Young healthy women	No hemodynamic changes were observed	2.5 mg GSNO over 30 min (about 4.1 nmol/kg/min)	90
		Patients with unstable angina and patients with acute myocardial infarction		2.2 or 4.4. nmol/kg/min	91
		Coronary bypass patients		40 nmol/min (0.67 nmol/kg/min)	92
	Reduced hypertension and platelet aggregation	Preeclamptic pregnant women		50-250 µg/min for 60-90 min (2.5 to 12.5 nmol/kg/min)	93
	Inhibition of platelet activation	Percutaneous transluminal coronary angioplasty patients	No hemodynamic changes were observed	Not mentioned	94
	Reduced embolization	Endarterectomy patients, Carotid angioplasty patients	Dose titrated not to induce hypotension	2.2 or 4.4. nmol/kg/min	95-97

Formulation type	Effects	Application	Note	Dosage (eq infusion rate)	Ref
Free GSNO	Platelet activation Inhibition and vasodilation	Healthy humans	Not significant vasodilation	0.2, 1, and 5 nmol/min (0.003-0.083 nmol/kg/min)	28
	Vasodilation and hypotension			30 µmol over 1 minute (500 nmol/kg/min)	99
	Vasodilation in dorsal hand vein and forearm arteries		Comparative *in vivo* and *in vitro* study among nitro vasodilators	1 pmol/min to 160 nmol/min (0-2.7 nmol/kg/min)	100
Nanoparticles	Liver accumulation	Rats			101

1.6.2 Topical administration

Besides IV, topical administration has been considered as another important delivery way of GSNO with several advantages: the drug can act locally or reach the bloodstream, while avoiding the first pass metabolism (as IV route); it also provides a prolonged contact with the drug (Table 2). In the report of Seabra et al.[102], an hydrogel containing GSNO was applied on the skin of healthy humans, thus increasing the local microcirculatory flux with no systemic side effect. In addition to skin, GSNO was applied to mucosal surfaces (especially airway mucosa) as well. It was reported that mucosal GSNO can induce bronchodilation by releasing NO, which is an important therapeutic agent in pulmonary diseases such as asthma[103]. In the study of Hurley et al.[104], a nebulized GSNO inhaler effectively improved oxygenation in cystic fibrosis patients. However, a lot of studies reported in the literature with interesting results only include *in vitro* and preclinical tests on cells or animals. For example, through incorporation of GSNO into poly(ethylene glycol) (PEG) matrices, Seabra et al.[105] obtained a formulation suitable for topical administration and showed its potential to enhance the percutaneous absorption of NO. In addition, Seabra et al.[106,107] also succeeded in incorporating GSNO into films of blended poly(vinyl alcohol)/poly(vinyl pyrrolidone) (PVA/PVP). These films could be applied to enhance wound healing in diabetes through releasing GSNO/NO. As these polymeric films protect GSNO from degradation and provide controlled local NO release, several GSNO loaded films made of different materials have also been developed. Simoes and de Oliveira[108] applied PVA to encapsulate GSNO and the final product films promoted local vasodilation. Kim et al.[109] found that chitosan films containing GSNO were able to help wound healing with antibacterial effects. In the work of Yoo et al.[110], GSNO was incorporated into films made of three different materials (Carbopol, hydroxypropyl

methylcellulose (HPMC) and PEG). These films enhanced the vaginal blood perfusion in a rat model and showed no cytotoxic effects, which means they might be regarded as potential treatments for female sexual arousal disorder. In addition, Pluronic®F-127 hydrogel[111–113] or chitosan[114] gel have also been developed to load GSNO with sustained and biologically effective release of NO. This Pluronic®F-127 hydrogel was used to different topical applications such as GSNO delivering to targeted tissues[111], decreasing pain related to inflammation[112] as well as acceleration of ischemic wounds healing[113]. In the work of Hlaing et al.[115], GSNO loaded poly(lactide-co-glycolide) (PLGA) microparticles were obtained through solid-in-oil-in-water (S/O/W) double emulsion with solvent evaporation technology. These microparticles were applied onto skin lesions infected with methicillin-resistant *Staphylococcus aureus* and enhanced drastically their healing, in a rat model.

Table 2. GSNO related topical delivery systems

Formulation type	Polymer	Effects or treatments	Administration area	Note	Ref
Hydrogel	F-127	local microcirculatory flux increase without any systemic side effects	Human skin		102
Free GSNO		Bronchodilation	Pig lung		103
Patent inhalation		Improving oxygenation without any systemic side effect	Lung of cystic fibrosis patients		104
Matrices	PEG	Potential to enhance the percutaneous absorption	Not mentioned		105
Films	PVA/PVP	Accelerate the wound healing in diabetes	Not mentioned		106,107
	PVA	Local vasodilation promotion effects or as dermal wound dressing	Human skin		108
	Chitosan	Wound healing and antibacterial effects	Rat skin		109

Formulation type	Polymer	Effects or treatments	Administration area	Note	Ref
Films	HPMC and PEG	Enhanced the vaginal blood perfusion in a rat model; no cytotoxic effects	Vaginal mucosa of rat	Potential treatment option for female sexual arousal disorder	110
Hydrogel	F-127	Deliver GSNO to target tissues	Not mentioned	Sustained and biologically effective release of NO	111
		Inflammation pain	Not mentioned		112
		Ischemic wounds	Human skin		113
Gel	Chitosan	Not mentioned	Rat skin		114
Microparticles	PLGA	Antibacterial	Rat skin		115

1.6.3 Implants

Some researchers worked on delivering GSNO through different types of implants, which are complex parenteral delivery systems (Table 3). Advantages of theses formulations are to be effective, with reduced side effects and with long periods of steady delivery, so it is easier to maintain the plasma drug levels in the desirable range for the treatment. Parent et al.[116] elaborated porous biodegradable 3D scaffolds made of PLGA)/poly(E-caprolactone) (PCL) blend loaded with GSNO. When muscle cells were dropped onto it, it allowed intermediate cells anchorage with an increase in protein production while cellular metabolic activity and redox balance were maintained. These preliminary results could pave the way for a potential application in cardiovascular tissue engineering. In addition, Parent et al.[117] also developed *in situ* GSNO-loaded formulations (implants and microparticles) using PLGA. After a single subcutaneous administration to healthy rats, these formulations showed a less pronounced but more sustained hypotension compared to free drug, and were able to prevent transient platelet hyper-responsiveness. Moreover, in a rat model, a single administration 2 h after induction of a stroke provided cerebroprotection (histological and functional benefits), while free drug was deleterious. Similarly, other scaffolds were developed such as nanocomposites made of polyhedral oligomeric silsesquioxane/poly(carbonate-urea) urethane by de Mel[118], and PLGA)/ PEG/PCL stents by Acharya[119]. All these implants were developed as the treatment methods for cardiovascular diseases and they showed a stable, sustained and consistent release of NO from 1 day to several weeks *in vitro*.

Table 3. GSNO loaded implants

Formulation type	Polymer	Effects	Application	Note	Ref
Scaffolds	PLGA/ PCL	Cardiovascular tissue engineering			116
Microparticles	PLGA	Potential treatment of stroke	Rats with stroke	Longer and slight hypotension effect, ability to prevent transient platelet hyper-responsiveness as well as to provide cerebroprotection after stroke	117
Nanocomposite	Polyhedral oligomeric silsesquioxane/poly(carbonate-urea) urethane	CVD			118
Polymeric stents	PLGA/ PEG / PCL	Antiplatelet			119

1.6.4 Oral administration

Studies about GSNO delivery mainly focused on parenteral and topical administrations, whereas a little attention has been paid to its oral delivery (Table 4). As one of the most preferred administration methods, oral delivery has several advantages over other routes such as compliance and convenience of patient (which helps to increase therapeutic efficacy), lower cost of production considering the manufactured conditions (sterility is unnecessary). In addition, oral route is interesting for physiological reasons: the gastrointestinal tract supplies extensive surface (300 to 400 m^2)[120] for drugs absorption but also poses challenges to prevent their degradation.

In the work of Shunmugavel et al.[121], free GSNO was directly applied orally to rats with spinal cord injury. Then ameliorated inflammatory sequelae were observed in bladder and renal tissues, compared with control group. Similarly, several other applications have been proposed for oral administration of GSNO to animals: Giri et al.[122] used the GSNO to inhibit proliferation of chemo responsive and chemo resistant ovarian cancer cell lines with oral dosage 1 mg/kg to rats. In the work of Nath et al.[123] the progression of a chronic experimental autoimmune encephalomyelitis was slowed in mice after applying GSNO. In a rat model of experimental autoimmune uveitis[124], a significant suppression of inflammatory mediators was shown after oral administration of GSNO. However, due to the degradation of GSNO along the gastrointestinal tract, high dosage of free GSNO (1 mg/kg) has to be used in these experiments. In order to protect GSNO from degradation, several particles adapted to oral route administration have been developed in our lab. For example, Wu et al developed GSNO-loaded nanoparticles[125] (GSNO-NP) using polymer Eudragit® RL PO through a double emulsion/solvent evaporation method, and they showed a protection and a sustained release of GSNO. GSNO-NP were then embedded

into an alginate, chitosan, or alginate/chitosan matrix to form nanocomposite particles[126,127] (GSNO-aNCP, GSNO-cNCP and GSNO-acNCP, respectively). All these nanocomposites showed higher encapsulation efficiency and better sustained release of GSNO. The GSNO-acNCP also led to the formation of a NO store in the aorta wall after a single oral administration to rats.

Table 4. GSNO related oral delivery systems

Formulation type	Polymer	Effects	Application	Note	Ref
Free GSNO		Ameliorates inflammatory sequelae observed in bladder and renal tissues	Spinal cord injury induced rats		121
		Inhibited proliferation of chemoresponsive and chemoresistant ovarian cancer cell lines	Rats		122
		Reduced disease progression in chronic models	Experimental autoimmune encephalomyelitis mice		123
		Significantly suppressed the levels of inflammatory mediators in the retinas of EAU mice	Experimental autoimmune uveitis (eau)		124
Nanoparticles	Eudragit				125
Nanocomposite	Eudragit, alginate, chitosan				126
			Rats	NO store formation in the vessel wall	127

1.6.5 Gastrointestinal barrier

All along the gastrointestinal tract various parameters can trigger RSNOs decomposition: enzymes and metal ions (described in the degradation of RSNOs) as well as pH variations. For the stomach, it produces gastric juice, which contains potassium chloride, sodium chloride and hydrochloric acid (HCl). The HCl keeps the acidic environment at pH 1.5 to 3.5 and induces the degradation of proteins and peptides into aminoamides. After entering the duodenum, pH increased rapidly from 2 to 6. The extreme pH and rapid change may accelerate the degradation of RSNOs and decrease its bioavailability. In addition, the enzymes or the metal ions existing in the gastrointestinal tract can also cause GSNO decomposition.

The barrier of intestine is a complex multilayer system which is composed of an external "physical" barrier and an inner immunological barrier[128]. The epithelial cell layer is covered with two mucus layers, which forms the protective external barrier. The single epithelial cells layer interspersed with various other cells, such as goblet cells, which produce mucus, Paneth cells, which produce anti-microbial peptide, as well as enterocytes M-cells, which specialize in luminal sampling. All of these cells forms the main barrier between the outside world and the proper function in the body. The layer under epithelium is the lamina propria, where exists various innate and adaptive immune cells such as B cells, T cells, mast cells, eosinophils and macrophages. All of these consist of the immune system, which responds with “toleragenic-reaction” or “active” eradication towards foreign antigens. The intestinal barrier plays an important role in the absorption and the bioavailability of drugs through oral administration[129–131]. Epithelial cells lining is a kind of tight junctions that repels harsh fluids, which may injure mucosa. The transport of drugs through the cells is the key factor of bioavailability (will be discussed in the Chapter 2). The mucus blanket is secreted by mucosal neck cells and surface epithelial cells. It forms a gel-like coating on the surface of mucosa with protecting effect. The bicarbonate is also secreted by epithelial cells. All these mucosal barriers prevent drugs (like GSNO) from entering blood vessels. With the viscosity and interactive nature, the mucus layers offer a resistance to the diffusion of drugs and limit their bioavailability. In addition, GSNO/RSNOs is also easy to be degraded during the gastrointestinal tract, *via* the different enzymes (such as Trx, PDI, GGT) on the cells.

1.7 Nanoparticles/microparticles for oral delivery of biological molecules

The bioavailability of biological molecules is always reduced by their susceptibility to degradation and low penetration across the intestinal barrier. Thus, the challenge to deliver GSNO through the oral route is to improve its bioavailability. Several strategies are on ongoing investigations such as chemical modification, encapsulation, use of absorption enhancers… Among all the methods, encapsulation into nanoparticles/microparticles seems to have advantages over others[131]:

1. The size and surface characteristics of particles are easy to manipulate to achieve drug targeting after administration.
2. The control of particles and the sustain of drug release will help to increase therapeutic efficacy with less side effects.
3. The degradation of particles and their controlled release effect can be modulated through the choice of matrix constituents.
4. Particles provide a good protection for drugs through the gastrointestinal tract and preserve the drug activity
5. Intestinal permeability can be enhanced using different polymers.

1.7.1 Nanoparticles targeting the gastrointestinal tract

The main aims to design nanoparticles to deliver biomolecular drugs are to control their size, surface properties and release kinetic parameters in order to get site-specific action with therapeutic drug concentrations. According to the targeted sites, developed nanoparticles can be classified into stomach targeting, small intestine targeting, intestinal lymphatic system targeting as well as colon targeting[129] (Figure 13).

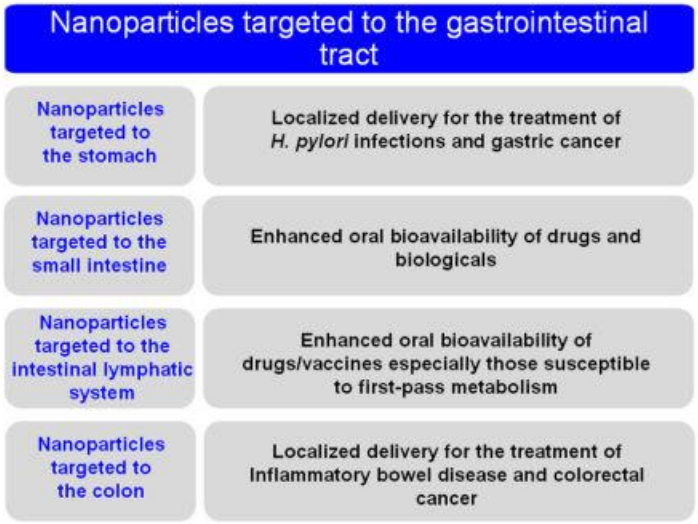

Figure 13. Nanoparticles targeted to the gastrointestinal tract[129].

Stomach targeting nanoparticles

Most of the nanoparticles designed to target the stomach were applied to increase the gastric retention using mucoadhesive polymer such as chitosan. As a natural polysaccharide composed of *N*-acetyl-D-glucosamine and β-(1–4)-linked D-glucosamine[132], chitosan contains amines, which can interact with negatively charged sugars on mucin and thus is widely used as mucoadhesive reagent. However, chitosan is easy to dissolve in acidic pH, so it should be complexed with polyanions to prevent its rapid dissolution. For example, Chang et al.[133] developed amoxicillin-loaded nanoparticles through complexing chitosan and poly-glutamic acid polyelectrolytes, which can be used for the treatment of *H. pylori* infections. In another investigation, Lin et al.[134] described fucose-chitosan-heparin nanoparticles crosslinked with genipin and loaded with berberine, which have the potential to treat *H. pylori* infection.

Small intestinal targeting nanoparticles

Targeting the small intestine has been regarded as a useful way to improve systemic absorption of drugs such as vaccines, peptides, proteins and other macromolecules. This kind of nanoparticles often uses enteric polymers alone or complexed with other polymers, to protect drug from decomposition in the stomach and/or to get specific site release[129]. In order to target small intestine, He and colleagues[135] fabricated insulin-loaded solid lipid nanoparticles with a vitamin B12 stearate conjugate for targeting. These nanoparticles presented more than 2-fold higher bioavailability compared to non-modified ones. Similar nanoparticles were synthesized by Verma[136], through coating insulin-loaded calcium phosphate

nanoparticles (Insu-Cap NPs) with sodium alginate and chitosan-vitamin layer congaing B12 conjugate.

Intestinal lymphatic system targeting nanoparticles

The targeting of nanoparticles to the intestinal lymphatic system has been extensively tested for improving drugs bioavailability especially for the ones with extensive degradation along gastrointestinal tract and/or hepatic first-pass metabolism. For lymphatic system targeting, various fatty acid monoglycerides, diglycerides and triglycerides were applied. Alex et al.[137] improved oral bioavailbility of lopinavir, a drug with low water solubility and low bioavailability, part of the highly active antiretroviral therapy, using glyceryl behenate solid lipid nanoparticles. During the work of Zhang et al.[138], candesartan cilexetil-loaded glyceryl monostearate nanoparticles were obtained and turned out to improve the in oral bioavailability of the drug in rats around 12-fold.

Colon targeting nanoparticles

The majority of formulation designed to target colon through oral route are mainly applied to treat inflammatory bowel diseases (IBD). To target the colon, pH sensitive polymers are commonly used alone or in combination with other polymers, which assist to target like azo containing moieties. Among all these polymers, Eudragit S is the most frequently used. For example, the group of Gugulothu[139] developed pH sensitive nanoparticles using Eudragit S100. These nanoparticles contained curcumin and celecoxib, which can be used for the treatment of IBD. After oral administration to Trinitrobenzene sulfonic acid induced rats, nanoparticles significantly lowered inflammatory cell activity in rat colon homogenates compared to the free drug.

1.7.2 Microparticles for oral delivery

Similar with nanoparticles, microparticles offer numerous advantages such as targeted delivery, protection of drug during gastrointestinal tract, and intestinal permeability enhancement according to the polymer applied. Despite the impressive progress made in targeting delivery, which allows good drug protection with less side effects, only a few drug-delivering nanoparticles have really reached the market. The following shortcomings are the main limits to their development[140,141]:

1. Low drug loading capacity. The drug loading (the weight of drug compared with the

weight of carrier material) of nanoparticles is usually less than 5%[142]. Due to this poor value, either the quantity of drug administrated is not enough to reach a pharmacologically active concentration at the target, or the required quantity of carrier material is too great, producing toxicity or other side-effects.

2. Burst release. The other main limit of nanoparticles is the rapid drug release after administration. It may come mainly from either the quick release of drug simply adsorbed or anchored at the surface of nanoparticles, or from its fast across the short length radius of nanoparticles. As a result, a significant part of drug will be released before reaching targets, leading to low efficacy as well as side-effects.

Compared with nanoparticles, microparticles usually offer better drug loading as well as longer sustained release time. On the one hand, with bigger size, microparticles can load more drugs than nanoparticles with the same amount of polymer. On the other hand, as the mechanisms of drug release from particles (especially polymeric particles) include diffusion, particle erosion and degradation (for nanoparticle using biodegradable material), it takes a longer time for erosion-triggers to penetrate the particle, and to the drugs or debris to release out in the bigger microparticles[142–144].

Chapter 2: Intestinal permeability of *S*-nitrosothiols

2.1 Transport mechanism through intestinal barrier

The main routes which drugs cross the intestine membrane can be divided into two pathways: paracellular pathway and transcellular pathway. Paracellular pathway means drugs cross through the aqueous pores at the tight junctions between the intestinal cells while transcellular pathway requires drug diffusion across the lipid cell membrane. The mechanism of intestinal transport can also be divided into passive diffusion or active transport. The active transport can be divided by two part: influx and efflux. A lot of influx transporters are expressed by the small intestinal mucosa. Influx is important for the absorption of nutrients and vitamins, it also plays important roles in the drugs absorption, such as the large neutral amino acids, di-/tripeptides, nucleosides bile acids, and monocarboxylic acid transporters. However, the main function of efflux is as an absorptive barrier to limit oral bioavailability of many drugs and xenobiotics. These transporters include breast cancer resistance protein, P-glycoprotein, organic ion transporters and multi-drug resistance-associated protein[145–147].

In order to apply RSNOs through the oral delivery route, it is important to know more about the intestinal permeability of different RSNOs. Different mechanisms could be involved in the absorption of molecules through the intestinal barrier: paracellular way, transcellular way (including carrier-mediated way as well as receptor-mediated transport)[128,129] (Figure 14).

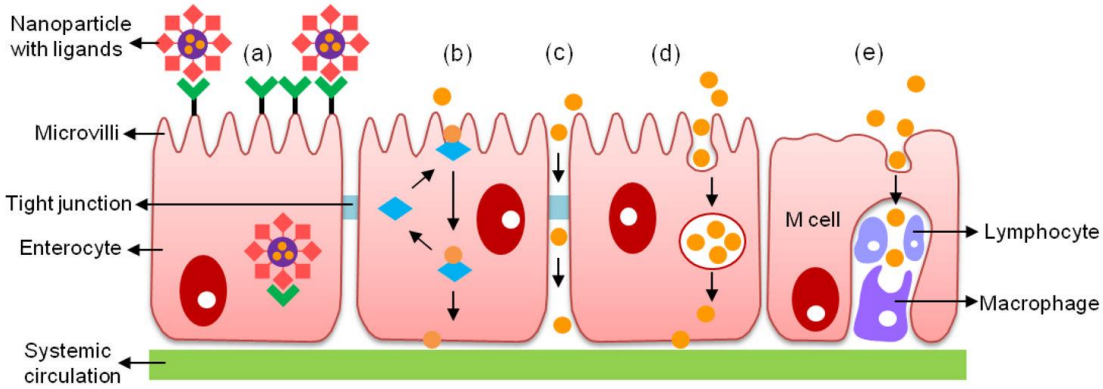

Figure 14. mechanisms of molecules crossing through the intestinal barrier[131]. (a) receptor-mediated transport; (b) carrier-mediated transport; (c) paracellular transport; (d) transcellular transport; and (e) M cell mediated transport (i.e., phagocytosis by M cells).

Paracellular transport

In paracellular transport, molecules cross the epithelium through the intercellular spaces between the epithelial cells. As a passive transport, the paracellular transport always results from diffusion and is controlled by the tight junctions. The tight junctions are the main barriers that limit the permeation rate during the paracellular transport of ions and large molecules[148]. The size of the paracellular space is around 10 Å and the sizes of aqueous pores resulting from epithelial tight junctions differ from their location: 7-9 Å, approximately 3–4 Å and 8–9 Å in human jejunum, ileum, and colon, respectively[149]. Thus, molecules with a radius above 15 Å (around 3.5 kDa) cannot be transported through the paracellular way[150]. Furthermore, tight junctions represent only around 0.01% of the total area on the intestine surface[151]. In addition, paracellular transport varies depending on electrical resistance among epithelia but is not largely influenced by the physicochemical properties of drugs, such as lipophilicity or hydrogen bonding capacity[152,153].

Transcellular transport

The transcellular transport occurs by transcytosis across intestinal epithelial cells, a special process through which cells take up particles. A typical example of transcellular transport is the transport of glucose from the intestinal lumen to the extracellular side through epithelial cells. An endocytic process takes place first at the cell apical membrane, followed with transport through the cell and finally release of glucose at the basolateral side[154]. Compared with the apical membrane, the basolateral membrane is thinner and more permeable due to the low protein-to-lipid ratio. Two key factors are significant to the transcellular transport: (i) physicochemical properties of molecular or particles, such as liophilicity, size, charge and hydrogen bond potential (ii) physiology of the gastrointestinal tract[155,156]. The two primary intestinal cells for transport are enterocytes and M cells. Enterocytes are the main cells lining the gastrointestinal tract whereas M cells represent a very small proportion of the intestinal epithelium[157]. M cells are mainly located in the epithelium of Peyer's patches and they deliver peptides and proteins from the lumen to the underlying lymphoid tissues to help inducing immune responses. M cells can transport a wide variety of materials with their high transcytosis capacity[158,159]. M cells take up particles, macromolecules and microorganisms through adsorptive endocytosis *via* clathrin-

coated pits and vesicles, fluid phase endocytosis and phagocytosis[160].

Carrier-mediated transport is an active absorption, which requires energy and carriers to uptake specific molecules. The carrier recognizes the target molecules and transport them even against the concentration gradient. Through carrier-mediated transport, drugs can be transferred across the intestine barrier and then released into circulation[161]. The process is especially adapted to small hydrophilic molecules[162], such as small di/tripeptides, amino acids and monosaccharides[163].

Protein drugs are the main clients in receptor-mediated transport. During this process, protein drugs usually act as a receptor for surface-attached ligands or as a receptor-specific ligand for surface-attached receptors[164]. It has been reported that receptor-mediated transport can be exploited to increase a protein bioavailability through oral delivery. The receptor-mediated transport comprises cell invagination, resulting in the formation of a vesicle. This transportation is called endocytosis and includes pinocytosis and phagocytosis, or the receptor-mediated potocytosis (nonclathrin-mediated) and endocytosis (clathrin-mediated).

As both carrier- and receptor-mediated transport also drive the target molecule into circulation through the cell or cell membrane, they can be regarded as transcellular pathways.

2.2 Intestinal permeability measurement with Caco-2 cell monolayer model

It is critical to select the right techniques to assess the intestinal permeability of drugs. A wide range of methods have been applied to measure the intestinal permeability according to the different settings (*in vivo*, *ex vivo* or *in vitro*). The *in vivo* measurement is the most direct method to check the intestinal permeability. For example, the typical measurement for intestinal permeability in humans is testing the urinary excretion of lactulose and mannitol (non-metabolized sugars) after oral administration over a 6 h period. The ratio of lactulose/mannitol can reflect the intestinal permeability state[165]. In addition, the *in vivo* measurement method has also been applied in the animal studies after oral gavage of PEG, sugars, or fluorescently labeled dextrans followed by detection in the blood or urine[166,167]. However, *in vivo* measurement is time-consuming and has several drawbacks, such as variation between the humans and animals or just the different genotype and phenotype of

humans[165]. *Ex vivo* test is another method applied to the intestinal permeability. One of the commonly used is Ussing Chamber, which mimics the *in vivo* compartmentalization between the intestine lumen and the intestine mucosa[168]. An intestine segment separates the system into two compartments (donor and acceptor) with equal volumes. Through adding different permeability markers (such as sodium fluorescein (paracellular), propranolol (transcellular), mannitol…) to donor compartment and harvesting in acceptor compartment, the intestinal permeability can be measured. This method is limited by its short time of measurement because of the low *ex vivo* viability (approximately 2 h)[168].

Compared with *in/ex vivo,* the *in vitro* models have several advantages such as lower cost, high accessibility and higher throughput. Furthermore, it may reduce the use of animals for experimental purposes[169]. Cell monolayer cultures have been regarded as one of the most important models for intestinal permeability. Through incubating the differentiated intestinal epithelial cells (such as Caco-2, HT-29, and T-84 cells) on semipermeable filter, an oriented cell monolayer is formed thus defining an apical and a basolateral compartment[170]. Among these different cell lines, Caco-2 is the most widely applied to mimic the intestinal epithelial barrier. Despite Caco-2 cells were derived from human colorectal adenocarcinoma, they are close to enterocytes from small intestine after differentiation and polarization[171]. For many compounds, strong correlations have been observed between permeability (passive transcellular and paracellular) across Caco-2 cell monolayers and oral bioavailability in humans[172,173]. Thus, this *in vitro* model has also been applied to rapidly predict the intestinal permeability of a as well as the pathways utilized during transport[174,175].

2.3 Biopharmaceutical Classification System

The drugs are categorized into 4 classes according to the Biopharmaceutical Classification System (BCS) based on the solubility and permeability to bio-membranes (as shown in Figure 15[176]). The BSC is regarded as a guideline for the formulation scientists, for the proper selection and design of the formulation of different drug substance.

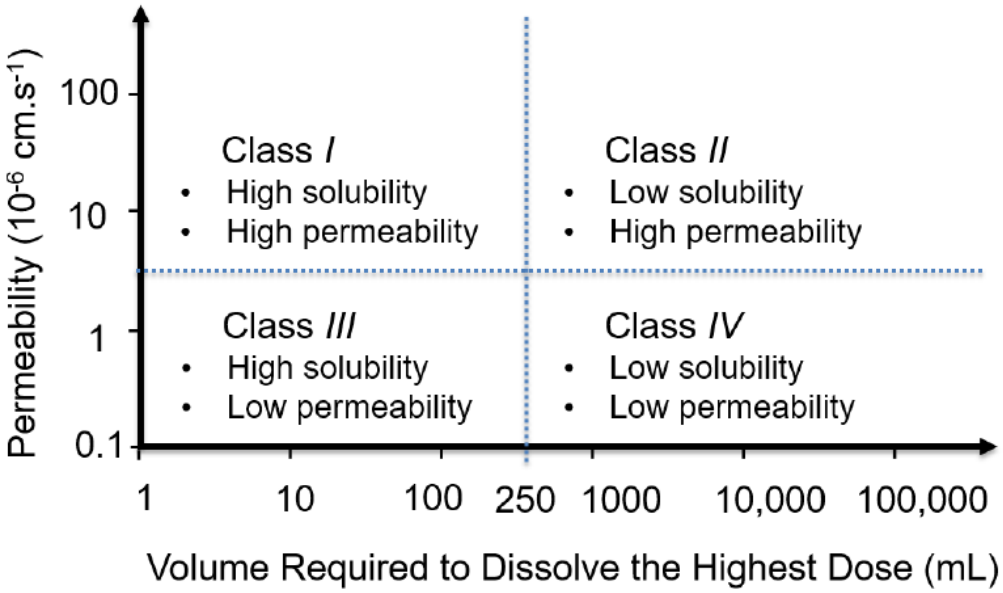

Figure 15. drugs classification according to the Biopharmaceutical Classification System (BCS)

Class I: Drugs belonging to Class I have fast dissolution and rapid bioavailability after oral administration. If they qualify pharmacokinetically and pharmacodynamically for the purpose, these drugs are good candidates for controlled drug delivery.

Class II: These drugs have low solubility but high permeability, thus, the dissolution rate becomes the key parameter for bioavailability. These drugs display variable bioavailability and need enhancement of their dissolution rate to improve their bioavailability. They are also suitable for controlled drug delivery.

Class III: Permeation through the intestinal membrane becomes the rate-determining step for drugs of Class III. As absorption is limited by permeation rate, their bioavailability is independent of drug release from the dosage form. These drugs are problematic for controlled release application and they need improvement of intestinal permeability to enhance the bioavailability.

Class IV: Drugs belonging to this class exhibit poor and variable bioavailability. Several parameters govern their bioavailability, such as intestinal permeability, rate of dissolution, gastric emptying, and so on. They are generally not suitable for oral drug delivery.

Thus, it is important to make clear the mechanism about the intestinal permeability of different RSNOs and which class it belongs to. In the article 2, intestinal permeability of three different RSNOs (GSNO, NACNO and SNAP) have been tested through a Caco-2 monolayer transwell model:

Article 2: Intestinal absorption of *S*-nitrosothiols: permeability and transport mechanisms

Absorption intestinale des S-nitrosothiols : Mécanismes de transport et de perméabilité

Justine Bonetti[#], Yi Zhou[#], Marianne Parent, Igor Clarot, Haiyan Yu, Isabelle Fries-Raeth, Pierre Leroy, Isabelle Lartaud, Caroline Gaucher*

[#] Les deux auteurs ont contribué à parts égales à ce travail.

Biochemical Pharmacology 155 (2018) 21–31

Contents lists available at ScienceDirect

Biochemical Pharmacology

journal homepage: www.elsevier.com/locate/biochempharm

Intestinal absorption of *S*-nitrosothiols: Permeability and transport mechanisms

Justine Bonetti[1], Yi Zhou[1], Marianne Parent, Igor Clarot, Haiyan Yu, Isabelle Fries-Raeth, Pierre Leroy, Isabelle Lartaud, Caroline Gaucher*

Université de Lorraine, CITHEFOR, F-54000 Nancy, France

ARTICLE INFO

Keywords:
S-Nitrosothiols
Nitric oxide
Intestinal permeability
Caco-2 cells
Passive diffusion

ABSTRACT

S-Nitrosothiols, a class of NO donors, demonstrate potential benefits for cardiovascular diseases. Drugs for such chronic diseases require long term administration preferentially through the oral route. However, the absorption of *S*-nitrosothiols by the intestine, which is the first limiting barrier for their vascular bioavailability, is rarely evaluated. Using an *in vitro* model of intestinal barrier, based on human cells, the present work aimed at elucidating the mechanisms of intestinal transport (passive or active, paracellular or transcellular pathway) and at predicting the absorption site of three *S*-nitrosothiols: *S*-nitrosoglutathione (GSNO), *S*-nitroso-*N*-acetyl-L-cysteine (NACNO) and *S*-nitroso-*N*-acetyl-D-penicillamine (SNAP). These *S*-nitrosothiols include different skeletons carrying the nitroso group, which confer different physico-chemical characteristics and biological activities (antioxidant and anti-inflammatory). According to the values of apparent permeability coefficient, the three *S*-nitrosothiols belong to the medium class of permeability. The evaluation of the bidirectional apparent permeability demonstrated a passive diffusion of the three *S*-nitrosothiols. GSNO and NACNO preferentially cross the intestinal barrier though the transcellular pathway, while SNAP followed both the trans- and paracellular pathways. Finally, the permeability of NACNO was favoured at pH 6.4, which is close to the pH of the jejunal part of the intestine. Through this study, we determined the absorption mechanisms of *S*-nitrosothiols and postulated that they can be administrated through the oral route.

1. Introduction

Nitric oxide (NO) is a gaseous mediator with a short half-life (less than 5 s [1]). Due to its radical nature and oxidative activity, NO is involved in various signalling pathways among different cellular types and physiological systems. NO is continuously synthesised by oxydoreductases, *i.e.* the three endothelial, inducible or neuronal isoforms of NO synthases. The decrease in NO bioavailability, linked to vascular endothelium dysfunction and oxidative stress, plays a major role in ageing and cardiovascular chronic diseases like atherosclerosis, angina pectoris and stroke. As a result, the restoration of NO bioavailability, using among NO donors the physiologically occurring *S*-nitrosothiols, is a therapeutic key to treat cardiovascular diseases [2–7]. *S*-Nitrosothiols are formed by *S*-nitrosation – *i.e.* formation of a covalent bond between NO and a reduced thiol function of a cysteine residue belonging to high or low molecular weight proteins or peptides. *In vivo*, *S*-nitrosothiols like *S*-nitrosoalbumin, *S*-nitrosohemoglobin and *S*-nitrosoglutathione (GSNO) are the physiological forms of NO storage and transport [8]. Indeed, the formation of the *S*-NO bond extends NO half-life from 45 min up to several hours [9–10] and limits the oxidative/nitrosative stress induced by NO oxidation into peroxynitrite ions ($ONOO^-$) [11]. Despite the therapeutic potential of *S*-nitrosothiols, their half-life linked to their physico-chemical instability (heat, light, metallic cations,…) and/or enzymatic (redoxines or, for GSNO only, γ-glutamyltransferase) degradation, is too short for chronic diseases treatment [12].

Nowadays, many preclinical studies focused on cardiovascular therapeutics using *S*-nitrosothiols [6,13–17]. For example, daily intraperitoneal administration of *S*-nitroso-*N*-acetyl-L-cysteine (NACNO) for two weeks shows anti-atherosclerotic effects in mice [13]. However, compared to the oral route, the intraperitoneal administration is less suitable for chronic treatments. GSNO administration through the oral route in a context of stroke [14] results in neuroprotective effects: GSNO maintains the blood-brain barrier integrity, reduces peroxynitrite formation and stabilises several deleterious factors *via* *S*-nitrosation [13–16]. Despite such beneficial effects following oral administration, to the best of our knowledge, no study evaluated the mechanisms of

* Corresponding author at: Université de Lorraine, CITHEFOR EA 3452, Faculté de Pharmacie, BP 80403, F-54001 Nancy Cedex, France.
E-mail address: caroline.gaucher@univ-lorraine.fr (C. Gaucher).
[1] Both authors contributed equally to this work.

https://doi.org/10.1016/j.bcp.2018.06.018
Received 12 April 2018; Accepted 19 June 2018
Available online 21 June 2018

intestinal absorption of GSNO and other *S*-nitrosothiols. Only Pinheiro et al. [17] demonstrated that oral administration of nitrite and nitrate ions (stable NO derived species) to rats increased the concentration of circulating *S*-nitrosothiols, thus produced antihypertensive effects. This study indirectly proves the intestinal absorption of *S*-nitrosothiols without elucidated the underlying mechanisms. However, the understanding of the intestinal absorption mechanisms of *S*-nitrosothiols is a prerequisite to control the dose and the kinetic of NO reaching its action sites.

To predict the intestinal absorption of drugs, the Biopharmaceutical Classification System (BCS) [18] defines four classes based on the physico-chemical properties (solubility) and intestinal permeability of drugs. The intestinal permeability of a drug is characterised, using *in vitro* or *ex vivo* models, by apparent permeability coefficient (Papp) from low permeability ($< 1 \times 10^{-6}$ cm.s^{-1}) to high permeability ($\geq 10 \times 10^{-6}$ cm.s^{-1}) including also a medium permeability class [19]. Thus far, only one of our studies was interested in the improvement and the prolongation of GSNO intestinal absorption by proposing alginate/chitosan nanocomposite formulation [20]. Using an *in vitro* intestinal barrier model of differentiated Caco-2 cells, we showed low intestinal permeability for GSNO with a Papp of 0.83×10^{-7} cm.s^{-1}. The nanocomposite formulation delayed GSNO absorption up to 24 h (1 h for free GSNO) and multiplied by four the Papp value (3.41×10^{-7} cm.s^{-1}) even if GSNO stayed in the low class of permeability [20]. This study showed the ability for GSNO to cross the intestinal barrier model and the possibility to modulate its kinetics of absorption. This opens new therapeutic applications in the treatment of chronic pathologies linked to a decrease of NO bioavailability.

Intestinal absorption of low molecular weight molecules is mainly driven by their physico-chemical properties such as lipophilicity, correlated with the octanol/water partition coefficient, expressed as a logarithmic value (log P), and the ionisation constant (pKa). For *S*-nitrosothiols, the log P value is driven by the skeleton carrying NO. GSNO, NACNO and *S*-nitroso-*N*-acetyl-D-penicillamine (SNAP), the three main *S*-nitrosothiols described in the literature, are characterised by calculated log P value of −2.70, −0.47 and 1.08, respectively [2]. The skeleton carrying NO presents also different therapeutic properties linked with its chemical structure. GSNO is a physiological *S*-nitrosothiol [21], present in the cytosol at a high concentration especially in erythrocytes [22], platelets and cerebral tissue. Its reduced glutathione (GSH) skeleton shows an antioxidant chemical structure thanks to its thiol functional group and forms, with the glutathione disulphide (GSSG), the intracellular redox buffer. NACNO and SNAP are synthetic *S*-nitrosothiols. NACNO with its *N*-acetyl-L-cysteine (NAC) skeleton possesses also an antioxidant activity in accordance with its chemical structure (thiol function). Furthermore, NAC is already used in human medicine as a mucolytic agent (oral administration) or as the antidote in acetaminophen intoxication [23]. SNAP shows in addition to its antioxidant properties (thiol function), an anti-inflammatory skeleton, *N*-acetyl-D-penicillamine (NAP) is used in the treatment of Wilson's disease (Trolovol®) and rheumatoid arthritis.

In this study, using an *in vitro* cell model of intestinal barrier, we propose to elucidate the intestinal transport mechanisms of *S*-nitrosothiols and NO in relation to their physico-chemical properties. Three different conditions were studied, i) permeability from the apical to the basolateral compartment, ii) permeability from the basolateral to the apical compartment to highlight an active transport such as drug influx/efflux, or a passive diffusion, and iii) permeability from an acidified apical compartment, mimicking the luminal intestinal pH of the jejunum, the major site of amino acid absorption [24].

2. Material and methods

2.1. Material and reagents

Eagle's Minimum Essential Medium (EMEM), foetal bovine serum (FBS), sodium pyruvate, penicillin 10 000 U.mL^{-1} and streptomycin 10 mg.mL^{-1} mix, trypsin, non-essential amino acids, glutamine, Hank's Balanced Salt Solution (HBSS Ca^{2+}/Mg^{2+}), sodium nitrate ($NaNO_3$), 2,3-diaminonaphthalene (DAN), 1.0 M hydrochloric acid (HCl) solution, propranolol hydrochloride, furosemide salt, triethylamine, 2-(*N*-morpholino)ethanesulfonic acid (MES), Trisma base (Tris), sodium chloride (NaCl), Igepal CA-630, sodium dodecyl sulfate (SDS), ethylenediaminetetraacetic acid (EDTA), neocuproine and *N*-ethylmaleimide (NEM) were purchased from Sigma, France. Mercuric chloride ($HgCl_2$), orthophosphoric acid and sodium tetraborate were purchased from Prolabo (VWR). Sodium nitrite ($NaNO_2$) from Merck, sodium hydroxide (NaOH) from VWR Chemicals, methanol from Carlo Erba Reagents and acetonitrile was from Biosolve. Nitrite/nitrate fluorimetric kit was purchased from Cayman Chemical (Ref. 780051).

2.2. S-Nitrosothiols synthesis

GSNO, NACNO and SNAP were synthesised according to a previously described method [25]. Briefly, GSH, NAC or NAP were incubated with one equivalent of sodium nitrite under acidic condition. Then, the pH was shifted to 7.4 using a phosphate buffered saline (PBS 0.148 M) solution. The final concentration was assessed by UV–Vis. spectrophotometry (Shimadzu; UV-spectrophotometer; UV-1800) using the specific molar absorbance of the *S*-NO bond at 334 nm for GSNO and NACNO (ε_{GSNO} = 922 M^{-1} cm^{-1}; ε_{NACNO} = 900 M^{-1} cm^{-1}) and at 340 nm for SNAP (ε_{SNAP} = 1020 M^{-1} cm^{-1}).

2.3. Caco-2 cells culture and cytocompatibility

Intestinal Caco-2 cells (ATCC® HTB-37™) from passage 36 to 45 were grown in complete medium consisting of EMEM supplemented with 10% (v/v) of FBS, 4 mM of glutamine, 100 U/mL of penicillin, 100 U/mL of streptomycin, 1% (v/v) of non-essential amino acids. Cells were cultivated at 37 °C under 5% CO_2 (v/v) in a humidified incubator. Caco-2 cells were seeded in 96-wells plates at 2×10^4 cells/well 24 h before experiment. They were then exposed to each *S*-nitrosothiol (from 10 to 100 µM) for 24 h at 37 °C, complete medium being used as control. Cytocompatibility was assessed through metabolic activity with the 3(4,5-dimethylthiazol-2-yl)-2,5-diphenyltetrazolium bromide (MTT) assay. The absorbance of extracted formazan crystals was read at 570 nm with a reference at 630 nm (EL 800 microplate reader, Bio-TEK Instrument, Inc®, France). Metabolic activity in control condition was considered as 100%.

2.4. Intestinal permeability of reference molecules and S-nitrosothiols

Caco-2 cells were seeded at 2×10^6 cell/cm^2 on cell culture inserts (Transwell®, Corning, USA, membrane with 0.4 µm pore size, 1.12 cm^2 area or 4.97 cm^2) disposed in a 12-wells or 6-wells plate, respectively. The complete medium was replaced every two days during the first week of cell proliferation. During the second week, the medium was replaced every day until the differentiated cell monolayer was formed (14–15 days). The formation of the barrier was followed by transepithelial electrical resistance (TEER) measurement using a Millicell®-Electrical Resistance system (Millipore, USA) and validated for TEER values higher than 500 Ω.cm^2.

The bidirectional permeability of each *S*-nitrosothiol across the Caco-2 monolayer was evaluated from the apical to basolateral (A-B) compartment, mimicking physiological permeability conditions (intestinal lumen to blood compartment), and from the basolateral to the apical (B-A) (Fig. 1) compartment in HBSS at pH 7.4 to evaluate possible efflux mechanisms. A third condition evaluates the importance of the influence of luminal pH adjusted to 6.4 with 0.5 M MES solution in the apical compartment to determine the intestinal site of absorption (intestinal segment).

The concentration of *S*-nitrosothiols used to study the permeability

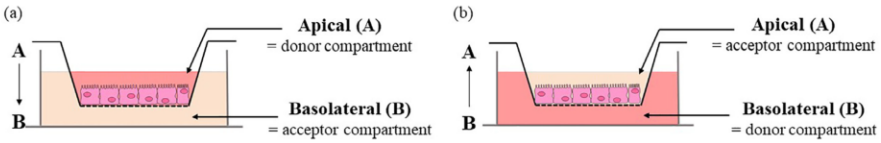

Fig. 1. Schematic representation of the bidirectional permeability of *S*-nitrosothiols across the Caco-2 monolayer. (a) From the apical (intestinal lumen) to the basolateral (bloodstream) compartment (on the left, A → B) to study physiological intestinal permeability, (b) from the basolateral to the apical compartment (on the right, B → A) to study *S*-nitrosothiol efflux.

in each direction was the same (100 µM). Since the apical and the basolateral compartments have different volumes (0.5 and 1.5 mL, respectively), the initial amounts of *S*-nitrosothiol for A-B and for B-A permeability studies were 50 and 150 nmol, respectively. $NaNO_2$ treatment (100 µM) was used as a positive control for nitrite ions permeability. The bidirectional permeability of propranolol (50 µM) and furosemide (100 µM), two reference molecules belonging to the high and low permeability class, respectively, was also assessed to surround the permeability of *S*-nitrosothiols [26,27] and to validate our model faced to the literature.

Permeability tests were conducted during 4 h under orbital shaking (500 rpm) at 37 °C. In the acceptor compartment, *S*-nitrosothiols were considered as RSNO because the R skeleton carrying NO cannot be identified by the methodology of quantification used. Reference molecules as well as NOx species (RSNO, nitrite ions and nitrate ions) were quantified after 1 h (entire volume of acceptor compartment removed) in the acceptor compartment and after 4 h in both compartments (for methodologies, see Sections 2.5. and 2.6.). RSNO and nitrite ions were also quantified inside the cells after 1 h and 4 h of permeability study.

At the end of the study, the integrity of the intestinal cell monolayer was checked by measuring the TEER value and the permeability of sodium fluorescein (5 µM), a marker of low paracellular permeability. A TEER value higher than 300 $\Omega.cm^2$ as well as a 5% of fluorescein permeability validated the integrity of the intestinal monolayer at the end of the experiment [28,29].

2.5. Quantification of S-nitrosothiols, nitrite and nitrate ions

S-Nitrosothiols and nitrite ions were immediately quantified using a fluorimetric method [30] with standard curves of GSNO and sodium nitrite, respectively (Table 1). Briefly, N_2O_3 generated from acidified nitrite ions reacts with DAN in the presence (for RSNO) or absence (for nitrite ions) of $HgCl_2$ producing 2,3-naphthotriazole that emits fluorescence at 415 nm after excitation at 375 nm (JASCO FP-8300, France). Nitrate ions quantification, using a standard curve of sodium nitrate included a reduction step to nitrite ions by reacting with nitrate reductase and its cofactors before the addition of DAN reagent (fluorimetric kit nitrite/nitrate Cayman Chemical) (Table 1). The concentration of nitrite ions (DAN assay) was subtracted from the value obtained by DAN-Hg^{2+} quantification to obtain the RSNO concentration and from the nitrate reductase quantification to obtain the nitrate ions concentration. The cumulative amounts of RSNO, NO_2^- and NO_3^- crossing the Caco-2 monolayer were calculated from the concentrations measured at 1 h and 4 h of the permeability studies in the acceptor compartment.

For intracellular quantifications, cells were lysed in 50 mM Tris buffer pH 6.8 added with 150 mM of NaCl, 1% of Igepal CA-630 (v/v), 0.1% of SDS (v/v), 1 mM of EDTA, 0.1 mM of neocuproine, 20 mM of sodium tetraborate and 10 mM of NEM.

2.6. Quantification of furosemide and propranolol

This procedure was adapted from [31–33] for propranolol and from [34] for furosemide. Briefly, the separation was performed on a C18 analytical column (Macherey-Nagel LiChrospher RP 18e; 5 µm; 125 × 4 mm) eluted with a mobile phase composed of acetonitrile added with 14 mM triethylamine in water buffered with orthophosphoric acid, pH 2.5 (30/70; v/v) at a flow rate of 1.0 $mL.min^{-1}$ and with a column temperature of 40 °C. The injection volume was 20 µL. Propranolol and furosemide were detected using a spectrofluorometric detector (model Jasco FP-920) set at λ_{ex} = 230 nm/λ_{em} = 340 nm, and λ_{ex} = 235 nm/λ_{em} = 402 nm, respectively. Standard curves of propranolol and furosemide were established between 0.5 and 10.0 µM and 62.5 nM to 2.0 µM, respectively.

2.7. Calculation of apparent permeability coefficients and recovery rates

2.7.1. Apparent permeability coefficient

The apparent permeability coefficient (Papp) values were calculated using the following equation (Eq. (1):

$$Papp = \frac{dQ}{dt} \times \frac{1}{A \times C_0} \quad (1)$$

dQ/dt ($mol.s^{-1}$) refers to the permeability rate of reference molecules, RSNO or NOx species (mol) in the acceptor compartment at the time (s) of quantification, A (cm^2) refers to membrane diffusion area, and C_0 (mol.mL-1 or $mol.cm^{-3}$) refers to the initial concentration in the donor compartment.

2.7.2. Recovery rate

Mass balance was calculated as the addition of the amount of drug recovered in the acceptor compartment after each interval and in the donor compartment at the end of the experiment.

2.8. Statistical analysis

Results are shown as mean ± standard deviation (SD), based on 3 or 4 independent experiments in duplicate. Values were compared with

Table 1
Standard curves validation parameters for *S*-nitrosothiols (RSNO), nitrite ions (NO_2^-) and nitrate ions (NO_3^-) in HBSS with Ca^{2+}/Mg^{2+}. Mean ± SD; n = 3.

	Concentration range (µM)	Standard curves equation	Relative standard deviation (%)	R^2
RSNO	0.1–2.0	y = (1451 ± 236)x + (399 ± 98)	0.1 µM: 12.3 2 µM: 1.2	0.99
NO_2^-		y = (1527 ± 96)x + (435 ± 89)	0.1 µM: 4.3 2 µM: 3.2	
NO_3^-	0.01–3.75	y = (264 ± 22)x + (1719 ± 116)	0.01 µM: 8.4 3.75 µM: 5.1	

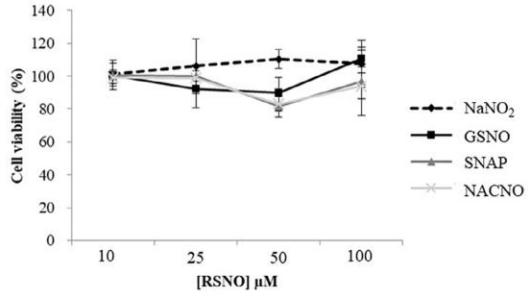

Fig. 2. Cytocompatibility of *S*-nitrosothiols with Caco-2 cells. Cell activity was assessed with the MTT test, 24 h after incubation with different *S*-nitrosothiols or $NaNO_2$. Values are expressed as mean ± SD of three independent experiments done in duplicate.

one-way ANOVA (treatments) or two-way ANOVA (treatment and time) followed by a Bonferroni's post-test using the Graphpad Prism 5 software; $p < 0.05$ was considered as statistically significant. Statistics are analysed excluding $NaNO_2$ treatments, which too high permeability values interfered with the statistical comparison of *S*-nitrosothiols.

3. Results

3.1. Cytocompatibility

Cell viability was not affected by any of the *S*-nitrosothiols presently tested and $NaNO_2$, with more 80% of viability independently of the concentration used (Fig. 2). For all the forthcoming experiments, a concentration of 100 µM of each *S*-nitrosothiol will be safely used.

Table 2
Values of apparent permeability coefficient (Papp) for NOx species (RSNO + NO_2^- + NO_3^-) and the RSNO molecular form after 4 h of permeation from the apical to the basolateral compartment. nd: not determined, LOQ: Limit of quantification. Mean ± SD of four independent experiments done in duplicate.

Treatments	NOx Papp ($\times 10^{-6}$ cm.s^{-1})	RSNO Papp ($\times 10^{-6}$ cm.s^{-1})
GSNO	2.6 ± 0.9	0.2 ± 0.1
NACNO	5.0 ± 2.1	0.21 ± 0.08
SNAP	3.3 ± 1.6	0.13 ± 0.09
$NaNO_2$	12.3 ± 3.2	Under LOQ
Propranolol	24.4 ± 1	nd
Furosemide	0.3 ± 0.1	nd

3.2. S-Nitrosothiols permeability from the apical to the basolateral compartment

S-Nitrosothiols permeation through the intestinal barrier model, evaluated in the A-B direction, showed the same profile for each treatment (GSNO, NACNO and SNAP) (Fig. 3). Each *S*-nitrosothiol (treatment) was permeated under three different chemical species. The RSNO form (Fig. 3A) was less permeated (0.50% ± 0.14% of the initial amount deposited in the donor compartment) than the NO_2^- (the first stable oxidation degree of NO in aqueous media) and NO_3^- ionic forms (4.8% ± 1.9% and 7.9% ± 2.4% of the initial amount, respectively). The NACNO treatment led to a higher permeation under the RSNO form than the GSNO and SNAP treatments (Fig. 3A). The duration of the study has no impact on the permeability of each treatment under the RSNO form while the permeability under the nitrite ions and nitrate ions (the oxidation product of nitrite ions) forms depended on time (Fig. 3B and 3C, $p_{time} < 0.05$) and on the treatment. Indeed, the NACNO treatment induced a higher absorption of NO_2^- (and NO_3^-) ionic forms than the GSNO and the SNAP treatments

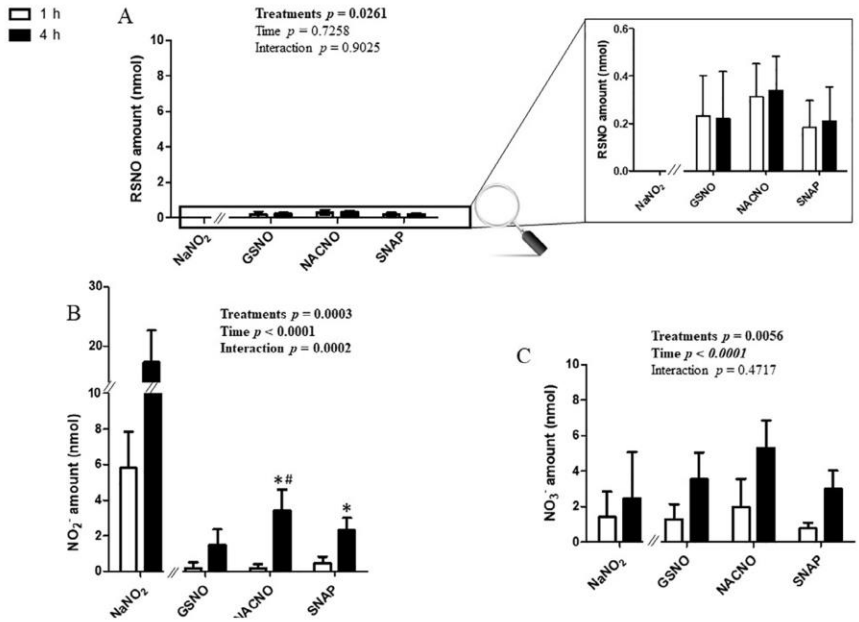

Fig. 3. Apical (pH 7.4) to basolateral compartment – Quantification in the basolateral compartment of permeated (A) RSNO, (B) NO_2^- and (C) NO_3^- after 1 h and 4 h of exposure to 50 nmol of each treatment. Results are shown as mean ± SD of four independent experiments done in duplicate and are compared using two-way ANOVA ($p_{treatment}$ (GSNO, NACNO, SNAP; excluding $NaNO_2$), p_{time} (1h, 4 h) and $p_{interaction}$). * *vs.* GSNO; # *vs.* SNAP at the same time; $p < 0.05$ (Bonferroni's multiple comparisons test).

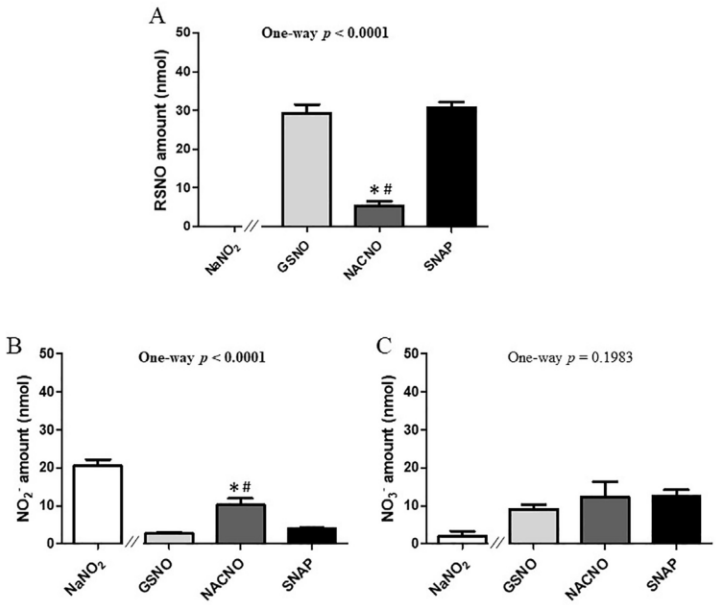

Fig. 4. Apical (pH 7.4) o basolateral compartment – Quantification in the apical compartment of remaining (A) RSNO, (B) NO_2^- and (C) NO_3^- and 4 h of exposure to 50 nmol of each treatment. Results are shown as mean ± SD of four independent experiments done in duplicate and are compared using one-way ANOVA (excluding $NaNO_2$) Bonferroni post-test. * *vs.* GSNO; # *vs.* SNAP at the same time; $p < 0.05$.

Table 3
Mass balance for each treatment (initial amount: 50 nmol) after 4 h of permeation from the apical to the basolateral compartment. Mean ± SD of four independent experiments done in duplicate.

Treatments	Amount (nmol)	Percentage of initial amount
GSNO	46 ± 4	92 ± 8
NACNO	38 ± 6	77 ± 12
SNAP	53 ± 7	106 ± 13
$NaNO_2$	41 ± 8	83 ± 16

($p_{treatment}$ = 0.0003 and $p_{interaction}$ 0.0002), especially after 4 h ($p_{time} < 0.0001$) (Fig. 3B).

The $NaNO_2$ treatment led to the permeability of the two ionic species only (Fig. 3). The permeability under the NO_2^- form was time dependent and 30% higher than the permeability of each *S*-nitrosothiol treatment under NO_2^- form (Fig. 3B). The permeability under the nitrate ionic form (Fig. 3C), representing 5% of the initial amount, supposes a spontaneous oxidation of nitrite ions into nitrate ions within our experimental conditions (presence of dioxygen).

The Papp values for the NOx species (addition of RSNO, NO_2^- and NO_3^-) were situated within the medium class of permeability (BCS definition) for each *S*-nitrosothiol treatment and surrounded by the Papp values of the reference drugs, propranolol and furosemide (Table 2). The permeability of *S*-nitrosothiols under the RSNO form was 25–40 times lower (Papp ≈ 0.17×10^{-6} cm.s^{-1}) than that of NOx species, confirming the higher absorption of *S*-nitrosothiols under the NO_2^- and NO_3^- ionic forms. The $NaNO_2$ treatment allowed to define a high permeability under the NO_2^- ionic form.

After 4 h of permeability, 60% of the initial amount (50 nmol) of *S*-

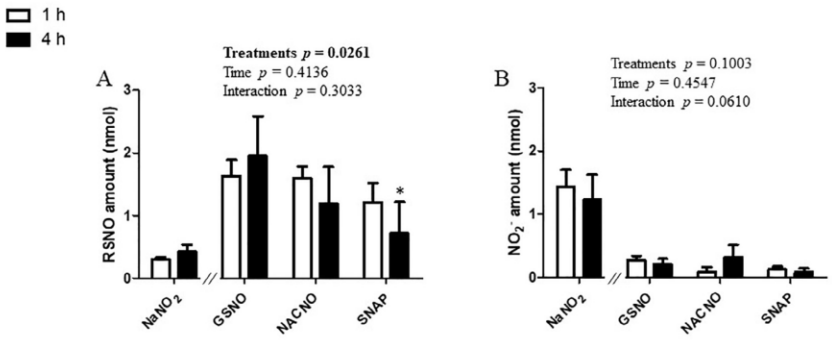

Fig. 5. Apical (pH 7.4) to basolateral permeability – Intracellular quantifications of (A) RSNO, (B) NO_2^-, (subtracted from the control cells) after 1 h and 4 h of exposure to 50 nmol of each treatment. Results are shown as mean ± SD of four independent experiments done in duplicate and are compared using two-way ANOVA ($p_{treatment}$ (GSNO, NACNO, SNAP; excluding $NaNO_2$), p_{time} (1h, 4 h) and $p_{interaction}$). * *vs.* GSNO at the same time; $p < 0.05$ (Bonferroni's multiple comparisons test).

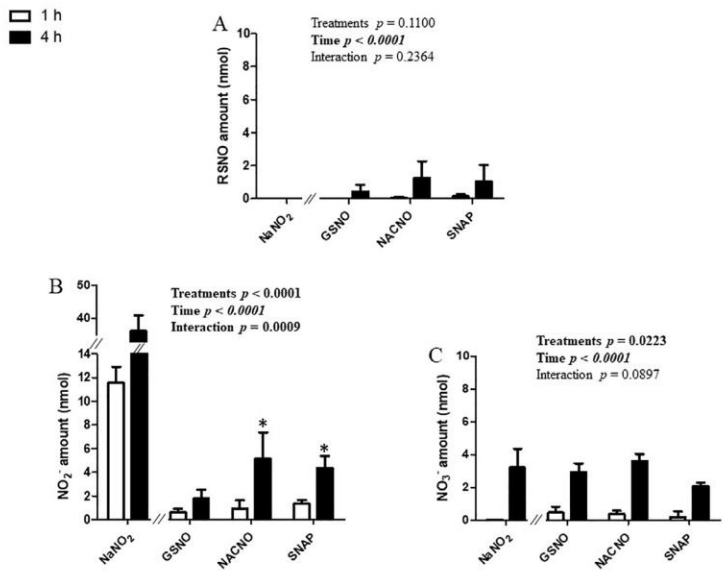

Fig. 6. Basolateral to Apical permeability – Quantification in the apical compartment of permeated (A) RSNO, (B) NO_2^- and (C) NO_3^- after 1 h and 4 h from 150 nmol of each treatment. Results are shown as mean ± SD of four independent experiments done in duplicate and are compared using two-way ANOVA ($p_{treatment}$ (GSNO, NACNO, SNAP; excluding $NaNO_2$), p_{time} (1h, 4 h) and $p_{interaction}$). * *vs.* GSNO at the same time; $p < 0.05$ (Bonferroni's multiple comparisons test).

Table 4
Values of apparent permeability coefficient (Papp) for NOx species (RSNO + NO_2^- + NO_3^-) and the RSNO form after 4 h of permeation from basolateral to apical compartment. nd: not determined, LOQ: Limit of quantification. Mean ± SD of four independent experiments done in duplicate.

Treatments	NOx Papp ($\times 10^{-6}$ cm.s^{-1})	RSNO Papp ($\times 10^{-6}$ cm.s^{-1})
GSNO	2.8 ± 1.2	0.3 ± 0.2
NACNO	4.5 ± 1.5	0.6 ± 0.6
SNAP	4.1 ± 0.7	0.5 ± 0.5
$NaNO_2$	97.5 ± 16.4	Under LOQ
Propranolol	33.1 ± 0.8	nd
Furosemide	15.2 ± 0.8	nd

nitrosothiols remained in the apical compartment for the GSNO and SNAP treatments, and only 10% for the NACNO treatment (Fig. 4A). Furthermore, the NACNO treatment led to a higher amount of nitrite ions remaining in the apical compartment compared to the GSNO and SNAP treatments (Fig. 4B), suggesting a higher degradation of NACNO into NO_2^-. Non-permeated nitrate ions amounts were around 23% for each treatment (Fig. 4C). The $NaNO_2$ treatment was still presenting 41% of non-permeated nitrite ions after 4 h (Fig. 4B) and lower spontaneous oxidation into nitrate ions (4%) within the apical compartment compared to *S*-nitrosothiol treatments (Fig. 4C).

Finally, the calculation of the mass balance (addition of all species quantified in the two compartments) after 4 h of permeability study, showed 83 ± 16% to 106 ± 13% of recovery for GSNO, SNAP and $NaNO_2$ (Table 3). Nevertheless, the NACNO treatment showed a loss of 23% of the initial amount deposited in the apical compartment. This missing can be trapped inside the cell monolayer, so cells were lysed and only RSNO and nitrite ions were quantified. Indeed, due to intracellular reducing power [35], the nitrate ions cannot exist inside cells. Quantities of RSNO found inside the cells were higher for *S*-nitrosothiol treatments than for the $NaNO_2$ treatment (Fig. 5A). This was the opposite for the NO_2^- intake (Fig. 5B). For each *S*-nitrosothiol treatment, the intracellular incorporation of the RSNO form was higher than the nitrite ions form. Intracellular quantity of the RSNO form depended on the *S*-nitrosothiol chemical structure ($p_{treatment} < 0.05$) with the lowest incorporation obtained for the SNAP treatment (< 2% of the initial amount) (Fig. 5A). Intracellular incorporation of nitrite ions was independent on time and treatments (Fig. 5B).

For intracellular quantification, the surface area of cells was increased 4.17 times (from 1.12 to 4.67 cm^2) in order to be able to quantify NOx species inside the cells. So, the intracellular amounts of RSNO and NO_2^- form were divided by 4.17 to calculate the mass balance (Table 2). The intracellular incorporation of RSNO and NO_2^- represented only 1.1%, 1.0% and 0.4% of the initial amount, for the GSNO, NACNO and SNAP treatments, respectively. Therefore, 22% of the initial amount are still missing for the NACNO treatment.

3.3. S-Nitrosothiols permeability from the basolateral to apical compartment

In order to determine the permeability modality (passive *vs.* active) for each *S*-nitrosothiol, the study was carried out in the opposite direction, from the basolateral to the apical compartment.

In this condition, the permeability of the RSNO form (Fig. 6A) was only dependent on time for each *S*-nitrosothiol treatment. The permeability of the NO_2^- and NO_3^- ionic forms was dependent on time and treatment (Fig. 6B and 6C). Higher amounts were permeated under the NO_2^- ionic form for the NACNO and SNAP treatments (≈ 3% of initial amounts) compared to the GSNO treatment (1.2% of initial amount, Fig. 6B). As in the experiments performed from the apical to the basolateral compartment (Section 3.2), NO_2^- and NO_3^- were the major permeated species.

For each *S*-nitrosothiol treatment, the Papp values in both directions (apical to basolateral versus basolateral to apical) were equivalent (Tables 2 and 4), the *S*-nitrosothiols intestinal permeability can be postulated as a passive diffusion [36]. This postulate is also based on the validation of our intestinal barrier model comparing the Papp values of reference molecules with the literature [19]. Propranolol with equivalent bidirectional Papp values follows a passive diffusion whereas furosemide with a higher Papp value from basolateral to apical than from apical to basolateral, follows an active efflux transport.

After 4 h of permeability study, 95% of the initial amount (150 nmol) of each *S*-nitrosothiol treatment remained unpermeated

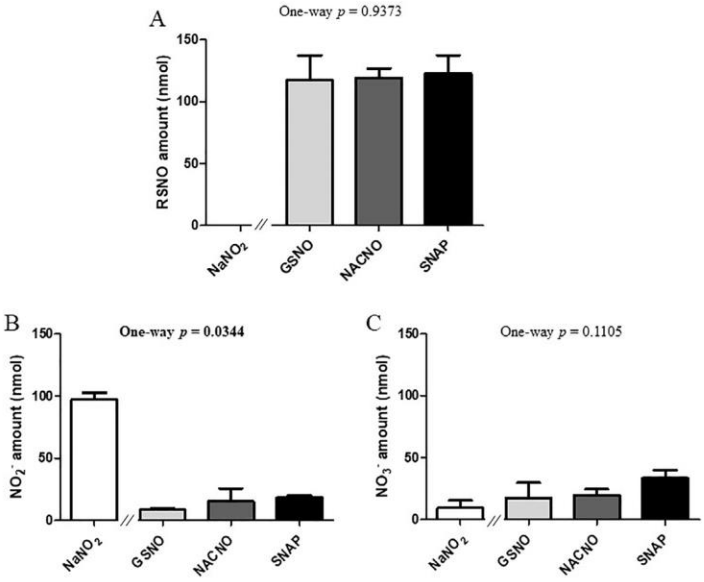

Fig. 7. Basolateral to apical permeability – Quantification in the basolateral compartment of remaining (A) RSNO, (B) NO_2^- and (C) NO_3^- after 4 h of exposure to 150 nmol of each treatment. Results are shown as mean ± SD of four independent experiments done in duplicate and are compared using one-way ANOVA (excluding $NaNO_2$).

Table 5
Mass balance for each tested treatment (initial amount 150 nmol) after 4 h of permeability from the basolateral to the apical compartment. Mean ± SD of four independent experiments done in duplicate.

Treatments	Amount (nmol)	Percentage of the initial amount
GSNO	169 ± 40	113 ± 36
NACNO	159 ± 24	106 ± 21
SNAP	162 ± 49	108 ± 44
$NaNO_2$	155 ± 18	103 ± 17

(Fig. 7). The amounts of unpermeated NO_2^- ions (Fig. 7B) were the only form that depended on *S*-nitrosothiol chemical structure ($p_{treatment} = 0.0344$). As *S*-nitrosothiols are separated from cells by the porous membrane of the device, they cannot be metabolised by cell membrane enzymes showing the great importance of *S*-nitrosothiol metabolism in their permeability. Furthermore, the high amount of remaining RSNO form (Fig. 7A) attested from the stability of each *S*-nitrosothiol in our operating conditions.

This also showed that the degradation of *S*-nitrosothiols into ionic forms observed in the apical to basolateral permeability study (Fig. 4) was due to cell membrane enzymes activity. Finally, the study of *S*-nitrosothiols permeability from the basolateral to the apical compartment showed a mass balance of 100% for each *S*-nitrosothiol treatment (Table 5).

3.4. Influence of the apical pH on S-nitrosothiols permeability

The principal site of absorption of small molecules including peptides and amino acids is the jejunum part of the intestine, which physiological pH ranges from 6 to 7. In order to study the permeability of *S*-nitrosothiols close to physiological conditions, the pH of the apical compartment mimicking the intestinal lumen was shifted of one log from pH 7.4 to pH 6.4. pH acidification has no impact on propranolol and furosemide permeability [27], so the experiment was not performed.

At pH 6.4, the permeability of each *S*-nitrosothiol under the RSNO and the ionic forms (Fig. 8) followed the same profile than at pH 7.4 (Fig. 3). However, the NACNO treatment showed a 7 times increase of permeability under the RSNO form (Fig. 8A) compared to pH 7.4. The $NaNO_2$ treatment showed a permeability under the RSNO form (Fig. 8A) and a large (10 times at 1 h and 20 times at 4 h) increase of the permeability under the NO_3^- form (Fig. 8C). So, at pH 6.4, the Papp values of NOx species and RSNO form rose for the $NaNO_2$ treatment (Table 6) compared to pH 7.4 (Table 2).

The Papp values at pH 6.4 (Table 6) maintained each *S*-nitrosothiol in the medium class of permeability for NOx species and in the low permeability class for the RSNO form. However, the Papp value of the NACNO treatment under the RSNO form increased from $0.21 \pm 0.08 \times 10^{-6}$ cm.s^{-1} (Table 2) at pH 7.4 to $0.9 \pm 0.7 \times 10^{-6}$ cm.s^{-1} at pH 6.4, bringing NACNO close to the medium permeability class (from 1 to 10×10^{-6} cm.s^{-1}, [19]).

The distribution of non-permeated species remaining in the apical compartment after 4 h of permeability at pH 6.4 (Fig. 9) was similar to that at pH 7.4 (Fig. 4).

The absorption of *S*-nitrosothiols from the apical compartment at pH 6.4 to the basolateral compartment at pH 7.4 presented a mass balance from 58% to 78% of the initial amount (Table 7).

4. Discussion

The human intestinal barrier model based on Caco-2 cells is widely used in the pharmaceutical industry to determine the parameters of intestinal permeability of new drugs. The results obtained depend mainly on cell culture parameters (time, medium and age [29]). In the present study, we validated our conditions using two reference molecules, *i.e.* propranolol and furosemide, in comparison with already published Papp values. These Papp values, as well as TEER values (> 500 Ω.cm^2), are quality guaranties of our model and results. From the literature, propranolol, with a Papp value between 3.30×10^{-6} and 41.90×10^{-6} cm.s^{-1} [26,27] belongs to the high permeability class, and furosemide, with a Papp value varying from 0.04×10^{-6} to 0.11×10^{-6} cm.s^{-1} [26,37] belongs to the low permeability class. Such a low permeability for furosemide was attributed to an efflux

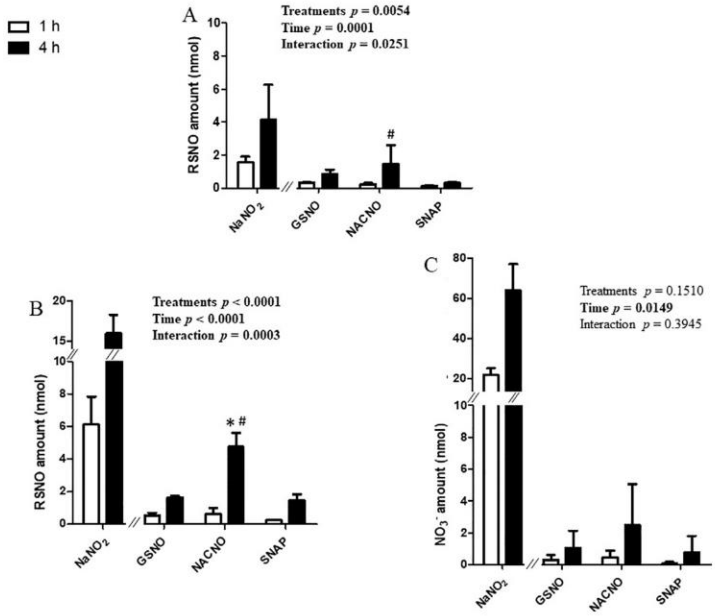

Fig. 8. Apical pH 6.4 to Basolateral permeability – Quantification in the basolateral compartment of remaining (A) RSNO, (B) NO_2^- and (C) NO_3^- after 1 h and 4 h of exposure to 50 nmol of each treatment. Results are shown as mean ± SD of three independent experiments done in duplicate and are compared using two-way ANOVA ($p_{treatment}$ (GSNO, NACNO, SNAP; excluding $NaNO_2$), p_{time} (1h, 4 h) and $p_{interaction}$). * *vs.* GSNO; # *vs.* SNAP at the same time; $p < 0.05$ (Bonferroni's multiple comparisons test).

Table 6
Values of apparent permeability coefficient (Papp) for NOx species ($RSNO + NO_2^- + NO_3^-$) and the RSNO form after 4 h of permeability study from the apical compartment (pH 6.4) to the basolateral compartment (pH 7.4). Mean ± SD of three independent experiments done in duplicate.

Treatments	NOx Papp ($\times 10^{-6}$ cm.s^{-1})	RSNO Papp ($\times 10^{-6}$ cm.s^{-1})
GSNO	1.9 ± 0.6	0.5 ± 0.2
NACNO	4.8 ± 2.4	0.9 ± 0.7
SNAP	1.4 ± 0.8	0.20 ± 0.05
$NaNO_2$	207.0 ± 37.9	7.7 ± 6.5

driven by the intestinal P-glycoprotein to the luminal direction [38]. The Papp values for propranolol (24.4×10^{-6} cm.s^{-1}) and furosemide (0.3×10^{-6} cm.s^{-1}) obtained using our intestinal barrier model confirm the already published values and probably attest for the presence and activity of the P-glycoprotein in this model.

S-Nitrosothiols are NO donors allowing the release of NO with a relative short half-life (within a few hours) [2]. Thereby, in aqueous medium, NO is spontaneously and quickly oxidized into nitrite and nitrate ions. So, it is mandatory to study the intestinal permeability of these ionic species as well as the permeability of the RSNO form to evaluate the bioavailability of NO in the blood stream after oral administration. In the present study, each *S*-nitrosothiol increased their permeability following time, in each of the three proposed conditions (apical to basolateral compartments at pH 7.4 direction, opposite direction, apical compartment at pH 6.4 to basolateral compartment at pH 7.4).

The study of *S*-nitrosothiols permeability from the compartment mimicking the intestinal lumen (apical compartment) to the compartment mimicking the lumen of blood vessels (basolateral compartment) revealed a weak absorption of each *S*-nitrosothiol treatment under the RSNO form compared to the ionic species, which are the major absorbed species (Fig. 10A). In a general point of view, the ionic species are more absorbed by the intestine than the neutral molecules. Indeed, specific ionic transporters such as the Organic Cation Transporters (OCT) and the Zwitterion Transporters (OCTN), implied in the absorption of Na^+ and Ca^{2+}, are expressed within the intestinal tissue and Caco-2 cells [39,40].

The Papp values of all permeated species placed each *S*-nitrosothiol studied within the medium permeability class for NOx species, class that was surrounded by our two reference molecules (propranolol and furosemide). The Papp value was the same for each *S*-nitrosothiol even if they presented different physico-chemical properties with a higher hydrophilicity for GSNO than SNAP [2]. In this way, the physico-chemical properties of the skeleton (R) carrying the nitroso group are not prevalent for the intestinal permeability of the *S*-nitrosothiols. The mass balance within both compartments allowed a recovery of 100% of the initial amount deposited for the SNAP treatment. The small missing amount for the GSNO treatment was recovered by the intracellular quantification, rising the mass balance to almost 100%. However, the NACNO treatment showed a mass balance of 75%, which was not completed to 100% after intracellular quantification.

The amount of NOx species found inside the cells was higher for the GSNO treatment than for the SNAP treatment, with the NACNO treatment situated between each other. SNAP promotes drug intestinal absorption [41] by opening tight junctions without affecting barrier integrity. Indeed, SNAP increases insulin rectal absorption, transepithelial transport of fluorescein sulfonic acid (low absorbable molecule) [41,42] and macromolecules absorption through the intestine by the reversible opening of tight junctions [41,43,44] and a thickening of ileal mucosal membrane [45]. So, in our study, paracellular absorption of SNAP can be speculated. GSNO and NACNO were partially absorbed *via* a transcellular pathway. The mass imbalance observed for the NACNO treatment can be attributed to its higher metabolism within the apical compartment. Moreover, the metabolism of each *S*-nitrosothiol was abolished in the donor compartment when studying the permeability from the basolateral to the apical compartments. This phenomenon is a proof of the intestinal barrier orientation with a brush border including metabolic enzymes like redoxins and gamma-glutamyl transferase [46], faced to the apical compartment, and a basal lamina without any metabolic activity faced to the basolateral compartment.

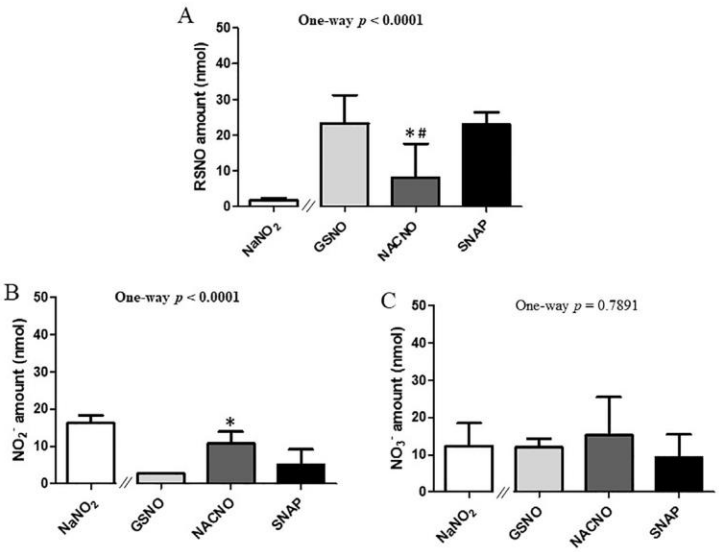

Fig. 9. Apical (pH 6.4) to basolateral compartment – Quantification in the apical compartment of remaining (A) RSNO, (B) NO_2^- and (C) NO_3^- after 1 h and 4 h of exposure to 50 nmol of each treatment. Results are shown as mean ± SD of three independent experiments done in duplicate and are compared using one-way ANOVA (excluding $NaNO_2$). * *vs.* GSNO; # *vs.* SNAP at the same time; $p < 0.05$ (Bonferroni post-test).

Table 7
Mass balance for all tested treatments (initial amount 50 nmol) after 4 h of permeability from the apical compartment at pH 6.4 to the basolateral compartment at pH 7.4. Mean ± SD of three independent experiments done in duplicate.

Treatments	Amount (nmol)	Percentage of the initial amount
GSNO	34 ± 10	68 ± 20
NACNO	37 ± 10	78 ± 20
SNAP	31 ± 5	58 ± 8
$NaNO_2$	114 ± 18	227 ± 35

The equal Papp values obtained permeability studies from the apical to the basolateral compartments and permeability studies from the basolateral to the apical compartments revealed that the absorption of *S*-nitrosothiols is driven by a passive diffusion through the intestinal barrier (Fig. 10B). This transport modality excluded the participation of all transport systems and energy consumption in the permeability of *S*-nitrosothiols [47]. In that way, *S*-nitrosothiols permeability may be improved using pharmaceutical formulations, which are aimed at opening tight junctions and increasing the local concentration and the residence time of the molecule.

Finally, the acidification (pH 6.4) of the apical compartment to mimic the physiological condition of the jejunum part of the intestine (Fig. 10C) showed a permeability dependent on the *S*-nitrosothiol treatment. The very low permeability of the RSNO form for the NACNO treatment at pH 7.4 was multiplied by ten at pH 6.4. However, this favoured permeability of NACNO seemed to be related neither to the lipophilic balance – as NACNO showed a log P intermediate between GSNO and SNAP – nor to the ionization state – as the isoelectric point (pI) of NACNO is intermediate (3.24) between GSNO and SNAP (4.8 and 4.85, respectively) and far away from the studied pHs. As the thiol functions are blocked by NO, their pKa values are not involved in the pI of the *S*-nitrosothiols. However, it may be involved in the stability of the S-NO bound, *e.g* the *S*-nitrosocysteine (cysNO) is less stable than GSNO due to a lower pKa of the thiol function of the cysteine residue. The permeability of the RSNO form for the $NaNO_2$ treatment suggested that pH 6.4 favoured the formation of RSNO starting from NO_2^-. This can also be postulated for all the experiments where permeability of the RSNO forms was observed. However, the formation of RSNO following the $NaNO_2$ treatment should certainly occur thanks to intracellular thiols, which are the only available source of thiol in the experimental system. This phenomenon will lead to cell thiol depletion, which will induce tolerance at it was already seen in clinics for organic nitrate treatments [48]. However, our experiments showed that *S*-nitrosothiol treatments bringing the thiol function itself, won't induce thiol depletion neither tolerance phenomenon. Furthermore, Pinheiro and coworkers demonstrated that oral administration of nitrite ions allowed the formation of RSNO in the stomach leading to an increased plasma RSNO concentration [17]. Our work precises that the formation of RSNO may also occur in the jejunum part of the intestine at acidic pH.

Finally, according to the BCS, *S*-nitrosothiols can be classified between class I and class III, regarding their high solubility and medium permeability. From Le Ferrec et al. [49], the result obtained *in vitro* with high permeability molecules (class I and class II) can be easily transposed to *in vivo* intestinal absorption unlike results obtained for low permeability molecules (class III and class IV). So, the *S*-nitrosothiols included in the medium class of permeability can be considered as drugs suitable for oral administration. Thereafter, it would be interesting to study the permeability of *S*-nitrosothiols in the presence of albumin in the basolateral compartment to mimic the blood stream compartment [50]. Furthermore, albumin including a free reduced cysteine residue in position 34 will increase the amount of RSNO found in the basolateral compartment through *S*-nitrosation process.

In conclusion, our study suggested that *S*-nitrosothiols can be administrated by the oral route to be absorbed at the intestinal level, mainly in the jejunum part. The passive diffusion of *S*-nitrosothiols under three different kinds of species such as nitrite and nitrate ions and the RSNO form was demonstrated using a model of human intestinal barrier. The permeation of the RSNO species will improve the interest for *S*-nitrosothiols oral administration compared to nitrite ions. Indeed, *S*-nitrosothiols would not deplete the intracellular stock of reduced thiols. Even if *S*-nitrosothiols are good candidates for NO oral supplementation, they will need appropriate protection from enzymatic degradation using nanotechnologies [20,51–53].

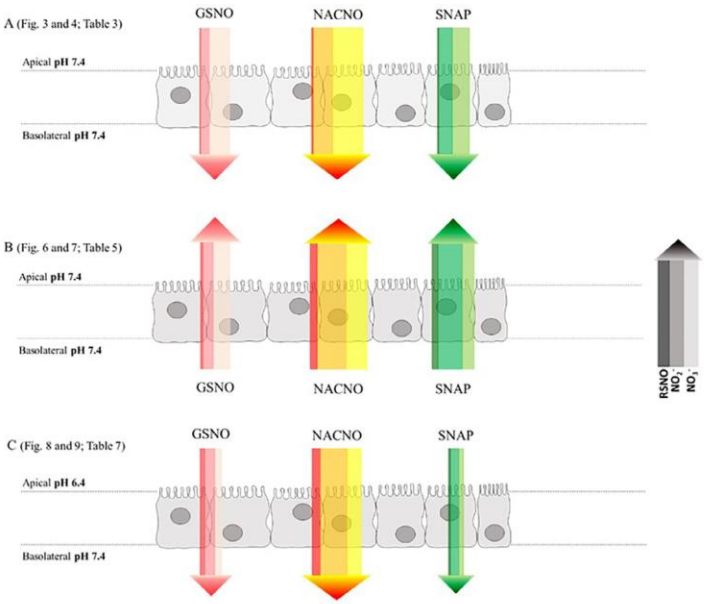

Fig. 10. Summary of NOx species permeability for each *S*-nitrosothiol treatment. The colour code of each arrow from the left to the right is the amount (width) of RSNO, NO_2^- and NO_3^-. The 4 h-permeability for each treatment is represented from (A) apical to basolateral compartment, (B) basolateral to apical compartment and (C) apical (pH 6.4) to basolateral compartment (pH 7.4).

Acknowledgments

The authors acknowledge Dr Wen WU for her help in preliminary experiment settings. The CITHEFOR EA3452 lab was supported by the "Impact Biomolecules" project of the "*Lorraine Université d'Excellence*" (*Investissements d'avenir – ANR*).

References

[1] T.S. Hakim, K. Sugimori, E.M. Camporesi, G. Anderson, Half-life of nitric oxide in aqueous solutions with and without haemoglobin, Physiol. Meas. 17 (1996) 267–277.
[2] C. Gaucher, A. Boudier, F. Dahboul, M. Parent, P. Leroy, S-nitrosation/denitrosation in cardiovascular pathologies: facts and concepts for the rational design of S-nitrosothiols, Curr. Pharm. Des. 19 (2013) 458–472.
[3] Z. Kaposzta, P.A. Baskerville, D. Madge, S. Fraser, J.F. Martin, H.S. Markus, L-Arginine and S-nitrosoglutathione reduce embolization in humans, Circulation 103 (2001) 2371–2375.
[4] Z. Kaposzta, A. Clifton, J. Molloy, J.F. Martin, H.S. Markus, S-nitrosoglutathione reduces asymptomatic embolization after carotid angioplasty, Circulation 106 (2002) 3057–3062.
[5] Z. Kaposzta, J.F. Martin, H.S. Markus, Switching off embolization from symptomatic carotid plaque using S-nitrosoglutathione, Circulation 105 (2002) 1480–1484.
[6] T. Rassaf, P. Kleinbongard, M. Preik, A. Dejam, P. Gharini, T. Lauer, J. Erckenbrecht, A. Duschin, R. Schulz, G. Heusch, M. Feelisch, M. Kelm, Plasma nitrosothiols contribute to the systemic vasodilator effects of intravenously applied NO: experimental and clinical Study on the fate of NO in human blood, Circ. Res. 91 (2002) 470–477.
[7] T. Rassaf, L.W. Poll, P. Brouzos, T. Lauer, M. Totzeck, P. Kleinbongard, P. Gharini, K. Andersen, R. Schulz, G. Heusch, U. Mödder, M. Kelm, Positive effects of nitric oxide on left ventricular function in humans, Eur. Heart J. 27 (2006) 1699–1705, http://dx.doi.org/10.1093/eurheartj/ehl096.
[8] S. Moncada, A. Higgs, The L-arginine-nitric oxide pathway, N. Engl. J. Med. 329 (1993) 2002–2012, http://dx.doi.org/10.1056/NEJM199312303292706.
[9] B. Meyer, A. Genoni, A. Boudier, P. Leroy, M.F. Ruiz-Lopez, Structure and stability studies of pharmacologically relevant S-nitrosothiols: a theoretical approach, J. Phys. Chem. A 120 (2016) 4191–4200, http://dx.doi.org/10.1021/acs.jpca.6b02230.
[10] B.A. Maron, S.-S. Tang, J. Loscalzo, S-nitrosothiols and the S-nitrosoproteome of the cardiovascular system, Antioxid. Redox Signal. 18 (2013) 270–287, http://dx.doi.org/10.1089/ars.2012.4744.
[11] E. Belcastro, W. Wu, I. Fries-Raeth, A. Corti, A. Pompella, P. Leroy, I. Lartaud, C. Gaucher, Oxidative stress enhances and modulates protein S-nitrosation in smooth muscle cells exposed to S-nitrosoglutathione, Nitric Oxide Biol. Chem. 69 (2017) 10–21, http://dx.doi.org/10.1016/j.niox.2017.07.004.
[12] F. Dahboul, P. Leroy, K. Maguin Gate, A. Boudier, C. Gaucher, P. Liminana, I. Lartaud, A. Pompella, C. Perrin-Sarrado, Endothelial γ-glutamyltransferase contributes to the vasorelaxant effect of S-nitrosoglutathione in rat aorta, PloS One 7 (2012) e43190, , http://dx.doi.org/10.1371/journal.pone.0043190.
[13] M.H. Krieger, K.F.R. Santos, S.M. Shishido, A.C.B.A. Wanschel, H.F.G. Estrela, L. Santos, M.G. De Oliveira, K.G. Franchini, R.C. Spadari-Bratfisch, F.R.M. Laurindo, Antiatherogenic effects of S-nitroso-N-acetylcysteine in hypercholesterolemic LDL receptor knockout mice, Nitric Oxide Biol. Chem. 14 (2006) 12–20, http://dx.doi.org/10.1016/j.niox.2005.07.011.
[14] M. Khan, B. Sekhon, S. Giri, M. Jatana, A.G. Gilg, K. Ayasolla, C. Elango, A.K. Singh, I. Singh, S-Nitrosoglutathione reduces inflammation and protects brain against focal cerebral ischemia in a rat model of experimental stroke, J. Cereb. Blood Flow Metab. Off. J. Int. Soc. Cereb. Blood Flow Metab. 25 (2005) 177–192, http://dx.doi.org/10.1038/sj.jcbfm.9600012.
[15] M. Khan, M. Jatana, C. Elango, A.S. Paintlia, A.K. Singh, I. Singh, Cerebrovascular protection by various nitric oxide donors in rats after experimental stroke, Nitric Oxide Biol. Chem. 15 (2006) 114–124, http://dx.doi.org/10.1016/j.niox.2006.01.008.
[16] M. Khan, T.S. Dhammu, M. Baarine, J. Kim, M.K. Paintlia, I. Singh, A.K. Singh, GSNO promotes functional recovery in experimental TBI by stabilizing HIF-1α, Behav. Brain Res. 340 (2018) 63–70, http://dx.doi.org/10.1016/j.bbr.2016.10.037.
[17] L.C. Pinheiro, J.H. Amaral, G.C. Ferreira, R.L. Portella, C.S. Ceron, M.F. Montenegro, J.C. Toledo, J.E. Tanus-Santos, Gastric S-nitrosothiol formation drives the antihypertensive effects of oral sodium nitrite and nitrate in a rat model of renovascular hypertension, Free Radic. Biol. Med. 87 (2015) 252–262, http://dx.doi.org/10.1016/j.freeradbiomed.2015.06.038.
[18] M. Levin (Ed.), Pharm. Process Scale-Up, Informa Healthcare, 2001, , http://dx.doi.org/10.1201/9780824741969.axh.
[19] Y. Peng, P. Yadava, A.T. Heikkinen, N. Parrott, A. Railkar, Applications of a 7-day Caco-2 cell model in drug discovery and development, Eur. J. Pharm. Sci. Off. J. Eur. Fed. Pharm. Sci. 56 (2014) 120–130, http://dx.doi.org/10.1016/j.ejps.2014.02.008.
[20] W. Wu, C. Perrin-Sarrado, H. Ming, I. Lartaud, P. Maincent, X.-M. Hu, A. Sapin-Minet, C. Gaucher, Polymer nanocomposites enhance S-nitrosoglutathione intestinal absorption and promote the formation of releasable nitric oxide stores in rat aorta, Nanomed. Nanotechnol. Biol. Med. 12 (2016) 1795–1803, http://dx.doi.org/10.1016/j.nano.2016.05.006.
[21] K.A. Broniowska, A.R. Diers, N. Hogg, S-nitrosoglutathione, Biochim. Biophys. Acta. 2013 (1830) 3173–3181, http://dx.doi.org/10.1016/j.bbagen.2013.02.004.
[22] P. Teixeira, P. Napoleão, C. Saldanha, S-nitrosoglutathione efflux in the erythrocyte, Clin. Hemorheol. Microcirc. 60 (2015) 397–404, http://dx.doi.org/10.3233/CH-141855.
[23] L.F. Prescott, R.N. Illingworth, J.A. Critchley, M.J. Stewart, R.D. Adam, A.T. Proudfoot, Intravenous N-acetylcystine: the treatment of choice for paracetamol poisoning, Br. Med. J. 2 (1979) 1097–1100.

[24] Y. Wang, J. Cao, X. Wang, S. Zeng, Stereoselective transport and uptake of propranolol across human intestinal Caco-2 cell monolayers, Chirality 22 (2010) 361–368, http://dx.doi.org/10.1002/chir.20753.
[25] M. Parent, A. Boudier, F. Dupuis, C. Nouvel, A. Sapin, I. Lartaud, J.-L. Six, P. Leroy, P. Maincent, Are in situ formulations the keys for the therapeutic future of S-nitrosothiols? Eur. J. Pharm. Biopharm. Off. J. Arbeitsgemeinschaft Pharm. Verfahrenstechnik EV 85 (2013) 640–649, http://dx.doi.org/10.1016/j.ejpb.2013.08.005.
[26] E.H. Kerns, L. Di, S. Petusky, M. Farris, R. Ley, P. Jupp, Combined application of parallel artificial membrane permeability assay and Caco-2 permeability assays in drug discovery, J. Pharm. Sci. 93 (2004) 1440–1453, http://dx.doi.org/10.1002/jps.20075.
[27] C. Zhu, L. Jiang, T.-M. Chen, K.-K. Hwang, A comparative study of artificial membrane permeability assay for high throughput profiling of drug absorption potential, Eur. J. Med. Chem. 37 (2002) 399–407.
[28] S.I. Khan, E.A. Abourashed, I.A. Khan, L.A. Walker, Transport of harman alkaloids across Caco-2 cell monolayers, Chem. Pharm. Bull. (Tokyo) 52 (2004) 394–397.
[29] B. Srinivasan, A.R. Kolli, M.B. Esch, H.E. Abaci, M.L. Shuler, J.J. Hickman, TEER measurement techniques for in vitro barrier model systems, J. Lab. Autom. 20 (2015) 107–126, http://dx.doi.org/10.1177/2211068214561025.
[30] W.S. Jobgen, S.C. Jobgen, H. Li, C.J. Meininger, G. Wu, Analysis of nitrite and nitrate in biological samples using high-performance liquid chromatography, J. Chromatogr. B Analyt. Technol. Biomed. Life. Sci. 851 (2007) 71–82, http://dx.doi.org/10.1016/j.jchromb.2006.07.018.
[31] H.K. Kim, J.H. Hong, M.S. Park, J.S. Kang, M.H. Lee, Determination of propranolol concentration in small volume of rat plasma by HPLC with fluorometric detection, Biomed. Chromatogr. BMC 15 (2001) 539–545, http://dx.doi.org/10.1002/bmc.110.
[32] G.S. Rekhi, S.S. Jambhekar, P.F. Souney, D.A. Williams, A fluorimetric liquid chromatographic method for the determination of propranolol in human serum/plasma, J. Pharm. Biomed. Anal. 13 (1995) 1499–1505.
[33] J.M. Ryu, S.J. Chung, M.H. Lee, C.K. Kim, C.K. Shim, Increased bioavailability of propranolol in rats by retaining thermally gelling liquid suppositories in the rectum, J. Control. Release Off. J. Control. Release Soc. 59 (1999) 163–172.
[34] T. Galaon, S. Udrescu, I. Sora, V. David, A. Medvedovici, High-throughput liquid-chromatography method with fluorescence detection for reciprocal determination of furosemide or norfloxacin in human plasma, Biomed. Chromatogr. 21 (2007) 40–47, http://dx.doi.org/10.1002/bmc.715.
[35] O. Parodi, R. De Maria, E. Roubina, Redox state, oxidative stress and endothelial dysfunction in heart failure: the puzzle of nitrate-thiol interaction, J. Cardiovasc. Med. 8 (2007) 765–774, http://dx.doi.org/10.2459/JCM.0b013e32801194d4.
[36] E.C. Sherer, A. Verras, M. Madeira, W.K. Hagmann, R.P. Sheridan, D. Roberts, K. Bleasby, W.D. Cornell, QSAR prediction of passive permeability in the LLC-PK1 cell line: trends in molecular properties and cross-prediction of Caco-2 permeabilities, Mol. Inform. 31 (2012) 231–245, http://dx.doi.org/10.1002/minf.201100157.
[37] S. Yamashita, T. Furubayashi, M. Kataoka, T. Sakane, H. Sezaki, H. Tokuda, Optimized conditions for prediction of intestinal drug permeability using Caco-2 cells, Eur. J. Pharm. Sci. Off. J. Eur. Fed. Pharm. Sci. 10 (2000) 195–204.
[38] P.-A. Billat, E. Roger, S. Faure, F. Lagarce, Models for drug absorption from the small intestine: where are we and where are we going? Drug Discov. Today. 22 (2017) 761–775, http://dx.doi.org/10.1016/j.drudis.2017.01.007.
[39] T. Han, R.S. Everett, W.R. Proctor, C.M. Ng, C.L. Costales, K.L.R. Brouwer, D.R. Thakker, Organic cation transporter 1 (OCT1/mOct1) is localized in the apical membrane of caco-2 cell monolayers and enterocytes, Mol. Pharmacol. 84 (2013) 182–189, http://dx.doi.org/10.1124/mol.112.084517.
[40] T. Hirano, S. Yasuda, Y. Osaka, M. Kobayashi, S. Itagaki, K. Iseki, Mechanism of the inhibitory effect of zwitterionic drugs (levofloxacin and grepafloxacin) on carnitine transporter (OCTN2) in Caco-2 cells, Biochim. Biophys. Acta BBA – Biomembr. 1758 (2006) 1743–1750, http://dx.doi.org/10.1016/j.bbamem.2006.07.002.
[41] G. Fetih, F. Habib, H. Katsumi, N. Okada, T. Fujita, M. Attia, A. Yamamoto, Excellent absorption enhancing characteristics of NO donors for improving the intestinal absorption of poorly absorbable compound compared with conventional absorption enhancers, Drug Metab. Pharmacokinet. 21 (2006) 222–229.
[42] A. Yamamoto, H. Tatsumi, M. Maruyama, T. Uchiyama, N. Okada, T. Fujita, Modulation of intestinal permeability by nitric oxide donors: implications in intestinal delivery of poorly absorbable, Drugs 7 (2018).
[43] A.L. Salzman, M.J. Menconi, N. Unno, R.M. Ezzell, D.M. Casey, P.K. Gonzalez, M.P. Fink, Nitric oxide dilates tight junctions and depletes ATP in cultured Caco-2BBe intestinal epithelial monolayers, Am. J. Physiol. 268 (1995) G361–373, http://dx.doi.org/10.1152/ajpgi.1995.268.2.G361.
[44] N. Numata, K. Takahashi, N. Mizuno, N. Utoguchi, Y. Watanabe, M. Matsumoto, T. Mayumi, Improvement of intestinal absorption of macromolecules by nitric oxide donor, J. Pharm. Sci. 89 (2000) 1296–1304.
[45] D.-Z. Xu, Q. Lu, E.A. Deitch, Nitric oxide directly impairs intestinal barrier function, Shock Augusta Ga 17 (2002) 139–145.
[46] N. Hogg, R.J. Singh, E. Konorev, J. Joseph, B. Kalyanaraman, S-Nitrosoglutathione as a substrate for gamma-glutamyl transpeptidase, Biochem. J. 323 (Pt 2) (1997) 477–481.
[47] B. Alberts, A. Johnson, J. Lewis, M. Raff, K. Roberts, P. Walter, Carrier Proteins and Active Membrane Transport, 2002. https://www.ncbi.nlm.nih.gov/books/NBK26896/ (accessed January 23, 2018).
[48] A. Daiber, T. Münzel, Organic nitrate therapy, nitrate tolerance, and nitrate-induced endothelial dysfunction: emphasis on redox biology and oxidative stress, Antioxid. Redox Signal. 23 (2015) 899–942, http://dx.doi.org/10.1089/ars.2015.6376.
[49] E. Le Ferrec, C. Chesne, P. Artusson, D. Brayden, G. Fabre, P. Gires, F. Guillou, M. Rousset, W. Rubas, M.L. Scarino, In vitro Models of the Intestinal Barrier. The Report and Recommendations of ECVAM Workshop 46, European Centre for the Validation of Alternative methods, Altern. Lab. Anim. ATLA, 2001, pp. 649–668.
[50] J.E. Gonçalves, M. Ballerini Fernandes, C. Chiann, M.N. Gai, J. De Souza, S. Storpirtis, Effect of pH, mucin and bovine serum on rifampicin permeability through Caco-2 cells, Biopharm. Drug Dispos. 33 (2012) 316–323, http://dx.doi.org/10.1002/bdd.1802.
[51] W. Wu, C. Gaucher, R. Diab, I. Fries, Y.-L. Xiao, X.-M. Hu, P. Maincent, A. Sapin-Minet, Time lasting S-nitrosoglutathione polymeric nanoparticles delay cellular protein S-nitrosation, Eur. J. Pharm. Biopharm. Off. J. Arbeitsgemeinschaft Pharm. Verfahrenstechnik EV 89 (2015) 1–8, http://dx.doi.org/10.1016/j.ejpb.2014.11.005.
[52] W. Wu, C. Gaucher, I. Fries, X.-M. Hu, P. Maincent, A. Sapin-Minet, Polymer nanocomposite particles of S-nitrosoglutathione: a suitable formulation for protection and sustained oral delivery, Int. J. Pharm. 495 (2015) 354–361, http://dx.doi.org/10.1016/j.ijpharm.2015.08.074.
[53] K.U. Shah, S.U. Shah, N. Dilawar, G.M. Khan, S. Gibaud, Thiomers and their potential applications in drug delivery, Expert Opin. Drug Deliv. 14 (2017) 601–610, http://dx.doi.org/10.1080/17425247.2016.1227787.

Chapter 3: Vascular NO storage and its vasoactivity

3.1 NO storage

In the previous work of our lab[127], nitric oxide storage has been found in the vascular wall after the administration of GSNO loaded nanocomposite to Wistar rats. As described in the Chapter 1, *S*-nitrosothiol (RSNOs) is one of the main NO storage forms in our body. The transnitrosation (such as transfer NO from cysteine residue to another, from GSNO to other proteins) plays an important role in both the production and degradation of RSNOs. Several studies have proven the existence of NO stores. For example, photosensitive NO stores have been identified through the relaxation of precontracted blood vessels after exposition to light[177,178]. In further study, photosensitivity was lost after exposed the endothelium removed vessels repeatedly exposed to light, but it recovered when these vessels were exposed to a NO donor[179]. Another evidence is the relaxation effect of blood vessels after adding the low molecular weight thiols like *N*-acetylcysteine (NAC). NAC can displace NO from other high molecular weight RSNOs then produce NO to vasodilate the vessels[180]. The existence of NO stores has been proposed as the explanation for the persistence of endothelium-dependent relaxion effects after using inhibitors to block the NO synthase[181]. It is also the reason for the lasting hyporesponsiveness of vessels to vasoconstrictors elicited by NO donors[182]. To conclude, all these studies proven the existence of NO stores and support the idea that *S*-nitrosation of thiols in tissues is a mechanism of NO stores (RSNOs) formation from which NO can be subsequently released.

Main forms of NO storage

In fact, RSNOs and dinitrosyl iron complexes (DNIC) are the two main forms of NO transport and storage in the organism. These two types of compounds can be of high or low molecular weight. The protein complexes are usually more stable compared to the one with low molecular weight. Among the low molecular weight nitrosothiols, *S*-nitrosocysteine has the closest physicochemical and virtually identical vasodilatory properties to endothelium derived relaxing factor[183]. GSNO has been regarded as the intermediate between NOS activation and free NO formation. It was suggested that NOS nitrosates glutathione to form GSNO, which releases NO in the presence of Cu^{+}[179,184,185]. In addition, low molecular weight RSNOs can also pass NO to the cysteine residues of proteins through transnitrosylation[186]. *S*-nitrosylation or *S*-nitrosation of certain proteins give rise to NO transport–storage forms such as *S*-

nitrosoalbumin[187,188] and *S*-nitrosohemoglobin (SNO-Hb)[189]. Iron-nitrosyl-hemoglobin is formed through the interaction of heme-Fe(II) with NO. Under high O_2 pressure, NO moiety is then transfer from the heme group to the cysteine 93 residue of Hb, resulting in the formation of SNO-Hb. Conversely, NO is released from SNO-Hb when O_2 tension decreases. This results in vasodilation and the improvement of tissue perfusion and gas exchange[190]. In addition, *S*-nitrosoalbumin also serves as an important NO-transporter.

Except RSNOs, DNIC with thiol-containing ligands [$(RS)_2Fe(NO)_2$] are other possible endogenous NO storage form[191]. DNIC were found in animal tissues over 50 years ago *via* their specific electron paramagnetic resonance signal[192]. The main biological activity of DNIC is due to release of NO, transfer NO to cysteine group of proteins, or transfer $Fe(NO)_2$ groups to proteins dithiols to form new DNIC. In the work of Galagan[193], exogenous DNIC were administrated to rats and resulted in quickly spread over tissues followed with hypotensive effects.

These two kinds of NO storage forms (RSNOs and DNIC) are capable of interconversions according to the level of Fe^{2+}, NO, as well as low molecular weight thiols in the cell (Figure 16). When thiols content decreases, both DNIC and RSNOs amount decrease. When NO level decreases while the thiols and iron concentration remain constant, DNIC and RSNOs mainly serve as NO donors, which transfer NO to the acceptor cell. Excessive iron accelerates RSNOs dissociation more than DNIC dissociation. NO is principally stabilized in the form of RSNOs with excessive thiols as compared to iron[194]. Apparently, RSNOs is the main NO transport form between the cells. When RSNOs arrives in the region where content of non-heme iron and thiols increased, it initiates DNIC formation, while dissociation of DNIC releases NO[195,196].

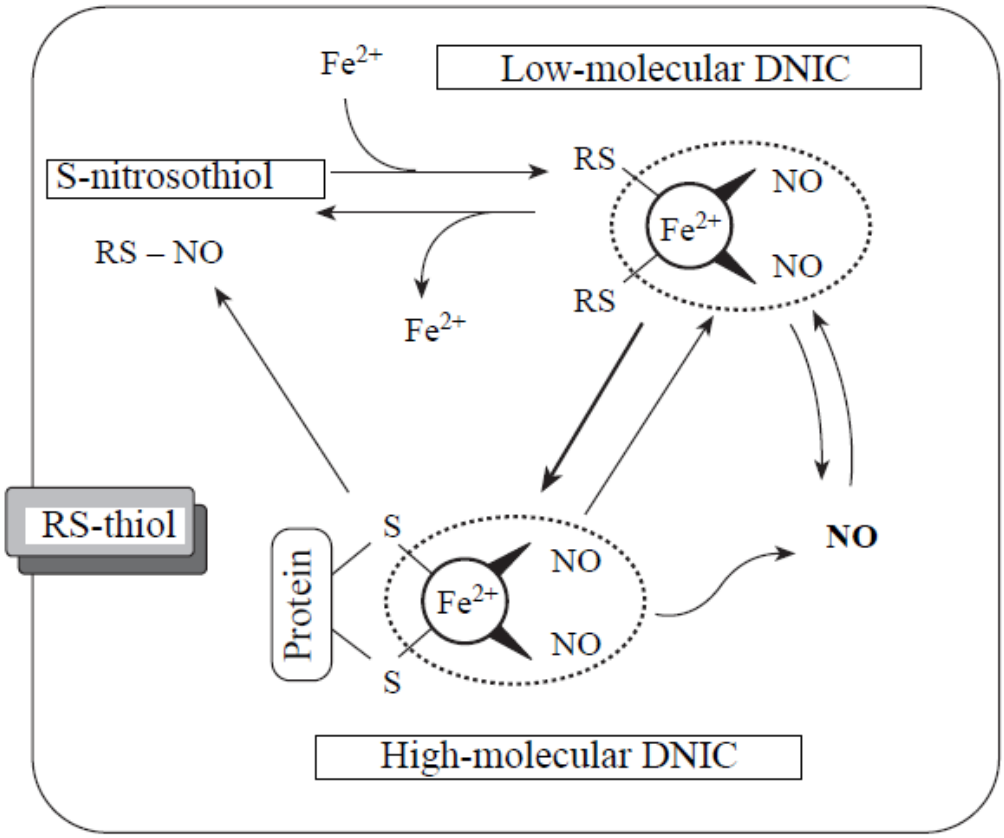

Figure 16. **NO storage in the form of *S*-nitrosothiols (RS-NO), dinitrosyl iron complexes (DNIC) with protein ligands, and low molecular weight DNIC[197]**.

***S*-nitroso-proteins and its functional significance**

As one of the main forms of NO storage in organisms, *S*-nitroso-proteins (such as SNO-Hb and *S*-nitrosoalbumin) play an important role in the transport and prolong the lifetime of NO. However, the *S*-nitrosation and denitrosation of proteins (enzymes) may also change their activity. For example, cysteine 69 (C69) is the nitrosable thiol of Trx[198]. It has been suggested that the *S*-nitrosation of C69 results in the increase of Trx activity compared with control. Whereas, this increase is not inducible using the C69S mutant Trx[199]. In addition, the enzyme PDI, a member of thioredoxin superfamily, has also proven to be nitrosable *in vitro*[200]. Some investigations have shown that PDI losses its activity after *S*-nitrosation with a fivefold excess of the SNO donor[201]. However, no data has been presented about the existence of PDI-SNO *in vivo*. Caspases are a family of proteolytic enzymes that play important role in cellular death. SNO is believed to exert a portion of its anti-apoptotic effects *via* nitrosation of cysteine from the active site of at least two members from the caspase family[202]. To conclude, *S*-nitrosation activity is

of significance to the activity of enzyme.

3.2 Endothelial dysfunction

Endothelial dysfunction is characterized by the decrease of the bioavailability of vasodilators, especiallyNO, and/or an increased production of endothelium derived contracting factors[203]. It is involved in most forms of cardiovascular diseases, such as atherosclerosis, hypertension, peripheral artery disease, chronic heart failure, coronary artery disease, diabetes, and chronic renal failure.

Several factors participate in the formation of endothelial dysfunction, such as cardiovascular risk factors including aging, smoking, hypertension, hyperglycemia, hypercholesterolemia, and genetic factors like family premature atherosclerotic disease history[203,204]. Endothelial dysfunction causes a chronic inflammatory process with a reduction of antithrombotic factors as well as an increase in prothrombotic products and vasoconstrictors, resulting in abnormal vasoreactivity and elevating risk of cardiovascular diseases[203,205,206] (Figure 17). In addition, endothelial dysfunction has also been related to obesity, elevated C-reactive protein, and chronic systemic infection[207–212].

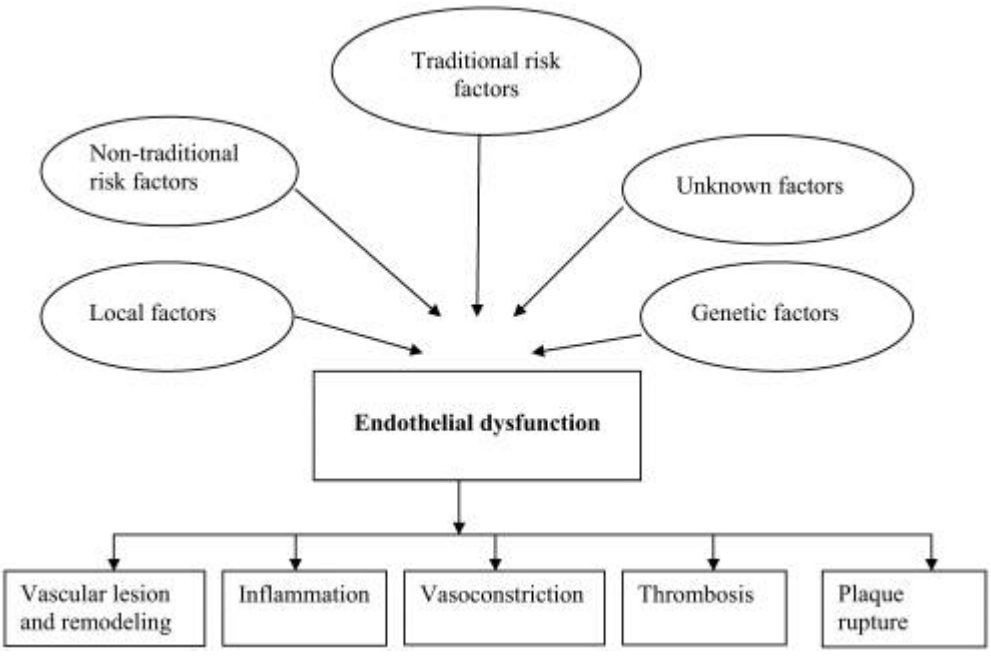

Figure 17. **The various factors that affect the endothelium and the consequences of endothelial dysfunction[204]**.

As the imbalance in the production of vasodilating factors (NO) is the key point of endothelial dysfunction, the formation of a NO store may restore the physiological role of NO which helps counteracting endothelial dysfunction.

To make clear the NO storage in vascular wall, different rat aorta (endothelium intact and removed) have been incubated with different NO donors to induce NO storage. The vasoactivity of NO storage has also been tested, as shown in article 3:

Article 3: *S*-nitrosothiols as potential therapeutics to induce a mobilizable vascular store of nitric oxide to counteract endothelial dysfunction.

Les *S*-nitrosothiols : de potentiels médicaments induisant la formation d'un stock mobilisable de monoxyde d'azote au sein des vaisseaux afin de contrer la dysfonction endothéliale.

Caroline Perrin-Sarrado[#], Yi Zhou[#], Valérie Salgues, Marianne Parent, Philippe Giummelly, Isabelle Lartaud, Caroline Gaucher*

[#] Les deux auteurs ont contribué à parts égales à ce travail.

Article soumis au journal *Biochemical Pharmacology* le 28 juin 2019.
(FI : 4,7). Q1 Pharmacology and Pharmacy).

S-nitrosothiols as potential therapeutics to induce a mobilizable vascular store of nitric oxide to counteract endothelial dysfunction

Caroline Perrin-Sarrado[1], Yi Zhou[1], Valérie Salgues, Marianne Parent, Philippe Giummelly, Isabelle Lartaud, Caroline Gaucher*

Université de Lorraine, CITHEFOR, F-54000 Nancy, France

[1] Both authors contributed equally to this work

* Corresponding author: Dr Caroline Gaucher. Université de Lorraine, CITHEFOR EA 3452, Campus Brabois Santé, 9, avenue de la Forêt de Haye, 54500 Vandœuvre-lès-Nancy Cedex, France.

E-mail address: caroline.gaucher@univ-lorraine.fr; Tel.: +33 3 72 74 73 49.

Keywords: *S*-nitrosothiols; NO-derived species; NO stores; vascular contraction; endothelium

Abstract:

Endothelial dysfunction predisposing to cardiovascular diseases is defined as an imbalance in the production of vasodilating factors, such as nitric oxide (NO), and vasoconstrictive factors. To insure its physiological role, NO, a radical with very short half-life, requires to be stored and transported to its action site. *S*-nitrosothiols (RSNOs) like *S*-nitrosoglutathione (GSNO) represent the main form of NO storage within the vasculature. The NO store formed by RSNOs is still bioavailable to trigger vasorelaxation. In this way, RSNOs are an emerging class of NO donors with a potential to restore NO bioavailability within cardiovascular disorders.

The aim of this study was to compare the ability of *S*-nitrosothiols, the physiologic GSNO and the synthetics *S*-nitroso-*N*-acetylcysteine (NACNO) and *S*-nitroso-*N*-acetylpenicillamine (SNAP) to produce a vascular store of NO either in endothelium-intact or endothelium-removed aortae in order to evaluate whether RSNOs can be used as therapeutics to compensate endothelial dysfunction. Sodium nitroprusside (SNP), a marketed drug already in clinics, was used as a non-RSNO NO-donor. Endothelium-intact or endothelium-removed aortae, isolated from normotensive Wistar rats, were exposed to RSNOs or SNP. Then, NO-

derived (NOx) species, representing the NO store inside the vascular wall, were quantified using the diaminonaphthalene probe coupled to mercuric ions. The bioavailability of the NO store and its ability to induce vasodilation was tested using *N*-acetylcysteine, then its ability to counteract vasoconstriction was challenged using phenylephrine (PHE).

All the studied RSNOs were able to generate a NO store materialized a three to five times increase of NOx species inside aortae. NACNO was the most potent RSNO to produce a vascular NO store bioavailable for vasorelaxation and the most efficient to induce vascular hyporeactivity to PHE in endothelium removed aortae. GSNO and SNAP were equivalent and more efficient than SNP. In endothelium-intact aortae, the NO store was also formed whereas it seemed less available for vasorelaxation and did not influence PHE-induced vasoconstriction. In conclusion, RSNOs - NACNO in a better extent - are able to restore NO bioavailability as a functional NO store within the vessel wall, especially when the endothelium is removed. This was associated with a hyporeactivity to the vasoconstrictive agent phenylephrine. Treatment with RSNOs could present a benefit to restore NO-dependent functions in pathological states associated with injured endothelium.

1. Introduction

Cardiovascular diseases (CVD) are an important leading causes of morbidity and mortality in the world and mainly originate from the disruption of endothelial homeostasis. Various physio-pathological conditions, including hyperglycemia, hyperlipidemia, hypertension [1] and aging [2], may impact endothelial function. Endothelium impairment is a complex pathophysiological event that includes endothelial cells activation and dysfunction. Endothelial dysfunction is defined as an imbalance in the production of vasodilating and vasoconstrictive factors, anti- and prothrombotic factors as well as anti- and proinflammatory factors [3,4]. The production and/or the bioavailability of vasodilating factors like nitric oxide (NO) or endothelium-hyperpolarizing factor and prostacyclin decrease [5,6]. In the meantime, the production of endothelium-dependent vasoconstrictive agents such as endothelin-1 increases [7,8]. The decreased synthesis, release and/or activity of endothelium derived NO is the earliest and one of the most important events that characterize endothelial dysfunction [9]. In endothelial cells, NO is responsible for the maintenance of vascular homeostasis through the coordination of the communication between endothelial and smooth muscle cells (SMC) in the vessel wall for example. The decrease in NO bioavailability results either from (i) a reduction of NO synthesis, linked to a decrease in eNOS protein expression [10] and/or eNOS activity impairment (uncoupling) [11], or from (ii) an increase in NO degradation. NO, as a gazotransmitter showing a very short half-life (less than 5 s [12]), is stored and transported as *S*-nitrosothiols (RSNOs), in relation with the *S*-nitrosation process (the formation of the S-NO bond). Thanks to such *S*-nitrosation processes, NO half-life is drastically extended (at least several min and up to several hours, depending of the structure of the carrying thiol) [13,14]. Moreover, *S*-nitrosation limits the oxidative/nitrosative stress induced by NO oxidation into peroxynitrite ions ($ONOO^-$) [15]. So, RSNOs can be envisaged as therapeutics with a potential use in cardiovascular disorders associated with endothelial dysfunction to restore

NO bioavailability. Indeed, RSNOs are currently investigated (clinical trials) to reduce cerebral embolization after carotid angioplasty, recurrent stroke or systemic embolization for example see [14].

In *ex vivo* models, these RSNOs, as NO donors, induce an immediate vasorelaxation (*e.g.* within 5 min following exposure in isolated aortae). This phenomenon is linked to the fast release of NO induced by denitrosating enzymes such as protein disulfide isomerase (PDI) and gamma-glutamyl transferase (GGT) - present at the endothelial level - and subsequent activation of the soluble guanylate cyclase (sGC)/GMPc pathway within smooth muscle cells [16,17]. The presence of a functional endothelium is crucial for the NO release from RSNOs as shown by a higher potency of RSNOs to induce vasodilation in the presence rather than in the absence of endothelium [16,18]. This was highlighted by a higher *ex vivo* vasorelaxant effects (1 log increase in pD_2 values) of RSNOs on endothelium-intact aortic rings than on endothelium-denuded aortic rings [16].

Besides these immediate vasorelaxant effects related to nitrosylation of sGC (NO coordination to the iron of the heme), RSNOs are able to induce the vascular storage of NO either *ex vivo* or *in vivo* [19–21]. This NO store is mainly composed of NO-derived (NOx) species like nitrite ions and *S*-nitrosated proteins or peptides made by transnitrosation reactions [15]. Those transnitrosation reactions with circulating or vascular peptides/proteins play important roles in NO transport and storage as well as NO signaling. The NO store can be mobilized for sGC activation leading to vasorelaxation [19–22]. Transnitrosation processes depend on the physico-chemical properties of the molecules carrying SNO [12,23] and their metabolism by denitrosating enzymes [24].

As endothelium plays an important role in the immediate vasorelaxant effect of RSNOs, we wonder whether it influences the storage of NO from RSNOs. We therefore compare the ability of three *S*-nitrosothiols, the *S*-nitrosoglutathione (GSNO) a physiological RSNO, and

two synthetic RSNOs, the *S*-nitroso-*N*-acetylcysteine (NACNO) and the *S*-nitroso-*N*-acetylpenicillamine (SNAP) to generate NO storage. Sodium nitroprusside (SNP) is evaluated as a non-RSNO NO-donor.

Aortic rings are pre-incubated with RSNOs or SNP in order to stimulate transnitrosation processes. The generation of a NO store within the vascular wall is evaluated by quantifying NOx species inside of the vascular wall. Then, the bioavailability of such NO storage to regulate vasoactivity is revealed by measuring aortic vasoconstriction to phenylephrine (PHE) and the vasorelaxation induced in response to *N*-acetylcysteine (NAC). Indeed, NAC can enter inside the cells where it is deacetylated in cysteine. Then, the cysteine residue, in the presence of NO storage, displaces NO by transnitrosation process to produce *S*-nitrosocysteine. This instable *S*-nitrosocysteine immediately releases NO available to stimulate the sGC/GMPc pathway inducing vasorelaxation. In the absence of NO store, the aortic rings do not relax under this NAC protocol. These two protocols (NAC and PHE) give functional proofs of the NO stored within the vascular wall, either in endothelium-intact or in endothelium removed aortae.

2. Material and methods

2.1. Chemicals

All reagents were of analytical grade. Mercuric chloride ($HgCl_2$) and sodium hydroxide (NaOH) were purchased from Prolabo (VWR). Carbachol, PHE, SNP and all other reagents were obtained from Sigma-Aldrich (Saint Quentin Fallavier, France). Ultrapure deionized water (18.2 MΩ.cm) was used to prepare all solutions.

GSNO, SNAP and NACNO were synthesized extemporaneously at a final concentration of 10^{-2} M, by *S*-nitrosation of glutathione, *N*-acetylpenicillamine or *N*-acetylcysteine with sodium nitrite (ratio 1:1) under acidic condition as previously described [25]. The purity of RSNO was assessed by ultraviolet spectrophotometry using the specific molar absorbance of

the S-NO bond at 334 nm (ε_{GSNO} = 922 M^{-1} cm^{-1}; ε_{NACNO} = 900 M^{-1} cm^{-1}) and at 340 nm for SNAP (ε_{SNAP} = 1020 M^{-1} cm^{-1}). All RSNO solutions were used in a concentration range >95% of the initial concentration. All manipulations and assays involving NO donors were performed with subdued lighting, in order to minimize light-induced degradation of RSNOs.

2.2. Rats and ethical statements

All experiments were performed in accordance with the European Community guidelines (2010/63/EU) for the use of experimental animals in the respect of the 3 Rs' requirements for Animal Welfare. The projects untitled "Nitro-Vivo" and "BisNitro-Vivo" (n°APAFIS#1614-2015090216575422v2 and #15598-2018061619129620v3, respectively) were positively evaluated by the regional ethical committee for animal experiments and approved by the French Ministry of Research.

Twelve week-old, male, normotensive Wistar rats (300-325 g) were purchased from Janvier Laboratories (Le Genest St Isle, France) and kept under standard conditions (temperature: 21 ± 1°C, hygrometry 60 ± 10%, light on 6 am to 6 pm). They ate standard diet (A04, Safe, Villemoisson-sur-Orge, France) and drank water (reverse osmosis system, Culligan, Brussels, Belgium) *ad libitum*.

Rats were anesthetized with sodium pentobarbitone (60 $mg.kg^{-1}$, intraperitoneal injection, Sanofi Santé Nutrition Animale, Libourne, France) and the adequacy of anesthesia was checked by testing the loss of the corneal and pinch paw withdrawal reflexes. If a change in the reflexes occurred, a bolus of sodium pentobarbitone was immediately administered. After administration of heparin (1000 $IU.kg^{-1}$ heparine Choay, penis vein), rats were sacrificed by exsanguination and segments (3 cm) of the descending thoracic aorta were removed, cleaned from surrounding connective tissues, cut into 2-mm long rings (8 rings per rat) and immediately used for vasoactivity. In some rings, the endothelium was removed by gently rubbing the intimal surface with forceps. For NOx species quantification, aortas

(endothelium-intact or endothelium-removed) were frozen in liquid nitrogen immediately after collection and stored at -80 °C (less than 2 months) until the incubation with NO donors.

2.3. Quantification of NO derived species

The NOx species (RSNO and nitrite ions) were quantified inside endothelium-intact and endothelium-removed aortae. Aortae were thawed at 37 °C for 2 min and cut into two pieces of 20 ± 2 mg each (one piece for control and one piece for RSNO incubation). All experiments were performed in the same condition as vasoactivity studies (section 2.4): each piece of aorta was equilibrated during 60 min at 37 °C in 75 mL of Krebs' solution containing 119 mM NaCl, 4.7 mM KCl, 1.2 mM KH_2PO_4, 1.2 mM $MgSO_4$, 1.6 mM $CaCl_2$, 24 mM $NaHCO_3$, 5.5 mM glucose, adjusted to pH 7.4 and under 95% O_2 and 5% CO_2 continuous bubbling. Then, GSNO, SNAP, NACNO or SNP (2 µM), or Krebs' solution as control, were incubated during 30 min (n = 3-15 per group, from 3-15 different rats in each group) Aortae were rinsed 3 times during 20 min with 75 mL of Krebs' solution to remove the excess of RSNO and dried with a paper tissue. Dry aortae were then snap frozen in liquid nitrogen and crushed with a pestle in a mortar. Aortae powder was mixed for 30 s with 600 µL of 0.105 mM 2,3-diaminonaphthalene (DAN) and 1.05 mM $HgCl_2$ prepared in HCl 0.6 M. The mixture was incubated 10 min at 37 °C under rotation. The reaction was stopped with 40 µL of 10 M NaOH to reach the maximum of naphthotriazole (NAT) fluorescence. After 15 min of centrifugation 18,000 *g* at 4 °C, the supernatant intensity of fluorescence was read in a black 96-wells plate at 415 nm after excitation at 375 nm (JASCO FP-8300, France). NOx species quantity was calculated upon a standard curve built with GSNO (0.1 to 2 µM).

2.4. Vasoactivity studies

Vasoactivity was evaluated on endothelium-intact or endothelium-removed aortic rings using an isometric tension recording system in 10 mL organ chambers (EMKABATH, Emka Technology, France) [18]. The organ chambers were filled with Krebs' solution (10 mL,

37°C) and continuously bubbled with 95% O_2 and 5% CO_2. Following 60-min equilibration at a basal resting tension of 2 g, rings were exposed 2 times to KCl (60 mM, 5 min) to check viability.

Aortae were exposed for 30 min to GSNO, SNAP, NACNO or SNP (2 µM) [20,22], followed by 3 times of washing (20 min each) with Krebs' solution to remove the excess of RSNO. Then, aortae were submitted to two different protocols to evaluate (i) NO storage in the aortic wall (NAC protocol) and (ii) vasoreactivity to a vasoconstrictor (PHE protocol):

1. NAC at 10^{-5} M (n = 8-10 per group, from 4-8 different rats in each group) was added on pre-constricted aortae (10^{-6} M PHE) in order to displace NO from cysteine-NO residue and mobilize NO for nitrosylation of soluble guanylate cyclase, cGMP production and vasodilation.
2. Cumulative concentration response curves to PHE from 3×10^{-10} M to 3×10^{-5} M (n = 6-17 per group, from 3-7 different rats in each group) were performed in order to evaluate whether the NO storage decreases vasoconstrictive capacities.

The role of the endothelium was investigated by performing experiments in either endothelium-intact or endothelium-removed aortae. Endothelium integrity or removal was assessed on 10^{-6} M PHE pre-constricted aortae using 10 µM carbachol, a muscarinic acetylcholine receptor agonist inducing vasorelaxation when the endothelium is intact. Aortic rings showing less than 17±1% of relaxation were considered as endothelium-removed.

2.5.Data analysis and statistical tests

All the results were presented as means ± standard deviation and analyzed (Graph Pad prism® software version 6.0); $p<0.05$ was considered as significant.

Results of NOx species quantification were analyzed using the Kruskal Wallis test for non-parametric (as some groups contained only 3 aortic rings) values followed by a Dunn's post-test. The vasorelaxant effect of NAC was calculated using the following equation (Eq. 1):

$$\%\ Vasorelaxation = 100 - \left(\frac{\Delta\ Tension_{NAC}}{Tension\ of\ PHE\ precontraction}\right) * 100$$

Results were analyzed by the One-Way ANOVA test followed by the Bonferroni's multiple comparisons test. For PHE response curves, half maximal effective concentrations (EC_{50}) and maximal responses (E_{max}) were calculated by fitting each concentration response curve using the Hill logistic equation (Eq. 2):

$$\%\ Contraction = E_{min} + \left(\frac{E_{max} - E_{min}}{1 + 10^{((\log EC_{50} - Concentration) * Hill\ slope)}}\right.$$

The pD_2 values were calculated as -log EC_{50} and analyzed by the One-Way ANOVA test followed by the Bonferroni's multiple comparisons test.

3. Results

Endothelium-intact (Fig. 1A) and endothelium-removed (Fig. 1B) aortae showed an increase in NOx species content following each NO-donor treatment compared to control. The control represents the physiological NO store inside of the aortic wall, which was higher in endothelium-intact aorta compared to endothelium-removed aorta. The amount of NOx species was greater for NACNO treatments in both types of aortae compared to other NO-donor treatments, and reached similar values whatever the presence or the absence of the endothelium. However, for GSNO, SNAP and SNP treatments, the amount of NOx species tended to be higher in endothelium-intact compared to endothelium-removed aortae.

To assess whether the NO store formed following NO-donors incubation is available for vasorelaxation, aortae were submitted to the NAC protocol, which allows the release of NO from *S*-nitrosated peptides or proteins (Fig. 2). In endothelium-intact aortae, NAC-induced vasorelaxation was only shown for NACNO treatment with 13% of vasorelaxation from PHE-preconstricted aortic rings (Fig. 2A). In endothelium-removed aortae, NAC-induced vasorelaxation was shown for GSNO, NACNO and SNAP treatments with 27 ± 4%, 43 ± 3% and 23 ± 4% of vasorelaxation from PHE-preconstricted aortic rings, respectively (Fig. 2B).

The highest values of NAC-induced vasorelaxation were reached for NACNO treatment in both endothelium-intact and endothelium-removed aortae. The vasorelaxation induced by NAC following SNP treatment did not lead to significant vasorelaxation compared to the control (Fig. 2B).

The functional availability of this mobilized NO store was challenged by comparing PHE-induced vasoconstriction curves with or without NO-donor pretreatments (Fig. 3). Concentration-dependent response curves to PHE were not modified by any NO-donor treatment compared to the control condition in endothelium-intact aortae (Fig. 3A). However, in endothelium-removed aortae the curves were shifted to the right (one log unit) for GSNO, NACNO, SNAP and SNP treatments compared to control (Fig. 3B). The curves shifting to the right was materialized by an increase in EC_{50} and a decrease of pD_2 values, without any change in E_{max} values (Table 1). Moreover, the treatment of endothelium-removed aortae with GSNO, NACNO, SNAP and SNP decreased the pD_2 values close to the pD_2 values of endothelium-intact aortae. As expected, E_{max} values of PHE were higher in endothelium-removed compared to endothelium-intact aortae.

4. Discussion

RSNOs as a physiological storage and transport form of NO may be potential therapeutics to restore NO bioavailability. In this study, we evaluated whether (i) a RSNO treatment is able to produce NO store in vascular tissues - this was measured as the NOx species content - and whether (ii) this NO store is available to achieve the physiological roles of NO. For the first time, the NO store produced by RSNO treatment was quantified in both endothelium-intact and endothelium-removed aortae. We used endothelium-removed aortae as a model of endothelial dysfunction. The three RSNO treatments studied here increased NOx content, and thus NO store in the aortic wall. This NO store is available for the NAC-induced vasodilation, as well as for the opposition to PHE-induced vasoconstriction. However, while endothelium-

intact and endothelium-removed aortae seemed to accumulate NO store in the same quantities (a little bit higher in endothelium-intact aortae certainly due to the endogenous production of NO by the endothelium), the physiological responses to its mobilization did not follow the same profile.

This might be explained by a higher catabolism of RSNOs and SNP by enzymes present both at the endothelial and smooth muscle cell levels in endothelium-intact aortae. Gamma glutamyl transferase (GGT, responsible for GSNO catabolism) and redoxins like PDI and thioredoxin (Trx) are distributed on endothelial cells and smooth muscle cells [15,16,24] (Fig. 4). In previous studies, we showed that the GGT activity is higher on endothelial cells (2.46±0.20 nmol/min/mg proteins) than on smooth muscle cells (1.35±0.20 nmol/min/mg of proteins) [15,16,24]. That could explain the small increase in NOx species in endothelium-intact aortae. Concerning SNP, its transfer of NO has been shown to be catalyzed by thiols like glutathione [26]. As our system does not include GSH in the medium surrounding aortae, the transfer was probably assumed by thiols present at the cell membrane level (Fig. 4). However, this transfer seems less efficient than those catalyzed by GGT and redoxins for GSNO, NACNO or SNAP (Fig. 4). The NACNO treatment produced a similar amount of NO store either in endothelium-intact and in endothelium-removed aortae. This phenomenon was probably due to the mechanism of NACNO incorporation into the cells using the *L*-type amino acid transporter (L-AT) present either on endothelial cells [27] or on smooth muscle cells [28] without any catabolism.

In order to proof the bioavailability of NO following treatments, NAC was applied to displace NO from the NO store and induce vasorelaxation. The NO store produced by NACNO treatment was shown to be more available for vasorelaxation compared to GSNO, SNAP and SNP either in endothelium-intact and endothelium-removed aortae. However, the NAC-induced vasorelaxation was higher in endothelium-removed than in endothelium-intact aortae.

This might be explained the formation of a bigger NO store in the endothelium due to the presence of more active enzymes than the ones present on smooth muscle cells. The NAC-induced release of NO from this endothelial store can either create a new store through protein *S*-nitrosation process or diffuse in smooth muscle cells before inducing the vasorelaxation (Fig. 5A). The access of NAC to smooth muscle cells is weaker (Stated in grey in Fig. 5A) so the direct release of NO from the NO store present in smooth muscle cells is less implicated in the vasorelaxation. In endothelium-removed aortae, the NO store is made directly in smooth muscle cells when upon release induced by NAC can produce directly the vasorelaxation (Fig. 5B)

Concerning the responses to alpha-1 adrenergic receptor agonists, it is well known that the vasoconstriction induced by PHE in endothelium-intact aortae is a balance between the activation of alpha-1 adrenergic receptors on smooth muscle cells (vasoconstriction) and that of alpha-1 adrenergic receptors on endothelial cells (leading to the activation of the NO/sGC signaling pathway and then attenuation of the smooth muscle cells vasoconstriction). In the present study, as in others [19–22], the vasoconstriction induced by agonists of alpha-1 adrenergic receptors was modified by RSNOs treatment only in endothelium-removed aortae. Furthermore, as pD_2 values of PHE are equivalent in control endothelium-intact aortae and endothelium-removed aortae treated with NO-donors, we may hypothesize that these treatments, through the storage of NO in smooth muscle cells, might mimic the role of the (lacking) endogenous NO production and the function of the endothelium. However, as Emax was not modified, the vasoconstriction efficiency of PHE is retained even after NO-donor treatments. This phenomenon was already described – but only for GSNO - in a model of induced endothelial dysfunction [29].

In conclusion, our study proposes NO-donors as a potential treatment for endothelial dysfunction using endothelium-removed aortae in direct comparison with endothelium-intact

aortae. These NO-donors were shown to induce the formation of a store of NO, which was quantified and assessed for vasoactivity. The bioavailability of the NO store was challenged with NAC-induced vasorelaxation and PHE-induced vasoconstriction. The NO store formed by NO-donor, mainly by NACNO, was available for vasorelaxation and produced a hyporeactivity to PHE. However, these functional results (PHE and NAC protocols) were not in total agreement with the NO store formed by NO-donors pretreatments. Indeed, on one side, increased quantities of NOx species in both endothelium-intact and removed aortae was highlighted and on the other side, higher functional mobilization and vasoactivity capacities were observed only in endothelium-removed aortae. The NACNO treatment was more potent than other treatments regarding the amount of NO store and the amplitude of its impact on the functional study. We also showed that the bioavailability of the NO store for vasorelaxation is not only a matter of quantity, but is also dependent from the presence of the endothelium. And finally, we suggested that NO-donors, mainly NACNO, should be used as therapeutics to compensate endothelium function lost along cardiovascular diseases.

Acknowledgments

The PhD thesis of Mr Yi ZHOU is financially supported by the Chinese Scolarship Council. The authors acknowledge the NutRedOx (Cost project CA16112). The CITHEFOR EA3452 lab was supported by the "Impact Biomolecules" project of the "*Lorraine Université d'Excellence*" (*Investissements d'avenir – ANR*). The authors thank *Animalerie du Campus Biologie Santé, Université de Lorraine*, for its expertise in animal welfare and experiments. The Servier Medical Art by Served, licensed under a Creative Commons Attribution 3.0 Unported License was used to create figure 4 and figure 5.

REFERENCES

[1] K. Dharmashankar, M.E. Widlansky, Vascular endothelial function and hypertension: insights and directions, Curr. Hypertens. Rep. 12 (2010) 448–455. doi:10.1007/s11906-010-0150-2.

[2] M.D. Herrera, C. Mingorance, R. Rodríguez-Rodríguez, M. Alvarez de Sotomayor, Endothelial dysfunction and aging: an update, Ageing Res. Rev. 9 (2010) 142–152. doi:10.1016/j.arr.2009.07.002.

[3] S. Verma, T.J. Anderson, Fundamentals of endothelial function for the clinical cardiologist, Circulation. 105 (2002) 546–549. doi:10.1161/hc0502.104540.

[4] R. Dhananjayan, K.S.S. Koundinya, T. Malati, V.K. Kutala, Endothelial Dysfunction in Type 2 Diabetes Mellitus, Indian J. Clin. Biochem. 31 (2016) 372–379. doi:10.1007/s12291-015-0516-y.

[5] J. Deanfield, A. Donald, C. Ferri, C. Giannattasio, J. Halcox, S. Halligan, A. Lerman, G. Mancia, J.J. Oliver, A.C. Pessina, D. Rizzoni, G.P. Rossi, A. Salvetti, E.L. Schiffrin, S. Taddei, D.J. Webb, Working Group on Endothelin and Endothelial Factors of the European Society of Hypertension, Endothelial function and dysfunction. Part I: Methodological issues for assessment in the different vascular beds: a statement by the Working Group on Endothelin and Endothelial Factors of the European Society of Hypertension, J. Hypertens. 23 (2005) 7–17. doi:10.1097/00004872-200501000-00004.

[6] V.B. Schini-Kerth, N. Etienne-Selloum, T. Chataigneau, C. Auger, Vascular protection by natural product-derived polyphenols: in vitro and in vivo evidence, Planta Med. 77 (2011) 1161–1167. doi:10.1055/s-0030-1250737.

[7] R.M. Touyz, E.L. Schiffrin, Reactive oxygen species in vascular biology: implications in hypertension, Histochem. Cell Biol. 122 (2004) 339–352. doi:10.1007/s00418-004-0696-7.

[8] M. Félétou, T.J. Verbeuren, P.M. Vanhoutte, Endothelium-dependent contractions in SHR: a tale of prostanoid TP and IP receptors, Br. J. Pharmacol. 156 (2009) 563–574. doi:10.1111/j.1476-5381.2008.00060.x.

[9] J.K. Liao, Linking endothelial dysfunction with endothelial cell activation, J. Clin. Invest. 123 (2013) 540–541. doi:10.1172/JCI66843.

[10] J.N. Wilcox, R.R. Subramanian, C.L. Sundell, W.R. Tracey, J.S. Pollock, D.G. Harrison, P.A. Marsden, Expression of multiple isoforms of nitric oxide synthase in normal and atherosclerotic vessels, Arterioscler. Thromb. Vasc. Biol. 17 (1997) 2479–2488.

[11] M. Federici, R. Menghini, A. Mauriello, M.L. Hribal, F. Ferrelli, D. Lauro, P. Sbraccia, L.G. Spagnoli, G. Sesti, R. Lauro, Insulin-dependent activation of endothelial nitric oxide synthase is impaired by O-linked glycosylation modification of signaling proteins in human coronary endothelial cells, Circulation. 106 (2002) 466–472. doi:10.1161/01.cir.0000023043.02648.51.

[12] T.S. Hakim, K. Sugimori, E.M. Camporesi, G. Anderson, Half-life of nitric oxide in aqueous solutions with and without haemoglobin, Physiol. Meas. 17 (1996) 267–277. doi:10.1088/0967-3334/17/4/004.

[13] B. Meyer, A. Genoni, A. Boudier, P. Leroy, M.F. Ruiz-Lopez, Structure and Stability Studies of Pharmacologically Relevant S-Nitrosothiols: A Theoretical Approach, J. Phys. Chem. A. 120 (2016) 4191–4200. doi:10.1021/acs.jpca.6b02230.

[14] C. Gaucher, A. Boudier, F. Dahboul, M. Parent, P. Leroy, S-nitrosation/denitrosation in cardiovascular pathologies: facts and concepts for the rational design of S-nitrosothiols, Curr. Pharm. Des. 19 (2013) 458–472. doi:10.2174/1381612811306030458.

[15] E. Belcastro, W. Wu, I. Fries-Raeth, A. Corti, A. Pompella, P. Leroy, I. Lartaud, C. Gaucher, Oxidative stress enhances and modulates protein S-nitrosation in smooth muscle cells exposed to S-nitrosoglutathione, Nitric Oxide Biol. Chem. 69 (2017) 10–21. doi:10.1016/j.niox.2017.07.004.
[16] F. Dahboul, P. Leroy, K. Maguin Gate, A. Boudier, C. Gaucher, P. Liminana, I. Lartaud, A. Pompella, C. Perrin-Sarrado, Endothelial γ-glutamyltransferase contributes to the vasorelaxant effect of S-nitrosoglutathione in rat aorta, PloS One. 7 (2012) e43190. doi:10.1371/journal.pone.0043190.
[17] F. Dahboul, C. Perrin-Sarrado, A. Boudier, I. Lartaud, R. Schneider, P. Leroy, S,S'-dinitrosobucillamine, a new nitric oxide donor, induces a better vasorelaxation than other S-nitrosothiols, Eur. J. Pharmacol. 730 (2014) 171–179. doi:10.1016/j.ejphar.2014.02.034.
[18] C. Perrin-Sarrado, M. Pongas, F. Dahboul, P. Leroy, A. Pompella, I. Lartaud, Reduced Activity of the Aortic Gamma-Glutamyltransferase Does Not Decrease S-Nitrosoglutathione Induced Vasorelaxation of Rat Aortic Rings, Front. Physiol. 7 (2016) 630. doi:10.3389/fphys.2016.00630.
[19] J.L. Alencar, K. Chalupsky, M. Sarr, V. Schini-Kerth, A.F. Vanin, J.-C. Stoclet, B. Muller, Inhibition of arterial contraction by dinitrosyl-iron complexes: critical role of the thiol ligand in determining rate of nitric oxide (NO) release and formation of releasable NO stores by S-nitrosation, Biochem. Pharmacol. 66 (2003) 2365–2374. doi:10.1016/j.bcp.2003.07.017.
[20] J.L. Alencar, I. Lobysheva, K. Chalupsky, M. Geffard, F. Nepveu, J.-C. Stoclet, B. Muller, S-nitrosating nitric oxide donors induce long-lasting inhibition of contraction in isolated arteries, J. Pharmacol. Exp. Ther. 307 (2003) 152–159. doi:10.1124/jpet.103.052605.
[21] W. Wu, C. Perrin-Sarrado, H. Ming, I. Lartaud, P. Maincent, X.-M. Hu, A. Sapin-Minet, C. Gaucher, Polymer nanocomposites enhance S-nitrosoglutathione intestinal absorption and promote the formation of releasable nitric oxide stores in rat aorta, Nanomedicine Nanotechnol. Biol. Med. 12 (2016) 1795–1803. doi:10.1016/j.nano.2016.05.006.
[22] J.L. Alencar, I. Lobysheva, M. Geffard, M. Sarr, C. Schott, V.B. Schini-Kerth, F. Nepveu, J.-C. Stoclet, B. Muller, Role of S-nitrosation of cysteine residues in long-lasting inhibitory effect of nitric oxide on arterial tone, Mol. Pharmacol. 63 (2003) 1148–1158. doi:10.1124/mol.63.5.1148.
[23] M.-L. Bouressam, B. Meyer, A. Boudier, I. Clarot, P. Leroy, A. Genoni, M. Ruiz-Lopez, P. Giummelly, P. Liminana, V. Salgues, M. Kouach, C. Perrin-Sarrado, I. Lartaud, F. Dupuis, In vivo and in silico evaluation of a new nitric oxide donor, S,S'-dinitrosobucillamine, Nitric Oxide Biol. Chem. 71 (2017) 32–43. doi:10.1016/j.niox.2017.10.004.
[24] E. Belcastro, C. Gaucher, A. Corti, P. Leroy, I. Lartaud, A. Pompella, Regulation of protein function by S-nitrosation and S-glutathionylation: processes and targets in cardiovascular pathophysiology, Biol. Chem. 398 (2017) 1267–1293. doi:10.1515/hsz-2017-0150.
[25] J. Bonetti, Y. Zhou, M. Parent, I. Clarot, H. Yu, I. Fries-Raeth, P. Leroy, I. Lartaud, C. Gaucher, Intestinal absorption of S-nitrosothiols: Permeability and transport mechanisms, Biochem. Pharmacol. 155 (2018) 21–31. doi:10.1016/j.bcp.2018.06.018.
[26] L. Grossi, S. D'Angelo, Sodium nitroprusside: mechanism of NO release mediated by sulfhydryl-containing molecules, J. Med. Chem. 48 (2005) 2622–2626. doi:10.1021/jm049857n.

[27] K. Hayashi, P. Jutabha, T. Kamai, H. Endou, N. Anzai, LAT1 is a central transporter of essential amino acids in human umbilical vein endothelial cells, J. Pharmacol. Sci. 124 (2014) 511–513.
[28] J.A. Riego, K.A. Broniowska, N.J. Kettenhofen, N. Hogg, Activation and inhibition of soluble guanylyl cyclase by S-nitrosocysteine: involvement of amino acid transport system L, Free Radic. Biol. Med. 47 (2009) 269–274. doi:10.1016/j.freeradbiomed.2009.04.027.
[29] M. Sarr, M. Chataigneau, N. Etienne-Selloum, A.S. Diallo, C. Schott, M. Geffard, J.-C. Stoclet, V.B. Schini-Kerth, B. Muller, Targeted and persistent effects of NO mediated by S-nitrosation of tissue thiols in arteries with endothelial dysfunction, Nitric Oxide Biol. Chem. 17 (2007) 1–9. doi:10.1016/j.niox.2007.04.003.

FIGURE CAPTIONS

Fig. 1. Quantity of nitric oxide-derived (NOx) species in endothelium-intact (A) or endothelium-removed (B) rat aortae after incubation or not (control) with 2 µM of *S*-nitrosoglutathione (GSNO), *S*-nitroso-*N*-acetylcysteine (NACNO), *S*-nitroso-*N*-acetylpenicillamine (SNAP) or sodium nitroprusside (SNP) for 30 min. Results are presented as mean ± SD of n = 3-15 per group, from 3-15 different rats in each group and compared with a Kruskal-Wallis test; * $p < 0.05$ *versus* control.

Fig. 2. Vasorelaxant effects of *N*-acetylcysteine (10^{-5} M) in endothelium-intact (A) and endothelium-removed (B) rat aortae after incubation or not (control) with 2 µM of *S*-nitrosoglutathione (GSNO), *S*-nitroso-*N*-acetylcysteine (NACNO), *S*-nitroso-*N*-acetylpenicillamine (SNAP) or sodium nitroprusside (SNP) for 30 min followed by one hour of washing with Krebs' solution. Results are expressed as the percentage of 10^{-6} M phenylephrine preconstriction, presented as mean ± SD of n = 8-10 per group, from 4-8 different rats in each group and compared with one-way ANOVA; *$p<0.05$ *versus* control, $^{\#}p<0.05$ *versus* NACNO (Bonferroni's multiple comparisons test).

Fig. 3. Concentration-dependent responses curves to phenylephrine of endothelium-intact (A) and endothelium-removed (B) rat aortae after incubation or not (control) with 2 µM of *S*-nitrosoglutathione (GSNO), *S*-nitroso-*N*-acetylcysteine (NACNO), *S*-nitroso-*N*-acetylpenicillamine (SNAP) or sodium nitroprusside (SNP) for 30 min. Results are presented as mean ± SD of n = 6-17 per group, from 3-7 different rats in each group and analyzed using the Hill equation.

Fig. 4. Schematic representation of *S*-nitrosoglutathione (GSNO), *S*-nitroso-*N*-acetylcysteine (NACNO), *S*-nitroso-*N*-acetylpenicillamine (SNAP) and sodium nitroprusside (SNP) metabolism to produce a NO store of *S*-nitrosated proteins (Pr-SNO) in cells. Protein disulfide isomerase (PDI), gamma-glutamyltransferase (GGT), L-type amino acid transporter (L-AT), *S*-nitrosocysteine (Cys-NO).

Fig. 5. Schematic representation of *N*-acetylcysteine (NAC)-induced vasorelaxation either in endothelium-intact (A) and in endothelium-removed aortae (B). NAC enters inside endothelial cells (A) or smooth muscle cells (B) using the L-type amino acid transporter (L-AT). Then, NAC is deacetylated in cysteine residues that, in the presence of a NO store (PrS-NO), forms Cys-NO by transnitrosation process. The unstable Cys-NO immediately releases

NO that either diffuse to smooth muscle cells to activate the soluble guanylate cyclase (sGC) (A) or activate directly the sGC in the case of endothelium-removed aortae (B)

Table

Table 1. Pharmacodynamic parameters calculated from phenylephrine concentration curves established on endothelium-intact and endothelium removed aortae subjected or not to 2 µM of *S*-nitrosoglutathione (GSNO), *S*-nitroso-*N*-acetylcysteine (NACNO), *S*-nitroso-*N*-acetylpenicillamine (SNAP) or sodium nitroprusside (SNP) treatment.

		Control	GSNO	NACNO	SNAP	SNP
Endothelium Intact	**pD_2**	6.1 ± 0.43	5.9 ± 0.2	5.9 ± 0.2	5.9 ± 0.2	5.8 ± 0.1
	E_{max} (g)	2.0 ± 0.5	1.9 ±0.4	2.7 ± 0.3	2 ± 1	2 ± 1
Endothelium Removed	**pD_2**	7.5 ± 0.4	**6.5 ± 0.2***	**6.3 ± 0.2***	**6.5 ± 0.2***	**6.3 ± 0.3***
	E_{max} (g)	4.0 ± 0.6	3.5 ± 0.69	4.1 ± 0.7	3.7 ± 0.67	3.3 ± 1.3

Figure 1

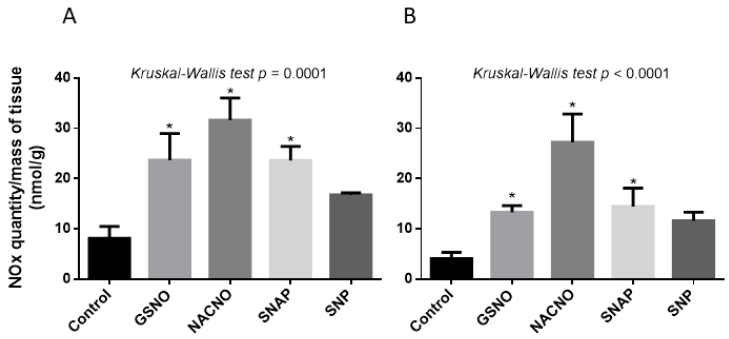

Figure 2

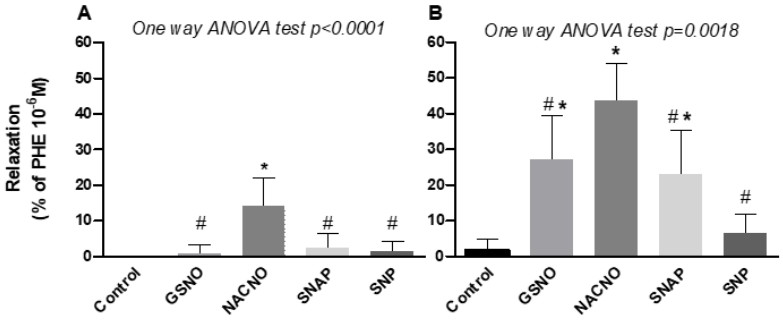

Figure 3.

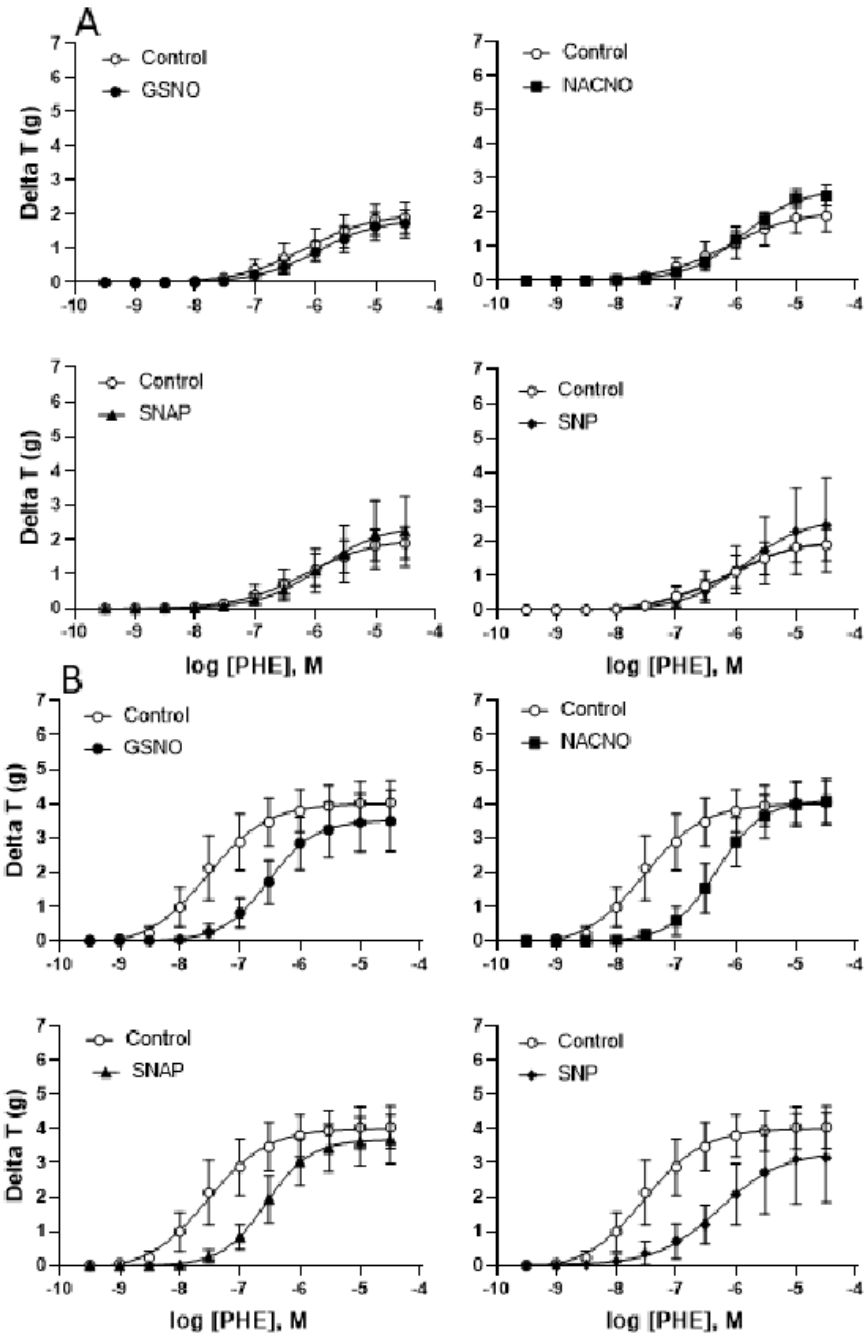
A
Control
GSNO
Control
NACNO
Control
SNAP
Control
SNP
Delta T (g)
log [PHE], M
B
Control
GSNO
Control
NACNO
Control
SNAP
Control
SNP
Delta T (g)
log [PHE], M

Figure 4

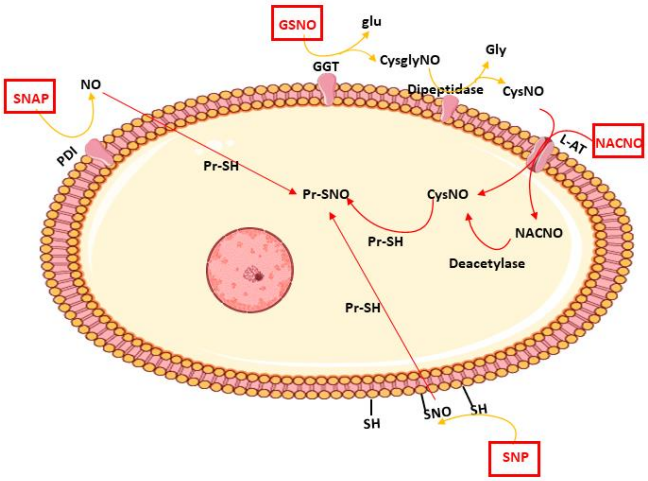

Figure 5

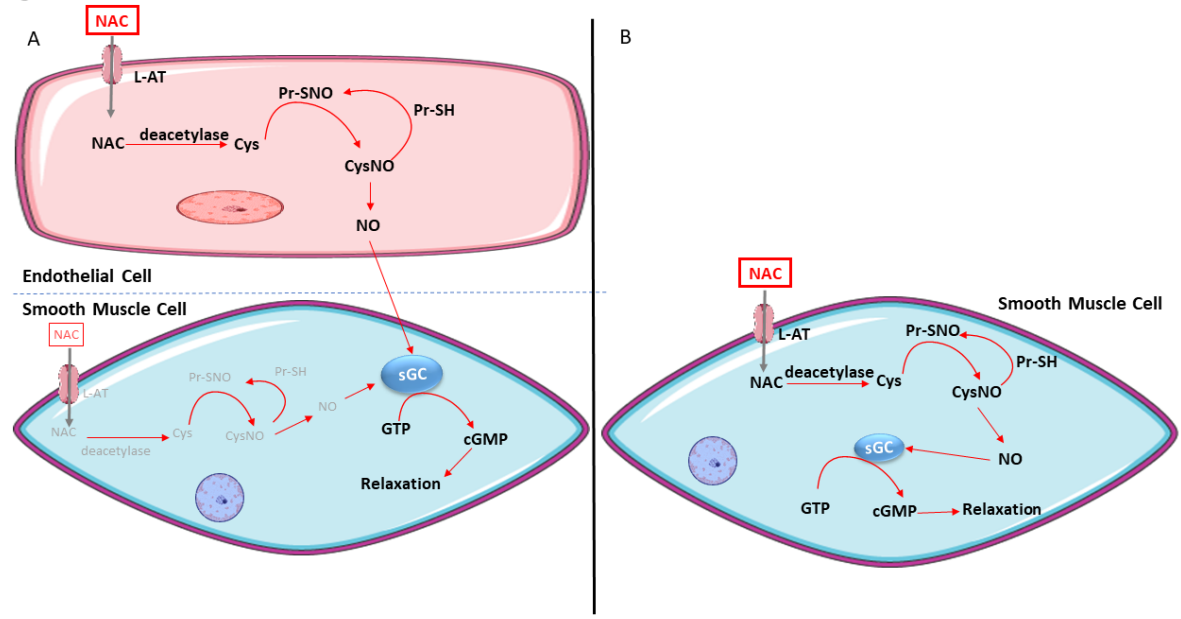

Chapter 4: Nano or micro? Three different particles to deliver GSNO through oral route.

As described in the chapter 2, GSNO showed a middle-class intestinal permeability preferentially through transcellular way. It was therefore postulated that GSNO can be administrated *via* the oral route. Oral delivery of GSNO seems to be a good method to apply GSNO with its advantages such as patient compliance, convenience, low cost, non-injection as well as lower infection risk. These merits are important especially when applied to chronic disease like cardiovascular diseases. However, GSNO is easy to degrade through different *in vitro* parameters and enzymes *in vivo.* The protection of GSNO through gastrointestinal tract is crucial for its applications through oral administration route. As shown in Tables 1-4, few oral formulations have been developed to deliver GSNO, which is a small hydrophilic molecule and easy to diffuse. To develop GSNO-loaded formulation through oral administration adapted to CVD application, several factors should be considered:

1. Material adapted to oral route.
2. Efficient encapsulation efficiency of GSNO
3. Sustained release
4. Intestinal permeability enhancement
5. Stability of encapsulated GSNO

As described in the Chapter 1, GSNO-NP have been developed in our lab using polymer **Eudragit® RL PO** through a water-in-oil-in-water (W/O/W) double emulsion/solvent evaporation method. In addition, microparticles share the advantages of nanoparticles but with additional ones such as higher drug loading and longer sustained release time. Thus, modification of GSNO-NP was considered in order to reach the four requirements above.

Eudragit® RL PO: The proper selection of material is of significant importance to develop a formulation. Eudragit® RL PO used in the GSNO-NP preparation belongs to Eudragit® family, which are nonabsorbable (in water), non-biodegradable and non-toxic polymers. Eudragit® RL PO is a copolymer consisting of methyl methacrylate, ethyl acrylate and methacrylic acid ester (low content) with quaternary ammonium groups. As a solid substance (white powder) with a faint amine-like smell, Eudragit® RL PO is used as coating material to get sustained drug release and is also suitable

for matrix structures. It is widely used in the development of drug delivery systems such as mucoadhesive tablets, nanoparticles, solid dispersions. Singh et al[213]. described that Eudragit® RLPO with iron oxide combination presented a high-level potential for developing gastroretentive and mucoadhesive drug delivery systems. Pandey et al[214] developed a site-specific patch using Eudragit® RLPO and RSPO, with a 12 h sustained release as well as mucoadhesion effect. Thus, Eudragit RLPO is a good candidate polymer for oral delivery system with sustained release.

Double emulsion (W/O/W and S/O/W)

After determining the polymer used to prepare the particles, the next step is to choose the preparation process. Several methods are potentially useful for the nano/microparticles preparation. One of the most common is single emulsion, it can encapsulate drugs, which are poorly soluble or lipophilic drugs successfully but it is not suitable for the highly water-soluble drugs. This problem can be solved using the double emulsion technique (also called “multiple emulsion”)[215].

Water in oil in water (W/O/W) double emulsion

The water in oil in water double emulsions separate the internal aqueous phase from external aqueous phases using an oil layer. The oil layer in the middle acts as a liquid membrane to constrain the hydrophilic drugs inside. Thus, this double emulsion system is regarded as a good candidate for controlled release of hydrophilic drugs. The water in oil in water double emulsion/solvent evaporation is the main method to prepare W/O/W microparticles. As shown in Figure 18, drugs are dissolved in an aqueous phase (inner aqueous phase, W1). W1 is then emulsified in an oil phase which is always the solution of polymer, resulting in the water in oil emulsion (W1/O). Then, this primary emulsion (W1/O) is dispersed in another aqueous phase (outside aqueous phase, W2) to produce the W1/O/W2 double emulsions. After removing the organic solvent through evaporation, the double emulsion particles can be collected

through centrifugation or filtration[216].

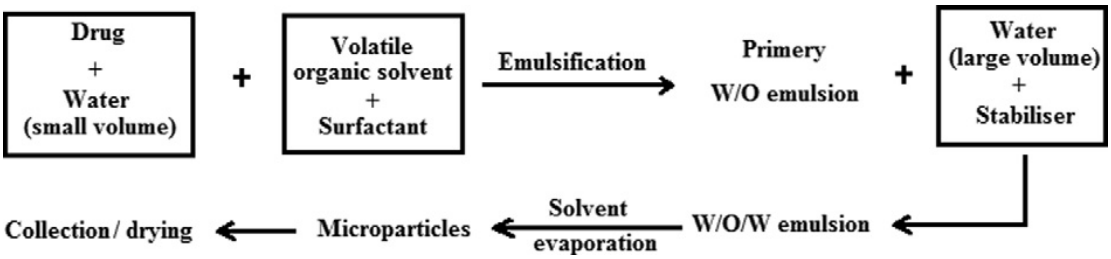

Figure 10. Scheme of the preparation procedure for drug loaded microparticles by the double emulsion solvent evaporation method[215].

Solid in oil in water (S/O/W) double emulsion

W/O/W double emulsion technique is the most commonly used for the microparticles preparation. However, some drugs may lose their activities during this process, or tend to aggregate such as proteins. When protein solution is emulsified under high shear with organic solvent, it is easy for protein to be adsorbed to the interface between water and oil phase[217,218]. Thus, S/O/W methodology has been applied to solve this problem since it can improve the protein stability during encapsulation, as it avoids the W1/O interface. The S/O/W double emulsion is prepared through a similar way than the W/O/W double emulsion, except that the solid drugs are dispersed directly in the polymer solutions to get the primary emulsion. This primary emulsion is then emulsified into a large volume of aqueous solutions with emulsifying agent. Compared with W/O/W double emulsion, S/O/W emulsion has several advantages. It avoids the first W/O emulsion, which limits the possible degradation or diffusion of inner drugs. Thus, it provides a more stable drug state and higher loading capacity. In addition, Lautner[219] and colleagues found that the encapsulation efficiency and release profile of S/O/W microparticles may be related to the size of inner phase, through preparation of SNAP loaded S/O/W PLGA microparticles.

In the article, three different particles (nanoparticles or microparticles) have been obtained through W/O/W double emulsion or S/O/W double emulsion using Eudragit® RL PO to deliver GSNO through oral route. As shown in article 4:

Article 4: Enhancing intestinal permeability of nitric oxide with storable microparticles for *S*-nitrosoglutathione oral delivery

Des microparticules préparables à l'avance pour la délivrance de *S*-nitroglutathion par voie orale et capables d'augmenter la perméabilité intestinale du monoxyde d'azote

Yi ZHOU, Caroline GAUCHER, Isabelle FRIES, Mehmet HOBBEKAYA, Charlène MARTIN, Clément LEONARD, Frantz DESCHAMPS, Anne SAPIN-MINET, Marianne PARENT*

*Manuscript
Click here to view linked References

Enhancing intestinal permeability of nitric oxide with storable microparticles for *S*-nitrosoglutathione oral delivery

Yi ZHOU[a], Caroline GAUCHER[a], Isabelle FRIES[a], Mehmet-Akif HOBEKKAYA[a], Charlène MARTIN[a], Clément LEONARD[b], Frantz DESCHAMPS[b], Anne SAPIN-MINET[a], Marianne PARENT[a,*]

[a] Université de Lorraine, CITHEFOR, F-54000 Nancy, France

[b] StaniPharm, 5 rue Jacques Monod, BP 10, 54250 Champigneulles, France

*Correspondence: marianne.parent@univ-lorraine.fr, EA 3452 CITHEFOR, Campus Brabois Santé, 9 avenue de la Forêt de Haye - BP 20199, 54505 Vandoeuvre Les Nancy Cedex, Tel +33-3-7274-7307

Mr Yi ZHOU is supported by a CSC (China Scholarship Council) funding.
The authors acknowledge support of EA 3452 CITHEFOR by the "Impact Biomolecules" project of the "Lorraine Université d'Excellence" (Investissements d'avenir – ANR).
These funding sources were not involved in study design, collection, analysis, interpretation of data, writing of the report nor in the decision to submit it for publication.

Declarations of interest: none

Abstract

Three kinds of particles encapsulating a physiological donor of nitric oxide, i.e. *S*-nitrosoglutathione (GSNO), were developed using the same raw materials but various double emulsion/solvent evaporation processes. W/O/W Nano- or micro-particles were compared to S/O/W micro-particles regarding size, encapsulation efficiency, *in vitro* release, cytocompatibility and intestinal permeability of GSNO (Caco-2 cells). All particles had an ~ 30% encapsulation efficiency but microparticles had a slower *in vitro* release and enhanced drastically GSNO permeation through the model of intestinal barrier. Moreover, size and GSNO content of all particles were maintained after lyophilization, and up to 1 month (microparticles) and 3 months (nanoparticles) after storage at 4°C. In conclusion, these GSNO-loaded particles might represent a new alternative for chronic oral treatment of pathologies associated with a deficit in nitric oxide.

Keywords: nitric oxide, *S*-nitrosoglutathione, nanoparticles, microparticles, oral delivery

1. Introduction

Nitric oxide (NO) is a gaseous messenger, produced by different cells like endothelial cells, macrophages or neutrophils, thanks to NO synthases[1]. Depending on the context and on its concentration, NO is implicated in controlling blood pressure (through relaxation of smooth muscle cells), wound healing and tissue regeneration, immune response, neurotransmission or anti-cancer defense[2-6]. As a result of these pleiotropic actions, the dysregulation of NO homeostasis through NO deficiency is linked to disorders like atherosclerosis, pulmonary hypertension, thrombosis and ischemia[3,4]. A treatment able to restore the physiological NO levels would therefore represent a major therapeutic advance for a growing number of patients. This is however quite challenging as NO gas may not be used directly in many cases. Its radical nature results in high reactivity and very short half-life (< 1s)[5].

In this context, NO donors have been developed over the past decades, including organic nitrates[6], nitrosamines[7], or metal-NO complex[8]. Among these NO donors, *S*-nitrosothiols (RSNO)[2,9-10] and diazeniumdiolates (NONOates)[11] are the most studied as promising drug candidates. NONOates are purely synthetic compounds, while RSNO are the physiologic forms of transport and storage of NO in our body[2]. In particular, *S*-nitrosoglutathione (GSNO) has recently gained a lot of attention for different biomedical applications[12]. This leadership could be explained by several advantages over other RSNO, in addition to its antiplatelet[13] and arterioselective vasodilator[12] effects: i) it is physiologic and safe, because the NO residue is grafted to glutathione (GSH), an anti-oxidant abundant in the cells; ii) it is relatively stable

compared to other endogenous RSNO; iii) it can release NO under the action of several enzymes. Most of them catabolize all types of RSNO (*e.g.* protein disulfide isomerases, thioredoxins[14]…) but the gamma-glutamyl transpeptidase is dedicated to GSNO metabolism.

All these properties could be of great interest in many conditions, including chronic cardiovascular diseases. In this context of long-term treatment, an oral delivery will be the most acceptable for the patients. Previously[15], we showed that RSNO can cross the intestinal barrier (Caco-2 intestinal model) with a medium apparent permeability rate using a passive mode, so they can be administrated through the oral route. Nevertheless, RSNO-delivery systems are needed to reveal the full potential of RSNO oral treatment. On the one hand, these systems could protect RSNO from the gastro-intestinal degrading factors (such as temperature, pH variation, metallic ions, enzymes…). On the other hand, they could modulate and/or sustain the NO release. Two approaches are commonly distinguished: *S*-nitrosation of thiol-containing prodrugs or encapsulation of RSNO in polymeric nano- or micro-structures. As examples of the first approach, dextran derivatives modified with cysteamine and cysteine have been *S*-nitrosated at their terminal thiol functions by Damodaran et al[16], generating a stable NO-releasing compound with antiplatelet effect. Shah et al[17] obtained a polymeric *S*-nitrosoglutathione-oligosaccharide-chitosan through the linkage of GSH to chitosan followed by a post-nitrosation with sodium nitrite. This new polymer showed a sustained release of NO for at least 6 hours. Similarly,

87 Katsumi et al[18] prepared a PEG-conjugated *S*-nitrosobovine serum albumin through
88 the *S*-nitrosation of the cysteine residue of the protein, thereby increasing NO half-life
89 and prolonging its vasorelaxant action. The encapsulation approach can itself be
90 divided into two strategies: direct encapsulation of RSNO (one-step) or encapsulation
91 of a thiol followed by its *S*-nitrosation (two-steps). For example, chitosan
92 nanoparticles encapsulating GSH have been prepared, then nitrosated before
93 incorporation in a Pluronic F-127 hydrogel for topical administration[19]. Some
94 attempts of direct encapsulation were reported in various delivery systems. Parent et
95 al[20] formulated GSNO and SNAP into *in situ* implants or microparticles. A sustained
96 and mild decrease in mean arterial pressure *versus* free drugs has been found after
97 their subcutaneous injection to rats. Moreover, beneficial effects of these formulations
98 have been observed in an acute model[21] of stroke. Regar et al[22] grafted
99 *S*-nitrosocysteamine onto the surface of poly(lactic-co-glycolic acid) (PLGA)
100 nanoparticles, thus increasing the antibiotic efficiency of tetracycline against *E. Coli*,
101 without any cytotoxicity to fibroblasts. Through the solid-in-oil-in-water (S/O/W)
102 double emulsion method, Lautner et al[23]. have encapsulated SNAP within
103 biodegradable PLGA microspheres with a high encapsulation efficiency (up to 61.9 %)
104 and long-time release. In sum, most of the systems described above focused on topical
105 or parenteral RSNO delivery, not oral one. Moreover, GSNO is poorly represented in
106 all previously reported studies, despite its specific strengths: this could be explained
107 by its high hydrophilicity, making it difficult to trap into polymeric matrices.
108 Nevertheless our lab succeeded previously[24–26]in encapsulating GSNO in polymeric

nanoparticles, with a satisfactory encapsulation efficiency and a delayed protein *S*-nitrosation in smooth muscle cells compared to free GSNO. The nanoparticles were prepared with a water in oil in water (W/O/W) double emulsion/evaporation process (suitable for such a hydrophilic drug) with Eudragit® RL PO polymer, commonly used for tablet coating. To enhance the encapsulation efficiency of GSNO and sustain its release, these nanoparticles have been incorporated into an alginate/chitosan matrix. A single oral administration of the resulting composite particles to rats was sufficient to generate a NO store in their aorta. Despite these very interesting results, the preclinical development of these composite formulations is hindered by several points. First, the multi-step preparation and adequate characterization of the composites take more than 6 hours, which is far too time-consuming. Second, these formulations are not stable and should be used immediately after preparation (no possibility to transfer them to other labs to be tested in preclinical models).

As a result, in this work we explored the possibilities to prepare GSNO-loaded microparticles from the same raw materials and double emulsion/evaporation process than for the previous nanoparticles. Microparticles were prepared with the W/O/W process (GSNO-MPW) but also with a S/O/W process (GSNO-MPS), as it often allows better encapsulation and more sustained release of drugs in the literature[22]. These particles were compared to nanoparticles (GSNO-NP) in terms of size, encapsulation efficiency and *in vitro* release. Moreover, to get particles in a stable solid state, a lyophilization process was applied. Potential modifications of critical product attributes (encapsulation efficiency and size) after drying were assessed, as

well as the stability of dried products. Caco-2 cells were used to evaluate the cytocompatibility of the 3 particle types. Intestinal permeability of NOx species was evaluated in an *in vitro* model of intestinal barrier.

2. Materials and Methods

All solutions were prepared with ultrapure deionized water (>18.2 MΩ.cm). GSNO was synthesized, purified and stored as previously described[26]. Eudragit® RLPO was a gift from Evonik industries (Germany). Mercuric chloride ($HgCl_2$) was purchased from Prolabo (Switzerland), sodium nitrite ($NaNO_2$) from Merck (Germany), sodium hydroxide (NaOH) from VWR Chemicals (Czech Republic), methanol from Carlo Erba Reagents (France) and Nitrite/nitrate fluorimetric kit from Cayman Chemical (Ref. *780051*, USA). 2,3-diaminonaphthalene (DAN), sulfanilamide, N-(1-naphthyl) ethylenediamine (NED) and all other reagents (including Kolliphor P188) were obtained from Sigma–Aldrich (France).

2.1. Preparation of GSNO-loaded nanoparticles (GSNO-NP), and GSNO-loaded microparticles by water-in-oil-in-water (GSNO-MPW) or solid-in-oil-in-water (GSNO-MPS) and lyophilization

GSNO-NP were prepared by a water-in-oil-in-water (W/O/W) emulsion/solvent evaporation technique. Briefly, 500 µL of 0.1% (w/v) Kolliphor P188 solution containing 10 mg of GSNO was emulsified by sonication for 60 s (11 W, 100% amplitude, Vibra cell™ 72434, France) in 5 mL of methylene chloride containing 500

153 mg of Eudragit, over an ice bath. The resulting primary emulsion was then poured in
154 19.5 mL of 0.1% (w/v) Kolliphor P188 solution with sonication (30 W, amplitude
155 maximum, Vibra cell™ 75022, France) for 30 s, to get the W/O/W emulsion. The
156 final NP suspension was obtained after 10 min of solvent evaporation.
157
158 GSNO-MPW were prepared as the GSNO-NP, except that the second emulsification
159 was performed with a vortex (VV3, VWR, USA) at maximum speed for 60 s, rather
160 than with ultrasonication. The whole process was conducted at controlled temperature
161 (24 ± 0.5 °C). The resulting suspension was hardened with a similar step of solvent
162 evaporation.
163
164 GSNO-MPS were prepared as GSNO-MPW, except that 10 mg of GSNO powder
165 (sieved at 40 µm) were directly suspended in the Eudragit/DCM solution.
166
167 After the preparation of particles, the suspensions were centrifuged (42,000 *g*, 4°C,
168 NP for 30 min and MP for 10 min) and the pellets were re-suspended in 10 mL of 10%
169 (w/v) sucrose solution. The re-suspensions were frozen at -80°C for 15 h ± 1 h then
170 lyophilizated for 24 h ±1 h (FreeZone6 LABCONCO USA, setups: condenser at
171 -50°C and pressure at 0.04 mbar). A preliminary study was conducted to optimize the
172 lyophilization of NP. Freezing the particles at -80 °C (instead of liquid nitrogen) and
173 using sucrose as protectant (instead of trehalose, and no mannitol) were selected as
174 the best and lowest-cost conditions.

175

176 After drying, the residual water content in the lyophilizate was immediately tested
177 with a Karl-Fischer apparatus (756 KF coulometer, France). All powders were placed
178 under nitrogen and stored at 4°C protected from light.

179

180 **2.2. Physicochemical characterization of particles**

181 The hydrodynamic diameter, polydispersity index (PDI) and zeta-potential of the NP
182 were measured in triplicate in 0.001 M NaCl by dynamic light scattering (Zetasizer
183 Nano ZS, Malvern Instrument, France). All measurements were performed at 25°C
184 after 30 s of equilibration with an angle detection of 173° backscatter.
185 The sizes of the MP were also measured in triplicate in 0.001 M NaCl by a
186 Mastersizer (hydro 2000 SM, Malvern Instruments, France). Span was calculated as
187 follows:

188 $$\mathbf{Span = (D_{v90} - D_{v10}) / D_{v50}}$$

189 where D_{v10}, D_{v50}, D_{v90} are values of size below which 10%, 50% or 90% of the
190 particles are contained.
191 The surface morphology of the particles was investigated by scanning electron
192 microscopy (SEM, Hitachi S4800, Japan, accelerating voltage 1 kV). Briefly, fresh
193 suspension of NP was diluted 10^6-fold. Then, a drop was deposited and dried
194 overnight at room temperature, and flash carbon coated (4 s). In the case of MP,
195 lyophilizates were observed after carbon coating.

196

197 **2.3. Determination of GSNO encapsulation efficiency**

198 The encapsulation efficiency (EE) was determined by quantifying the GSNO
199 contained inside the particles. After particles centrifugation (42,000 *g*, 30 min for NP,
200 10 min for MP), the pellets were collected and destroyed by methylene chloride.
201 GSNO was then extracted with phosphate buffer saline (0.148 M PBS, pH=7.4) (ratio
202 methylene chloride/PBS 1:10) using high speed shaking (2000 rpm, Heidolph
203 Vibramax 110, Germany). After centrifugation (2500 *g* for 10 min), GSNO was
204 quantified in the supernatant using Griess and Griess-Saville reactions[27]. Total
205 recovery of GSNO during the extraction process has been verified and potential
206 matrix effect with polymer residues have been ruled out in preliminary experiments.
207 The encapsulation efficiency was assessed immediately after particles preparation and
208 again after lyophilization, and was calculated according to:

209 $$EE = (m_e / m_i) * 100\%$$

210 Where EE is encapsulation efficiency (%), m_e the mass of drug entrapped in particles,
211 and m_i is the mass of initial drug. The residual water content in the powders after
212 lyophilization can affect the EE value, and calculations were therefore corrected
213 accordingly.

214

215 **2.4. Stability of particles before and after lyophilization.**

216 After preparation, fresh suspensions were centrifuged (42,000 g, 4°C, NP for 30 min
217 and MP for 10 min) and the pellets were re-suspended in 1 mL water and stored at 4 °C
218 protected from light. After 1, 2, 3, or 4 days, size and encapsulation efficiency were

219 measured as previously described.

220 After lyophilization, the particle powders were separated and stored at 4 °C under

221 nitrogen and protected from light. After 1, 2, 3, 4, 5, 8 and 12 weeks, size and

222 encapsulation efficiency were checked as previously described and compared to the

223 values obtained immediately after lyophilization.

224

225 **2.5. Kinetics of GSNO release**

226 Immediately after preparation, 1 mL of fresh particles suspensions were centrifuged

227 (42,000 *g*, 4 °C, NP for 30 min and MP for 10 min) and the pellets were suspended in

228 1 mL of 0.148 M PBS (pH 7.4) and transferred into dialysis cellulose membrane

229 (average flat width 10 mm (0.4 in), cut-off 14,000 Da). The membrane was immerged

230 in 200 mL PBS at 37 °C protected from light with magnetic agitation at 200 rpm. The

231 GSNO and nitrite ions released in the medium were quantified using the DAN and

232 DAN-Hg^{2+} methods[12] at different time intervals (every 30 min during two hours and

233 every hour from two to six hours).

234

235 **2.6. Cytocompatibility of particles**

236 Intestinal Caco-2 cells (ATCC® HTB-37™) were grown in complete medium

237 consisting of Eagle's Minimum Essential Medium supplemented with 10% (v/v) fetal

238 bovine serum (FBS), 4 mM of glutamine, 100 U/mL of penicillin, 100 U/mL of

239 streptomycin, 1 % (v/v) of non-essential amino acids. Cells were cultivated at 37 °C

240 under 5 % CO_2 (v/v) in a humidified incubator. Cells were then seeded in a 96-well

plates at 10^5 cells/well. After 24h, they were exposed to free GSNO (from 25 to 2500 µM) or to the lyophilizate particles (3 batches, in duplicate, at equivalent concentrations of GSNO 25 to 2500 µM) for 24 h in complete medium. After incubation, cytocompatibility was checked by the MTT[29] method. The absorbance was read at 570 nm with a reference at 630 nm using EL 800-microplate reader (Bio-TEK Instrument, France). Metabolic activity in the presence of treatments was compared to the control condition, *i.e.* medium alone (as 100%).

2.7. Intestinal Permeability

Caco-2 cells were seeded at 2×10^6 cell/cm^2 on cell culture inserts (Transwell®, Corning, USA) with 0.4 µm pore size disposed in a 12-wells plate. The medium (complete medium containing FBS) was replaced every two days during the first week and every day during the second week. The intestinal barrier was validated when the differentiated cell monolayer was obtained after 14-15 days of culture. This was verified by a transepithelial electrical resistance (TEER) value > 500 Ω.cm^2. Intestinal permeability of the 3 different lyophilizate particles (GSNO concentration 100 µM in all cases, 3 batches, in triplicate) was compared to free GSNO in HBSS $^+$ (containing Ca^{2+} and Mg^{2+}). HBSS $^+$ and HBSS $^-$ were used as controls for permeability and integrity of the intestinal barrier model, respectively. After 1 h of incubation, the amounts of NOx species (*i.e.* RSNO + nitrite ions + nitrate ions) were assessed in the apical medium, inside the particles and in the basolateral medium. A

TEER value higher than 300 $\Omega.cm^2$ and a fluorescein permeability lower than 5% at the end of the test validated the integrity of the intestinal monolayer.

The apparent permeability coefficients (Papp) were calculated as follows:

$$\mathbf{Papp = (dQ/dt) \times (1/(A \times C_0))}$$

Where dQ/dt ($mol.s^{-1}$) refers to the permeability rate (mol) of RSNO or NOx in the basolateral compartment at the time of quantification, A (cm^2) to membrane diffusion area, and C_0 ($mol.mL^{-1}$) to the initial concentration in the apical compartment.

The recovery rate of NOx species (mass balance of GSNO) was checked by comparing the amount of NOx species quantified in the different compartments (apical, basolateral, in the particles) with the initial amount of GSNO deposited.

2.8. Statistical analysis

All the results are shown as either mean ± standard deviation (sd, for characterization) or mean ± standard error of mean (sem, for cells results). In all cases, three independent batches (preparation and lyophilization) were used.

The one-way ANOVA or two-way ANOVA (Dunnett's multiple comparisons test or Tukey's multiple comparisons test) were used for the analysis of particles stability, release and Caco-2 cells experiments. $p < 0.05$ was considered as significantly different. Statistical analyses were performed using the GraphPad Prism software (GraphPad Software, USA).

3. Results

284 **3.1. Formulation and lyophilization of particles**

285 The three types of particles encapsulating GSNO were prepared starting from the
286 same amount of the same raw materials (GSNO and Eudragit® RL PO) using different
287 processes based on double emulsion/solvent evaporation. Microparticles were
288 obtained by decreasing the energy of the second emulsion (GSNO-MPW) and using
289 solid GSNO in the first emulsion (GSNO-MPS). These modifications were efficient to
290 increase particles size from 225.1 nm ± 3.3 nm for GSNO-NP to 68.9 µm ± 7.1 µm
291 for GSNO-MPW and 165.1 µm ± 13.9 µm for GSNO-MPS (Figure 1). However, the
292 process did not modify GSNO encapsulation efficiency (27.9% ± 1.9% for
293 GSNO-MPW, 25.8% ± 3.1% for GSNO-MPS *versus* 33.4% ± 6.1% for GSNO-NP).
294 In all cases, the amount of nitrite ions was lower that the LOQ value of the method
295 used, meaning that the encapsulation process is suitable for a sensitive drug such as
296 GSNO. The zeta-potential of GSNO-NP was highly positive (+ 38.3 mV ± 1.0 mV)
297 due to the positive charges of the Eudragit® polymer. This may explain the stability of
298 the size of GSNO-NP when stored as suspensions (Figure 2). However, their GSNO
299 content decreased quickly during storage, highlighting the poor overall stability of
300 these suspensions. A lyophilization process with sucrose was implemented to stabilize
301 the three particles types and did not modify their characteristics (size, zeta potential,
302 GSNO encapsulation efficiency, Figure 1).
303 SEM images show that the three kinds of particles are roughly spherical, with a more
304 or less smooth surface and no visible pores at the surface (Figure 1d). It was not
305 possible to observe freeze-dried powder of GSNO-NP (instead, fresh particles were

306 observed), because the sucrose included in the lyophilizate generated structures in the
307 same range of size than NP.
308
309 **3.2. Stability of the particles as fresh suspensions**
310 Although the sizes of all particles stayed stable (in the range of 90% to 110% of initial
311 values) during three days (Figure 2), their GSNO content dropped to less than 80% of
312 the initial value for all types of particles within two days, and below 50% after three
313 days. Similar results were previously obtained for NP[23,24].
314
315 **3.3. Stability of the particles after lyophilization**
316 After lyophilization, the powders of the three particles types were stored at 4 °C
317 protected from light and oxygen. The size and EE were measured on separated
318 aliquots every week during the first five weeks then after two and three months
319 (Figure 3).
320 During storage, the size of all particles stayed stable in the range 90-110% of the
321 post-lyophilization size. In contrast, the GSNO content in NP started to decrease
322 slowly after the 4 first weeks, with 90% of initial GSNO remaining after 3 months.
323 The GSNO content in MP decreased significantly after 3 or 4 weeks of storage. These
324 results might be linked to the different residual water content of the lyophilizates:
325 GSNO-NP 7.4% ± 4.6%; GSNO-MPW 8.9% ± 4.7%; GSNO-MPS 26.0% ± 10.8%.
326 However, more than 80% of initial GSNO remained inside GSNO-MPS after 1 month
327 and GSNO-MPW after 2 months. In the end, lyophilizate NP could be considered

328 stable for 3 months and MP for at least 1 month.

329

330 **3.3. *In vitro* release**

331 The *in vitro* release kinetics of GSNO from the fresh suspensions were determined in

332 a dialysis bag (Figure 4).

333

334 The *in vitro* release profiles of GSNO showed an initial burst in the first 1.5 h for all

335 types of particles. At 2 h, the cumulative release from microparticles is lower (around

336 70-75%) than for free GSNO and GSNO NP (around 90% released). Complete release

337 was achieved after 6h (no more GSNO released from the particles from 6h to 24h).

338 However, the GSNO already released in the medium continued to degrade into nitrite

339 ions (around 50% at 24 h).

340

341 **3.4. Cytocompatibility of particles.**

342 The 24-h cytocompatibility of the three types of particles is presented in Figure 5. For

343 all tested conditions, the cell viability decreased while increasing the GSNO

344 concentration. It went below 80% for concentrations above 500 µM of free GSNO,

345 and 50 µM of eq [GSNO] for all kind of particle. The IC_{50} value of free GSNO was

346 1717.9 ± 1.3 µM. It decreased for the particles, in the order GSNO-MPS (309.8 ± 1.1

347 µM), GSNO-MPW (198.5 ± 1.1 µM) and GSNO-NP (140.0 ± 1.1 µM).

348

349 **3.5. Intestinal Permeability of NOx from different particle types**

350 The intestinal permeability of NOx species from particles compared to free GSNO
351 was evaluated using an *in vitro* intestinal barrier model (Figure 6).
352
353 The mass balance (Table 1) and the values of apparent permeability coefficient (Papp)
354 (Table 2) were then calculated for all NOx species.
355
356 The mass balance calculated at the end of the permeability study showed that most of
357 the GSNO initially encapsulated or added (free) was recovered under RSNO, nitrite
358 ions and mostly nitrate ions species.
359 At the end of incubation, the amount of GSNO in the apical media was significantly
360 lower for GSNO-MPs conditions (*circa* 60% of initial load) than for GSNO-NP
361 (~75%) and free GSNO (~90%). While around 10% of GSNO remained inside NP,
362 almost 20% were still inside MP. This confirms the slower release of GSNO for MP
363 than NP, previously observed in the *in vitro* experiment. In the meantime, MP led to a
364 drastically higher concentration of nitrate ions in the basolateral side compared to free
365 GSNO or NP conditions.
366 The Papp values of each NO species are higher for GSNO-MPs than for GSNO-NP or
367 free GSNO (Table 2). This led to a global Papp (NOx species) at least two times
368 higher for GSNO-MPW and GSNO-MPS than for GSNO-NP and free GSNO. This
369 situation is mainly driven by a higher permeability of nitrate ions than nitrite ions and
370 RSNO.
371

4. Discussion

As mentioned previously, the therapeutic use of nitric oxide has been limited by its high reactivity and short half-life. Therefore, several NO donors such as RSNO have been developed for NO supplementation. As physiological intermediates in the metabolism of NO, RSNO (and especially GSNO) have been extensively studied for their potential therapeutic effects in cardiovascular diseases[3,4,12,14,30]. Although using donors improve the half-time of NO, the gain is often limited to few hours. Additionally, a fine tuning of NO concentration within time matters as NO may trigger different signalizations depending on its concentration. As a result, designing NO delivery systems is an on-trend challenge to achieve both increased half-life and controlled release. Several routes of administration have been considered in accordance with the targeted therapeutic applications. For example, many groups administered topical formulations of RSNO for wound healing[19,31,32,33]. Parenteral formulations were also developed to study biologic effects of RSNO[34], alleviate liver fibrosis/portal hypertension[35], or decrease brain damages after stroke[21]. As far as oral administration of RSNO is concerned, our team previously proved it feasibility, showing first that unformulated RSNO can cross an *in vitro* intestinal barrier model[15] and second developing GSNO-NP able to delay GSNO delivery to cells by 18 h[24]. Due to the hydrophilic nature of GSNO, the nanoparticles were obtained through a W/O/W double emulsion/solvent evaporation method using Eudragit RL PO as polymer. These GSNO-NP were next embedded in an alginate/chitosan matrix forming nanocomposite particles to constitute a releasable store of NO in aorta wall of

394 rats after a single oral administration[26]. The surrounding matrix improved NO loading,
395 slowed down NO release and provided mucoadhesion to optimize the contact between
396 the formulation and the intestine. Despite the promising proof of concept obtained
397 with these nanocomposite particles, their application in preclinical models is
398 drastically prevented by their low stability and high time-consuming preparation and
399 characterization before use.
400 As a result, the formulation process of the GSNO-NP has been modified starting from
401 the same raw materials. The double emulsion/solvent evaporation processes (W/O/W,
402 W/O/O or S/O/W) was adapted in order to produce microparticles. The two aims were
403 (i) to increase the encapsulation efficiency and (ii) to slow down the GSNO release
404 from these particles, thanks to their longer pathway of drug diffusion compared to
405 nanoparticles.
406
407 As a first step, the energy of the 2nd emulsion of the W/O/W process was reduced.
408 Ultra-sonication at low energy resulted in sub-micrometric particles, mechanical
409 stirring to aggregation. GSNO-MPW were finally obtained using vortex agitation,
410 with similar encapsulation efficiency compared to GSNO-NP. In an attempt to counter
411 the likely drug leakage from internal to external aqueous phase that can occur during
412 W/O/W emulsion[36], W/O/O processes were also tested with paraffin oil as external
413 phase[37,38]. In some cases, resulting MP aggregated, in others they were quite difficult
414 to isolate, while EE was not significantly modified. Finally, the encapsulation of
415 hydrophilic drugs is often increased using S/O/W processes. For example, Castellanos

et al succeeded in enhancing the EE of PLGA-Bovine serum albumin MP to 80% using S/O/W process[39] compared to less than 40% for the W/O/W one[40]. This approach was also tested and led to the GSNO-MPS, although the S/O/W process failed to increase EE in our case (still around 30% thus corresponding to a load of 0.02 µmol GSNO/mg particles). Nevertheless, the *in vitro* release profile of GSNO from these GSNO-MPS particles was modified compared to W/O/W particles (GSNO-NP or GSNO-MPW, see Fig 4). Although the *in vitro* GSNO release from our particles (around 90 $pmol.mg^{-1}$ $particles.min^{-1}$ for a 3h duration time) could be improved, it is in the range of other systems described in the literature (*e.g.* from 40 $pmol.mg^{-1}.min^{-1}$ for particles encapsulating SNAP[23] to 400 $pmol.mg^{-1}.min^{-1}$ for particles encapsulating DETA NONOate[41]).

S/0/W microparticles of RSNO have been previously described in the literature. Lautner et al. prepared SNAP-loaded microspheres with different PLGA polymers, after cryo-milling reduction of SNAP powder size to 25 µm. They obtained a loading up to 0.56 µmol of SNAP/mg of microspheres and an *in vitro* release sustained from 10 days to 4 weeks, depending on the polymer[23]. Recently, Hliang *et al*. described GSNO-loaded microparticles obtained with PLGA, aimed at healing cutaneous wounds infected with drug-resistant bacteria[32]. They are loaded with 0.15 µmol of GSNO/mg of particles and allowed a 1 week-release *in vitro*. Although there is no mention of a specific pretreatment of the GSNO powder, it seems that the size of their GSNO grain in particles is around 10 µm, according to a picture displayed in the

438 article. In our case, the size of raw GSNO grain was near 40 µm. Reducing the size of
439 drug particles up to a critical threshold is known to improve EE in S/O/W or S/O/O
440 processes[42,43]. As a result, and because of the fragility of GSNO, we tried to reduce
441 the size of GSNO grain with supercritical fluid technology[44] (Table 3). We used first a
442 SAS (supercritical antisolvent) process with DMSO but it led to a non-acceptable
443 degradation of the drug (>40% loss). Secondly, we tested a GAS (gaseous anti-solvent)
444 process in which we failed to obtain any solid product. Finally, the SAS process with
445 milder conditions led to a pink powder, with >80% purity, but so hygroscopic that it
446 turned to a sticky product before we could characterize it. As a result, we used directly
447 the raw GSNO powder in our experiments. EE was not significantly improved
448 compared to GSNO-MPW, which may be explained by a non-homogeneous
449 dispersion of GSNO particles, due to their size, and their consequential leakage during
450 emulsification[43]. We obtained an approximately 8 times lower loading than Hliang et
451 al., related to their lower size of GSNO particles and/or to the polymer (PLGA 50:50)
452 they used, which is less hydrophobic than ours (Eudragit RLPO). Interestingly, we
453 first tested PLGA with W/O/W processes but as Hliang et al., we obtained very low
454 EE. We then have switched towards Eudragit polymer, because Eudragit are classical
455 polymers for oral drug delivery systems, with good biocompatibility as well as high
456 stability through the gastro-intestinal tract, on the contrary to PLGA[45,46]. Additionally,
457 Eudragit imparts a positive charge at the surface of the particles. This charge will
458 foster the interaction between particles and intestinal cells, which may result in a
459 better drug bioavailability. Indeed, the three types of particles showed an

460 improvement of the intestinal permeability of NOx species (GSNO-MPS >
461 GSNO-MPW > GSNO-NP) after only 1h and without damaging the cells monolayer
462 (Figure 7). The Papp parameter characterizes the intestinal permeability of a drug in
463 *in vitro* or *ex vivo* models. Drugs could have low permeability (Papp < 1 $\times 10^{-6}$ cm.s^{-1})
464 or high permeability ($\geq$ 10 $\times 10^{-6}$ cm.s^{-1}), or be in a medium permeability class[47]. As a
465 result, considering NOx species, GSNO is in the medium permeability class when
466 administered as free GSNO or GSNO-NP, and reaches the high permeability class
467 using GSNO-MPs ($\geq$ 10 $\times 10^{-6}$ cm.s^{-1}).
468
469 In our study, we also overcame the challenge of getting stable and easy-to transport
470 particles. A lyophilization process was developed on GSNO-NP and transferred to MP
471 using sucrose as protectant. Critical parameters of the particles (*i.e.* size and GSNO
472 content) were maintained after drying, and the resulting products were stable at last 1
473 month for MP and 3 months for NP, when stored at 4°C protected from oxygen. In
474 this way, the lyophilization process has brought a very significant improvement, since
475 initial suspensions had to be used right after preparation. The discrepancies in water
476 residual content of the particles after drying indicate that MP (especially the
477 GSNO-MPS ones) still retain a high amount of water. This might be due to the
478 hygroscopic properties of GSNO powder. As GSNO is less stable in solution than in
479 dry state, optimization of the lyophilization process could be conducted in the future
480 in order to reduce residual water content and therefore to improve the stability of
481 these GSNO-MPS.

As a result, we prepared and characterized three types of particles loaded with a physiological RSNO, suitable for oral administration. Based on the same raw materials but obtained with different processes, they have similar EE of GSNO, with different *in vitro* release kinetics and different modulation of NOx species intestinal permeability. Moreover, they were stabilized by lyophilization thus facilitating their translation to preclinical testing.

ACKNOWLEDGEMENTS

Mr Yi ZHOU is supported by a CSC (China Scholarship Council) funding. The authors acknowledge support of EA 3452 CITHEFOR by the "Impact Biomolecules" project of the "Lorraine Université d'Excellence" (Investissements d'avenir – ANR).

REFERENCES

1 Nathan C. Nitric-Oxide as a Secretory Product of Mammalian-Cells. *Faseb J* 1992; **6**: 3051–3064.

2 Al-Sa'doni H, Ferro A. S-nitrosothiols: a class of nitric oxide-donor drugs. *Clin Sci* 2000; **98**: 507–520.

3 Gaucher C, Boudier A, Dahboul F, Parent M, Leroy P. S-nitrosation/Denitrosation in Cardiovascular Pathologies: Facts and Concepts for the Rational Design of S-nitrosothiols. *Curr Pharm Des* 2013; **19**: 458–472.

4 Maron BA, Tang S-S, Loscalzo J. S-Nitrosothiols and the S-Nitrosoproteome of the Cardiovascular System. *Antioxid Redox Signal* 2013; **18**: 270–287.

5 Hakim TS, Sugimori K, Camporesi EM, Anderson G. Half-life of nitric oxide in aqueous solutions with and without haemoglobin. *Physiol Meas* 1996; **17**: 267.

6 Bennett BM, McDonald BJ, Nigam R, Craig Simon W. Biotransformation of organic nitrates and vascular smooth muscle cell function. *Trends Pharmacol Sci* 1994; **15**: 245–249.

7 Messin R, Boxho G, Smedt JD, Buntinx IM. Acute and Chronic Effect of Molsidomine Extended Release on Exercise Capacity in Patients with Stable Angina, a Double-blind Cross-over Clinical Trial Versus Placebo. *J Cardiovasc Pharmacol* 1995; **25**: 558–563.

8 Hwang S, Meyerhoff ME. Polyurethane with tethered copper(II)–cyclen complex: Preparation, characterization and catalytic generation of nitric oxide from S-nitrosothiols.

515 *Biomaterials* 2008; **29**: 2443–2452.

516 9 Jen MC, Serrano MC, Lith R van, Ameer GA. Polymer- Based Nitric Oxide Therapies:
517 Recent Insights for Biomedical Applications. *Adv Funct Mater* 2012; **22**: 239–260.

518 10 Zhang Q-Y, Wang Z-Y, Wen F, Ren L, Li J, Teoh SH *et al.* Gelatin–siloxane nanoparticles to
519 deliver nitric oxide for vascular cell regulation: Synthesis, cytocompatibility, and cellular
520 responses. *J Biomed Mater Res A* 2015; **103**: 929–938.

521 11 Lam CF, Sviri S, Ilett KF, van Heerden PV. Inhaled diazeniumdiolates (NONOates) as
522 selective pulmonary vasodilators. *Expert Opin Investig Drugs* 2002; **11**: 897–909.

523 12 Hornyak I, Pankotai E, Kiss L, Lacza Z. Current Developments in the Therapeutic Potential
524 of S-Nitrosoglutathione, an Endogenous NO-Donor Molecule. *Curr Pharm Biotechnol* 2011;
525 **12**: 1368–1374.

526 13 Naseem KM, Bruckdorfer KR. Synergism between hydrogen peroxide and
527 S-nitrosoglutathione: Inhibition of activation of human platelets. *J Physiol-Lond* 1996; **491P**:
528 P8–P9.

529 14 Broniowska KA, Diers AR, Hogg N. S-Nitrosoglutathione. *Biochim Biophys Acta-Gen Subj*
530 2013; **1830**: 3173–3181.

531 15 Bonetti J, Zhou Y, Parent M, Clarot I, Yu H, Fries-Raeth I *et al.* Intestinal absorption of
532 S-nitrosothiols: Permeability and transport mechanisms. *Biochem Pharmacol* 2018; **155**:
533 21–31.

16 Damodaran VB, Leszczak V, Wold KA, Lantvit SM, Popat KC, Reynolds MM. Antithrombogenic properties of a nitric oxide-releasing dextran derivative: evaluation of platelet activation and whole blood clotting kinetics. *RSC Adv* 2013; **3**: 24406–24414.

17 Shah SU, Martinho N, Socha M, Reis CP, Gibaud S. Synthesis and characterization of S-nitrosoglutathione-oligosaccharide-chitosan as a nitric oxide donor. *Expert Opin Drug Deliv* 2015; **12**: 1209–1223.

18 Katsumi H, Nishikawa M, Yamashita F, Hashida M. Development of polyethylene glycol-conjugated poly-S-nitrosated serum albumin, a novel S-nitrosothiol for prolonged delivery of nitric oxide in the blood circulation in vivo. *J Pharmacol Exp Ther* 2005; **314**: 1117–1124.

19 Pelegrino MT, de Araújo DR, Seabra AB. S-nitrosoglutathione-containing chitosan nanoparticles dispersed in Pluronic F-127 hydrogel: Potential uses in topical applications. *J Drug Deliv Sci Technol* 2018; **43**: 211–220.

20 Parent M, Boudier A, Dupuis F, Nouvel C, Sapin A, Lartaud I *et al.* Are in situ formulations the keys for the therapeutic future of S-nitrosothiols? *Eur J Pharm Biopharm* 2013; **85**: 640–649.

21 Parent M, Boudier A, Perrin J, Vigneron C, Maincent P, Violle N *et al.* In Situ Microparticles Loaded with S-Nitrosoglutathione Protect from Stroke. *Plos One* 2015; **10**: e0144659.

22 Reger NA, Meng WS, Gawalt ES. Surface modification of PLGA nanoparticles to deliver nitric oxide to inhibit Escherichia coli growth. *Appl Surf Sci* 2017; **401**: 162–171.

554 23 Lautner G, Meyerhoff ME, Schwendeman SP. Biodegradable poly(lactic-co-glycolic acid)
555 microspheres loaded with S-nitroso-N-acetyl-D-penicillamine for controlled nitric oxide
556 delivery. *J Controlled Release* 2016; **225**: 133–139.

557 24 Wu W, Gaucher C, Diab R, Fries I, Xiao Y-L, Hu X-M *et al.* Time lasting
558 S-nitrosoglutathione polymeric nanoparticles delay cellular protein S-nitrosation. *Eur J*
559 *Pharm Biopharm* 2015; **89**: 1–8.

560 25 Wu W, Gaucher C, Fries I, Hu X, Maincent P, Sapin-Minet A. Polymer nanocomposite
561 particles of S -nitrosoglutathione: A suitable formulation for protection and sustained oral
562 delivery. *Int J Pharm* 2015; **495**: 354–361.

563 26 Wu W, Perrin-Sarrado C, Ming H, Lartaud I, Maincent P, Hu X-M *et al.* Polymer
564 nanocomposites enhance S -nitrosoglutathione intestinal absorption and promote the
565 formation of releasable nitric oxide stores in rat aorta. *Nanomedicine Nanotechnol Biol Med*
566 2016; **12**: 1795–1803.

567 27 Parent M, Dahboul F, Schneider R, Clarot I, Maincent P, Leroy P *et al.* A Complete
568 Physicochemical Identity Card of S-nitrosoglutathione. *Curr Pharm Anal* 2013; **9**: 31–42.

569 28 Sun J, Zhang X, Broderick M, Fein H. Measurement of Nitric Oxide Production in Biological
570 Systems by Using Griess Reaction Assay. *Sensors* 2003; **3**: 276–284.

571 29 Cole S. Rapid Chemosensitivity Testing of Human-Lung Tumor-Cells Using the Mtt Assay.
572 *Cancer Chemother Pharmacol* 1986; **17**: 259–263.

30 Radomski MW, Rees DD, Dutra A, Moncada S. S-nitroso-glutathione inhibits platelet activation in vitro and in vivo. *Br J Pharmacol* 1992; **107**: 745–749.

31 Seabra A. *Nitric Oxide Donors: Novel Biomedical Applications and Perspectives*. Academic Press, 2017.

32 Hlaing SP, Kim J, Lee J, Hasan N, Cao J, Naeem M *et al.* S-Nitrosoglutathione loaded poly(lactic-co-glycolic acid) microparticles for prolonged nitric oxide release and enhanced healing of methicillin-resistant Staphylococcus aureus-infected wounds. *Eur J Pharm Biopharm Off J Arbeitsgemeinschaft Pharm Verfahrenstechnik EV* 2018; **132**: 94–102.

33 Skeff MA, Brito GAC, de Oliveira MG, Braga CM, Cavalcante MM, Baldim V *et al.* S-nitrosoglutathione accelerates recovery from 5-fluorouracil-induced oral mucositis. *PloS One* 2014; **9**: e113378.

34 Nacharaju P, Tuckman-Vernon C, Maier KE, Chouake J, Friedman A, Cabrales P *et al.* A nanoparticle delivery vehicle for S-nitroso-N-acetyl cysteine: Sustained vascular response. *Nitric Oxide Biol Chem Off J Nitric Oxide Soc* 2012; **27**: 150–160.

35 Duong HTT, Dong Z, Su L, Boyer C, George J, Davis TP *et al.* The use of nanoparticles to deliver nitric oxide to hepatic stellate cells for treating liver fibrosis and portal hypertension. *Small Weinh Bergstr Ger* 2015; **11**: 2291–2304.

36 Giri TK, Choudhary C, Ajazuddin, Alexander A, Badwaik H, Tripathi DK. Prospects of pharmaceuticals and biopharmaceuticals loaded microparticles prepared by double emulsion technique for controlled delivery. *Saudi Pharm J SPJ Off Publ Saudi Pharm Soc* 2013; **21**:

593 125–141.

594 37 Aydogan E, Comoglu T, Pehlivanoglu B, Dogan M, Comoglu S, Dogan A *et al.* Process and
595 formulation variables of pregabalin microspheres prepared by w/o/o double emulsion solvent
596 diffusion method and their clinical application by animal modeling studies. *Drug Dev Ind*
597 *Pharm* 2015; **41**: 1311–1320.

598 38 Yousry C, Elkheshen SA, El-Laithy HM, Essam T, Fahmy RH. Studying the influence of
599 formulation and process variables on Vancomycin-loaded polymeric nanoparticles as
600 potential carrier for enhanced ophthalmic delivery. *Eur J Pharm Sci Off J Eur Fed Pharm Sci*
601 2017; **100**: 142–154.

602 39 Castellanos IJ, Carrasquillo KG, López JDJ, Alvarez M, Griebenow K. Encapsulation of
603 bovine serum albumin in poly(lactide-co-glycolide) microspheres by the solid-in-oil-in-water
604 technique. *J Pharm Pharmacol* 2001; **53**: 167–178.

605 40 Coombes AGA, Yeh M-K, Lavelle EC, Davis SS. The control of protein release from
606 poly(dl-lactide co-glycolide) microparticles by variation of the external aqueous phase
607 surfactant in the water-in oil-in water method. *J Controlled Release* 1998; **52**: 311–320.

608 41 Yoo J-W, Lee J-S, Lee CH. Characterization of nitric oxide-releasing microparticles for the
609 mucosal delivery. *J Biomed Mater Res A* 2010; **92A**: 1233–1243.

610 42 Han Y, Tian H, He P, Chen X, Jing X. Insulin nanoparticle preparation and encapsulation into
611 poly(lactic-co-glycolic acid) microspheres by using an anhydrous system. *Int J Pharm* 2009;
612 **378**: 159–166.

613 43 Morita T, Sakamura Y, Horikiri Y, Suzuki T, Yoshino H. Protein encapsulation into
614 biodegradable microspheres by a novel S/O/W emulsion method using poly(ethylene glycol)
615 as a protein micronization adjuvant. *J Control Release Off J Control Release Soc* 2000; **69**:
616 435–444.

617 44 Jung J, Perrut M. Particle design using supercritical fluids: Literature and patent survey. *J*
618 *Supercrit Fluids* 2001; **20**: 179-219.

619 45 Anwer MK, Al-Shdefat R, Ezzeldin E, Alshahrani SM, Alshetaili AS, Iqbal M. Preparation,
620 Evaluation and Bioavailability Studies of Eudragit Coated PLGA Nanoparticles for Sustained
621 Release of Eluxadoline for the Treatment of Irritable Bowel Syndrome. *Front Pharmacol*
622 2017; **8**. doi:10.3389/fphar.2017.00844.

623 46 Park M-H, Baek J-S, Lee C-A, Kim D-C, Cho C-W. The effect of Eudragit type on
624 BSA-loaded PLGA nanoparticles. *J Pharm Investig* 2014; **44**: 339–349.

625 47 Peng Y, Yadava P, Heikkinen AT, Parrott N, Railkar A. Applications of a 7-day Caco-2 cell
626 model in drug discovery and development. *Eur J Pharm Sci* 2014; **56**: 120–130.

Figure captions

Figure 1. Characterization of GSNO-loaded particles before and after lyophilization. Size and polydispersity index (PDI) of the GSNO-NP (a) as well as size and span of the GSNO-MP (b), encapsulation efficiencies (c) are presented as mean ± sd (n=3). Representative Scanning Electron Microscopy images are also presented (d).

Figure 2. Stability (size (a) and remaining GSNO content (b)) of GSNO-NP, GSNO-MPW and GSNO-MPS suspensions stored at 4 °C. Results are presented as mean ± sd (n = 3) and compared to the values obtained just after preparation (day 0, 100%). The grey areas delimit the sizes between 90% and 110% of the initial values. The percentages of remaining GSNO were analyzed with One-way ANOVA $p < 0.0001$ (Dunnett's multiple comparisons test): * $p < 0.05$ *versus* day 0.

Figure 3. Evolution of size and GSNO remaining for the GSNO-NP (a), GSNO-MPW (b) and GSNO-MPS (c) stored at 4 °C under inert atmosphere after lyophilization. Values measured immediately after lyophilization are considered as 100%. The grey areas delimit the sizes between 90% and 110% of the initial values. Results are presented as mean ± sd (n = 3). The data about GSNO remaining were analyzed with One-way ANOVA $p < 0.01$ (Dunnett's multiple comparisons test: GSNO-NP: $p = 0.0045$; GSNO-MPW: $p = 0.0016$; GSNO-MPS: $p = 0.0003$): * $p < 0.05$ *versus* week 0 (100%).

Figure 4. Drug release in PBS. Results are presented as mean ± sd (n = 3, free GSNO as control), two-way ANOVA (Turkey's multiple comparisons test): * $p < 0.05$ *versus* free GSNO and

649 GSNO-NP.

650

651 **Figure 5.** Cytocompatibility of Caco-2 cells after 24 h of incubation with GSNO (a), GSNO-NP
652 (b), GSNO-MPW (c), GSNO-MPS (d). Control condition = culture medium without fetal bovine
653 serum. Results are presented regarding GSNO loading, in equivalence of free GSNO from 25 µM
654 to 2500 µM. Results are shown as means ± sem, n = 3 in duplicate. ND = not determined

655

656 **Figure 6.** Quantity of GSNO, nitrite ions nitrate ions remaining in the apical medium (a, b and c,
657 respectively), as well as in the basolateral medium (e, f and g, respectively), and GSNO (d)
658 remaining inside the particles after 1 h of permeability study (GSNO initial amount = 50 nmol in
659 all cases). Results are shown as means ± sem, n=3 in duplicate, one-way ANOVA (Tukey's
660 multiple comparisons test): $*p < 0.05$ *versus* GSNO and $\# p < 0.05$ *versus* GSNO-NP.

661

662 **Figure 7.** Summary of NOx species permeability for each condition (free GSNO, GSNO-NP,
663 GSNO-MPW and GSNO-MPS). The width of each section of the arrows is correlated with the
664 amounts (from left to right) of NO^{3-}, NO^{2-} and GSNO.

665

666

667

668

669

670

Table 1

Table 1. Mass balance of NOx species for GSNO, GSNO-NP and GSNO-MPs conditions after 1 h of permeability study (GSNO initial amount 50 nmol). Results are presented as mean ± sem, n=3 in duplicate.

	Amount in nmol *(%)*			
	Apical		Basolateral	Total
	Free	In particles		
GSNO	44.7 ± 2.2 *(89.4 ± 4.4)*	-	0.8 ± 0.3 *(1.6 ± 0.6)*	45.5 ± 2.0 *(91.0 ± 4.0)*
GSNO-NP	37.6 ± 2.2 *(75.2 ± 4.4)*	5.3 ± 1.3 *(10.6 ± 2.6)*	1.5 ± 0.8 *(3.0 ± 1.6)*	44.4 ± 1.2 *(88.8 ± 2.4)*
GSNO-MPW	31.9 ± 3.1 *(61.8 ± 6.2)*	9.8 ± 1.8 *(19.6 ± 3.6)*	2.6 ± 1.1 *(5.2 ± 2.2)*	42.7 ± 1.2 *(85.4 ± 2.4)*
GSNO-MPS	30.0 ± 2.3 *(60.0 ± 4.6)*	10.7 ± 1.8 *(21.4 ± 3.6)*	2.4 ± 1.1 *(4.8 ± 2.2)*	43.1 ± 2.0 *(86.2 ± 4.0)*

Table 2

Table 2. Values of apparent permeability coefficient for RSNO, nitrite ions, nitrate ions and NOx (sum of all species) after 1 h of free GSNO, GSNO-NP or GSNO-MPs incubation. Results are presented as mean ± sem, n=3 in duplicate.

	Papp values ($\times 10^{-6}$ cm.s^{-1})			
Treatment	**RSNO**	**NO_2^-**	**NO_3^-**	**NOx**
GSNO	0.84 ± 0.41	0.26 ± 0.17	1.97 ± 0.20	3.07 ± 0.65
GSNO-NP	0.63 ± 0.25	0.92 ± 0.27	4.30 ± 1.15	5.87 ± 1.58
GSNO-MPW	1.14 ± 0.74	1.78 ± 0.29	7.47 ± 1.28	10.20 ± 1.56
GSNO-MPS	1.11 ± 0.57	1.31 ± 0.31	8.23 ± 2.09	10.60 ± 2.39

Table 3

Table 3. Conditions used in supercritical trials to decrease the size of GSNO grain and subsequent results.

Gaseous antisolvent (GAS) and supercritical antisolvent (SAS) processes rely on the use of the supercritical CO_2 as an anti-solvent. The crystallization of GSNO is induced by the mass transfer of the solvent (DMSO) in the supercritical phase.

Supercritical trials operating conditions and results				
Treatment	**Crystallization conditions**	**Drying conditions**	**Yield**	**Issue(s)**
GAS	• Crystallization pressure: 300 bar • Crystallization temperature: 40°C • GSNO 1%wt in DMSO • 10.9 g of solution injected • CO_2 pressurization: 150 bar/min • Equilibrium: agitation 54 rpm 10 min before drying • 20 mL autoclave	• 300 bar/40°C • CO_2 flowrate: 0.6 kg/h • Duration: 3h00min	0%	Probable too high solubility of GSNO in CO_2/DMSO mixture Too high DMSO fraction
SAS (1st trial)	• Crystallization pressure: 300 bar • Crystallization temperature: 40°C • GSNO 1%wt in DMSO • 15.8 g of solution injected • Molar CO_2 fraction: 0.984 2.2 kg_{CO2}/h – 1.0 g_{sol}/min) • Coaxial nozzle (100 µm i.d.) • 300 mL autoclave	• 300 bar/40°C • CO_2 flowrate: 1.0 kg/h • Duration: 2h30min	43.4 mg (27.5%) Purity: 92%	Probable too high solubility of GSNO in CO_2/DMSO mixture
SAS (2nd trial)	• Crystallization pressure: 160 bar • Crystallization temperature: 40°C • GSNO 1%wt in DMSO • 22.1 g of solution injected • Molar CO_2 fraction: 0.971 1.1 kg_{CO2}/h – 1.0 g_{sol}/min) • Coaxial nozzle (130 µm i.d.) • 300 mL autoclave	• 160 bar/40°C • CO_2 flowrate: 1.1 kg/h • Duration: 3h00min	157.8 mg (71.6%) Purity: >80%	Lower solubility of GSNO in CO_2/DMSO mixture but probable higher final DMSO residual content in powder resulting in a quasi-instantaneous product melting due to a hygroscopic effect

Figure 1.

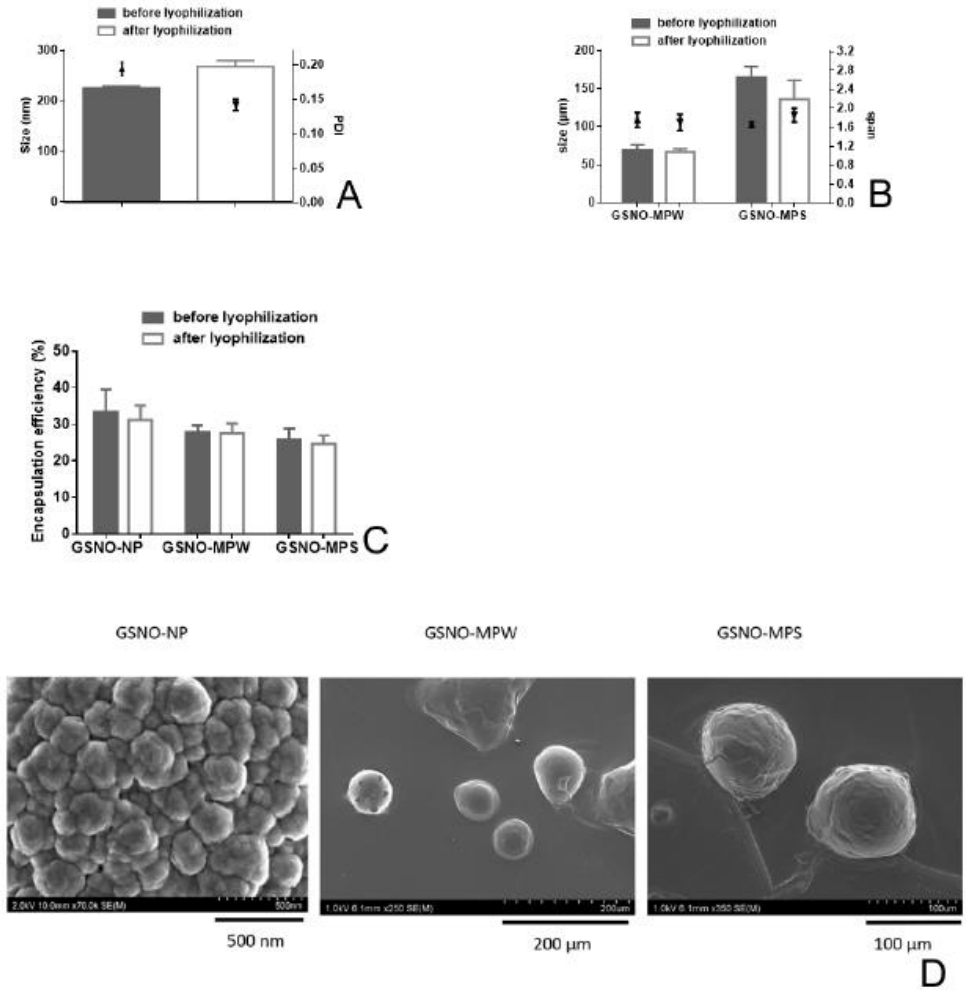

Figure 2.

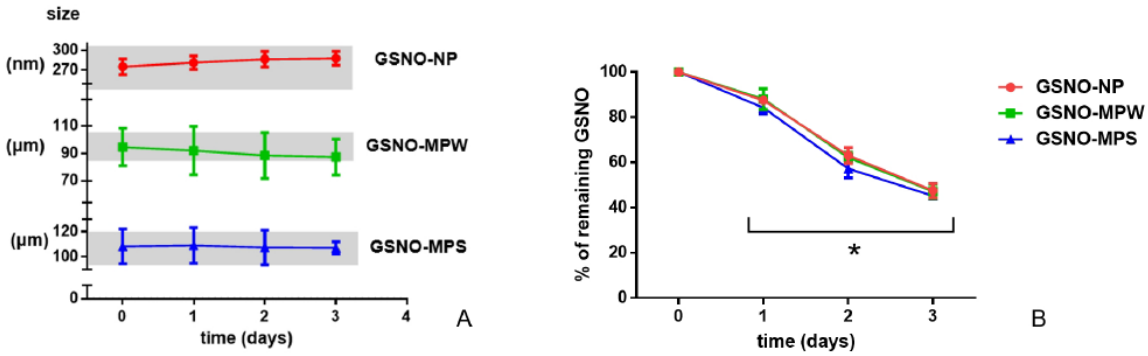

Figure 3.

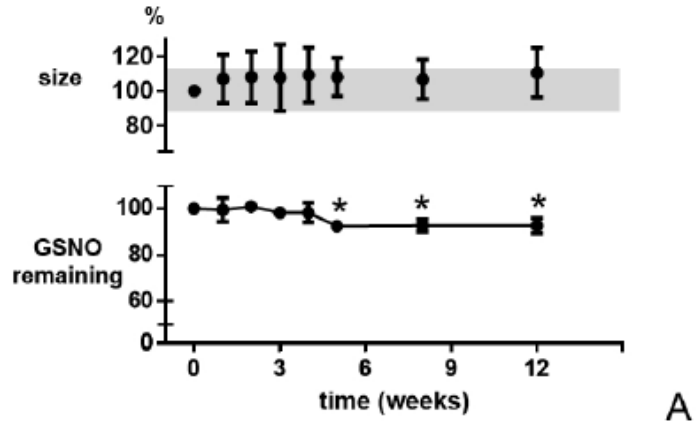
%
size
120
100
80
100
80
60
0
GSNO
remaining
*
*
*
0
3
6
9
12
time (weeks)

A

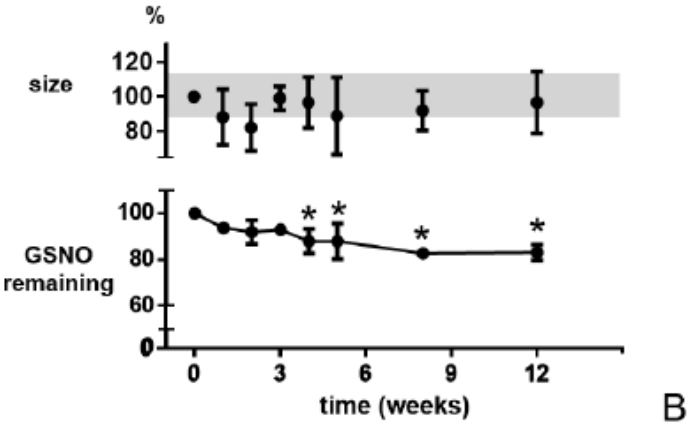
%
size
120
100
80
100
80
60
0
GSNO
remaining
*
*
*
*
0
3
6
9
12
time (weeks)

B

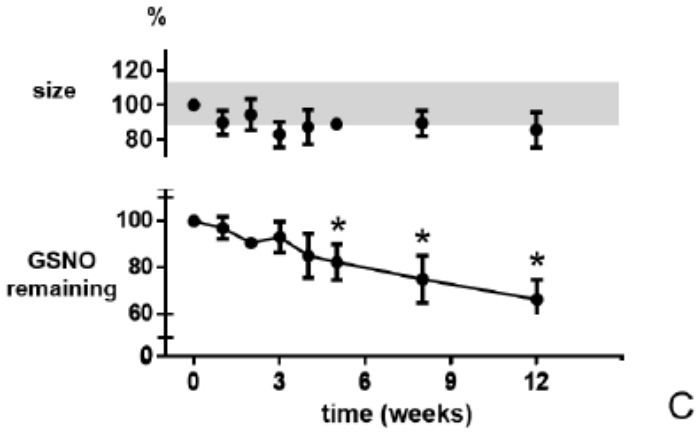
%
size
120
100
80
100
80
60
0
GSNO
remaining
*
*
*
0
3
6
9
12
time (weeks)

C

Figure 4.

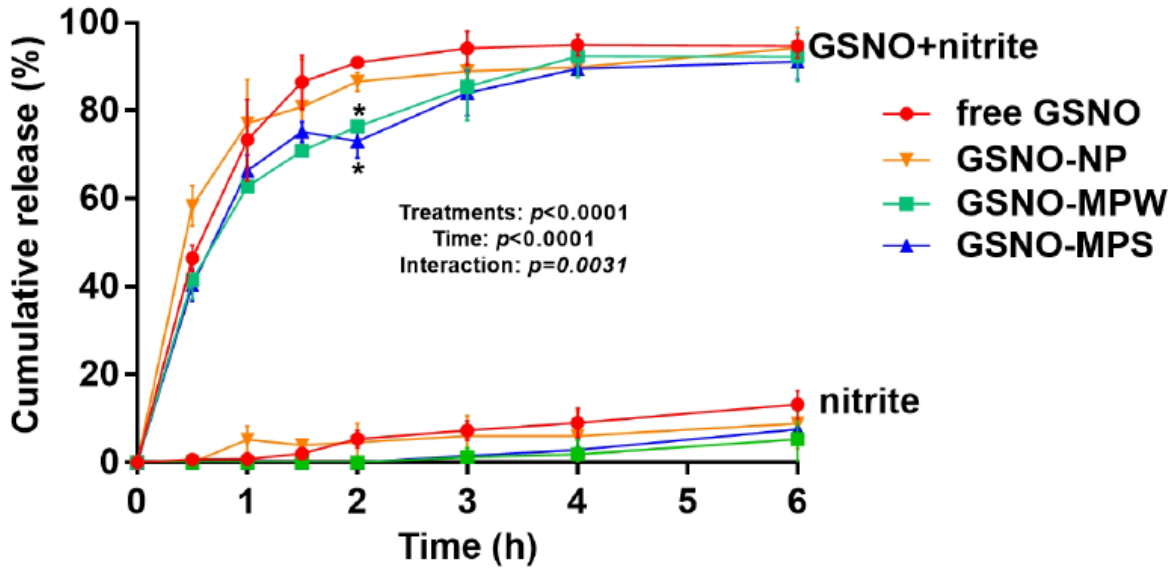
Cumulative release (%)
100
80
60
40
20
0
0
1
2
3
4
5
6
Time (h)
GSNO+nitrite
nitrite
free GSNO
GSNO-NP
GSNO-MPW
GSNO-MPS
Treatments: p<0.0001
Time: p<0.0001
Interaction: p=0.0031
*
*

Figure 5.

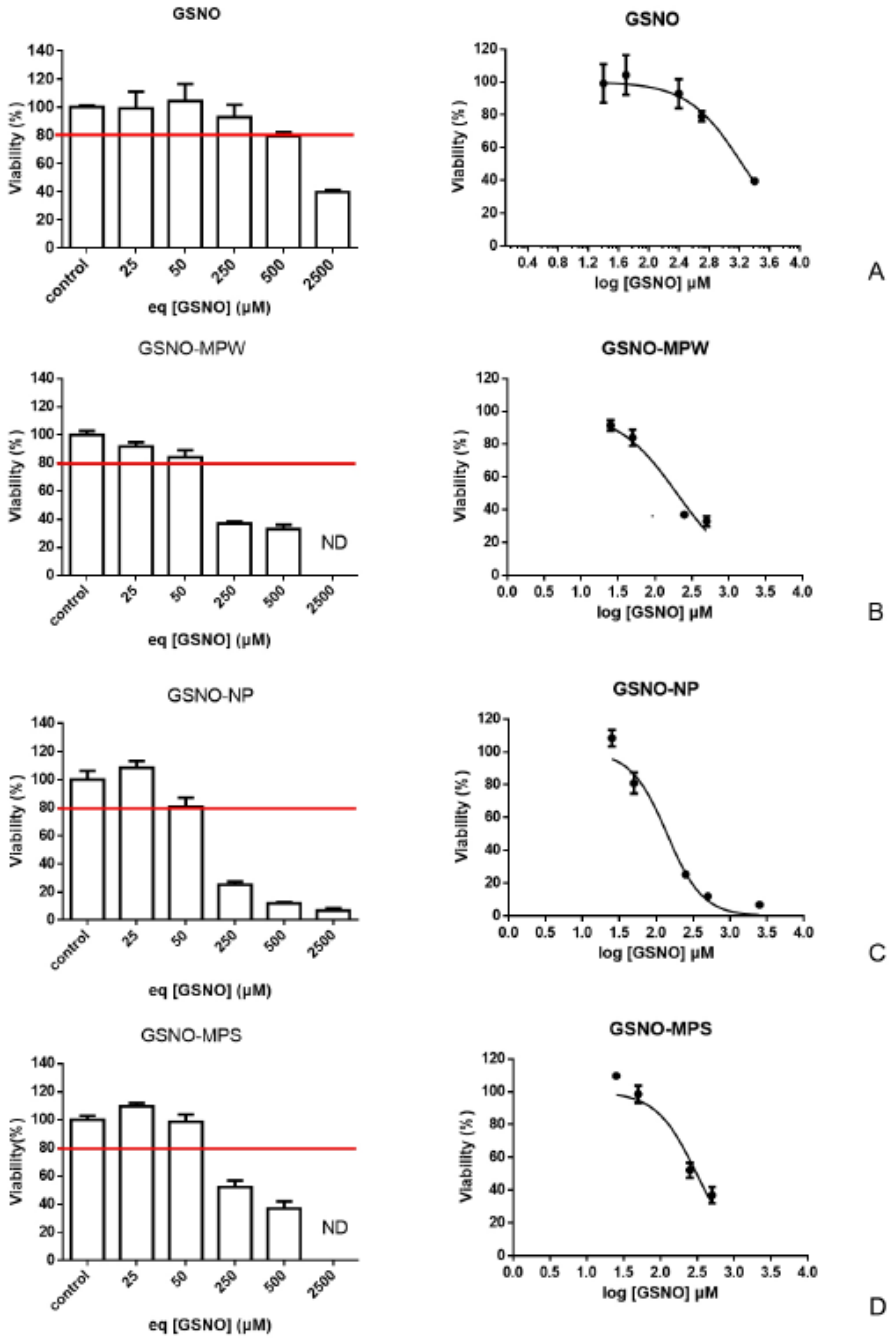
GSNO
Viability (%)
eq [GSNO] (μM)
control
25
50
250
500
2500
log [GSNO] μM
A
GSNO-MPW
ND
B
GSNO-NP
C
GSNO-MPS
Viability(%)
D

Figure 6.

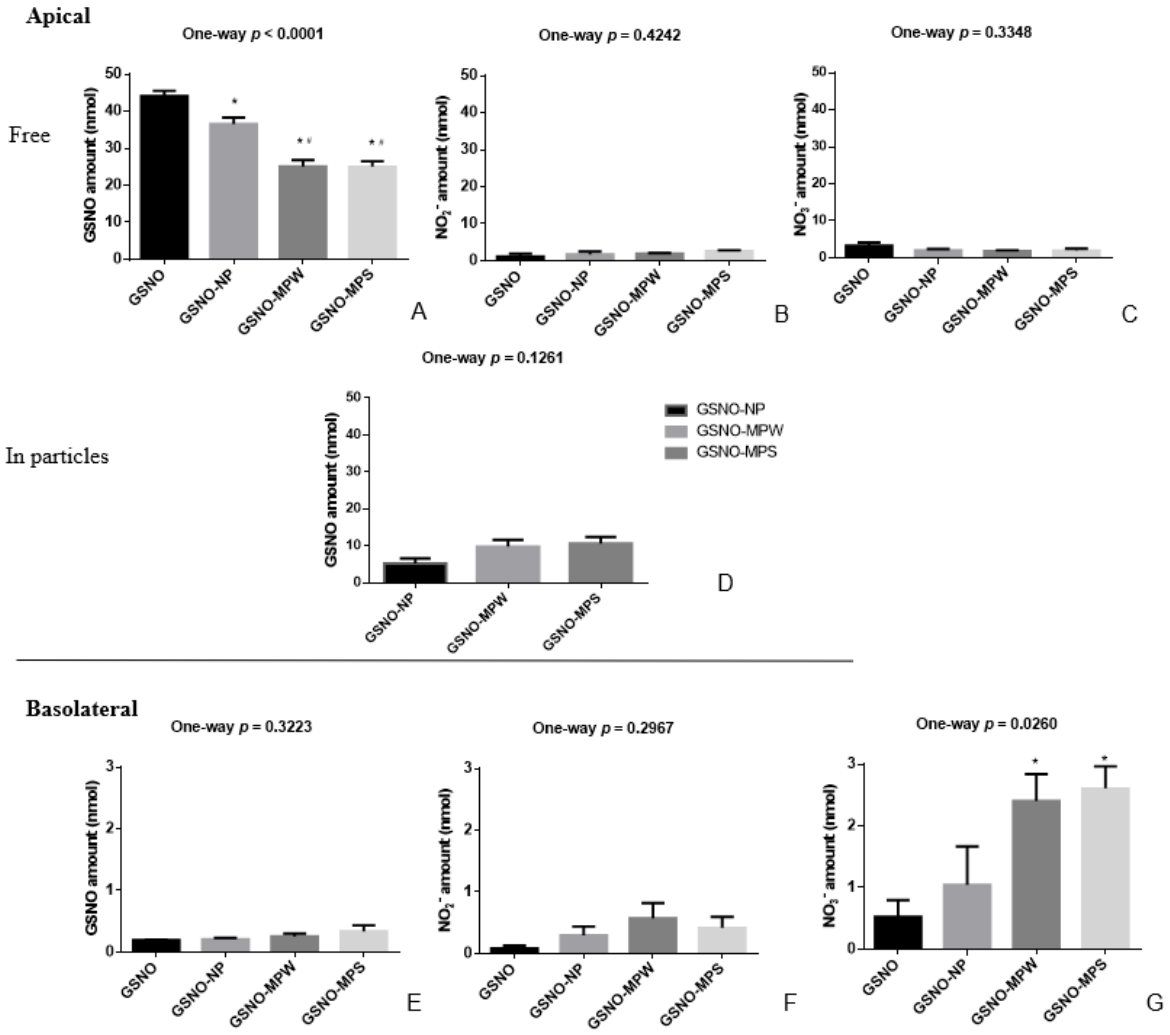

Figure 7.

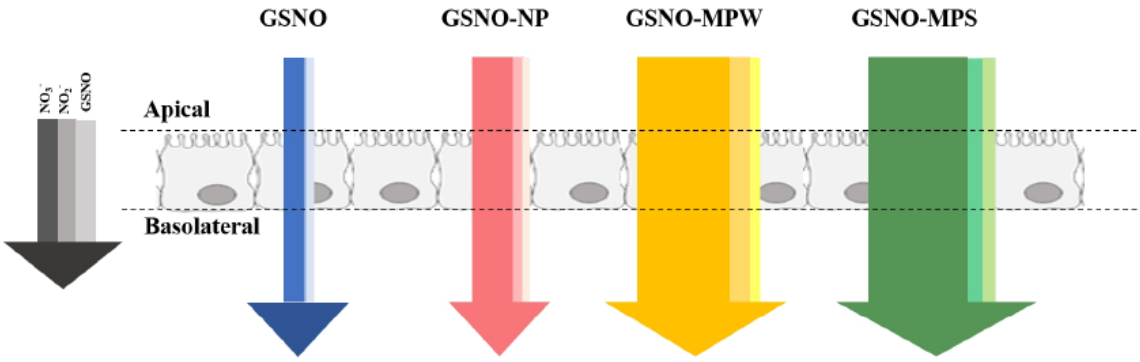

General discussion, conclusions and perspectives

General discussion

As an important second messenger, nitric oxide plays important roles in our body. NO deficiency is one of the key factors for the CVD. Due to its short half-time and the inconvenience of its application as gas, NO donors are good candidate drugs for CVD treatment. NO donors decompose in the body to generate NO or NO-derived species. NO donors have been applied in CVD for many years, in particular sodium nitroprusside for the treatment of hypertensive emergencies and organic nitrates for angina pectoris. However, long-term administration of organic nitrates generates tolerance, oxidative stress and other side effects. New NO donors, especially RSNOs offer advantages over existing drugs. They do not share side effects with organic nitrates and initial clinical studies suggest their therapeutic potential in a variety of cardiovascular disorders.

However, the application of RSNOs is limited by their poor stability. RSNOs are sensitive to different parameters *in vitro* (such as metal ions, light, oxygen, light, temperature) and are easy to be degraded by enzymes *in vivo* (as described in chapter 1).

In order to apply RSNOs to chronic CVD, oral delivery system with sustained release effect sounds like the best choice. In previous studies of our lab, Wu et al[127] developed GSNO-acNCP. After a unique oral administration of these GSNO-acNCP to Wistar rats, GSNO permeated through intestine and entered into vessels, resulting in the formation of a NO store within the vascular wall. However, some drawbacks arose: GSNO-acNCP are not easy to reproduce due to a time-consuming and multi-steps process of production; and they should be prepared right before administration due to their low stability as suspensions.

In this study, we aimed at evaluating the future of RSNOs to treat cardiovascular diseases through oral route and at developing suitable delivery systems. To that purpose we:

1. Made clear the intestinal permeability mechanisms of different RSNOs
2. Evaluated RSNOs capacity to form a bioavailable NO store within the vascular wall
3. Optimized the oral delivery system for *S*-nitrosoglutathione

The oral bioavailability of proteins, peptides or drugs depends mainly on their intestinal absorption[220,221]. As the RSNOs studied here are derived from peptides (GSH) or amino acids (cysteine, valine), it is therefore critical for us to evaluate the intestinal permeability (free or from particles). In the article 2, the intestinal permeability of RSNOs have been followed through the quantification of different NOx species (RSNOs, NO_2^- and NO_3^-). Indeed, as described in chapter 1, RSNOs are easy to degrade and produce NO_2^- and NO_3^-. NO_2^- and NO_3^- are capable of interconversion or able to release NO in a physiological environment, so both of them have been regarded as meaningful parts of NO intestinal permeability. Basically, NO, NO_2^- and NO_3^- constitute a complex biological cycle under physiological conditions in mammals. Several different mechanisms are thought to be involved in this cycling, such as reduction or oxidation through bacteria[222–224], hemoglobin[225–227] or other heme proteins[228], NOS[229,230], xanthine oxidoreductase[231–235], hypoxia[236], acid catalyzed[237–240], and UV radiation[241]. Nitrate ions in the blood can be circled and concentrated in the salivary glands and secreted into our mouth[222–224], where they are finally reduced to nitrite ions. Nitrite ions can also be reduced to NO under acidic conditions in the stomach[242], and enter the blood vessels as RSNOs after permeating the intestine. Nitrite ions in the blood are reduced by enzymes (such as xanthine oxidoreductase) or *via* hemoglobin under hypoxic conditions. Thus, NO_2^- and NO_3^- can also be regarded as possible NO sources in the body.

In order to develop the proper formulation for RSNOs oral delivery, RSNOs were classified according to the BCS. BCS is a system which has been widely used to differentiate the drugs according to their solubility and intestinal permeability. The

permeability of three different RSNOs (physiologic GSNO and two synthetic RSNOs: SNAP and NACNO) was evaluated using an *in vitro* model of intestinal barrier made of Caco-2 cells, which has been widely used for intestinal permeability evaluation and drug screening[243,244]. As presented in article 2, NACNO showed the highest Papp value, which means the best intestinal permeability of these three RSNOs. GSNO displayed similar intestinal permeability as SNAP. However, all the three RSNOs belong to the medium intestinal permeability class. The intestinal permeability of NACNO belongs to the middle of medium class and GSNO and SNAP belong to the beginning of medium class. So, NACNO tends to be closer to the class I type drugs (according to BCS) and should be a better option for formulations than other RSNOs (GSNO and SNAP). However, these three RSNOs display different biological properties linked to their own chemical structures. SNAP and NACNO are synthetic RSNOs derived from valine and cysteine, respectively. Furthermore, SNAP is made of *N*-acetyl-*D*-penicillamine an anti-inflammatory drug, used to treat rheumatoid polyarthritis, with an antioxidant thiol function. NACNO is made of *N*-acetyl-*L*-cysteine, a mucolytic, showing an antioxidant activity linked to the thiol function of the cysteine. Less RSNOs and nitrite ions have been found in the cells incubated with SNAP compared to NACNO and GSNO. We speculated that SNAP may cross the intestine mainly through paracellular way, whereas NACNO and GSNO mainly through transcellular way. In fact, SNAP has been shown to promote intestinal absorption of different model drugs (insulin, fluorescein-labelled compounds) by reversible opening of tight junctions[245,30]. In addition, we demonstrated that the transport of RSNOs through the intestine barrier is driven by passive diffusion rather than active transport. With high solubility and medium intestinal permeability, RSNOs can be regarded as drugs classified between class I and class III according to BCS. As described by Le Ferrec et al.[249], the results obtained *in vitro* with high permeability molecules (class I and class II) can be easily transposed to *in vivo* intestinal absorption unlike results obtained for low permeability molecules (class III and class IV). Thus, RSNOs can be regarded as suitable for oral administration route with their medium class of permeability.

After permeating the intestine barrier, RSNOs enter in the bloodstream where they

promote the formation of NO store. This latter is vital to vascular homeostasis, as described in the chapter 3, thus the reconstitution of this stock is mandatory in the context of cardiovascular diseases linked to NO depletion. In the literature, two main methods were described to evaluate the vascular NO store: one is the relaxation of vessels representing the existence of photosensitive NO store, during the exposure of the precontracted blood vessels to light[178–180]; the other is the usage of NO scavengers such as low molecular weight thiols. For example, NAC can displace NO from the NO store especially from *S*-nitrosated proteins or protein-bound dinitrosyl-iron complexes. Thus, the relaxation induced by NAC in precontracted vessels also indicates the presence of a NO store[181,250]. We evaluated the NO store produced by GSNO, SNAP and NACNO on endothelium-intact and endothelium-removed aortae in order to mimic healthy condition and endothelial dysfunction, respectively. As shown in article 3, the three RSNOs, with NACNO as the leader, were able to form a NO store within the aorta, no matter which kind of aorta was studied. The NAC-induced vasodilation protocol confirmed also the superiority of NACNO, being the RSNOs forming the highest NO store with the highest bioavailability in both types of aortae. This may probably due to the mechanism of NACNO incorporation into cells using the *L*-type amino acid transporter without metabolism[251,252], whereas other RSNOs (GSNO and SNAP) transfer into cells using enzymes activity present either on the endothelium or on smooth muscle cells[253,254]. Moreover, the NO store produced by NACNO induces also a higher hyporeactivity to vasoconstrictor than other NO donors. In addition, all these NO donors showed their ability to counteract the vasoconstriction induced by phenylephrine in endothelium-removed aorta. It has been illustrated that endogenous NO or NO derived from exogenous NO donors is responsible for the vascular hyporeactivity to vasoconstrictors[255,256]. In fact, in the study of Alencar et al.[250], they induced NO storage in rat aorta by administration of GSNO through infusion, which finally caused similar aortic hyporeactivity to vasoconstrictors like phenylephrine. In our study, we have not only checked the ability of RSNOs to induce NO store as well as its vasoactivity, but we also linked this pharmacological action to the quantification of NOx species either in endothelium-intact or endothelium-removed aortae.

Phenylephrine effect on vessels is a balance between the activation of alpha-1 adrenergic receptors on smooth muscle cells (vasoconstriction) and alpha-1 adrenergic receptors on endothelial cells (leading to the activation of the NO/sGC signaling pathway and then attenuation of the vasoconstriction). We confirmed that the vasoconstriction induced by agonists of alpha-1 adrenergic receptors was modified by three different RSNOs treatment only in endothelium-removed aortae, which has been supported by the work of others (mainly treatment of GSNO and DNIC)[127,250,257,258]. In addition, it was suggested that *S*-nitrosation of alpha-1 adrenergic receptors by RSNOs was also one possible mechanism of alpha-1 adrenergic receptors inhibition[259]. To conclude, RSNOs, in particular NACNO, are able to induce NO storage, which present a benefit to restore NO-related functions especially when the endothelium is absent (mimic of endothelial dysfunction).

For the quantification of the NO store, a lot of work has been focused on the optimization of the DAN/DAN+Hg^{2+} method. We first transferred the DAN/DAN+Hg^{2+} method from simple media (PBS, Kreb's buffer…) to the quantification in more complex media like cell lysates from smooth muscle cells (article 1) or intestinal cells (article 2). Basically, the cells were lysed in a medium containing a complex of sodium tetraborate and L-serine[260] (as GGT inhibitor) as well as N-ethylmaleimide[261] (free thiols blocker) and the NOx species were quantified with the DAN/DAN+Hg^{2+} method. However, with a more complex matrix and lower concentrations of NOx species, the quantification in tissues like aortae (article 3) is more difficult. First, the tissues (aorta) were crushed in liquid nitrogen with a mortar and then reacted directly with an overdosage of DAN+Hg^{2+} reagent in acidic solution. During this procedure, by avoiding lysis buffer, the dilution of samples has been eliminated. However, this method did not enable us to quantify nitrite ions and RSNOs separately, but small amount of NOx species (nitrite ions + RSNOs) could be quantified.

After studying the ability of RSNOs to cross the intestinal barrier and developing suitable methodology to study the NO store in vascular wall they can trigger, we also developed an oral delivery system to administer them. This formulation is

aimed at protecting the RSNOs from degradation all along the gastrointestinal tract, increasing their intestinal permeability as well as their release time. Regarding articles 2 and 3, NACNO seems to be the best drug candidate to formulate with both the highest intestinal permeability and the induction of the highest and most bioavailable NO store compared to SNAP and GSNO. However, we choose GSNO as the RSNOs model in the preparation of oral delivery systems due to its several advantages: it is a physiological RSNOs and its skeleton, reduced GSH, is very abundant in the body, which means lower side effects; GSNO can be synthesized and stored as solid, which is a prerequisite for the preparation of S/O/W particles (NACNO cannot). Thus, GSNO was chosen as the drug candidate to prepare oral delivery systems.

As it has a simple and reproducible preparation method with efficient encapsulation efficiency (about 30%), the GSNO-NP[125] has been chosen as the starting material for optimization. In recent literature[115,219], different RSNOs were successfully encapsulated in PLGA microparticles through S/O/W double emulsion. As described in chapter 1 and chapter 3, microparticles display several advantages over nanoparticles such as higher loading capacity as well as longer sustained release time. Moreover, among microparticles, S/O/W microparticles are often described as surpassing W/O/W microparticles, with possible higher encapsulation efficiency as well as better release profile. So, two different types of particles (GSNO-MPW and GSNO-MPS) were obtained through the modification of the energy of the 2nd emulsion and the inner phase during GSNO-NP preparation. However, the encapsulation efficiency of these two microparticles kept similar to the GSNO-NP. This may result from the quick diffusion of GSNO as a small hydrophilic molecular, and regarding the GSNO-MPS it may also result from the big size of inner solid GSNO powder. Increasing the encapsulation efficiency was not our principal aim, but it could be beneficial, as high encapsulation efficiency presents several advantages: 1) efficient therapeutic effects with higher possible drug concentration; 2) economical and fewer side effects with less excipient like polymer; 3) compliance of patient with less dosage and lower frequencies. In the work of Castellanos[262] et al, the EE of PLGA-Bovine serum albumin W/O/W MP (less than 40%) has been enhanced to 80% using S/O/W process. However, for our

particles, the encapsulation efficiency still kept around 30% (corresponding to a load of 0.02 µmol GSNO/mg particles). Nevertheless, microparticles presented a sustained release time (2-4 hours) compared to GSNO-NP.

Stabilizing the formulations to get storable and easy-to-transport products was however a key objective of our work. Transforming particles suspensions to dry drug products can indeed provide several advantages[263], such as easier delivery and storage of the drug product, with long stability. Several methods could be applied to remove the liquid medium and get dry drug products[263–265]: spray-drying, direct drying, vacuum drying, lyophilization and so on. However, with the low stability of GSNO, it is important to control the environment during the drying of GSNO loaded particles, such as the light, oxygen, temperature, and to get a low residual water content. Lyophilization, often used for pharmaceutics, can achieve those requirements and therefore was tested in this work. However, microparticles powders displayed a high residual water content after lyophilization, which may be related to the lyophilization process or the hygroscopic properties of GSNO. Lyophilization is a stressful process for both the particles and the drug. We did not explore in this work the optimization of this complex process, in particular because we had nor the time neither the suitable apparatus to do it properly. It might also be difficult to obtain lower residual water content without destroying the drug, due to its peptidic, hygroscopic and labile nature.

Even with their high residual water content, our particles had a satisfying stability, lower for GSNO-MPS (one month) than for GSNO-NP (more than 3 months). Besides, all these three types of particles displayed an enhancement of GSNO intestinal permeability: GSNO-NP promoted the intestinal permeability of GSNO to the middle of medium class whereas GSNO-MPW and GSNO-MPS enhanced GSNO to the high permeability class. This improvement may be attributed to the positive charge at the surface of particles, which comes from the methacrylic acid and ethylacrylate polymer (Eudragit). The particles may interact with intestinal cells (negative charge) and cause an increase in bioavailability, enhanced in the case of microparticles by a sustained NO delivery. These microparticles seem to be good candidates for the oral delivery of

GSNO.

When applying RSNOs through oral administration, they have to cross not only the intestinal epithelium (after surviving the harsh conditions in the upper tract), but also the mucus layer and the intestinal microbiota. The drug delivery system might offer some key features for the interaction with the mucus layer. In the meantime, NO, the main product of RSNOs decomposition, has anti-bacterial effect through several possible ways[266,267]: it attacks DNA of bacterial, disturbs protein (enzymes) synthesis and damages the amino acids in membrane. GSNO and NACNO are bactericidal against common Gram-negative and Gram-positive pathogens[267–269]. GSNO is bactericidal at low concentrations (4.6 ± 3.2 mM), which are safe to human cells: around twice the concentration of GSNO in serum[269,270]. The antibacterial effect of NACNO not only comes from NO but also from NAC. On the one hand, the interaction of RSNOs with microbiota in intestine provides another application of RSNOs loaded particles; on the other hand, the interaction may decrease the bioavailability of RSNOs in the treatment of CVD. Thus, it could be important to evaluate the impact of GSNO loaded particles/free GSNO on the intestinal flora of animals if we want to apply them to the *in vivo* experiment.

Conclusion and Perspectives

This work aims at making clear the mechanisms of intestinal permeability of different RSNOs as well as their ability to form NO store within the vascular wall, which helps to improve RSNOs-loaded oral delivery system dedicated to CVD treatment. We demonstrated that:

1. All the three RSNOs can cross the intestinal barrier (medium class of permeability) by passive diffusion. GSNO and NACNO preferentially cross intestinal barrier by the transcellular pathway and SNAP followed not only the transcellular but also paracellular way. They belong to class I or class III according to BCS and can be administrated through oral route.

2. All RSNOs showed their ability to induce the formation of a NO store, which represent a three to five times increase in NOx species content inside aorta (endothelium-intact or endothelium-removed). The vascular NO store, produced by each RSNOs (NACNO was the most potent), was available for vasorelaxation and induced hyporeactivity to the vasoconstrictive agent PHE. RSNOs, particularly NACNO, are able to restore NO bioavailability within the vascular wall, especially for the endothelium-removed aortae. They can be regarded as potent therapeutics to counteract endothelial dysfunction.

3. Two microparticles types (GSNO-MPW and GSNO-MPS) were obtained through the modification of GSNO-NP preparation with similar encapsulation efficiency (about 30%) but longer GSNO release time (more than 2 hours). Through lyophilization, all these three particles were transferred to powders with long time stability (more than 3 months for GSNO-NP and 1 month for two microparticles). In addition, all these three particles presented an ability to enhance the intestinal permeability of GSNO. They might represent a good choice for chronic oral treatment of NO deficiency caused pathologies like CVD.

With regard to these studies, several parts deserve further study or our attention. In the study of amidoxime (article 1), compound 2d bearing aromatic and aliphatic

amidoximes functions was the most potent molecule for NO release with cytocompatibility with human smooth muscle cells. In order to study its potentiality for CVD, its intestinal permeability and ability to induce NO storage could also be evaluated using similar experiments as in article 2 and 3. During these procedures, the logP value may also guide the selection of amidoximes molecule. According to 'Lipinski's Rule of 5' (developed at Pfizer) the logP of a compound intended for oral administration should be smaller than 5[271]. A suitable logP value is important for the oral administration, a more lipophilic compound (logP > 5) will have low aqueous solubility and result in compromising bioavailability; or it may be easy sequestered by fatty tissue and difficult to excrete. Normally, for oral administration through intestinal absorption, the idea logP value is 1.35–1.8[271,272]. The amidoximes tested in article 1 had logP values between 0 and 2, thus suitable for oral administration and also probably easier to encapsulate into polymeric formulations than GSNO (logP - 2.7) with more sustained release. However, the decomposition of amidoximes exclusively by CYP450 could raise a tolerance issue under chronic administration, as observed with organic nitrates.

The future of RSNOs application either in free or formulated form will pass by an evaluation of their *in vivo* properties after oral administration. First the pharmacokinetic of these compounds should be followed using methods developed in the literature[273], especially, the one based on N^{15} developed in our lab[62,63]. Indeed, Yu et al, developed a DAN assay followed by liquid chromatography with tandem mass spectrometry based on N^{15} quantification. This method deciphers between naturally occurring NOx species (nitrite ions, nitrate ions and RSNOs) and N^{15} enriched administrated GSNO. This method was validated on Caco-2 cell[274] as well as intestine tissue[275] (Ussing chamber) with a 5 nM limit of quantification (for memory, Griess method has a limit of quantification about 10^{-6} to 10^{-5} M whereas DAN with 10^{-7} to $2*10^{-6}$ M). The possibility to quantify NOx species in the nanomolar range, in cells and in tissues, will render easier the *in vivo* pharmacokinetic studies (release, distribution, degradation and excretion) of RSNOs and RSNOs formulations.

In addition, the study of the effects of RSNOs on the intestinal mucus and flora could also be interesting. As RSNOs have anti-bacterial effect, the intestinal flora balance may be destroyed, which may cause the changes of intestinal absorption of RSNOs. In addition, some of RSNOs could be degraded during the reaction with different bacteria during the intestinal tract. As described by Björne et al.[276], nitrite-containing human saliva increases not only gastric mucosal blood flow but also mucus thickness in the rat. Similarly, the degradation of RSNOs can produce nitrite, which could change the thickness of mucus and impact the intestinal permeability of RSNOs

The description of the vascular NO store should be also continued in terms of localization and identification. The NO store could be localized within vascular wall either by comparing the quantity of NO store in the whole *versus* in an endothelium-removed vessel, or by immunofluorescence microscopy. To further make clear if the NO store is within organelles, in extracellular matrix, or in the cytosol, we can use an intracellular NO probe such as 4,5-Diaminofluorescein diacetate[277], combined with specific probes of each cell compartment or tissue layer. The identification of *S*-nitrosated proteins forming the NO store in the vascular wall could be achieved using the biotin switch method coupled with mass spectrometry already developed in the lab[278]. *S*-nitrosated proteins identification might help us to find new NO target and will open further studies on the impact of the *S*-nitrosation process on these proteins' activity and/or expression.

As mentioned in the discussion part, NACNO could be an interesting treatment for CVD, so we can also prepare NACNO loaded nanoparticles and microparticles through W/O/W method, starting from NACNO solutions. However, the initial NACNO concentration after preparation is always 0.01 M in our lab, which is six times lower than the one of GSNO (about 0.06 M). Thus, NACNO solution should be condensed to get a higher concentration before particles preparation. In addition, NACNO cannot be entrapped through S/O/W double emulsion method without way to isolate NACNO solid powder. The post-*S*-nitrosation of NAC (previously encapsulated as solid powder) with $NaNO_2$ might be another potent way to get NACNO S/O/W microparticles. As

described in the work of Nacharaju[279] et al, NACNO loaded nanoparticles were successfully prepared through the *S*-nitrosation of NAC by $NaNO_2$. These nanoparticles were suspended in tetramethoxysilane based sol-gel and showed long time (24 h) release. In addition, Souza[280] et al have found a novel way to deliver NACNO through the oral route using the intratablet *S*-nitrosation of NAC. Basically, a tablet containing NAC and $NaNO_2$ powder were obtained and NACNO was sustain released during the absorption of water. Thus, NACNO loaded particles can be obtained with W/O/W method through direct encapsulation, and with S/O/W by indirect way.

Lyophilization has been applied to get long time stability. However, the stability time of microparticles (1 month) is less than nanoparticles (3 months). To get a longer stability time (more than 3 months or longer), we can optimize the lyophilization procedure for GSNO loaded particles according to the property of GSNO: the annealing procedure to decrease the duration time; the temperature and duration time of primary drying and second drying[281–283].

It is possible to enhance the encapsulation efficiency and to sustain the release through different methods:

1. Choose the proper Eudragit: It has been suggested that the mechanism of drug release from dosage forms coated with Eudragit is mainly through control of fluid permeation with subsequent dissolution and diffusion of the active substance. However, the pores of Eudragit films have been shown to be larger (which means the diffusion of the drug through these pores is higher) in Eudragit RL films than in Eudragit RS films. The larger pores can cause the quick release speed of GSNO from the particles. Besides, the high permeability of Eudragit RL PO may also induce the low drug loading capacity[284,285].

2. Use two different emulsifiers to prepare the double emulsion. In the double emulsion of these three particles, only one surfactant Kolliphor P188 has been applied as emulsifier. The polymer Eudragit RL PO acts partly as emulsifier, which may be not

so efficient.

After optimization of the particles, we can obtain different particles and choose the right one (size, encapsulation efficiency, release, dosage) for *in vivo* experiments. Then, capacity of chosen particles to counteract CVD can be determined through *in vivo* experiments after oral administration to murine model of atherosclerosis or stroke for example.

References

1 Furchgott RF, Cherry PD, Zawadzki JV, Jothianandan D. Endothelial cells as mediators of vasodilation of arteries. *J Cardiovasc Pharmacol* 1984; **6 Suppl 2**: S336-343.

2 Hibbs JB, Taintor RR, Vavrin Z. Macrophage cytotoxicity: role for L-arginine deiminase and imino nitrogen oxidation to nitrite. *Science* 1987; **235**: 473–476.

3 Stuehr DJ, Marletta MA. Mammalian nitrate biosynthesis: mouse macrophages produce nitrite and nitrate in response to Escherichia coli lipopolysaccharide. *Proc Natl Acad Sci U S A* 1985; **82**: 7738–7742.

4 Furchgott RF, Zawadzki JV. The obligatory role of endothelial cells in the relaxation of arterial smooth muscle by acetylcholine. *Nature* 1980; **288**: 373–376.

5 Arnold WP, Mittal CK, Katsuki S, Murad F. Nitric oxide activates guanylate cyclase and increases guanosine 3':5'-cyclic monophosphate levels in various tissue preparations. *Proc Natl Acad Sci USA* 1977; **74**: 3203–3207.

6 Ignarro LJ, Buga GM, Wood KS, Byrns RE, Chaudhuri G. Endothelium-derived relaxing factor produced and released from artery and vein is nitric oxide. *Proc Natl Acad Sci USA* 1987; **84**: 9265–9269.

7 Garthwaite J, Charles SL, Chess-Williams R. Endothelium-derived relaxing factor release on activation of NMDA receptors suggests role as intercellular messenger in the brain. *Nature* 1988; **336**: 385–388.

8 Foster MW, McMahon TJ, Stamler JS. S-nitrosylation in health and disease. *Trends Mol Med* 2003; **9**: 160–168.

9 Moncada S, Palmer RM, Higgs EA. Nitric oxide: physiology, pathophysiology, and pharmacology. *Pharmacol Rev* 1991; **43**: 109–142.

10 Torregrossa AC, Aranke M, Bryan NS. Nitric oxide and geriatrics: Implications in diagnostics and treatment of the elderly. *J Geriatr Cardiol* 2011; **8**: 230–242.

11 Bredt D, Snyder S. Nitric-Oxide - a Physiological Messenger Molecule. *Annu Rev Biochem* 1994; **63**: 175–195.

12 Groves JT, Wang CCY. Nitric oxide synthase: models and mechanisms. *Curr Opin Chem Biol* 2000; **4**: 687–695.

13 Alderton WK, Cooper CE, Knowles RG. Nitric oxide synthases: structure, function and inhibition. *Biochem J* 2001; **357**: 593–615.

14 Nathan C, Xie Q. Nitric-Oxide Synthases - Roles, Tolls, and Controls. *Cell* 1994; **78**: 915–918.

15 Farah C, Michel LYM, Balligand J-L. Nitric oxide signalling in cardiovascular health and disease. *Nature Reviews Cardiology* 2018; **15**: 292–316.

16 Calver A, Collier J, Vallance P. Nitric-Oxide and Cardiovascular Control. *Exp Physiol* 1993; **78**: 303–326.

17 Palmer RM, Ashton DS, Moncada S. Vascular endothelial cells synthesize nitric oxide from L-arginine. *Nature* 1988; **333**: 664–666.

18 Dinerman J, Lowenstein C, Snyder S. Molecular Mechanisms of Nitric-Oxide Regulation - Potential Relevance to Cardiovascular-Disease. *CircRes* 1993; **73**: 217–222.

19 Napoli C, de Nigris F, Williams-Ignarro S, Pignalosa O, Sica V, Ignarro LJ. Nitric oxide and atherosclerosis: An update. *Nitric Oxide-Biol Chem* 2006; **15**: 265–279.

20 Foerstermann U. Nitric oxide and oxidative stress in vascular disease. *Pflugers Arch* 2010; **459**: 923–939.

21 Chatterjee A, Catravas JD. Endothelial nitric oxide (NO) and its pathophysiologic regulation. *Vasc Pharmacol* 2008; **49**: 134–140.

22 Higashi Y, Noma K, Yoshizumi M, Kihara Y. Endothelial Function and Oxidative Stress in Cardiovascular Diseases. *Circ J* 2009; **73**: 411–418.

23 Li HG, Forstermann U. Nitric oxide in the pathogenesis of vascular disease. *J Pathol* 2000; **190**: 244–254.

24 Debelder A, Macallister R, Radomski M, Moncada S, Vallance P. Effects of S-Nitroso-Glutathione in the Human Forearm Circulation - Evidence for Selective-Inhibition of Platelet Activation. *Cardiovasc Res* 1994; **28**: 691–694.

25 Lundberg JO. Nitric Oxide Metabolites and Cardiovascular Disease: Markers, Mediators, or Both? *Journal of the American College of Cardiology* 2006; **47**: 580–581.

26 Smith BC, Marletta MA. Mechanisms of S-nitrosothiol formation and selectivity in nitric oxide signaling. *Curr Opin Chem Biol* 2012; **16**: 498–506.

27 Zhang Y, Hogg N. S-Nitrosothiols: cellular formation and transport. *Free Radical Biology and Medicine* 2005; **38**: 831–838.

28 Hogg N. The biochemistry and physiology of S-nitrosothiols. *Annu Rev Pharmacol Toxicol* 2002; **42**: 585–600.

29 Loscalzo J, Welch G. Nitric oxide and its role in the cardiovascular system. *Prog Cardiovasc Dis* 1995; **38**: 87–104.

30 Richardson G, Benjamin N. Potential therapeutic uses for S-nitrosothiols. *Clin Sci* 2002; **102**: 99–105.

31 Wang PG, Xian M, Tang XP, Wu XJ, Wen Z, Cai TW *et al.* Nitric oxide donors: Chemical activities and biological applications. *Chem Rev* 2002; **102**: 1091–1134.

32 Carpenter AW, Schoenfisch MH. Nitric oxide release: Part II. Therapeutic applications. *Chem Soc Rev* 2012; **41**: 3742–3752.

33 Parratt JR. Nitroglycerin--the first one hundred years: new facts about an old drug. *J Pharm Pharmacol* 1979; **31**: 801–809.

34 Nelin LD, Hoffman GM. The use of inhaled nitric oxide in a wide variety of clinical problems. *Pediatr Clin North Am* 1998; **45**: 531–548.

35 Nitroprusside. In: *Drugs and Lactation Database (LactMed)*. National Library of Medicine (US): Bethesda (MD), 2006http://www.ncbi.nlm.nih.gov/books/NBK500662/ (accessed 21 Jun2019).

36 Cobb A, Thornton L. Sodium Nitroprusside as a Hyperinflation Drug and Therapeutic Alternatives. *J Pharm Pract* 2018; **31**: 374–381.

37 Ware RW, King SB. P-Nitrosophosphate compounds: new N-O heterodienophiles and nitroxyl delivery agents. *J Org Chem* 2000; **65**: 8725–8729.

38 Ellis A, Li CG, Rand MJ. Differential actions of L-cysteine on responses to nitric oxide, nitroxyl anions and EDRF in the rat aorta. *Br J Pharmacol* 2000; **129**: 315–322.

39 Ng SS, Pang CC. Venous versus arterial actions of diethylamine/nitric oxide (DEA/NO) complex and S-nitroso-N-acetylpenicillamine (SNAP) in vivo. *Br J Pharmacol* 1998; **125**: 1247–1251.

40 Fernández-Tomé P, Lizasoain I, Leza JC, Lorenzo P, Moro MA. Neuroprotective effects of DETA-NONOate, a nitric oxide donor, on hydrogen peroxide-induced neurotoxicity in cortical neurones. *Neuropharmacology* 1999; **38**: 1307–1315.

41 Schönafinger K. Heterocyclic NO prodrugs. *Farmaco* 1999; **54**: 316–320.

42 Ignarro LJ, Napoli C, Loscalzo J. Nitric oxide donors and cardiovascular agents modulating the bioactivity of nitric oxide - An overview. *CircRes* 2002; **90**: 21–28.

43 Gruetter CA, Gruetter DY, Lyon JE, Kadowitz PJ, Ignarro LJ. Relationship between cyclic guanosine 3':5'-monophosphate formation and relaxation of coronary arterial smooth muscle by glyceryl trinitrate, nitroprusside, nitrite and nitric oxide: effects of methylene blue and methemoglobin. *J Pharmacol Exp Ther* 1981; **219**: 181–186.

44 Gruetter CA, Barry BK, McNamara DB, Gruetter DY, Kadowitz PJ, Ignarro L. Relaxation of bovine coronary artery and activation of coronary arterial guanylate cyclase by nitric oxide, nitroprusside and a carcinogenic nitrosoamine. *J Cyclic Nucleotide Res* 1979; **5**: 211–224.

45 McGuire JJ, Anderson DJ, McDonald BJ, Narayanasami R, Bennett BM. Inhibition of NADPH-cytochrome P450 reductase and glyceryl trinitrate biotransformation by diphenyleneiodonium sulfate. *Biochem Pharmacol* 1998; **56**: 881–893.

46 Kurz MA, Boyer TD, Whalen R, Peterson TE, Harrison DG. Nitroglycerin metabolism in vascular tissue: role of glutathione S-transferases and relationship between NO. and NO2- formation. *Biochem J* 1993; **292 (Pt 2)**: 545–550.

47 Münzel T, Sayegh H, Freeman BA, Tarpey MM, Harrison DG. Evidence for enhanced vascular superoxide anion production in nitrate tolerance. A novel mechanism underlying tolerance and cross-tolerance. *J Clin Invest* 1995; **95**: 187–194.

48 Münzel T, Kurz S, Rajagopalan S, Thoenes M, Berrington WR, Thompson JA *et al.* Hydralazine prevents nitroglycerin tolerance by inhibiting activation of a membrane-bound NADH oxidase. A new action for an old drug. *J Clin Invest* 1996; **98**: 1465–1470.

49 Skatchkov null, Larina null, Larin null, Fink null, Bassenge null. Urinary NItrotyrosine Content as a Marker of Peroxynitrite-induced Tolerance to Organic NItrates. *J Cardiovasc Pharmacol Ther* 1997; **2**: 85–96.

50 Molina CR, Andresen JW, Rapoport RM, Waldman S, Murad F. Effect of in vivo nitroglycerin therapy on endothelium-dependent and independent vascular relaxation and cyclic GMP accumulation in rat aorta. *J Cardiovasc Pharmacol* 1987; **10**: 371–378.

51 Münzel T, Li H, Mollnau H, Hink U, Matheis E, Hartmann M *et al.* Effects of long-term nitroglycerin treatment on endothelial nitric oxide synthase (NOS III) gene expression, NOS III-mediated superoxide production, and vascular NO bioavailability. *Circ Res* 2000; **86**: E7–E12.

52 Fylaktakidou KC, Hadjipavlou-Litina DJ, Litinas KE, Varella EA, Nicolaides DN. Recent developments in the chemistry and in the biological applications of amidoximes. *Curr Pharm Des* 2008; **14**: 1001–1047.

53 Clement B. Reduction of N-hydroxylated compounds: amidoximes (N-hydroxyamidines) as pro-drugs of amidines. *Drug Metab Rev* 2002; **34**: 565–579.

54 Kang S, Zeng H, Li H, Wang H, Wang P. 4-Chlorobenzamidoxime. *Acta Crystallographica Section E* 2007; **63**: o4698–o4698.

55 Al-Sa'Doni H, Ferro A. S-Nitrosothiols: a class of nitric oxide-donor drugs. *Clin Sci* 2000; **98**: 507–520.

56 Williams DL. S-nitrosothiols and role of metal ions in decomposition to nitric oxide. *Meth Enzymol* 1996; **268**: 299–308.

57 Singh RJ, Hogg N, Joseph J, Kalyanaraman B. Mechanism of nitric oxide release from S-nitrosothiols. *J Biol Chem* 1996; **271**: 18596–18603.

58 Sexton DJ, Muruganandam A, McKenney DJ, Mutus B. Visible light photochemical release of nitric oxide from S-nitrosoglutathione: potential photochemotherapeutic applications. *Photochem Photobiol* 1994; **59**: 463–467.

59 Broniowska KA, Diers AR, Hogg N. S-Nitrosoglutathione. *Biochim Biophys Acta-Gen Subj* 2013; **1830**: 3173–3181.

60 Hogg N. Biological chemistry and clinical potential of S-nitrosothiols. *Free Radical Biology and Medicine* 2000; **28**: 1478–1486.

61 Hogg N. The kinetics of S-transnitrosation--a reversible second-order reaction. *Anal Biochem* 1999; **272**: 257–262.

62 Wang K, Wen Z, Zhang W, Xian M, Cheng JP, Wang PG. Equilibrium and kinetics studies of transnitrosation between S-nitrosothiols and thiols. *Bioorg Med Chem Lett* 2001; **11**: 433–436.

63 Butler AR, Al-Sa'doni HH, Megson IL, Flitney FW. Synthesis, decomposition, and vasodilator action of some new S-nitrosated dipeptides. *Nitric Oxide* 1998; **2**: 193–202.

64 Stamler JS. S-nitrosothiols and the bioregulatory actions of nitrogen oxides through reactions with thiol groups. *Curr Top Microbiol Immunol* 1995; **196**: 19–36.

65 Arnelle DR, Stamler JS. NO+, NO, and NO- donation by S-nitrosothiols: implications for regulation of physiological functions by S-nitrosylation and acceleration of disulfide formation. *Arch Biochem Biophys* 1995; **318**: 279–285.

66 Hogg N, Singh RJ, Kalyanaraman B. The role of glutathione in the transport and catabolism of nitric oxide. *FEBS Lett* 1996; **382**: 223–228.

67 Mohr S, Hallak H, de Boitte A, Lapetina EG, Brüne B. Nitric oxide-induced S-glutathionylation and inactivation of glyceraldehyde-3-phosphate dehydrogenase. *J Biol Chem* 1999; **274**: 9427–9430.

68 Ji Y, Akerboom TP, Sies H, Thomas JA. S-nitrosylation and S-glutathiolation of protein sulfhydryls by S-nitroso glutathione. *Arch Biochem Biophys* 1999; **362**: 67–78.

69 Padgett CM, Whorton AR. Cellular responses to nitric oxide: role of protein S-thiolation/dethiolation. *Arch Biochem Biophys* 1998; **358**: 232–242.

70 Haj-Yehia AI, Benet LZ. In vivo depletion of free thiols does not account for nitroglycerin-induced tolerance: a thiol-nitrate interaction hypothesis as an alternative explanation for nitroglycerin activity and tolerance. *J Pharmacol Exp Ther* 1996; **278**: 1296–1305.

71 Hornyak I, Pankotai E, Kiss L, Lacza Z. Current Developments in the Therapeutic Potential of S-Nitrosoglutathione, an Endogenous NO-Donor Molecule. *Curr Pharm Biotechnol* 2011; **12**: 1368–1374.

72 Hart TW. Some observations concerning the S-nitroso and S-phenylsulphonyl derivatives of L-cysteine and glutathione. *Tetrahedron Letters* 1985; **26**: 2013–2016.

73 Parent M, Dahboul F, Schneider R, Clarot I, Maincent P, Boudier PL and A. A Complete Physicochemical Identity Card of S-nitrosoglutathione. Current Pharmaceutical Analysis. 2013.http://www.eurekaselect.com/105996/article (accessed 21 Jun2019).

74 Jensen DE, Belka GK, Du Bois GC. S-Nitrosoglutathione is a substrate for rat alcohol dehydrogenase class III isoenzyme. *Biochem J* 1998; **331**: 659–668.

75 Koivusalo M, Baumann M, Uotila L. Evidence for the identity of glutathione-dependent formaldehyde dehydrogenase and class III alcohol dehydrogenase. *FEBS Lett* 1989; **257**: 105–109.

76 Staab CA, Hartmanová T, El-Hawari Y, Ebert B, Kisiela M, Wsol V *et al.* Studies on reduction of S-nitrosoglutathione by human carbonyl reductases 1 and 3. *Chem Biol Interact* 2011; **191**: 95–103.

77 Barnett SD, Buxton ILO. The role of S-nitrosoglutathione reductase (GSNOR) in human disease and therapy. *Crit Rev Biochem Mol Biol* 2017; **52**: 340–354.

78 Benhar M, Forrester MT, Hess DT, Stamler JS. Regulated protein denitrosylation by cytosolic and mitochondrial thioredoxins. *Science* 2008; **320**: 1050–1054.

79 Sengupta R, Holmgren A. Thioredoxin and thioredoxin reductase in relation to reversible S-nitrosylation. *Antioxid Redox Signal* 2013; **18**: 259–269.

80 Mitchell DA, Marletta MA. Thioredoxin catalyzes the S-nitrosation of the caspase-3 active site cysteine. *Nat Chem Biol* 2005; **1**: 154–158.

81 Zai A, Rudd MA, Scribner AW, Loscalzo J. Cell-surface protein disulfide isomerase catalyzes transnitrosation and regulates intracellular transfer of nitric oxide. *J Clin Invest* 1999; **103**: 393–399.

82 Sliskovic I, Raturi A, Mutus B. Characterization of the S-denitrosation activity of protein disulfide isomerase. *J Biol Chem* 2005; **280**: 8733–8741.

83 Allison RD. gamma-Glutamyl transpeptidase: kinetics and mechanism. *Meth Enzymol* 1985; **113**: 419–437.

84 Meister A, Tate SS, Griffith OW. Gamma-glutamyl transpeptidase. *Meth Enzymol* 1981; **77**: 237–253.

85 Abbott WA, Griffith OW, Meister A. Gamma-glutamyl-glutathione. Natural occurrence and enzymology. *J Biol Chem* 1986; **261**: 13657–13661.

86 Hou Y, Guo Z, Li J, Wang PG. Seleno compounds and glutathione peroxidase catalyzed decomposition of S-nitrosothiols. *Biochem Biophys Res Commun* 1996; **228**: 88–93.

87 Trujillo M, Alvarez MN, Peluffo G, Freeman BA, Radi R. Xanthine oxidase-mediated decomposition of S-nitrosothiols. *J Biol Chem* 1998; **273**: 7828–7834.

88 Jourd'heuil D, Laroux FS, Miles AM, Wink DA, Grisham MB. Effect of superoxide dismutase on the stability of S-nitrosothiols. *Arch Biochem Biophys* 1999; **361**: 323–330.

89 Staab CA, Hellgren M, Höög J-O. Medium- and short-chain dehydrogenase/reductase gene and protein families : Dual functions of alcohol dehydrogenase 3: implications with focus on formaldehyde dehydrogenase and S-nitrosoglutathione reductase activities. *Cell Mol Life Sci* 2008; **65**: 3950–3960.

90 Ramsay B, Radomski M, Debelder A, Martin J, Lopezjaramillo P. Systemic Effects of S-Nitroso-Glutathione in the Human Following Intravenous-Infusion. *Br J Clin Pharmacol* 1995; **40**: 101–102.

91 Langford EJ, Wainwright RJ, Martin JF. Platelet activation in acute myocardial infarction and unstable angina is inhibited by nitric oxide donors. *Arterioscler Thromb Vasc Biol* 1996; **16**: 51–55.

92 Salas E, Langford EJ, Marrinan MT, Martin JF, Moncada S, de Belder AJ. S-nitrosoglutathione inhibits platelet activation and deposition in coronary artery saphenous vein grafts in vitro and in vivo. *Heart* 1998; **80**: 146–150.

93 Lees C, Langford E, Brown AS, DeBelder A, Pickles A, Martin JF *et al.* The effects of S-nitrosoglutathione on platelet activation, hypertension, and uterine and fetal Doppler in severe preeclampsia. *Obstet Gynecol* 1996; **88**: 14–19.

94 Langford E, Brown A, Wainwright R, Debelder A, Thomas M, Smith R *et al.* Inhibition of Platelet Activity by S-Nitrosoglutathione During Coronary Angioplasty. *Lancet* 1994; **344**: 1458–1460.

95 Kaposzta Z, Baskerville PA, Madge D, Fraser S, Martin JF, Markus HS. L-arginine and S-nitrosoglutathione reduce embolization in humans. *Circulation* 2001; **103**: 2371–2375.

96 Kaposzta Z, Clifton A, Molloy J, Martin JF, Markus HS. S-nitrosoglutathione reduces asymptomatic embolization after carotid angioplasty. *Circulation* 2002; **106**: 3057–3062.

97 Molloy J, Martin JF, Baskerville PA, Fraser SCA, Markus HS. S-nitrosoglutathione reduces the rate of embolization in humans. *Circulation* 1998; **98**: 1372–1375.

98 Moncada S, Palmer RM, Higgs EA. Nitric oxide: physiology, pathophysiology, and pharmacology. *Pharmacol Rev* 1991; **43**: 109–142.

99 Macallister R, Calver A, Riezebos J, Collier J, Vallance P. Relative Potency and Arteriovenous Selectivity of Nitrovasodilators on Human Blood-Vessels - an Insight into the Targeting of Nitric-Oxide Delivery. *J Pharmacol Exp Ther* 1995; **273**: 154–160.

100 Rassaf T, Kleinbongard P, Preik M, Dejam A, Gharini P, Lauer T *et al.* Plasma nitrosothiols contribute to the systemic vasodilator effects of intravenously applied NO - Experimental and clinical study on the fate of NO in human blood. *CircRes* 2002; **91**: 470–477.

101 Duong HTT, Dong Z, Su L, Boyer C, George J, Davis TP *et al.* The use of nanoparticles to deliver nitric oxide to hepatic stellate cells for treating liver fibrosis and portal hypertension. *Small* 2015; **11**: 2291–2304.

102 Seabra AB, Fitzpatrick A, Paul J, De Oliveira MG, Weller R. Topically applied S-nitrosothiol-containing hydrogels as experimental and pharmacological nitric oxide donors in human skin. *Br J Dermatol* 2004; **151**: 977–983.

103 Bannenberg G, Xue J, Engman L, Cotgreave I, Moldeus P, Ryrfeldt A. Characterization of Bronchodilator Effects and Fate of S-Nitrosothiols. *J Pharmacol Exp Ther* 1995; **272**: 1238–1245.

104 Hurley KP, Bovet LL, Stamler JS. Stable S-nitrosthiol formulations, patent cooperation treaty. 2005.

105 Seabra AB, de Souza GFP, da Rocha LL, Eberlin MN, de Oliveira MG. S-nitrosoglutathione incorporated in poly(ethylene glycol) matrix: potential use for topical nitric oxide delivery. *Nitric Oxide-Biol Chem* 2004; **11**: 263–272.

106 Seabra AB, Da Rocha LL, Eberlin MN, De Oliveira MG. Solid films of blended poly(vinyl alcohol)/poly(vinyl pyrrolidone) for topical S-nitrosoglutathione and nitric oxide release. *J Pharm Sci* 2005; **94**: 994–1003.

107 Seabra AB, de Oliveira MG. Poly(vinyl alcohol) and poly(vinyl pyrrolidone) blended films for local nitric oxide release. *Biomaterials* 2004; **25**: 3773–3782.

108 Simões MM de SG, de Oliveira MG. Poly(vinyl alcohol) films for topical delivery of S-nitrosoglutathione: effect of freezing-thawing on the diffusion properties. *J Biomed Mater Res Part B Appl Biomater* 2010; **93**: 416–424.

109 Kim JO, Noh J-K, Thapa RK, Hasan N, Choi M, Kim JH *et al.* Nitric oxide-releasing chitosan film for enhanced antibacterial and in vivo wound-healing efficacy. *Int J Biol Macromol* 2015; **79**: 217–225.

110 Yoo J-W, Acharya G, Lee CH. In vivo evaluation of vaginal films for mucosal delivery of nitric oxide. *Biomaterials* 2009; **30**: 3978–3985.

111 Shishido SM, Seabra AB, Loh W, Ganzarolli de Oliveira M. Thermal and photochemical nitric oxide release from S-nitrosothiols incorporated in Pluronic F127 gel: potential uses for local and controlled nitric oxide release. *Biomaterials* 2003; **24**: 3543–3553.

112 Vercelino R, Cunha TM, Ferreira ES, Cunha FQ, Ferreira SH, de Oliveira MG. Skin vasodilation and analgesic effect of a topical nitric oxide-releasing hydrogel. *J Mater Sci Mater Med* 2013; **24**: 2157–2169.

113 Georgii JL, Amadeu TP, Seabra AB, de Oliveira MG, Monte-Alto-Costa A. Topical S-nitrosoglutathione-releasing hydrogel improves healing of rat ischaemic wounds. *J Tissue Eng Regen Med* 2011; **5**: 612–619.

114 Pelegrino MT, de Araújo DR, Seabra AB. S-nitrosoglutathione-containing chitosan nanoparticles dispersed in Pluronic F-127 hydrogel: Potential uses in topical applications. *Journal of Drug Delivery Science and Technology* 2018; **43**: 211–220.

115 Hlaing SP, Kim J, Lee J, Hasan N, Cao J, Naeem M *et al.* S-Nitrosoglutathione loaded poly(lactic-co-glycolic acid) microparticles for prolonged nitric oxide release and enhanced healing of methicillin-resistant Staphylococcus aureus-infected wounds. *Eur J Pharm Biopharm* 2018; **132**: 94–102.

116 Parent M, Boudier A, Fries I, Gostyńska A, Rychter M, Lulek J *et al.* Nitric oxide-eluting scaffolds and their interaction with smooth muscle cells in vitro. *J Biomed Mater Res A* 2015; **103**: 3303–3311.

117 Parent M, Boudier A, Perrin J, Vigneron C, Maincent P, Violle N *et al.* In Situ Microparticles Loaded with S-Nitrosoglutathione Protect from Stroke. *PLoS ONE* 2015; **10**: e0144659.

118 de Mel A, Naghavi N, Cousins BG, Clatworthy I, Hamilton G, Darbyshire A *et al.* Nitric oxide-eluting nanocomposite for cardiovascular implants. *J Mater Sci Mater Med* 2014; **25**: 917–929.

119 Acharya G, Lee CH, Lee Y. Optimization of cardiovascular stent against restenosis: factorial design-based statistical analysis of polymer coating conditions. *PLoS ONE* 2012; **7**: e43100.

120 Bhavsar MD, Amiji MM. Polymeric nano- and microparticle technologies for oral gene delivery. *Expert Opin Drug Deliv* 2007; **4**: 197–213.

121 Shunmugavel A, Khan M, Hughes FM, Purves JT, Singh A, Singh I. S-Nitrosoglutathione protects the spinal bladder: Novel therapeutic approach to post-spinal cord injury bladder remodeling: GSNO Protects Spinal Bladder. *Neurourology and Urodynamics* 2015; **34**: 519–526.

122 Giri S, Rattan R, Deshpande M, Maguire JL, Johnson Z, Graham RP *et al.* Preclinical Therapeutic Potential of a Nitrosylating Agent in the Treatment of Ovarian Cancer. *PLoS ONE* 2014; **9**: e97897.

123 Nath N, Morinaga O, Singh I. S-nitrosoglutathione a Physiologic Nitric Oxide Carrier Attenuates Experimental Autoimmune Encephalomyelitis. *Journal of Neuroimmune Pharmacology* 2010; **5**: 240–251.

124 Haq E, Rohrer B, Nath N, Crosson CE, Singh I. S-nitrosoglutathione prevents interphotoreceptor retinoid-binding protein (IRBP161-180)-induced experimental autoimmune uveitis. *J Ocular Pharmacol Ther* 2007; **23**: 221–231.

125 Wu W, Gaucher C, Diab R, Fries I, Xiao Y-L, Hu X-M *et al.* Time lasting S-nitrosoglutathione polymeric nanoparticles delay cellular protein S-nitrosation. *European Journal of Pharmaceutics and Biopharmaceutics* 2015; **89**: 1–8.

126 Wu W, Gaucher C, Fries I, Hu X, Maincent P, Sapin-Minet A. Polymer nanocomposite particles of S -nitrosoglutathione: A suitable formulation for protection and sustained oral delivery. *International Journal of Pharmaceutics* 2015; **495**: 354–361.

127 Wu W, Perrin-Sarrado C, Ming H, Lartaud I, Maincent P, Hu X-M *et al.* Polymer nanocomposites enhance S -nitrosoglutathione intestinal absorption and promote the formation of releasable nitric oxide stores in rat aorta. *Nanomedicine: Nanotechnology, Biology and Medicine* 2016; **12**: 1795–1803.

128 Ensign LM, Cone R, Hanes J. Oral Drug Delivery with Polymeric Nanoparticles: The Gastrointestinal Mucus Barriers. *Adv Drug Deliv Rev* 2012; **64**: 557–570.

129 Date AA, Hanes J, Ensign LM. Nanoparticles for oral delivery: Design, evaluation and state-of-the-art. *Journal of Controlled Release* 2016; **240**: 504–526.

130 Pagels RF, Prud'homme RK. Polymeric nanoparticles and microparticles for the delivery of peptides, biologics, and soluble therapeutics. *Journal of Controlled Release* 2015; **219**: 519–535.

131 Yun Y, Cho YW, Park K. Nanoparticles for oral delivery: Targeted nanoparticles with peptidic ligands for oral protein delivery. *Adv Drug Deliv Rev* 2013; **65**: 822–832.

132 George M, Abraham TE. Polyionic hydrocolloids for the intestinal delivery of protein drugs: alginate and chitosan--a review. *J Control Release* 2006; **114**: 1–14.

133 Chang C-H, Lin Y-H, Yeh C-L, Chen Y-C, Chiou S-F, Hsu Y-M *et al.* Nanoparticles incorporated in pH-sensitive hydrogels as amoxicillin delivery for eradication of Helicobacter pylori. *Biomacromolecules* 2010; **11**: 133–142.

134 Lin Y-H, Lin J-H, Chou S-C, Chang S-J, Chung C-C, Chen Y-S *et al.* Berberine-loaded targeted nanoparticles as specific Helicobacter pylori eradication therapy: in vitro and in vivo study. *Nanomedicine (Lond)* 2015; **10**: 57–71.

135 He H, Wang P, Cai C, Yang R, Tang X. VB12-coated Gel-Core-SLN containing insulin: Another way to improve oral absorption. *Int J Pharm* 2015; **493**: 451–459.

136 Verma A, Sharma S, Gupta PK, Singh A, Teja BV, Dwivedi P *et al.* Vitamin B12 functionalized layer by layer calcium phosphate nanoparticles: A mucoadhesive and pH responsive carrier for improved oral delivery of insulin. *Acta Biomater* 2016; **31**: 288–300.

137 Aji Alex MR, Chacko AJ, Jose S, Souto EB. Lopinavir loaded solid lipid nanoparticles (SLN) for intestinal lymphatic targeting. *Eur J Pharm Sci* 2011; **42**: 11–18.

138 Zhang Z, Gao F, Bu H, Xiao J, Li Y. Solid lipid nanoparticles loading candesartan cilexetil enhance oral bioavailability: in vitro characteristics and absorption mechanism in rats. *Nanomedicine* 2012; **8**: 740–747.

139 Gugulothu D, Kulkarni A, Patravale V, Dandekar P. pH-sensitive nanoparticles of curcumin-celecoxib combination: evaluating drug synergy in ulcerative colitis model. *J Pharm Sci* 2014; **103**: 687–696.

140 Couvreur P. Nanoparticles in drug delivery: Past, present and future. *Advanced Drug Delivery Reviews* 2013; **65**: 21–23.

141 Kohane DS. Microparticles and nanoparticles for drug delivery. *Biotechnology and Bioengineering* 2007; **96**: 203–209.

142 Couvreur P, Puisieux F. Nanoparticles and Microparticles for the Delivery of Polypeptides and Proteins. *Adv Drug Deliv Rev* 1993; **10**: 141–162.

143 Kumar MNVR. Nano and microparticles as controlled drug delivery devices. *Journal of Pharmacy and Pharmaceutical Sciences* 2000.

144 Mundargi RC, Babu VR, Rangaswamy V, Patel P, Aminabhavi TM. Nano/micro technologies for delivering macromolecular therapeutics using poly(D,L-lactide-co-glycolide) and its derivatives. *J Control Release* 2008; **125**: 193–209.

145 Doherty MM, Charman WN. The mucosa of the small intestine: how clinically relevant as an organ of drug metabolism? *Clin Pharmacokinet* 2002; **41**: 235–253.

146 Friend DR. Drug delivery to the small intestine. *Curr Gastroenterol Rep* 2004; **6**: 371–376.

147 Gotoh Y, Suzuki H, Kinoshita S, Hirohashi T, Kato Y, Sugiyama Y. Involvement of an organic anion transporter (canalicular multispecific organic anion transporter/multidrug resistance-associated protein 2) in gastrointestinal secretion of glutathione conjugates in rats. *J Pharmacol Exp Ther* 2000; **292**: 433–439.

148 Madara JL. Regulation of the movement of solutes across tight junctions. *Annu Rev Physiol* 1998; **60**: 143–159.

149 Tomita M, Shiga M, Hayashi M, Awazu S. Enhancement of colonic drug absorption by the paracellular permeation route. *Pharm Res* 1988; **5**: 341–346.

150 Rubas W, Cromwell ME, Shahrokh Z, Villagran J, Nguyen TN, Wellton M *et al.* Flux measurements across Caco-2 monolayers may predict transport in human large intestinal tissue. *J Pharm Sci* 1996; **85**: 165–169.

151 Pappenheimer JR. Physiological regulation of transepithelial impedance in the intestinal mucosa of rats and hamsters. *J Membr Biol* 1987; **100**: 137–148.

152 Barry PH. Ionic permeation mechanisms in epithelia: biionic potentials, dilution potentials, conductances, and streaming potentials. *Meth Enzymol* 1989; **171**: 678–715.

153 Powell DW. Barrier function of epithelia. *Am J Physiol* 1981; **241**: G275-288.

154 Shakweh M, Ponchel G, Fattal E. Particle uptake by Peyer's patches: a pathway for drug and vaccine delivery. *Expert Opin Drug Deliv* 2004; **1**: 141–163.

155 Burton PS, Conradi RA, Hilgers AR. (B) Mechanisms of peptide and protein absorption: (2) Transcellular mechanism of peptide and protein absorption: passive aspects. *Advanced Drug Delivery Reviews* 1991; **7**: 365–385.

156 Florence AT. Issues in oral nanoparticle drug carrier uptake and targeting. *J Drug Target* 2004; **12**: 65–70.

157 Giannasca PJ, Giannasca KT, Leichtner AM, Neutra MR. Human intestinal M cells display the sialyl Lewis A antigen. *Infect Immun* 1999; **67**: 946–953.

158 Frey A, Neutra MR. Targeting of mucosal vaccines to Peyer's patch M cells. *Behring Inst Mitt* 1997; : 376–389.

159 Clark MA, Hirst BH, Jepson MA. Lectin-mediated mucosal delivery of drugs and microparticles. *Adv Drug Deliv Rev* 2000; **43**: 207–223.

160 Buda A, Sands C, Jepson MA. Use of fluorescence imaging to investigate the structure and function of intestinal M cells. *Adv Drug Deliv Rev* 2005; **57**: 123–134.

161 Schué F. Encyclopedia of controlled drug delivery, Volumes 1 and 2 Edited by Edith Mathiowitz John Wiley and Sons, New York, 1999 Volume 1, pp 492; volume 2, pp 565, price ISBN Volume 1: 0-471-16662-6; Volume 2: 0-471-16663-4; 2 Volume set: 0-471-14828-8. *Polymer International* 2002; **51**: 263–263.

162 Barthe L, Woodley J, Houin G. Gastrointestinal absorption of drugs: methods and studies. *Fundam Clin Pharmacol* 1999; **13**: 154–168.

163 Bai JP, Amidon GL. Structural specificity of mucosal-cell transport and metabolism of peptide drugs: implication for oral peptide drug delivery. *Pharm Res* 1992; **9**: 969–978.

164 Russell-Jones GJ. The potential use of receptor-mediated endocytosis for oral drug delivery. *Adv Drug Deliv Rev* 2001; **46**: 59–73.

165 Camilleri M, Nadeau A, Lamsam J, Nord SL, Ryks M, Burton D *et al.* Understanding Measurements of Intestinal Permeability in Healthy Humans with Urine Lactulose and Mannitol Excretion. *Neurogastroenterol Motil* 2010; **22**: e15–e26.

166 Wang L, Llorente C, Hartmann P, Yang A-M, Chen P, Schnabl B. Methods to determine intestinal permeability and bacterial translocation during liver disease. *J Immunol Methods* 2015; **421**: 44–53.

167 González-González M, Díaz-Zepeda C, Eyzaguirre-Velásquez J, González-Arancibia C, Bravo JA, Julio-Pieper M. Investigating Gut Permeability in Animal Models of Disease. *Front Physiol* 2019; **9**. doi:10.3389/fphys.2018.01962.

168 Clarke LL. A guide to Ussing chamber studies of mouse intestine. *Am J Physiol Gastrointest Liver Physiol* 2009; **296**: G1151–G1166.

169 Gordon S, Daneshian M, Bouwstra J, Caloni F, Constant S, Davies DE *et al.* Non-animal models of epithelial barriers (skin, intestine and lung) in research, industrial applications and regulatory toxicology. *ALTEX* 2015; **32**: 327–378.

170 Moon C, VanDussen KL, Miyoshi H, Stappenbeck TS. Development of a primary mouse intestinal epithelial cell monolayer culture system to evaluate factors that modulate IgA transcytosis. *Mucosal Immunol* 2014; **7**: 818–828.

171 Hidalgo IJ, Raub TJ, Borchardt RT. Characterization of the human colon carcinoma cell line (Caco-2) as a model system for intestinal epithelial permeability. *Gastroenterology* 1989; **96**: 736–749.

172 Grüneberg S, Güssregen S. Drug Bioavailability. Estimation of Solubility, Permeability, Absorption and Bioavailability. (Series: Methods and Principles in Medicinal Chemistry, Vol. 18; series editors: R. Mannhold, H. Kubinyi, and G. Folkers). Edited by Han van de Waterbeemd, Hans Lennernäs and Per Artursson. *Angewandte Chemie International Edition* 2004; **43**: 146–147.

173 Gamboa JM, Leong KW. In vitro and in vivo models for the study of oral delivery of nanoparticles. *Adv Drug Deliv Rev* 2013; **65**: 800–810.

174 Li N, Sui Z, Liu Y, Wang D, Ge G, Yang L. A fast screening model for drug permeability assessment based on native small intestinal extracellular matrix. *RSC Adv* 2018; **8**: 34514–34524.

175 Nunes R, Silva C, Chaves L. 4.2 - Tissue-based in vitro and ex vivo models for intestinal permeability studies. In: Sarmento B (ed). *Concepts and Models for Drug Permeability Studies*. Woodhead Publishing, 2016, pp 203–236.

176 Sachan N, Bhattacharya A, Pushkar S, Mishra A. Biopharmaceutical classification system: A strategic tool for oral drug delivery technology. *Asian Journal of Pharmaceutics* 2009; **3**: 76.

177 Kubaszewski E, Peters A, McClain S, Bohr D, Malinski T. Light-activated release of nitric oxide from vascular smooth muscle of normotensive and hypertensive rats. *Biochem Biophys Res Commun* 1994; **200**: 213–218.

178 Furchgott RF, Ehrreich SJ, Greenblatt E. The Photoactivated Relaxation of Smooth Muscle of Rabbit Aorta. *J Gen Physiol* 1961; **44**: 499–419.

179 Flitney FW, Megson IL. Nitric Oxide and the Mechanism of Rat Vascular Smooth Muscle Photorelaxation. *The Journal of Physiology* 2003; **550**: 819–828.

180 Stoclet J-C, Troncy E, Muller B, Brua C, Kleschyov AL. Molecular mechanisms underlying the role of nitric oxide in the cardiovascular system. *Expert Opinion on Investigational Drugs* 1998; **7**: 1769–1779.

181 Kakuyama M, Vallance P, Ahluwalia A. Endothelium-dependent sensory NANC vasodilatation: involvement of ATP, CGRP and a possible NO store. *British Journal of Pharmacology* 1998; **123**: 310–316.

182 Terluk MR, da Silva-Santos JE, Assreuy J. Involvement of soluble guanylate cyclase and calcium-activated potassium channels in the long-lasting hyporesponsiveness to phenylephrine induced by nitric oxide in rat aorta. *Naunyn-Schmied Arch Pharmacol* 2000; **361**: 477–483.

183 Myers PR, Minor RL, Guerra R, Bates JN, Harrison DG. Vasorelaxant properties of the endothelium-derived relaxing factor more closely resemble S-nitrosocysteine than nitric oxide. *Nature* 1990; **345**: 161–163.

184 Mayer B, Pfeiffer S, Schrammel A, Koesling D, Schmidt K, Brunner F. A new pathway of nitric oxide/cyclic GMP signaling involving S-nitrosoglutathione. *J Biol Chem* 1998; **273**: 3264–3270.

185 Mülsch A, Vanin A, Mordvintcev P, Hauschildt S, Busse R. NO accounts completely for the oxygenated nitrogen species generated by enzymic L-arginine oxygenation. *Biochem J* 1992; **288**: 597–603.

186 Hogg N, Singh RJ, Konorev E, Joseph J, Kalyanaraman B. S-Nitrosoglutathione as a substrate for gamma-glutamyl transpeptidase. *Biochem J* 1997; **323 (Pt 2)**: 477–481.

187 Stamler JS, Jaraki O, Osborne J, Simon DI, Keaney J, Vita J *et al.* Nitric oxide circulates in mammalian plasma primarily as an S-nitroso adduct of serum albumin. *Proc Natl Acad Sci USA* 1992; **89**: 7674–7677.

188 Ewing JF, Young DV, Janero DR, Garvey DS, Grinnell TA. Nitrosylated bovine serum albumin derivatives as pharmacologically active nitric oxide congeners. *J Pharmacol Exp Ther* 1997; **283**: 947–954.

189 Jia L, Bonaventura C, Bonaventura J, Stamler JS. S-nitrosohaemoglobin: a dynamic activity of blood involved in vascular control. *Nature* 1996; **380**: 221–226.

190 Gow AJ, Stamler JS. Reactions between nitric oxide and haemoglobin under physiological conditions. *Nature* 1998; **391**: 169–173.

191 Lewandowska H, Kalinowska M, Brzóska K, Wójciuk K, Wójciuk G, Kruszewski M. Nitrosyl iron complexes—synthesis, structure and biology. *Dalton Trans* 2011; **40**: 8273–8289.

192 Vithayathil AJ, Ternberg JL, Commoner B. Changes in Electron Spin Resonance Signals of Rat Liver During Chemical Carcinogenesis. *Nature* 1965; **207**: 1246.

193 Galagan ME, Oranovskaia EV, Mordvintsev PI, Medvedev OS, Vanin AF. [Hypotensive effect of dinitrosyl iron complexes in experiments on waking animals]. *Biull Vsesoiuznogo Kardiol Nauchn Tsentra AMN SSSR* 1988; **11**: 75–80.

194 Vanin AF, Kubrina LN, Kiladze SV, Burbaev DS. [Factors influencing formation of dinitrosyl complexes of non-heme iron in vitro preparations of mouse liver and yeasts]. *Biofizika* 1977; **22**: 646–650.

195 Vanin AF. Endothelium-derived relaxing factor is a nitrosyl iron complex with thiol ligands. *FEBS Letters* 1991; **289**: 1–3.

196 Vanin AF, Malenkova IV, Serezhenkov VA. Iron Catalyzes both Decomposition and Synthesis ofS-Nitrosothiols: Optical and Electron Paramagnetic Resonance Studies. *Nitric Oxide* 1997; **1**: 191–203.

197 Manukhina EB, Smirin BV, Malyshev IY, Stoclet JC, Muller B, Solodkov AP *et al.* Nitric oxide storage in the cardiovascular system. *Biol Bull* 2002; **29**: 477–486.

198 Haendeler J, Hoffmann J, Tischler V, Berk BC, Zeiher AM, Dimmeler S. Redox regulatory and anti-apoptotic functions of thioredoxin depend on S-nitrosylation at cysteine 69. *Nat Cell Biol* 2002; **4**: 743–749.

199 Nikitovic D, Holmgren A. S-nitrosoglutathione is cleaved by the thioredoxin system with liberation of glutathione and redox regulating nitric oxide. *J Biol Chem* 1996; **271**: 19180–19185.

200 Zai A, Rudd MA, Scribner AW, Loscalzo J. Cell-surface protein disulfide isomerase catalyzes transnitrosation and regulates intracellular transfer of nitric oxide. *J Clin Invest* 1999; **103**: 393–399.

201 Sliskovic I, Raturi A, Mutus B. Characterization of the S-denitrosation activity of protein disulfide isomerase. *J Biol Chem* 2005; **280**: 8733–8741.

202 Dimmeler S, Haendeler J, Nehls M, Zeiher AM. Suppression of apoptosis by nitric oxide via inhibition of interleukin-1beta-converting enzyme (ICE)-like and cysteine protease protein (CPP)-32-like proteases. *J Exp Med* 1997; **185**: 601–607.

203 Hadi HA, Carr CS, Al Suwaidi J. Endothelial Dysfunction: Cardiovascular Risk Factors, Therapy, and Outcome. *Vasc Health Risk Manag* 2005; **1**: 183–198.

204 Endemann DH, Schiffrin EL. Endothelial dysfunction. *J Am Soc Nephrol* 2004; **15**: 1983–1992.

205 Fonseca V, Desouza C, Asnani S, Jialal I. Nontraditional Risk Factors for Cardiovascular Disease in Diabetes. *Endocr Rev* 2004; **25**: 153–175.

206 Rajendran P, Rengarajan T, Thangavel J, Nishigaki Y, Sakthisekaran D, Sethi G *et al.* The Vascular Endothelium and Human Diseases. *Int J Biol Sci* 2013; **9**: 1057–1069.

207 Celermajer DS, Sorensen KE, Gooch VM, Spiegelhalter DJ, Miller OI, Sullivan ID *et al.* Non-invasive detection of endothelial dysfunction in children and adults at risk of atherosclerosis. *Lancet* 1992; **340**: 1111–1115.

208 Steinberg HO, Chaker H, Leaming R, Johnson A, Brechtel G, Baron AD. Obesity/insulin resistance is associated with endothelial dysfunction. Implications for the syndrome of insulin resistance. *J Clin Invest* 1996; **97**: 2601–2610.

209 Thögersen Anna M., Jansson Jan-Håkan, Boman Kurt, Nilsson Torbjörn K., Weinehall Lars, Huhtasaari Fritz *et al.* High Plasminogen Activator Inhibitor and Tissue Plasminogen Activator Levels in Plasma Precede a First Acute Myocardial Infarction in Both Men and Women. *Circulation* 1998; **98**: 2241–2247.

210 Cushman M, Lemaitre RN, Kuller LH, Psaty BM, Macy EM, Sharrett AR *et al.* Fibrinolytic activation markers predict myocardial infarction in the elderly. The Cardiovascular Health Study. *Arterioscler Thromb Vasc Biol* 1999; **19**: 493–498.

211 Fichtlscherer S, Rosenberger G, Walter DH, Breuer S, Dimmeler S, Zeiher AM. Elevated C-reactive protein levels and impaired endothelial vasoreactivity in patients with coronary artery disease. *Circulation* 2000; **102**: 1000–1006.

212 Prasad A, Zhu J, Halcox JPJ, Waclawiw MA, Epstein SE, Quyyumi AA. Predisposition to atherosclerosis by infections: role of endothelial dysfunction. *Circulation* 2002; **106**: 184–190.

213 Singh I, Rana V. Iron oxide induced enhancement of mucoadhesive potential of Eudragit RLPO: formulation, evaluation and optimization of mucoadhesive drug delivery system. *Expert Opinion on Drug Delivery* 2013; **10**: 1179–1191.

214 Pandey SL, Jirwankar P, Mehta SP, Pandit SP, Tripathi PK, Patil A. Formulation and evaluation of bilayered gastroretentable mucoadhesive patch for stomach-specific drug delivery. *Current drug delivery* 2013; **10**: 374–383.

215 Ding S, Serra CA, Vandamme TF, Yu W, Anton N. Double emulsions prepared by two–step emulsification: History, state-of-the-art and perspective. *Journal of Controlled Release* 2019; **295**: 31–49.

216 Giri TK, Choudhary C, Ajazuddin, Alexander A, Badwaik H, Tripathi DK. Prospects of pharmaceuticals and biopharmaceuticals loaded microparticles prepared by double

emulsion technique for controlled delivery. *Saudi Pharmaceutical Journal* 2013; **21**: 125–141.

217 Crotts G, Park TG. Protein delivery from poly(lactic-co-glycolic acid) biodegradable microspheres: Release kinetics and stability issues. *Journal of Microencapsulation* 1998; **15**: 699–713.

218 van de Weert M, Hoechstetter J, Hennink WE, Crommelin DJ. The effect of a water/organic solvent interface on the structural stability of lysozyme. *J Control Release* 2000; **68**: 351–359.

219 Lautner G, Meyerhoff ME, Schwendeman SP. Biodegradable poly(lactic-co-glycolic acid) microspheres loaded with S-nitroso-N-acetyl-D-penicillamine for controlled nitric oxide delivery. *J Control Release* 2016; **225**: 133–139.

220 Kwan KC. Oral Bioavailability and First-Pass Effects. *Drug Metab Dispos* 1997; **25**: 1329–1336.

221 Renukuntla J, Vadlapudi AD, Patel A, Boddu SHS, Mitra AK. Approaches for enhancing oral bioavailability of peptides and proteins. *Int J Pharm* 2013; **447**: 75–93.

222 Doel JJ, Benjamin N, Hector MP, Rogers M, Allaker RP. Evaluation of bacterial nitrate reduction in the human oral cavity. *Eur J Oral Sci* 2005; **113**: 14–19.

223 Lundberg JO, Weitzberg E, Cole JA, Benjamin N. Nitrate, bacteria and human health. *Nat Rev Microbiol* 2004; **2**: 593–602.

224 Boehme A. Über Nitritvergiftung nach interner Darreichung von Bismuthum subnitricum. *Archiv für experimentelle Pathologie und Pharmakologie* 2005; **57**: 441–454.

225 Shiva S, Huang Z, Grubina R, Sun J, Ringwood LA, MacArthur PH *et al.* Deoxymyoglobin is a nitrite reductase that generates nitric oxide and regulates mitochondrial respiration. *Circ Res* 2007; **100**: 654–661.

226 Huang Z, Shiva S, Kim-Shapiro DB, Patel RP, Ringwood LA, Irby CE *et al.* Enzymatic function of hemoglobin as a nitrite reductase that produces NO under allosteric control. *J Clin Invest* 2005; **115**: 2099–2107.

227 Cosby K, Partovi KS, Crawford JH, Patel RP, Reiter CD, Martyr S *et al.* Nitrite reduction to nitric oxide by deoxyhemoglobin vasodilates the human circulation. *Nat Med* 2003; **9**: 1498–1505.

228 Alzawahra WF, Talukder MAH, Liu X, Samouilov A, Zweier JL. Heme proteins mediate the conversion of nitrite to nitric oxide in the vascular wall. *Am J Physiol Heart Circ Physiol* 2008; **295**: H499-508.

229 Webb AJ, Milsom AB, Rathod KS, Chu WL, Qureshi S, Lovell MJ *et al.* Mechanisms underlying erythrocyte and endothelial nitrite reduction to nitric oxide in hypoxia: role for xanthine oxidoreductase and endothelial nitric oxide synthase. *Circ Res* 2008; **103**: 957–964.

230 Gautier C, van Faassen E, Mikula I, Martasek P, Slama-Schwok A. Endothelial nitric oxide synthase reduces nitrite anions to NO under anoxia. *Biochem Biophys Res Commun* 2006; **341**: 816–821.

231 Zhang Z, Naughton DP, Blake DR, Benjamin N, Stevens CR, Winyard PG *et al.* Human xanthine oxidase converts nitrite ions into nitric oxide (NO). *Biochem Soc Trans* 1997; **25**: 524S.

232 Baker JE, Su J, Fu X, Hsu A, Gross GJ, Tweddell JS *et al.* Nitrite confers protection against myocardial infarction: role of xanthine oxidoreductase, NADPH oxidase and K(ATP) channels. *J Mol Cell Cardiol* 2007; **43**: 437–444.

233 Lu P, Liu F, Yao Z, Wang C-Y, Chen D-D, Tian Y *et al.* Nitrite-derived nitric oxide by xanthine oxidoreductase protects the liver against ischemia-reperfusion injury. *HBPD INT* 2005; **4**: 350–355.

234 Webb A, Bond R, McLean P, Uppal R, Benjamin N, Ahluwalia A. Reduction of nitrite to nitric oxide during ischemia protects against myocardial ischemia-reperfusion damage. *Proc Natl Acad Sci USA* 2004; **101**: 13683–13688.

235 Golwala NH, Hodenette C, Murthy SN, Nossaman BD, Kadowitz PJ. Vascular responses to nitrite are mediated by xanthine oxidoreductase and mitochondrial aldehyde dehydrogenase in the rat. *Can J Physiol Pharmacol* 2009; **87**: 1095–1101.

236 Maher AR, Milsom AB, Gunaruwan P, Abozguia K, Ahmed I, Weaver RA *et al.* Hypoxic modulation of exogenous nitrite-induced vasodilation in humans. *Circulation* 2008; **117**: 670–677.

237 Duncan C, Dougall H, Johnston P, Green S, Brogan R, Leifert C *et al.* Chemical generation of nitric oxide in the mouth from the enterosalivary circulation of dietary nitrate. *Nat Med* 1995; **1**: 546–551.

238 McKnight GM, Smith LM, Drummond RS, Duncan CW, Golden M, Benjamin N. Chemical synthesis of nitric oxide in the stomach from dietary nitrate in humans. *Gut* 1997; **40**: 211–214.

239 Lundberg JO, Weitzberg E, Lundberg JM, Alving K. Intragastric nitric oxide production in humans: measurements in expelled air. *Gut* 1994; **35**: 1543–1546.

240 Benjamin N, O'Driscoll F, Dougall H, Duncan C, Smith L, Golden M *et al.* Stomach NO synthesis. *Nature* 1994; **368**: 502.

241 Opländer C, Volkmar CM, Paunel-Görgülü A, van Faassen EE, Heiss C, Kelm M *et al.* Whole body UVA irradiation lowers systemic blood pressure by release of nitric oxide from intracutaneous photolabile nitric oxide derivates. *Circ Res* 2009; **105**: 1031–1040.

242 Zweier JL, Li H, Samouilov A, Liu X. Mechanisms of nitrite reduction to nitric oxide in the heart and vessel wall. *Nitric Oxide* 2010; **22**: 83–90.

243 Artursson P, Karlsson J. Correlation between oral drug absorption in humans and apparent drug permeability coefficients in human intestinal epithelial (Caco-2) cells. *Biochem Biophys Res Commun* 1991; **175**: 880–885.

244 Yamashita S, Furubayashi T, Kataoka M, Sakane T, Sezaki H, Tokuda H. Optimized conditions for prediction of intestinal drug permeability using Caco-2 cells. *Eur J Pharm Sci* 2000; **10**: 195–204.

245 Fetih G, Habib F, Katsumi H, Okada N, Fujita T, Attia M *et al.* Excellent Absorption Enhancing Characteristics of NO Donors for Improving the Intestinal Absorption of Poorly Absorbable Compound Compared with Conventional Absorption Enhancers. *Drug Metabolism and Pharmacokinetics* 2006; **21**: 222–229.

246 Numata N, Takahashi K, Mizuno N, Utoguchi N, Watanabe Y, Matsumoto M *et al.* Improvement of intestinal absorption of macromolecules by nitric oxide donor. *J Pharm Sci* 2000; **89**: 1296–1304.

247 Yamamoto A, Tatsumi H, Maruyama M, Uchiyama T, Okada N, Fujita T. Modulation of Intestinal Permeability by Nitric Oxide Donors: Implications in Intestinal Delivery of Poorly Absorbable Drugs. *J Pharmacol Exp Ther* 2001; **296**: 84–90.

248 Salzman AL, Menconi MJ, Unno N, Ezzell RM, Casey DM, Gonzalez PK *et al.* Nitric oxide dilates tight junctions and depletes ATP in cultured Caco-2BBe intestinal epithelial monolayers. *Am J Physiol* 1995; **268**: G361-373.

249 Le Ferrec E, Chesne C, Artusson P, Brayden D, Fabre G, Gires P *et al.* In vitro models of the intestinal barrier. The report and recommendations of ECVAM Workshop 46. European Centre for the Validation of Alternative methods. *Altern Lab Anim* 2001; **29**: 649–668.

250 Alencar JL, Lobysheva I, Geffard M, Sarr M, Schott C, Schini-Kerth VB *et al.* Role of S-nitrosation of cysteine residues in long-lasting inhibitory effect of nitric oxide on arterial tone. *Mol Pharmacol* 2003; **63**: 1148–1158.

251 Hayashi K, Jutabha P, Kamai T, Endou H, Anzai N. LAT1 is a central transporter of essential amino acids in human umbilical vein endothelial cells. *J Pharmacol Sci* 2014; **124**: 511–513.

252 Riego JA, Broniowska KA, Kettenhofen NJ, Hogg N. Activation and inhibition of soluble guanylyl cyclase by S-nitrosocysteine: involvement of amino acid transport system L. *Free Radic Biol Med* 2009; **47**: 269–274.

253 Belcastro E, Wu W, Fries-Raeth I, Corti A, Pompella A, Leroy P *et al.* Oxidative stress enhances and modulates protein S-nitrosation in smooth muscle cells exposed to S-nitrosoglutathione. *Nitric Oxide* 2017; **69**: 10–21.

254 Dahboul F, Leroy P, Maguin Gate K, Boudier A, Gaucher C, Liminana P *et al.* Endothelial γ-glutamyltransferase contributes to the vasorelaxant effect of S-nitrosoglutathione in rat aorta. *PLoS ONE* 2012; **7**: e43190.

255 Dahboul F, Perrin-Sarrado C, Boudier A, Lartaud I, Schneider R, Leroy P. S,S'-dinitrosobucillamine, a new nitric oxide donor, induces a better vasorelaxation than other S-nitrosothiols. *Eur J Pharmacol* 2014; **730**: 171–179.

256 Pastor CM, Billiar TR. Nitric oxide causes hyporeactivity to phenylephrine in isolated perfused livers from endotoxin-treated rats. *Am J Physiol* 1995; **268**: G177-182.

257 Alencar JL, Chalupsky K, Sarr M, Schini-Kerth V, Vanin AF, Stoclet J-C *et al.* Inhibition of arterial contraction by dinitrosyl-iron complexes: critical role of the thiol ligand in determining rate of nitric oxide (NO) release and formation of releasable NO stores by S-nitrosation. *Biochem Pharmacol* 2003; **66**: 2365–2374.

258 Alencar JL, Lobysheva I, Chalupsky K, Geffard M, Nepveu F, Stoclet J-C *et al.* S-nitrosating nitric oxide donors induce long-lasting inhibition of contraction in isolated arteries. *J Pharmacol Exp Ther* 2003; **307**: 152–159.

259 Nozik-Grayck E, Whalen EJ, Stamler JS, McMahon TJ, Chitano P, Piantadosi CA. S-nitrosoglutathione inhibits alpha1-adrenergic receptor-mediated vasoconstriction and ligand binding in pulmonary artery. *Am J Physiol Lung Cell Mol Physiol* 2006; **290**: L136-143.

260 Tate SS, Meister A. Serine-borate complex as a transition-state inhibitor of gamma-glutamyl transpeptidase. *Proc Natl Acad Sci USA* 1978; **75**: 4806–4809.

261 McLaggan D, Rufino H, Jaspars M, Booth IR. Glutathione-Dependent Conversion of N-Ethylmaleimide to the Maleamic Acid by Escherichia coli: an Intracellular Detoxification Process. *Appl Environ Microbiol* 2000; **66**: 1393–1399.

262 Castellanos IJ, Carrasquillo KG, López JDJ, Alvarez M, Griebenow K. Encapsulation of bovine serum albumin in poly(lactide-co-glycolide) microspheres by the solid-in-oil-in-water technique. *Journal of Pharmacy and Pharmacology* 2001; **53**: 167–178.

263 Emami F, Vatanara A, Park EJ, Na DH. Drying Technologies for the Stability and Bioavailability of Biopharmaceuticals. *Pharmaceutics* 2018; **10**. doi:10.3390/pharmaceutics10030131.

264 Levit SL, Stwodah RM, Tang C. Rapid, Room Temperature Nanoparticle Drying and Low-Energy Reconstitution via Electrospinning. *J Pharm Sci* 2018; **107**: 807–813.

265 Iskandar F, Gradon L, Okuyama K. Control of the morphology of nanostructured particles prepared by the spray drying of a nanoparticle sol. *Journal of Colloid and Interface Science* 2003; **265**: 296–303.

266 Schairer DO, Chouake JS, Nosanchuk JD, Friedman AJ. The potential of nitric oxide releasing therapies as antimicrobial agents. *Virulence* 2012; **3**: 271–279.

267 Marcinkiewicz J. Nitric oxide and antimicrobial activity of reactive oxygen intermediates. *Immunopharmacology* 1997; **37**: 35–41.

268 Laver JR, Stevanin TM, Messenger SL, Lunn AD, Lee ME, Moir JWB *et al.* Bacterial nitric oxide detoxification prevents host cell S-nitrosothiol formation: a novel mechanism of bacterial pathogenesis. *FASEB J* 2010; **24**: 286–295.

269 Rodrigo A. Souza-Lima S, Cariello AJ, Marcelo Bispo S, Gabriela De Souza S, Oliveira MD, Hofling-Lima AL *et al.* Bactericidal Effect Of Nitric Oxide Donors Against Clinical Isolates From Keratitis. *Invest Ophthalmol Vis Sci* 2011; **52**: 5839–5839.

270 Richie JP, Skowronski L, Abraham P, Leutzinger Y. Blood glutathione concentrations in a large-scale human study. *Clin Chem* 1996; **42**: 64–70.

271 Benet LZ, Hosey CM, Ursu O, Oprea TI. BDDCS, the Rule of 5 and Drugability. *Adv Drug Deliv Rev* 2016; **101**: 89–98.

272 Bhal S. LogP—Making Sense of the Value. ; : 4.

273 de Souza GFP, S. Ferreira E da, Baldim V, de Oliveira MG. Metabolic fate of S-nitrosoglutathione after oral administration: Where does NO go? *Nitric Oxide* 2012; **27**: S35.

274 Yu H, Bonetti J, Gaucher C, Fries I, Vernex-Loset L, Leroy P *et al.* Higher-energy collision-induced dissociation for the quantification by liquid chromatography/tandem ion trap mass spectrometry of nitric oxide metabolites coming from S-nitroso-glutathione in an in vitro model of the intestinal barrier. *Rapid Communications in Mass Spectrometry* 2019; **33**: 1–11.

275 Haiyan Y, Romain S, Anne S, Patrick C, Pierre L. Comparison between two derivatization methods of nitrite ion labeled with 15N applied to liquid chromatography-tandem mass spectrometry. *Anal Methods* 2018; **10**: 3830–3836.

276 Björne H, Petersson J, Phillipson M, Weitzberg E, Holm L, Lundberg JO. Nitrite in saliva increases gastric mucosal blood flow and mucus thickness. *J Clin Invest* 2004; **113**: 106–114.

277 Zhou X, He P. Improved measurements of intracellular nitric oxide in intact microvessels using 4,5-diaminofluorescein diacetate. *Am J Physiol Heart Circ Physiol* 2011; **301**: H108-114.

278 Liu R, Fu Q, Lonergan S, Huff-Lonergan E, Xing L, Zhang L *et al.* Identification of S-nitrosylated proteins in postmortem pork muscle using modified biotin switch method coupled with isobaric tags. *Meat Sci* 2018; **145**: 431–439.

279 Nacharaju P, Tuckman-Vernon C, Maier KE, Chouake J, Friedman A, Cabrales P *et al.* A nanoparticle delivery vehicle for S-nitroso-N-acetyl cysteine: sustained vascular response. *Nitric Oxide* 2012; **27**: 150–160.

280 Souza GFP de, Oliveira MG de. Intratablet S-nitrosation: A New Approach for the Oral Administration of S-nitrosothiols as Nitric Oxide Donors. *JPharmSci* 2016; **105**: 359–361.

281 Fonte P, Lino PR, Seabra V, Almeida AJ, Reis S, Sarmento B. Annealing as a tool for the optimization of lyophilization and ensuring of the stability of protein-loaded PLGA nanoparticles. *International Journal of Pharmaceutics* 2016; **503**: 163–173.

282 Fonte P, Reis S, Sarmento B. Facts and evidences on the lyophilization of polymeric nanoparticles for drug delivery. *Journal of Controlled Release* 2016; **225**: 75–86.

283 Niu L, Panyam J. Freeze concentration-induced PLGA and polystyrene nanoparticle aggregation: Imaging and rational design of lyoprotection. *Journal of Controlled Release* 2017; **248**: 125–132.

284 Thakral S, Thakral NK, Majumdar DK. Eudragit®: a technology evaluation. *Expert Opinion on Drug Delivery* 2013; **10**: 131–149.

285 Patra ChN, Priya R, Swain S, Kumar Jena G, Panigrahi KC, Ghose D. Pharmaceutical significance of Eudragit: A review. *Future Journal of Pharmaceutical Sciences* 2017; **3**: 33–45.

Appendix A, supplementary data in article 1

Synthesis of Novel Mono and Bis Nitric Oxide Donors with High Cytocompatibility and Release Activity

Tanya Sahyoun[a,c], Caroline Gaucher[b], Yi Zhou[b], Naïm Ouaini[c], Raphaël Schneider[d*], Axelle Arrault[a*]

[a] *Laboratoire de Chimie Physique Macromoléculaire, Université de Lorraine, CNRS, LCPM, F-54000 Nancy, France*

[b] *Université de Lorraine, CITHEFOR, F-54000 Nancy, France*

[c] *Faculty of Sciences, Holy Spirit University of Kaslik, BP446, Jounieh, Mount Lebanon, Lebanon*

[d] *Laboratoire Réactions et Génie des Procédés, Université de Lorraine, CNRS, LRGP, F-54000 Nancy, France*

Materials

β-Nicotinamide adenine dinucleotide 2′-phosphate reduced tetrasodium salt hydrate (NADPH, ≥97%), rat liver microsomes (20 mg/mL in saccharose), hydroxylamine hydrochloride (99%), hydroxylamine solution 50 wt. % in H_2O were purchased from Sigma-Aldrich. 4-hydroxybenzamidoxime (>98%) and 4-methoxybenzamidoxime (99%) were purchased from Alfa Aesar. Potassium cyanide (KCN, ≥97%) was purchased from Merck. Calcium carbonate (Na_2CO_3, ≥99.8%) was purchased from Carl Roth. Commercial products were used as received. Ultrapure deionized water (>18.2MΩ.cm) was used to prepare all the solutions.

The cells used were from human smooth muscular cells issued from human thoracic aorta (CRL-1999).

Characterization

All reactions were monitored by TLC silica plates. Melting points were measured on a Buchi M-560 Melting Point apparatus. FT-IR spectra were recorded by a Bruker Tensor 27 spectrometer equipped with liquid nitrogen cooled MCT-detector. FT-IR spectra were obtained at 6 cm^{-1} resolution using the Attenuated Total Reflectance (ATR) technique. NMR spectra were measured with a Bruker Avance 300 (300 MHz for ^{1}H and 75 MHz for ^{13}C) with tetramethylsilane as standard. Chemical shifts are reported in parts per million. Electron spray ionization mass spectra (ESI-MS) were recorded on a Brucker MicroTof-Q HR spectrometer, Faculté des Sciences et Techniques, Vandoeuvre-les-Nancy, France. HPLC spectra were recorded on a Shimadzu High Performance Liquid Chromatography apparatus with UV detection (245 nm). HPLC parameters: Reprospher RP-C18 (5 μM); 250×4.6 mm; gradient elution of solvent A= CH_3CN + 0.1% THF and solvent B = H_2O + 0.1% THF; eluent flow: 1 mL/min; volume of injected sample: 20 μL; UV detector at 254 nm.

The absorbance for the Griess assay was measured by using EL 800 microplate reader (Bio-TEK Instrument, INC®, France). All fluorescence for DAN assay was measured by using the FP-8300iRM fluorescence spectrophotometer (JASCO, France) coupled with FMP Micro-well plate reader.

Synthesis of nitriles 1c and 1d

To a stirred solution of the bromo derivative (15 mmol) in DMF (15 mL), was added potassium cyanide (4 eq). The mixture was heated to reflux for 72 h. After cooling to room temperature, the mixture was filtered over sintered glass and Celite and the solvent evaporated under reduced pressure. The residue was extracted with ethyl acetate (4 x 40 mL) and the organic phase washed with a 1M NaOH. The organic layer was dried over $MgSO_4$ and concentrated. The product was purified by flash chromatography using ethyl acetate/petroleum ether (8/2) as eluent.

5-Phenoxy-pentanenitrile **1c**

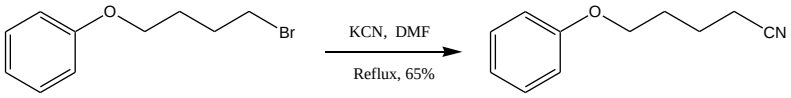

1c

Analytical Data:

Transparent oily liquid. $C_{11}H_{13}NO$. Yield: 1.71 g (65%).

^{1}H NMR (300 MHz, DMSO-d_6, 25°C): δ = 7.31-7.25 (m, 2H, H_{ar}), 6.94-6.90 (m, 3H, H_{ar}), 3.99 (t, *J* = 6.0 Hz, 2H, O-CH_2), 2.57 (t, *J* = 6.9 Hz, 2H, CN-CH_2), 1.83-1.69 (m, 4H, $(CH_2)_2$).

^{13}C NMR (75 MHz, DMSO-d_6, 25°C): δ = 158.4, 129.4, 120.6, 120.4, 114.4, 66.3, 27.7, 21.7, 15.9.

IR (neat): 3398 (br), 2924 (w), 2875 (w), 2246 (w), 1598 (m), 1495 (m), 1474 (m), 1427 (w), 1394 (w), 1294 (w), 1243 (s), 1173 (w), 1081 (w), 1058 (w).

4-(4-Cyano-butoxy)-benzonitrile **1d**

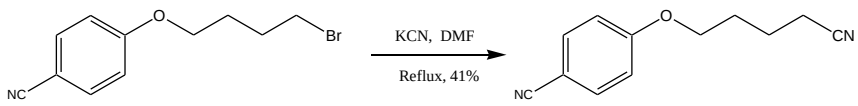

1d

Analytical Data:

Yellowish crystals. $C_{12}H_{12}N_2O$. Yield: 1.23 g (41%)

mp: 74.2°C.

^{1}H NMR (300 MHz, $CDCl_3$, 25°C): δ = 7.60-7.57 (m, 2H, H_{ar}), 6.95-6.92 (m, 2H, H_{ar}), 4.06 (t, *J* = 5.6 Hz, 2H, O-CH_2), 2.46 (t, *J* = 6.8 Hz, 2H, CN-CH_2), 2.03-1.84 (m, 4H, $(CH_2)_2$)

^{13}C NMR (75 MHz, $CDCl_3$, 25°C): δ= 162.6, 134.7, 119.9, 119.8, 115.8, 104.9, 67.8, 28.6, 23.0, 17.7.

IR (neat): 2961 (w), 2934 (w), 2225 (s), 1699 (w), 1606 (s), 1510 (s), 1646 (w), 1407 (w), 1299 (w), 1254 (s), 1176 (s), 1036 (m).

Amidoximes Synthesis Conditions

Table 1. Conditions used for the synthesis of amidoximes **2**.

Entry	Product	Conditions	Yield (%)
1	**2a**	$NH_2OH.HCl$ (3 x 2eq), Na_2CO_3 (3 x 2 eq), EtOH, reflux	98
2	**2b**	$NH_2OH.HCl$ (2 x 2eq), Na_2CO_3 (2 x 2 eq), EtOH, reflux	95
3	**2c**	$NH_2OH.HCl$ (2 x 2eq), Na_2CO_3 (2 x 2 eq), EtOH, reflux	37
4	**2c**	NH_2OH 50 wt. % in H_2O (1.5 eq), EtOH, reflux	60
5	**2d**	NH_2OH 50 wt. % in H_2O (2.5 eq), EtOH, reflux	40

Oxidation of amidoximes using rat liver microsomes

The incubation media was prepared by mixing the substrate (111 µM) with rat liver microsomes (0.25 mg of proteins) and 148 mM phosphate buffer pH 7.4 (final volume, 450 µL). This media was pre-incubated for 1 min at 37°C. NADPH (1.11 mM) was added to start the reaction and the mixture was incubated for 10 min at 37°C. The reaction was stopped by heating the mixture for 3 min at 100°C. The proteins were precipitated by centrifugation for 15 min at 10000 rpm at 4°C.

Griess assay

Briefly, 100 µL of sample were diluted with 100 µL acetoacetic solution 11% (v/v) (pH 2.5) and added with 40 µL of sulfanilamide solution in 0.4 M HCl. Finally, the diazonium salt formed was made to react with 10 µL of a 0.6% (w/v) *N*-(1-naphthyl) ethylenediamine solution in 0.4 M HCl to form a chromophoric azo product that absorbs at 540 nm. Results are expressed as means ± standard error of the mean (SEM). Statistical analyses were performed using one-way ANOVA test followed by Bonferroni's multiple comparisons test. The GraphPad Prism software (GraphPad Software version 5.0, San Diego, USA) was used for all the presented results.

Cytocompatibility assay

HVSMC cells (CRL-1999, ATCC, USA) were grown in F-12K (ATCC-30-2004) medium supplemented with 10% (v/v) fetal bovine serum, 1 % (v/v) penicilline-streptomycin cocktail (10000 units penicillin and 10 mg streptomycin per mL), 0.01 mg/mL insuline, 0.05 mg/mL acid ascorbic, 10 mM TES, 0.01 mg/mL transferrine, 10 ng/mL sodium selenite, 0.03 mg/mL ECGS et 10 mM HEPES. Cells were cultured at 37°C under 5% (v/v) CO_2 in a humidified incubator. HVSMC cells were seeded at 6.25×10^4 cells/cm^2 in 96-wells plates for 24 h before being incubated with amidoximes **2**. After 24 h at 37°C with 0.001 to 100 µM of compounds **2**, cytocompatibility regarding metabolic activity was checked using the MTT assay. Briefly, 0.5 mg/mL MTT was incubated with the cells for 3 h. Then, 50 µL DMSO was added under stirring for 5 min to extract the formazan crystals. The absorbance was read at 570 nm with a reference at 630 nm using EL 800 microplate reader (Bio-TEK Instrument, INC®, France). Metabolic activity in the presence of treatments was compared to the control condition.

NO release experiments

The reference GSNO was synthesized as previously described by Parent *et al*.[1] Briefly, reduced glutathione (GSH) was incubated with an equivalent amount of sodium nitrite under acidic conditions (0.626 M HCl). The concentration of GSNO was calculated using the specific molar absorbance of S-NO bond at 334 nm (ε = 922 M^{-1}cm^{-1}) and the Beer-Lambert law.

HVSMC cells were seeded at 6,400 cells/cm^2 in 6-wells plates 48 h before incubation with amidoximes **2**. After 1 h at 37°C with 100 µM (a concentration of 50 µM was used for **2d**) of each amidoxime, or 100 µM of GSNO, cells were washed with PBS and lysed in 50 mM of Tris, 150 mM of NaCl, 1% of Igepal CA-630 (v/v), 0.1% of SDS (v/v), 1 mM of EDTA, 0.1 mM of neocuproine, 20 mM of sodium tetraborate and 10 mM of NEM. RSNO and nitrite ions were immediately quantified using a fluorimetric method as previously described by Wu *et al*.[2] Briefly, N_2O_3 generated from acidified nitrite ions reacts with 1.05 mM 2,3-diaminonaphthlene with or without 1.05 mM of $HgCl_2$ producing naphthotriazole that emit fluorescence at 415 nm after excitation at 375 nm (JASCO FP-8300, France).[2]

Intracellular RSNO and nitrite ions were quantified after 1 h of incubation with different treatment (amidoxime or GSNO) in contact with smooth muscle cells. Control cells incubated

with PBS added with 0.1% DMSO were under the limit of detection for both RSNO and nitrite ions.

References

1. Parent, M.; Dahboul, F.; Schneider, R.; Clarot, I.; Maincent, P. *Curr. Pharm. Anal.* **2013**, *9*, 31.
2. Wu, W. ; Gaucher, C.; Diab, R.; Fries, I.; Xiao, Y.-L.; Hu, X.-M.; Maincent, P.; Sapin-Minet, A. *Eur. J. Pharm. Biopharm.* **2015**, *89*, 1.

Analytical data for nitrile compounds

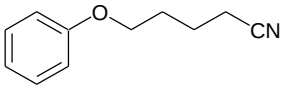

1c

[175.0997]

^{1}H and ^{13}C NMR Analysis: solvent DMSO-d_6

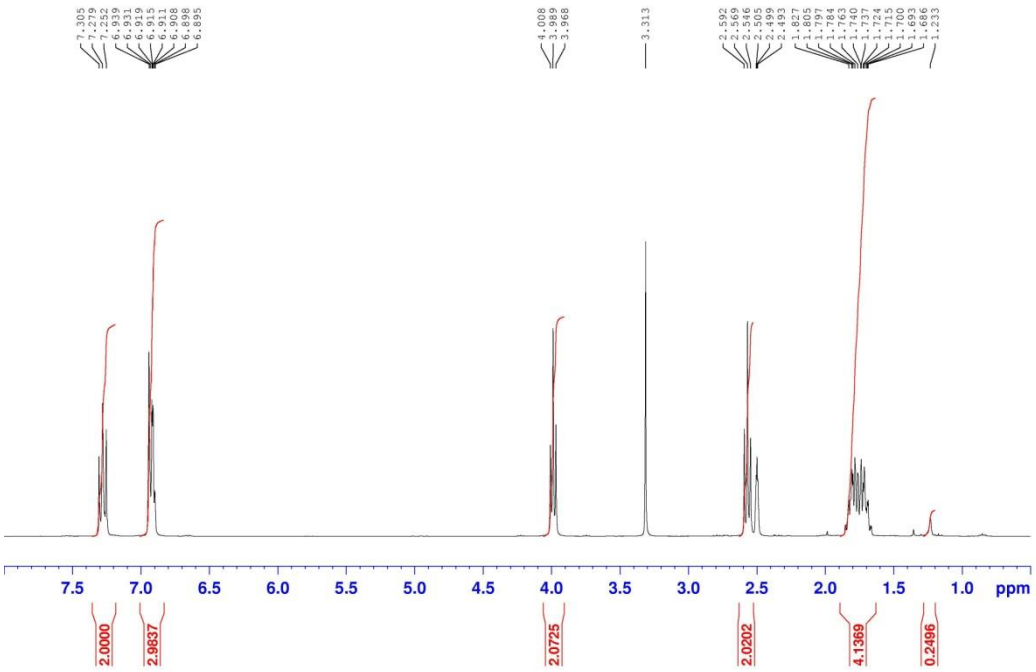

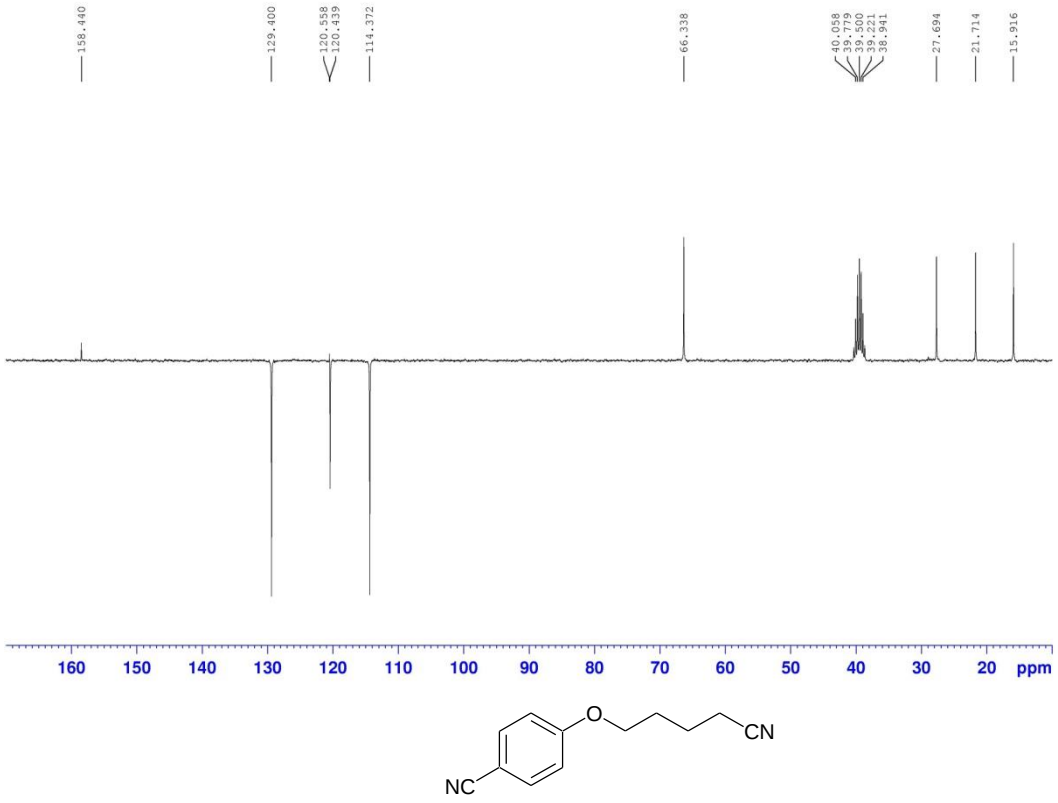

1d

[200.0950]

^{1}H and ^{13}C NMR Analysis: solvent $CDCl_3$

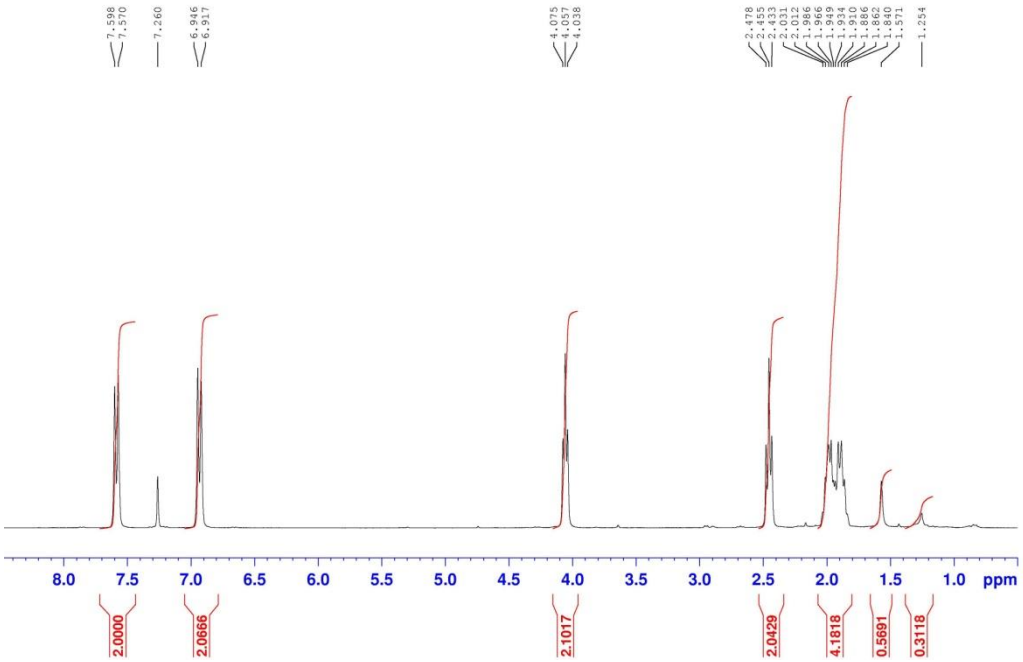

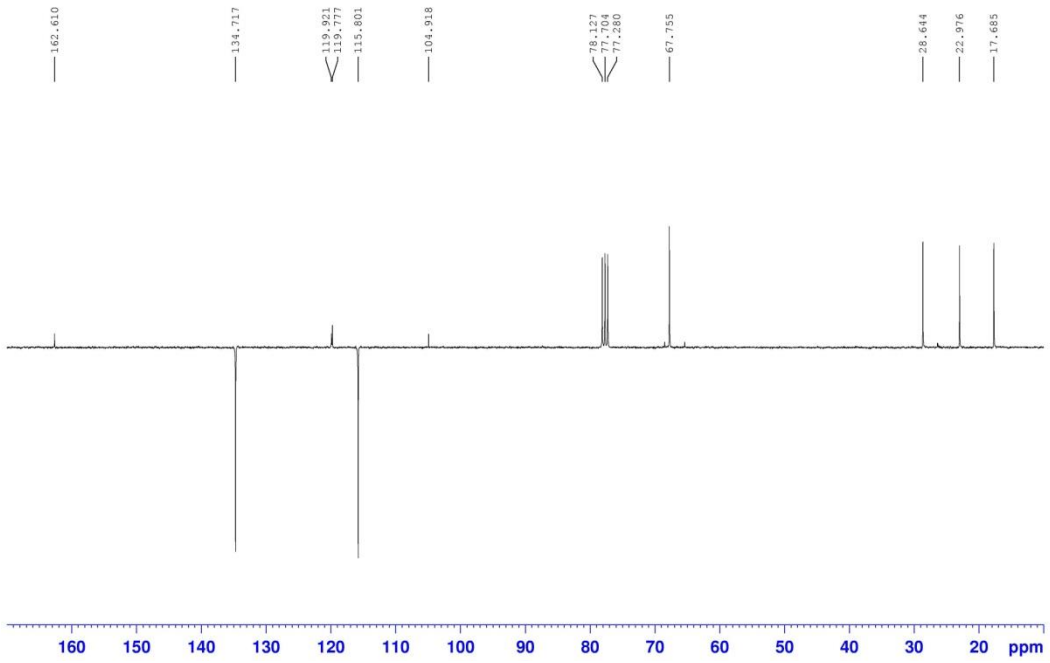

Analytical data for lead compounds

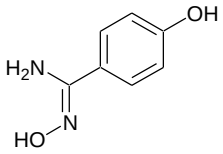

2a

[152.0586]

^{1}H and ^{13}C NMR Analysis: solvent DMSO-d_6

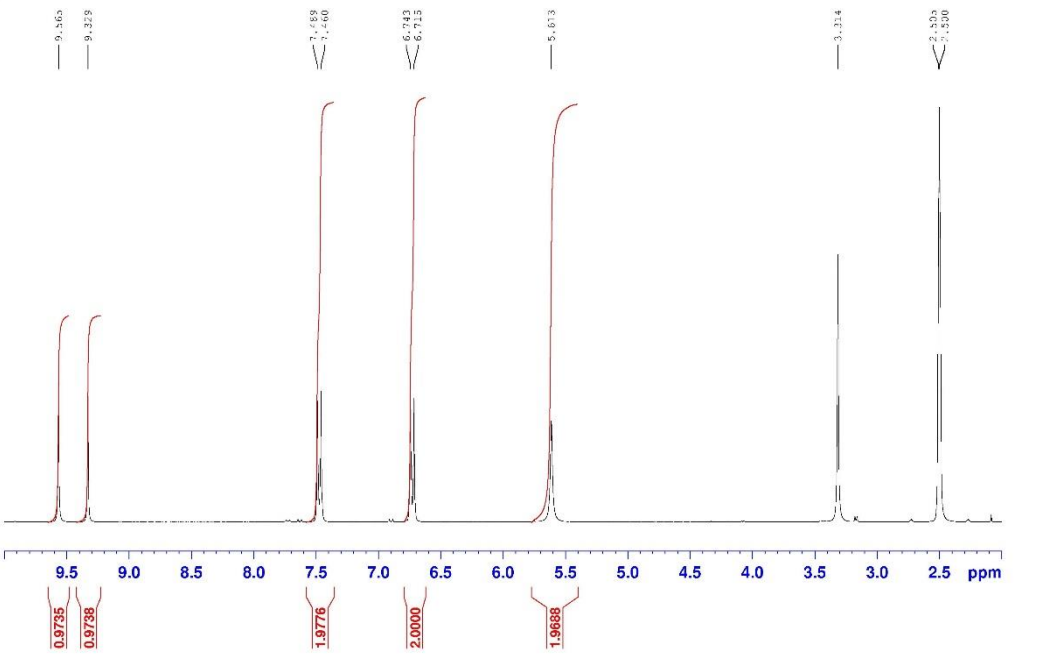

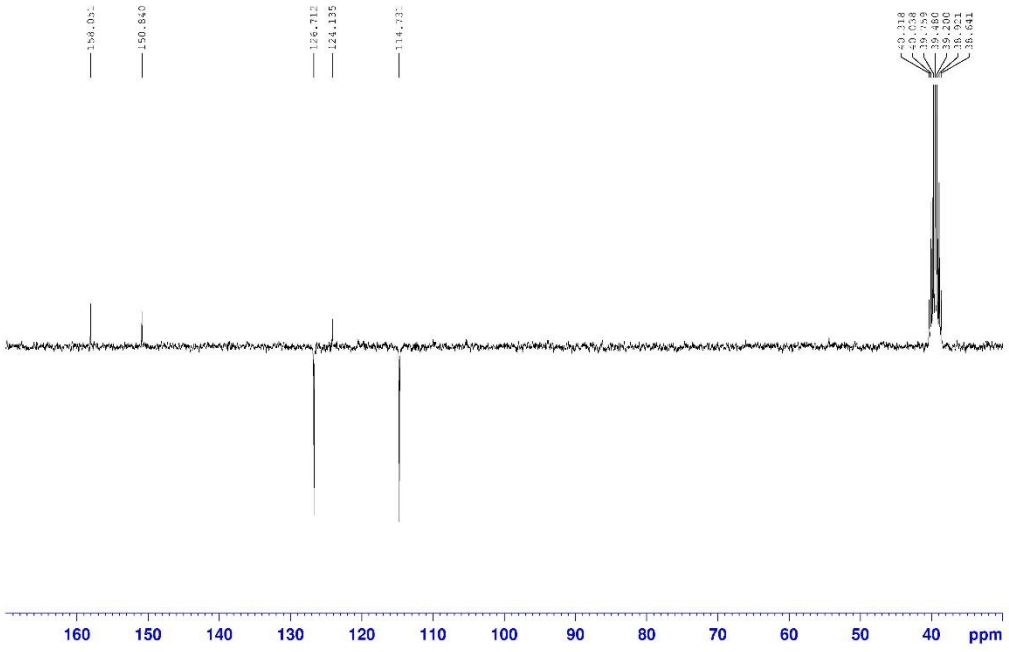

MS High Resolution

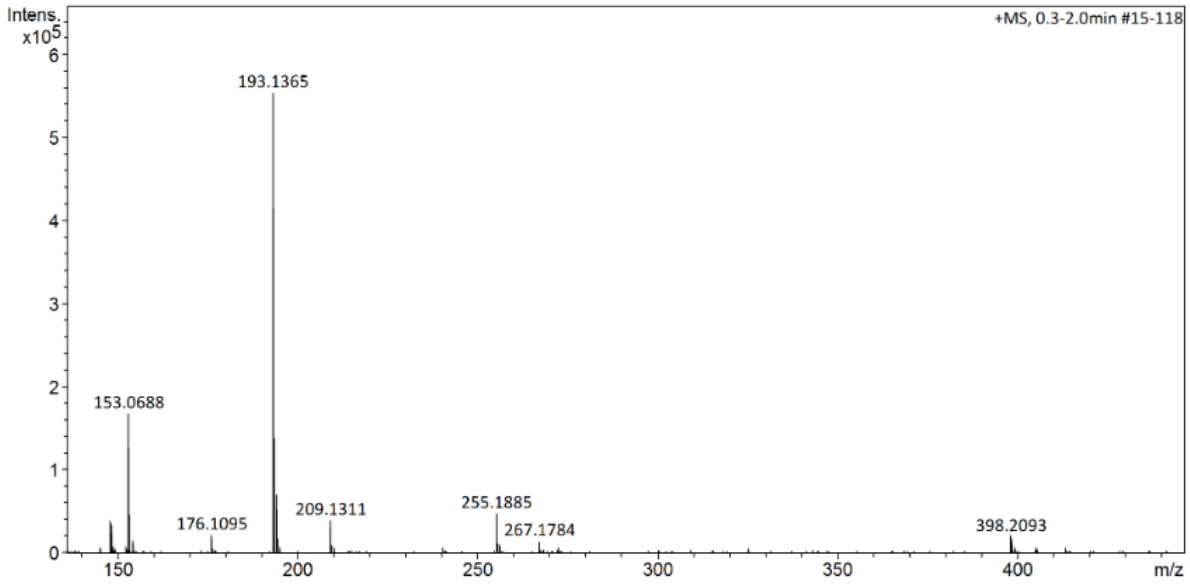

HPLC Analysis

R_t = 8.862, Area percentage = 96.791 %

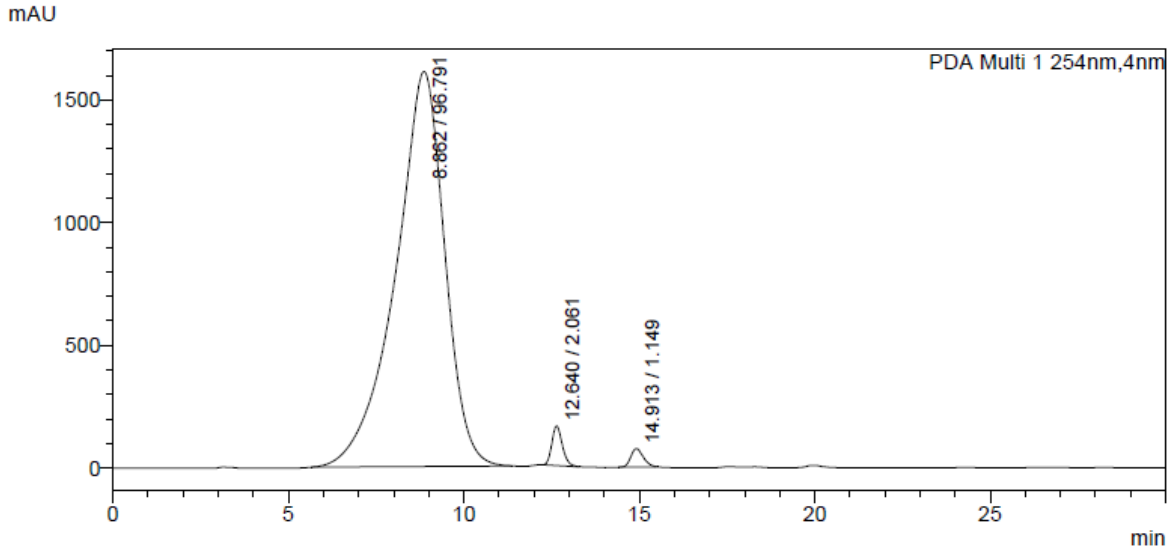

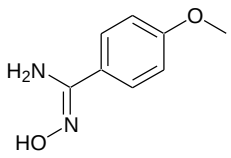

2b

[166.0742]

^{1}H and ^{13}C NMR Analysis: solvent DMSO-d_6

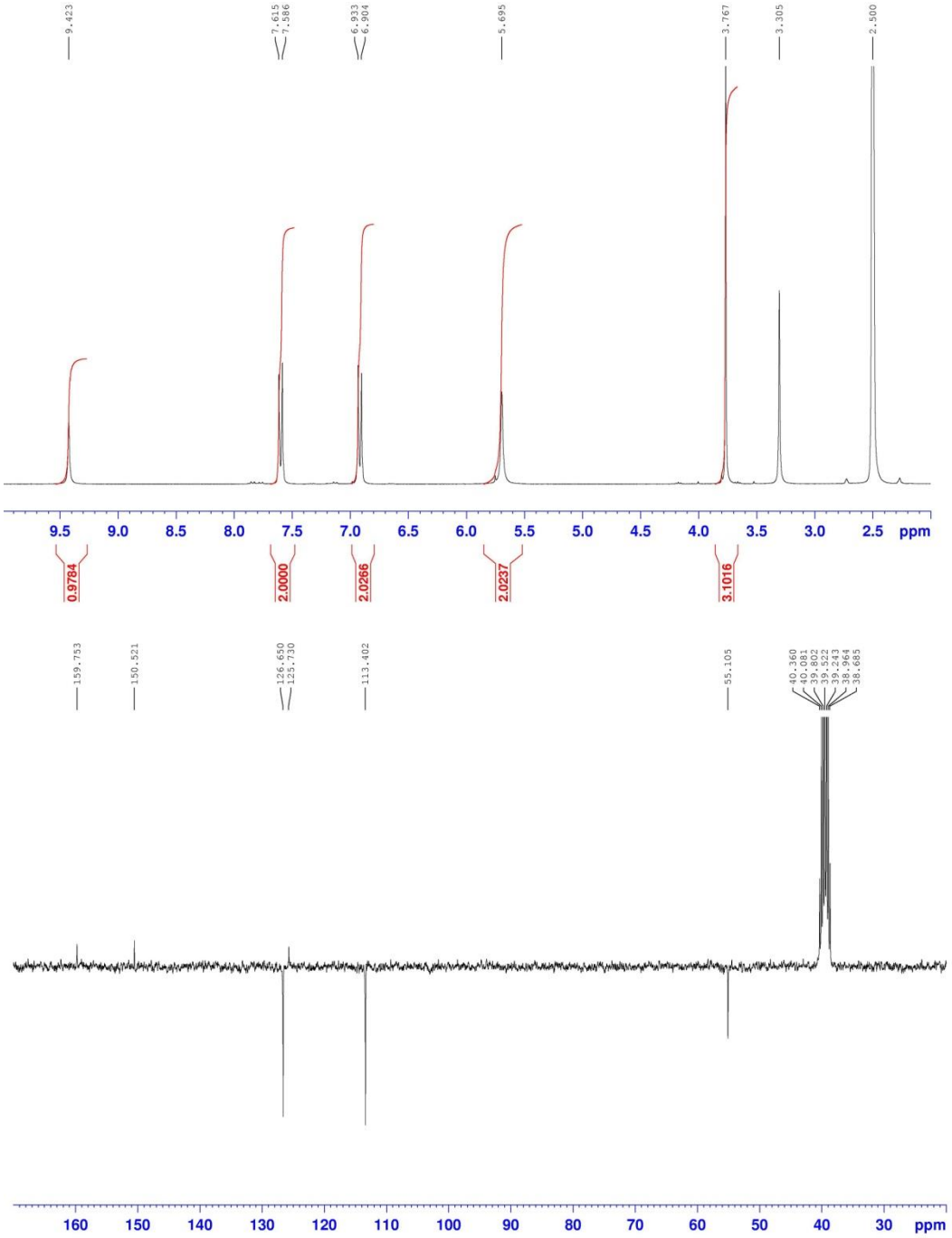

MS High Resolution

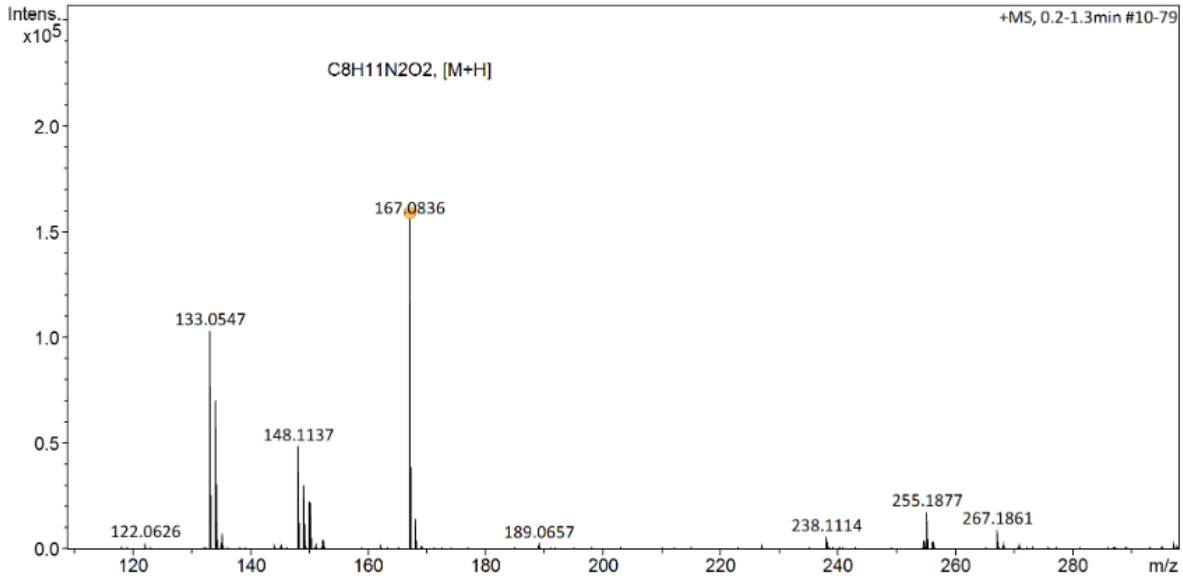

HPLC Analysis

R_t = 13.433, Area percentage = 98.886 %

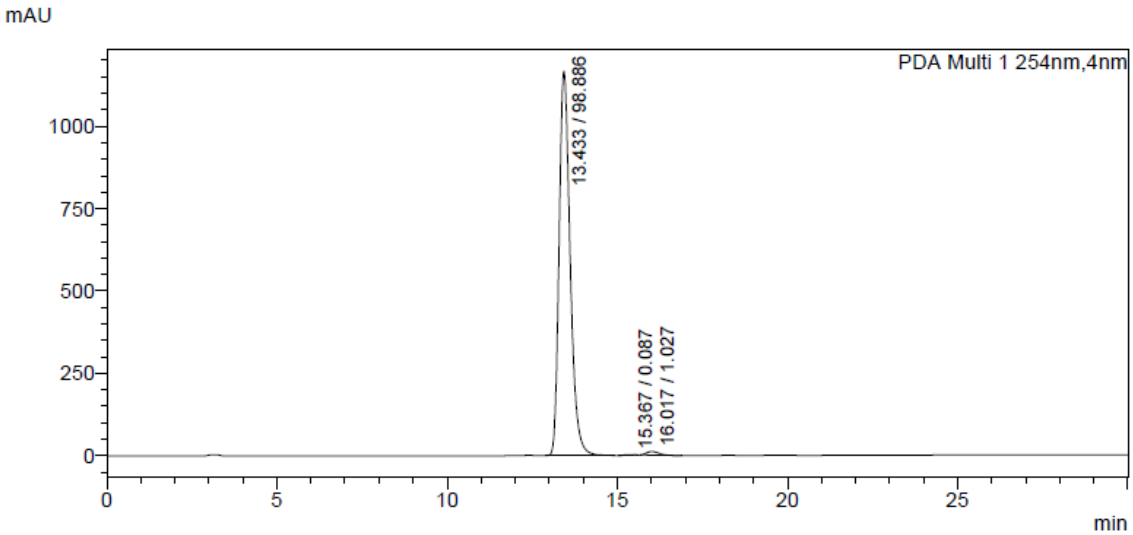

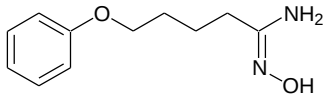

2c

[208.1212]

^{1}H and ^{13}C NMR Analysis: solvent DMSO-d_6

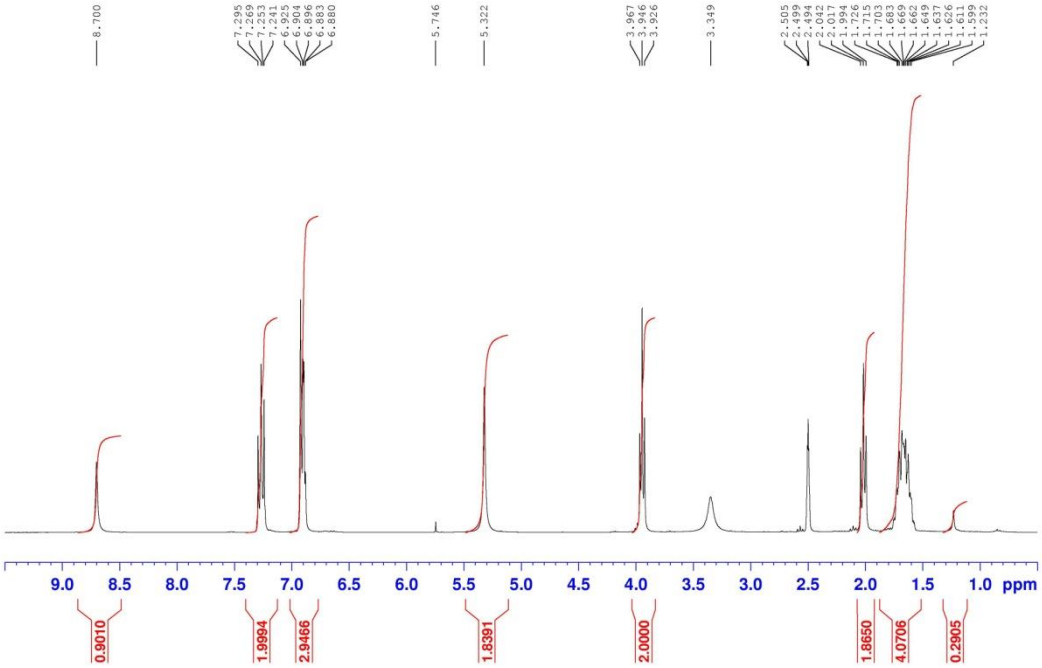

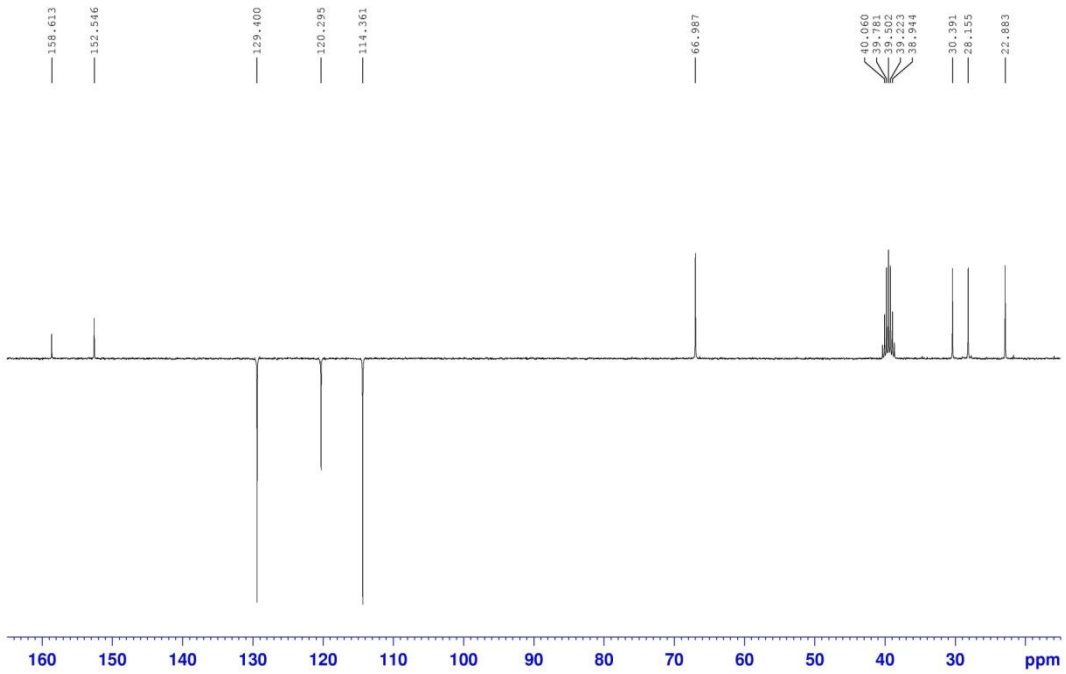

MS High Resolution

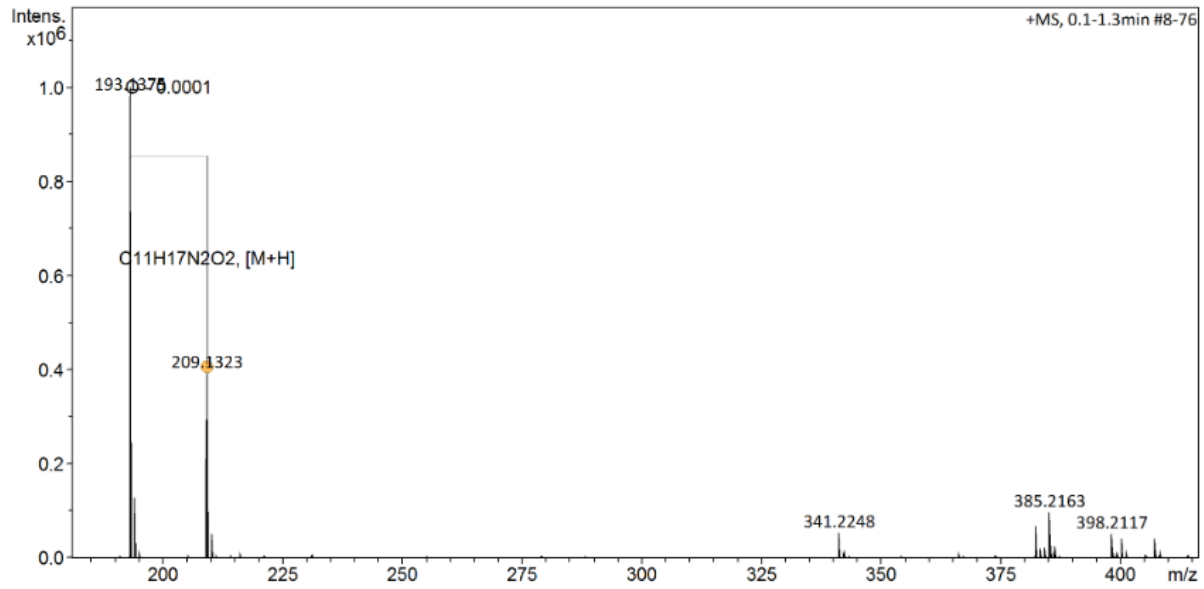

HPLC Analysis

R_t = 10.859, Area percentage = 96.731 %

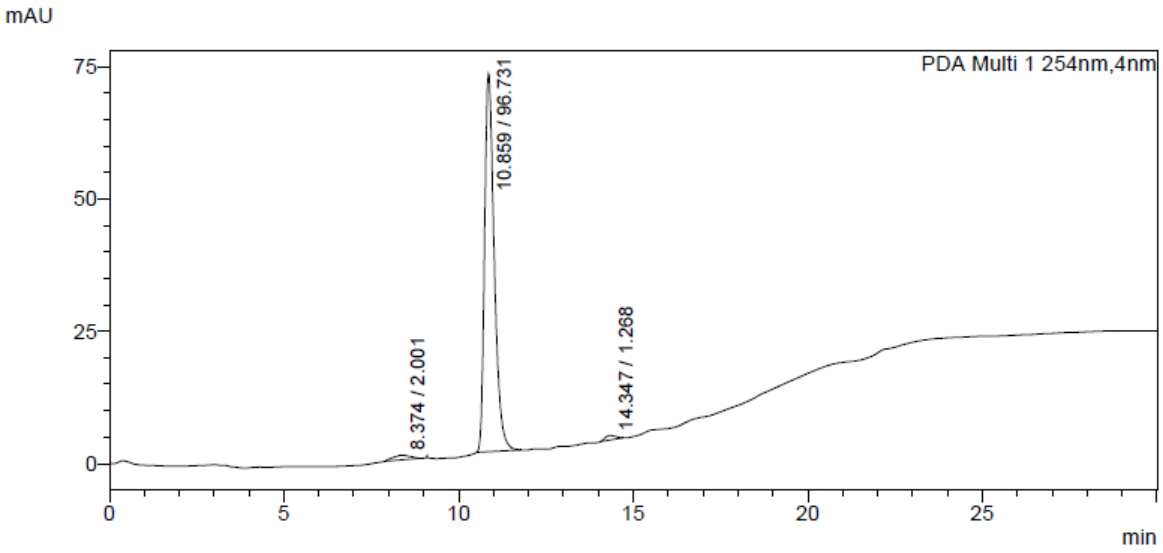

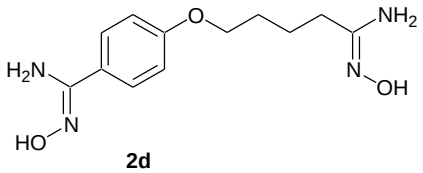

2d

[206.1379]

^{1}H and ^{13}C NMR Analysis: solvent DMSO-d_6

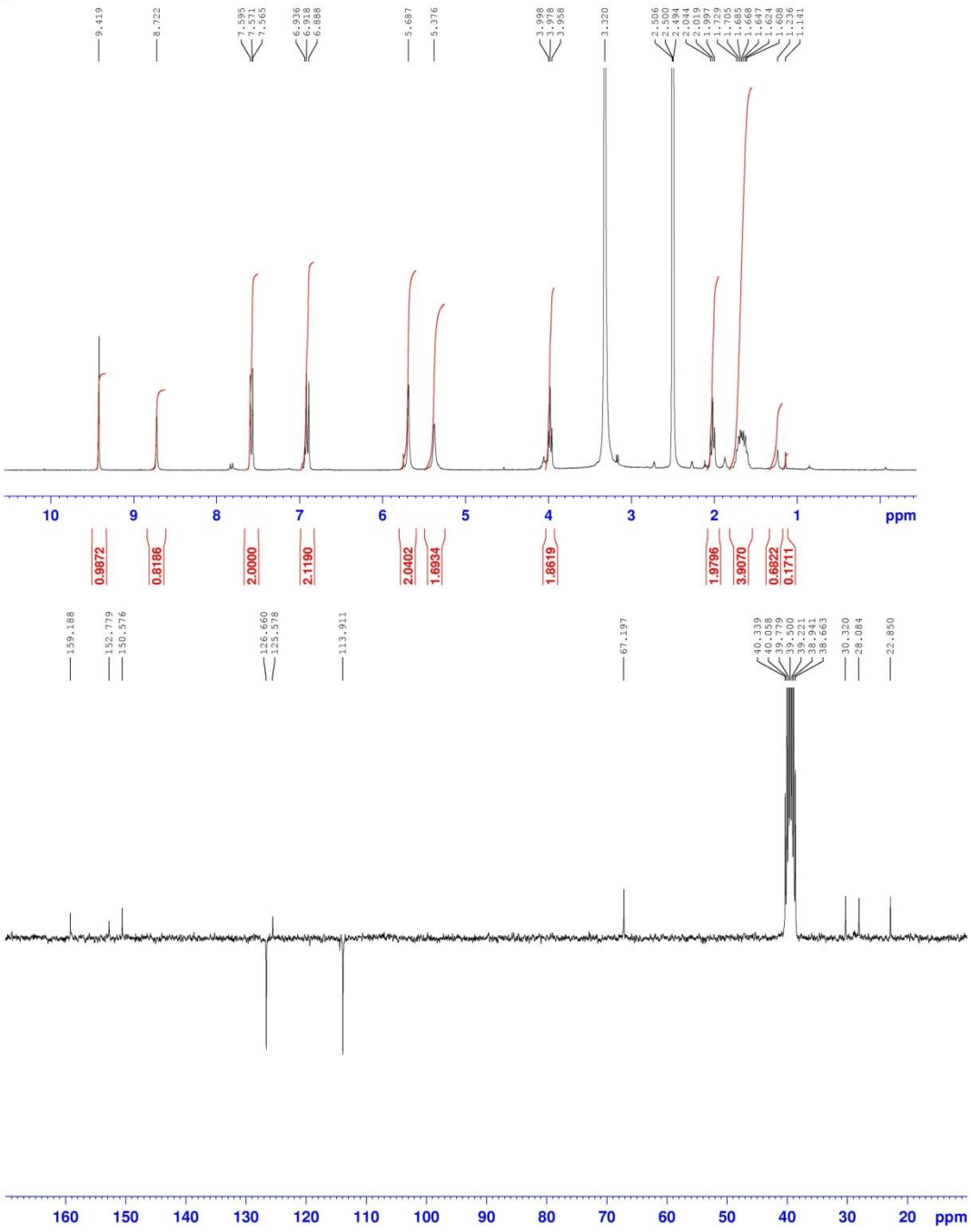

MS High Resolution

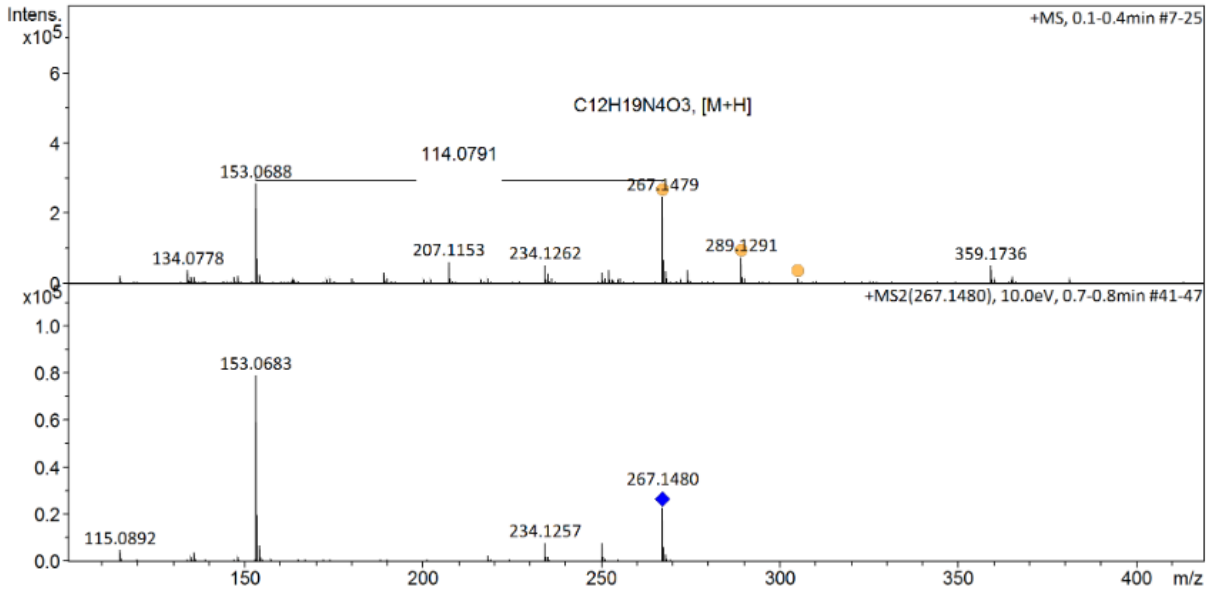

HPLC Analysis

R_t = 13.942, Area percentage = 95.183 %

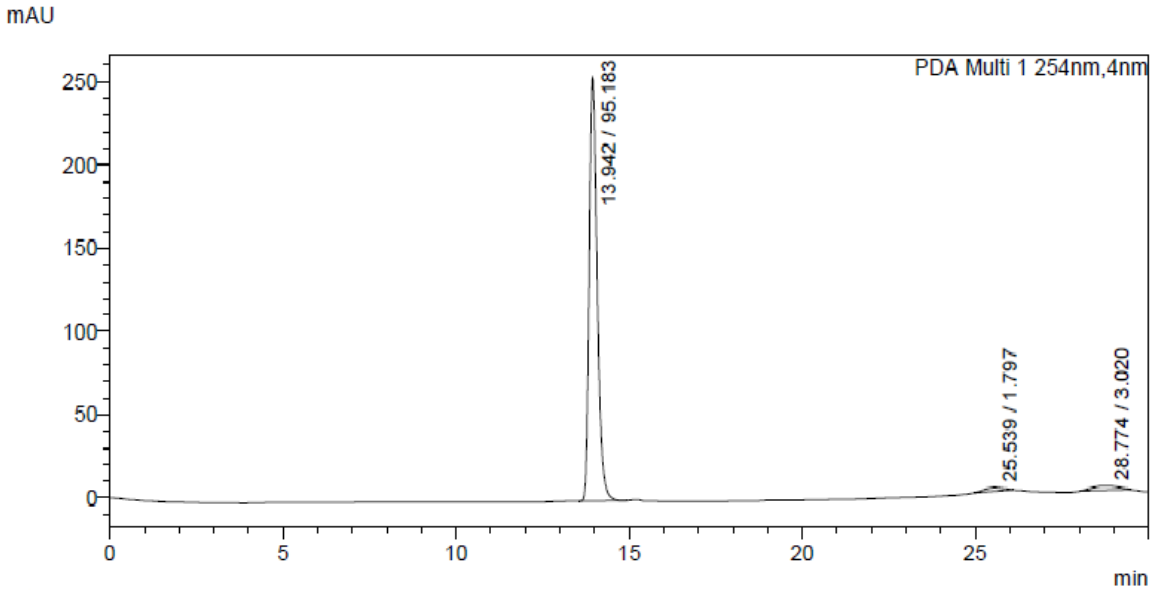

Mécanismes de franchissement de la barrière intestinale et de stockage vasculaire des S-nitrosothiols pour l'amélioration de formulations orales de NO

Les *S*-nitrosothiols (RSNO) comme le *S*-nitrosoglutathion (GSNO) sont des donneurs de monoxyde d'azote (NO) prometteurs pour le traitement des maladies cardiovasculaires. Cependant, ce sont des candidats médicaments peu stables. Précédemment, des nanoparticules chargées en GSNO (GSNO-NP) ont été incluses dans une matrice d'alginate/chitosan. Les particules composites ainsi produites avaient une bonne encapsulation et une libération prolongée de GSNO. De plus, leur administration orale à des rats produisait un stock de NO au niveau de la paroi de l'aorte. Elles avaient cependant plusieurs limitations : préparation et caractérisation longues, manque de stabilité et de reproductibilité. Ce travail avait donc trois objectifs : (1) déterminer le mécanisme d'absorption intestinale des RSNO non formulés ; (2) évaluer la capacité des RSNO non formulés à créer un stock vasculaire de NO ; 3) optimiser la formulation de GSNO.

Nous avons montré, dans un modèle *in vitro* de barrière intestinale, que la perméabilité intestinale de GSNO, *S*-nitroso-*N*-acétylcystéine (NACNO) et *S*-nitroso-*N*-acetylpénicillamine (SNAP) se fait par un mécanisme passif, principalement par voie transcellulaire (également paracellulaire pour SNAP), avec une perméabilité moyenne. Après avoir traversé la barrière intestinale, les RSNO atteindront les vaisseaux sanguins. Pour comparer leur capacité à former un stock vasculaire de NO dans des aortes (avec endothélium intact ou retiré), nous avons quantifié le stock, vérifié sa biodisponibilité pour la vasorelaxation et évalué son impact sur une vasoconstriction induite par la phénylephrine (PHE). L'incubation des aortes avec les RSNO augmente le stock basal de NO par un facteur trois à cinq. Ce stock est mobilisable pour induire la vasorelaxation et efficace pour diminuer la réactivité vasculaire à la PHE (NACNO>GSNO = SNAP), seulement dans les aortes dont l'endothélium a été retiré. Comme la perméabilité intestinale des RSNO est moyenne, l'intégration du GSNO dans une formulation appropriée est nécessaire. Vu l'impossibilité de résoudre les problèmes liés aux particules composites, le protocole de production des GSNO-NP a été modifié pour produire des microparticules (deux types selon l'état liquide ou solide de GSNO dans la phase interne de l'émulsion). Les deux types de microparticules avaient une libération de GSNO ralentie par rapport aux GSNO-NP. Les nano- comme les micro-particules ont pu être stabilisées par lyophilisation, et amélioraient la perméabilité intestinale de GSNO (jusqu'à une forte perméabilité avec les microparticules). Par conséquent, une administration orale de nano/microparticules chargées en GSNO/RSNO pourrait représenter une nouvelle approche thérapeutique pour les maladies cardiovasculaires.

Mots clés : *S*-nitrosoglutathion, particules, systèmes de délivrance pour la voie orale, stockage de monoxyde d'azote, perméabilité intestinale

Mechanisms of S-nitrosothiols intestinal permeability and NO store formation within vascular wall to improve NO oral delivery systems

S-nitrosothiols (RSNOs) such as *S*-nitrosoglutathione (GSNO) are promising nitric oxide (NO) donors for cardiovascular diseases treatment. However, they are poorly stable drug candidates. In previous studies, GSNO-loaded nanoparticles (GSNO-NP) were embedded into an alginate/chitosan matrix. Resulting nanocomposite particles showed high encapsulation and sustained release of GSNO, and led to the formation of a NO store in the wall of aorta after a single oral administration to rats. However, these nanocomposite particles have several limitations such as time-consuming preparation, lack of both stability and reproducibility. This thesis work aimed at: 1) Elucidate the mechanism of free RSNOs intestinal absorption; 2) Evaluate ability of free RSNOs to form a vascular NO store; 3) Optimize the GSNO formulation.

In this study, we showed that the intestinal permeability (in vitro model of intestinal barrier) of GSNO, *S*-nitroso-N-acetylcysteine (NACNO) and S-nitroso-N-acetylpenicillamine (SNAP) was a passive diffusion, following the transcellular pathway (and also the paracellular way for SNAP) and belonging to the medium permeability class. After crossing the intestinal barrier, RSNOs will reach the vasculature. In order to compare the ability of free RSNOs to form a vascular store of NO either in endothelium-intact or endothelium-removed aortae, we quantified the store, verified its bioavailability for vasorelaxation and evaluated its impact on phenylephrine (PHE)-induced vasoconstriction. Incubation with RSNOs increased the basal NO store three to five times. This store is still bioavailable to induce vasorelaxation and efficient to induce vascular hyporeactivity to PHE (NACNO> GSNO = SNAP) only in endothelium-removed aortae. As intestinal permeability of RSNOs was in the medium class, the integration of GSNO into an appropriate delivery system is essential. Limitations of previously developed nanocomposites particles were impossible to bypass so the production process of GSNO-NP was modified (liquid or solid GSNO in the internal phase of the emulsion) to produce microparticles. Both kinds of microparticles exhibited a slower release of GSNO than GSNO-NP. Nano-and micro-particles were stable after lyophilization and presented an enhancement of GSNO intestinal permeability (up to high permeability class for microparticles). Thus, oral administration of GSNO/RSNO loaded nano/micro particles seems to be a promising avenue for the treatment of cardiovascular diseases.

Keywords: *S*-nitrosoglutathione, particles, oral delivery systems, nitric oxide storage, intestinal permeability